AN ANALYTICAL INVESTIGATION OF PASSIVE AND ACTIVE SUSPENSION SYSTEMS FOR ARTICULATED FREIGHT VEHICLES

Faisal Oueslati

A Thesis
in
The Department
of
Mechanical Engineering

Presented in Partial Fulfillment of the Requirements
for the Degree of Doctor of Philosophy at
Concordia University
Montreal, Quebec
Canada

April 1995

ISBN 0-612-01286-7

Name FAISAL QUESCATI

Dissertation Abstracts International is arranged by broad, general subject categories. Please select the one subject which most nearly describes the content of your dissertation. Enter the corresponding four-digit code in the spaces provided.

Mechanical Engineering — SUBJECT TERM

0548 — SUBJECT CODE

U·M·I

Subject Categories

THE HUMANITIES AND SOCIAL SCIENCES

COMMUNICATIONS AND THE ARTS
- Architecture 0729
- Art History 0377
- Cinema 0900
- Dance 0378
- Fine Arts 0357
- Information Science 0723
- Journalism 0391
- Library Science 0399
- Mass Communications 0708
- Music 0413
- Speech Communication 0459
- Theater 0465

EDUCATION
- General 0515
- Administration 0514
- Adult and Continuing 0516
- Agricultural 0517
- Art 0273
- Bilingual and Multicultural 0282
- Business 0688
- Community College 0275
- Curriculum and Instruction 0727
- Early Childhood 0518
- Elementary 0524
- Finance 0277
- Guidance and Counseling 0519
- Health 0680
- Higher 0745
- History of 0520
- Home Economics 0278
- Industrial 0521
- Language and Literature 0279
- Mathematics 0280
- Music 0522
- Philosophy of 0998
- Physical 0523
- Psychology 0525
- Reading 0535
- Religious 0527
- Sciences 0714
- Secondary 0533
- Social Sciences 0534
- Sociology of 0340
- Special 0529
- Teacher Training 0530
- Technology 0710
- Tests and Measurements 0288
- Vocational 0747

LANGUAGE, LITERATURE AND LINGUISTICS
- Language
  - General 0679
  - Ancient 0289
  - Linguistics 0290
  - Modern 0291
- Literature
  - General 0401
  - Classical 0294
  - Comparative 0295
  - Medieval 0297
  - Modern 0298
  - African 0316
  - American 0591
  - Asian 0305
  - Canadian (English) 0352
  - Canadian (French) 0355
  - English 0593
  - Germanic 0311
  - Latin American 0312
  - Middle Eastern 0315
  - Romance 0313
  - Slavic and East European 0314

PHILOSOPHY, RELIGION AND THEOLOGY
- Philosophy 0422
- Religion
  - General 0318
  - Biblical Studies 0321
  - Clergy 0319
  - History of 0320
  - Philosophy of 0322
- Theology 0469

SOCIAL SCIENCES
- American Studies 0323
- Anthropology
  - Archaeology 0324
  - Cultural 0326
  - Physical 0327
- Business Administration
  - General 0310
  - Accounting 0272
  - Banking 0770
  - Management 0454
  - Marketing 0338
- Canadian Studies 0385
- Economics
  - General 0501
  - Agricultural 0503
  - Commerce-Business 0505
  - Finance 0508
  - History 0509
  - Labor 0510
  - Theory 0511
- Folklore 0358
- Geography 0366
- Gerontology 0351
- History
  - General 0578
  - Ancient 0579
  - Medieval 0581
  - Modern 0582
  - Black 0328
  - African 0331
  - Asia, Australia and Oceania 0332
  - Canadian 0334
  - European 0335
  - Latin American 0336
  - Middle Eastern 0333
  - United States 0337
- History of Science 0585
- Law 0398
- Political Science
  - General 0615
  - International Law and Relations 0616
  - Public Administration 0617
- Recreation 0814
- Social Work 0452
- Sociology
  - General 0626
  - Criminology and Penology 0627
  - Demography 0938
  - Ethnic and Racial Studies 0631
  - Individual and Family Studies 0628
  - Industrial and Labor Relations 0629
  - Public and Social Welfare 0630
  - Social Structure and Development 0700
  - Theory and Methods 0344
- Transportation 0709
- Urban and Regional Planning 0999
- Women's Studies 0453

THE SCIENCES AND ENGINEERING

BIOLOGICAL SCIENCES
- Agriculture
  - General 0473
  - Agronomy 0285
  - Animal Culture and Nutrition 0475
  - Animal Pathology 0476
  - Food Science and Technology 0359
  - Forestry and Wildlife 0478
  - Plant Culture 0479
  - Plant Pathology 0480
  - Plant Physiology 0817
  - Range Management 0777
  - Wood Technology 0746
- Biology
  - General 0306
  - Anatomy 0287
  - Biostatistics 0308
  - Botany 0309
  - Cell 0379
  - Ecology 0329
  - Entomology 0353
  - Genetics 0369
  - Limnology 0793
  - Microbiology 0410
  - Molecular 0307
  - Neuroscience 0317
  - Oceanography 0416
  - Physiology 0433
  - Radiation 0821
  - Veterinary Science 0778
  - Zoology 0472
- Biophysics
  - General 0786
  - Medical 0760

EARTH SCIENCES
- Biogeochemistry 0425
- Geochemistry 0996
- Geodesy 0370
- Geology 0372
- Geophysics 0373
- Hydrology 0388
- Mineralogy 0411
- Paleobotany 0345
- Paleoecology 0426
- Paleontology 0418
- Paleozoology 0985
- Palynology 0427
- Physical Geography 0368
- Physical Oceanography 0415

HEALTH AND ENVIRONMENTAL SCIENCES
- Environmental Sciences 0768
- Health Sciences
  - General 0566
  - Audiology 0300
  - Chemotherapy 0992
  - Dentistry 0567
  - Education 0350
  - Hospital Management 0769
  - Human Development 0758
  - Immunology 0982
  - Medicine and Surgery 0564
  - Mental Health 0347
  - Nursing 0569
  - Nutrition 0570
  - Obstetrics and Gynecology 0380
  - Occupational Health and Therapy 0354
  - Ophthalmology 0381
  - Pathology 0571
  - Pharmacology 0419
  - Pharmacy 0572
  - Physical Therapy 0382
  - Public Health 0573
  - Radiology 0574
  - Recreation 0575
  - Speech Pathology 0460
  - Toxicology 0383
- Home Economics 0386

PHYSICAL SCIENCES
Pure Sciences
- Chemistry
  - General 0485
  - Agricultural 0749
  - Analytical 0486
  - Biochemistry 0487
  - Inorganic 0488
  - Nuclear 0738
  - Organic 0490
  - Pharmaceutical 0491
  - Physical 0494
  - Polymer 0495
  - Radiation 0754
- Mathematics 0405
- Physics
  - General 0605
  - Acoustics 0986
  - Astronomy and Astrophysics 0606
  - Atmospheric Science 0608
  - Atomic 0748
  - Electronics and Electricity 0607
  - Elementary Particles and High Energy 0798
  - Fluid and Plasma 0759
  - Molecular 0609
  - Nuclear 0610
  - Optics 0752
  - Radiation 0756
  - Solid State 0611
- Statistics 0463

Applied Sciences
- Applied Mechanics 0346
- Computer Science 0984
- Engineering
  - General 0537
  - Aerospace 0538
  - Agricultural 0539
  - Automotive 0540
  - Biomedical 0541
  - Chemical 0542
  - Civil 0543
  - Electronics and Electrical 0544
  - Heat and Thermodynamics 0348
  - Hydraulic 0545
  - Industrial 0546
  - Marine 0547
  - Materials Science 0794
  - Mechanical 0548
  - Metallurgy 0743
  - Mining 0551
  - Nuclear 0552
  - Packaging 0549
  - Petroleum 0765
  - Sanitary and Municipal 0554
  - System Science 0790
- Geotechnology 0428
- Operations Research 0796
- Plastics Technology 0795
- Textile Technology 0994

PSYCHOLOGY
- General 0621
- Behavioral 0384
- Clinical 0622
- Developmental 0620
- Experimental 0623
- Industrial 0624
- Personality 0625
- Physiological 0989
- Psychobiology 0349
- Psychometrics 0632
- Social 0451

ABSTRACT

AN ANALYTICAL INVESTIGATION OF PASSIVE AND ACTIVE SUSPENSION SYSTEMS FOR ARTICULATED FREIGHT VEHICLES

Faisal Oueslati, Ph.D.
Concordia University, 1995

Articulated freight vehicles transmit high levels of whole-body ride vibration to the driver and high magnitudes of dynamic tire forces to the pavements. The high levels of ride vibration and tire forces are attributed to the excessive sizes and weights of these vehicles. The driver health and safety risks posed by ride vibrations, and the significant tire induced road damage caused by heavy vehicles have prompted a growing demand for design of driver- and road-friendly vehicles. Different active and passive suspension systems are thus analyzed to enhance the performance characteristics of articulated freight vehicles. The investigation is carried out in five sequential phases: *(i)* development of a representative dynamic model of the vehicle; *(ii)* passive suspension design and optimization; *(iii)* ideal active suspension design; *(iv)* limited-state active suspension design; and *(v)* assessment of tire dynamic forces transmitted to the pavement. An articulated freight vehicle is characterized by an inplane nine degrees-of-freedom (*DOF*) dynamic system model. An analytical characterization of the randomly irregular road surface is presented and the time delays between the consecutive wheel inputs are incorporated using *Padé* approximation. The validity of the analytical vehicle model is asserted by comparing its response characteristics with the road measured data. A technique, based on covariance analysis, is employed to perform the multi-parameter sensitivity analysis and to design an "optimum" passive suspension. A performance index comprising ride quality, cargo safety, suspension rattle space and dynamic tire forces is formulated to derive the "optimum" suspension design. The effects of varying the suspension properties on the frequency response characteristics are investigated to further

verify the conclusions drawn from the covariance analysis. *Linear Quadratic Gaussian* (*LQG*) control technique is employed to design an ideal fail-safe active suspension scheme based on full-state feedback. Passive damping and stiffness elements are incorporated in the active suspension system to yield a fail-safe configuration with minimal power requirement. The performance characteristics of the ideal active suspension are compared to those of the "optimum" passive suspension to determine their potential performance benefits. In view of the excessive hardware and signal processing requirements, high cost and poor reliability of a full-state feedback active suspension design, a thorough analysis of a more realistic active suspension scheme, based on H_2 synthesis, is undertaken. Two suspension schemes based upon limited-state measurements are investigated. The performance characteristics of the proposed suspension designs are compared to those of the full-state active suspension and the "optimum" passive suspension systems. Finally, a comprehensive analysis is undertaken to assess the effects of the passive and various active suspension schemes on the dynamic tire forces. It is concluded that the reduced state active suspension systems yield performance characteristics comparable to those of an ideal active suspension.

ACKNOWLEDGMENT

The author is sincerely grateful to his supervisors, Dr. S. Rakheja and Dr. I. Stiharu for their guidance and encouragement throughout the course of this research. Sincere thanks are also due to Dr. S. Sankar for initiating the project and providing guidance and supervision until his departure in June 1994.

The author also wishes to thank members of the faculty and staff of *CONCAVE Research Centre* for their time and assistance during the progression of this work.

Financial support provided by *Concordia University* and *FCAR (Fonds pour la formation de chercheurs et l'aide à la recherche)* is gratefully acknowledged.

TABLE OF CONTENTS

CHAPTER 3

PASSIVE SUSPENSION DESIGN AND OPTIMIZATION

CHAPTER 4

IDEAL *LQG* ACTIVE SUSPENSION DESIGN

CHAPTER 5

ANALYSIS AND DESIGN OF AN ACTIVE SUSPENSION USING H_2 SYNTHESIS

CHAPTER 6

PAVEMENT DAMAGE EVALUATION

CHAPTER 7

CONCLUSIONS AND RECOMMENDATIONS FOR FUTURE WORK

LIST OF FIGURES

Figure

LIST OF TABLES

Table

NOMENCLATURE

$\tilde{A}$, $\tilde{B}_1$, $\tilde{B}_2$, $\tilde{C}_1$, $\tilde{D}_{11}$, $\tilde{D}_{12}$, $\tilde{C}_2$, $\tilde{D}_{21}$, and $\tilde{D}_{22}$,	state-space matrices describing the tractor-semitrailer dynamics in the H_2 formulation
A_1	horizontal distance from tractor CG to tractor steer axle
A_2	horizontal distance from semitrailer CG to fifth axle
AS1 to *AS5*	active suspension schemes based on full-state measurements
B_1	horizontal distance from tractor CG to tractor first drive axle
B_2	horizontal distance from tractor CG to tractor second drive axle
B_3	horizontal distance from semitrailer CG to semitrailer first axle
B_4	horizontal distance from semitrailer CG to semitrailer second axle
B_5	horizontal distance from tractor CG to fifth wheel
$\boldsymbol{C}$	damping matrix
$\boldsymbol{C}_1$	state-to-performance variables transformation matrix
C_1	tractor front suspension damping coefficient
C_2	tractor leading/trailing drive axle damping coefficient
C_3	Semitrailer leading/trailing axle suspension damping coefficient
C_5	fifth wheel damping coefficient
$\boldsymbol{C}_m$	controllability matrix
$\boldsymbol{D}_{12}$	control forces-to performance variables transformation matrix
DLC	*Dynamic Load Coefficient*
DOF	degrees-of-freedom

ESAL	*Equivalent Standard Axle Loads*
$E[\ ]$	denotes the expected value
$\boldsymbol{F}$	matrix of control forces
f_n	natural frequency (Hz)
$\boldsymbol{H}$	frequency response function relating the excitation to the vector of system response variables $\boldsymbol{z}$
$\boldsymbol{I}$	identity matrix
I_{y1}	tractor pitch moment of inertia
I_{y2}	semitrailer pitch moment of inertia
$\boldsymbol{J}_{H_2}$	H_2 performance index
$\boldsymbol{K}$	control gain matrix
K_1	tractor front suspension stiffness
K_2	tractor leading/trailing drive axle suspension stiffness
K_3	semitrailer leading/trailing axle suspension stiffness
K_5	fifth wheel stiffness
$\boldsymbol{K}_c$	full-state feedback gain
$\boldsymbol{K}_s$	stiffness matrix
$\boldsymbol{K}_o$	*Kalman* filter residual gain
$\boldsymbol{K}_T$	tire stiffness matrix
K_{ti}	stiffness of i^{th} tire
LQG	*Linear Quadratic Gaussian*
LSM1	active suspension system based on measurement of relative displacements and velocities across the suspensions

LSM2	active suspension system based on measurement of tractor and semitrailer bounce and pitch accelerations
$\boldsymbol{M}$	mass matrix,
Mf	multiplication factor associated with ρ_i
Mt	multiplication factor associated with μ_1 and μ_2
m_{s1}	tractor mass
m_{s2}	semitrailer mass
m_{u1}	tractor steering axle assembly mass
m_{u2}	tractor leading/trailing drive axle assembly mass
m_{u3}	semitrailer leading/trailing axle assembly mass
$\mathcal{P}$	transfer function matrix
$\boldsymbol{P}$	solution of the matrix *Riccati* equation
P(t)	instantaneous tire force
$\boldsymbol{P}_o$	*Kalman* filter error covariance matrix
PSD	power spectral density
P_{stat}	static tire force
$\boldsymbol{P}_{xx}, \boldsymbol{P}_{xw}, \boldsymbol{P}_{ww}$	partition matrices of $\boldsymbol{P}$
$\hat{\boldsymbol{Q}}, \boldsymbol{Q}, \hat{\boldsymbol{R}}, \boldsymbol{R}, \boldsymbol{N}$	weighting matrices
$\boldsymbol{q}$	road elevation vector
q_i	road elevation at the i^{th} wheel
$\boldsymbol{r}$	vector of generalized coordinates,
RSF	*Dynamic Road Stress Factor*

S_z	power spectral density of the response variables
S_ξ	auto spectral density of the white noise input excitation
s	*Laplace* operator
$\bar{s}$	coefficient of variation of dynamic tire force,
Tr	trace
$T_{\tilde{w}z}$	closed loop transfer function relating the disturbance $\tilde{w}$ to the penalized variables vector z
u	control forces vector
u_1 to u_5	control forces
V	sensor noise covariance matrix noises
W	filtered white noise covariance matrix
$\tilde{w}$	exogenous signal (includes disturbance and sensors noise)
X	covariance matrix of the state vector $x(t)$
x	augmented state vector
x_o	estimate of augmented state vector x
y	observation vector (or vector of measurable/accessible variables)
y_y	state vector
z	error vector (or vector of penalized variables)
z_1 to z_{14}	performance variables
α, σ	road roughness coefficients
Δ_n	time delay between the first and the n^{th} wheel
$\delta_{(t-\tau)}$	Dirac delta function
Φ_q	road irregularities power spectral density

ζ	white measurement noise
ζ_d	damping ratios
ξ	white plant noise
μ_i	weighting factors associated with the penalized response variables
ρ_i	weighting factors associated with the penalized actuator forces
v	vehicle speed
ω	temporal angular frequency *(rad/s)*
Ω	spatial frequency *(1/m)*
*	denotes the complex conjugate transpose
'	denotes the transpose

CHAPTER 1

INTRODUCTION

1.1 GENERAL

For reasons of freight transportation economy, the weights and dimensions of articulated freight vehicles have been increased considerably during the past decade. Various studies conducted by transportation research organizations and regulatory bodies have established that the directional stability and control, ride vibration environment, and dynamic tire forces of heavy vehicles are strongly affected by the increased sizes and weights in a highly adverse manner. The ride quality and dynamic tire forces of heavy vehicles are directly related to different vibration modes of the vehicle. The ride performance of an articulated freight vehicle is substantially different from that of a passenger car. The excessive masses of the coupled dynamic vehicle system yield vibration levels 9 to 16 times larger than those encountered in a passenger car. Vehicle drivers are exposed to such high levels of vibrations for approximately 10 hours a day during driving, and perhaps an additional 10 hours a day if they are employed in sleeper-line dual operation. The health and safety risks associated with the prolonged exposure to high levels of articulated vehicle vibration have prompted a demand for enhancement of ride quality performance of the vehicles. The high levels of vehicular vibration have also caused

many concerns related to cargo safety.

Freight vehicles with high axle loads and high tire inflation pressure transmit high magnitudes of dynamic forces to the pavement through the tires. The high magnitudes of dynamic tire forces are known to accelerate pavement fatigue and rut formation. Dynamic wheel loads of heavy vehicles transmitted to the pavement have been associated with high cost of highway infrastructure maintenance. The total annual cost of highway infrastructure maintenance by the federal and provincial governments in Canada, has been estimated at $ 8 billion. While part of this cost is due to environmental factors, a significant component has been directly attributed to the heavy vehicle tire loads. In recent years, *OECD (Organization for Economic Cooperation and Development)* has undertaken a major initiative to enhance the road-friendliness of heavy vehicles in an attempt to protect the public investments in highway infrastructures.

The ride vibration environment and the dynamic wheel loads are strongly influenced by various design and operating parameters in a highly complex manner. Among the various design parameters, vehicle suspension design and road roughness, are known to affect driver- and road-friendliness of the vehicle in a very most significant manner. The handling directional control and stability, ride quality and suspension rattle space, however, pose conflicting design requirements for suspension design. Tractor-semitrailer suspension systems are thus designed to achieve a compromise among the design requirements. For ride comfort and cargo safety, the suspension should isolate the driver and cargo from high frequency roadway inputs. On the other hand, for good vehicle handling, the tractor, semitrailer and wheels should closely follow the vertical inputs from the road at low frequencies. Enhancement of driver- and road-friendliness of heavy vehicles thus involves formulation of an adequate suspension design objective comprising ride quality, cargo safety, rattle space requirements and dynamic tire forces. Passive suspensions, while being

very reliable and easily implementable, exhibit inherent performance limitations in satisfying the various conflicting design requirements. Passive suspensions are constrained due to the constitutive laws of their elements. With recent advances in optimization techniques, automatic control, and reliable hardware, active suspensions offer considerable performance potentials to enhance the vehicle performance related to ride quality, cargo safety, suspension rattle space and dynamic tire loads. While active suspensions eliminate some of the inherent performance limitations of passive suspensions, the associated high costs and complexities prohibit their general implementation. The active suspensions are thus considered feasible when the performance benefits outweigh the increased cost and complexities. In view of the health and safety risks posed by the ride vibration environment of heavy vehicles, and the high cost associated with the tire induced road damage, the demand for reliable active suspensions has been growing. The cost and complexities of an active suspension system can be reduced considerably through suspension designs based upon limited-state measurements. The control gains, however, must be selected to enhance both the driver- and road-friendliness of the vehicle. This research is thus directed towards the design of "optimum" and limited-state active suspensions to improve the ride quality, cargo safety and reduce the tire generated road damage.

1.2 LITERATURE REVIEW

A review of previous investigations relevant to tractor-semitrailer suspension design aspects, such as vehicle mathematical modeling, performance evaluations, design and optimization of passive and active suspension systems, and tire generated pavement damage, is presented in the following subsections to develop the scope of the research.

1.2.1 Vehicle Mathematical Models

A study of ride dynamics and pavement interactions of a freight vehicle involves development of a representative dynamic model that closely describes the vehicle behavior. Many vehicle models ranging from linear quarter vehicle models with two degrees-of-freedom (*DOF*) to complex three-dimensional models with many *DOF* have been reported in literature. While the majority of the models consider the sprung and unsprung masses as rigid bodies, few models have incorporated the flexibility of the trailer structure to study contributions due to frame bending modes [1-5].

Simple one and two *DOF* vehicle models have been used by several investigators to study the performance characteristics of active, semi-active and passive suspension systems [6-10]. Such models permit the analysis of different suspension concepts under uncoupled vertical motions in a highly convenient manner. These models, however, can not be utilized to analyze the ride dynamics of heavy vehicles, which comprise various vibration modes associated with vertical, roll and pitch motions of sprung and unsprung masses.

Many analytical and experimental studies on ride dynamics of road vehicles have been reported in literature. The primary objectives of these studies, in general, include: assessment of vehicle ride quality, performance evaluation of different vehicle suspensions, assessment of cargo vibrations, and evaluation of dynamic tire loads transmitted to the pavement. Since the simple one-dimensional one- and two *DOF* vehicle models can not be used to predict the complex dynamics associated with articulated heavy vehicles, a number of comprehensive two- and three-dimensional vehicle models have been developed to study the ride quality and tire force characteristics. Ride dynamic models of articulated freight vehicles, reported in literature, vary from two-dimensional three *DOF* to three-

dimensional nineteen *DOF* models [11-13]. Analytical models with limited number of *DOF*, but realistic enough to provide reasonably accurate estimate of the ride dynamics, are desirable for design and optimization studies. In recent years, these analytical models have been further employed to study the dynamic wheel loads transmitted to the pavement [14-17]. Various studies on ride dynamics and vehicle-pavement interactions have concluded that contributions of the roll-plane dynamics of highway vehicles are insignificant [18]. The vehicle ride quality, and the dynamic wheel loads are strongly related to the pitch and vertical modes of the sprung masses and vertical deflection modes of the unsprung masses. An analogy between the vehicle ride vibrations and the pavement interactions has been further derived due to their strong dependence upon the vehicle vibration modes [19,20]. Results of these studies have demonstrated that three and six *DOF* inplane vehicle models can be effectively used to determine the ride dynamic behavior of articulated vehicles.

The ride dynamics of articulated freight vehicles are strongly dependent upon their weight and dimension, axle configuration, suspension and tire properties, etc. A wide range of freight vehicles operate on our highways, such as trucks, tractor-trailer combinations, B-trains, doubles and triples. Since the dynamics of the vehicle is strongly dependent upon the configuration, the vehicle models are developed to address the dynamics of specific a vehicle configuration. A survey conducted by *Road Transport Association of Canada* [21], reported that approximately 77% of all heavy vehicles operated in Canada are tractor-semitrailers. Tractor-semitrailers exhibit complex ride behavior due to interactions of the multiple axles and pavement, articulation properties, and excessive weights and dimensions. A study of dynamic performance behavior of articulated vehicles thus necessitates the development of a comprehensive analytical model. The *DOF* and thus the complexity of the model, however, are related to the objectives of the analysis. Tractor-semitrailer combinations comprise long semitrailer

structures supported on two-, or three-, or four axles at the rear end, and the articulation mechanism at the leading edge. Trailer frame deformations, that are known to exhibit bending modes in the 6 to 9 *Hz* frequency range, have been included in some of the reported models of heavy vehicles to study the contribution due to frame bending. Majority of the studies, however, have concluded that contributions of the frame bending modes to the overall dynamic behavior are insignificant [1-5]. The tractor and semitrailer sprung masses can thus be characterized by rigid bodies.

Development of an analytical vehicle model to determine the ride dynamics and pavement interactions primarily involves characterization of the suspension and tires. Vehicle suspension systems often exhibit nonlinearities associated with progressively hardening force-deflection and variable force-velocity properties of the stiffness and damping elements, respectively. A number of analytical techniques have been proposed to analyze the response characteristics of nonlinear dynamic systems. These techniques employ various approaches based on *Markov* process, perturbation, and simulation methods [22-24]. In view of the convenience of analysis using well established linear analytical tools, time and frequency domain equivalent linearization techniques are frequently employed to analyze nonlinear dynamic systems [25-28]. Analytical investigations of vehicle characteristics based on the assumption of linear suspension parameters, however, are frequently used to derive preliminary design guidelines and to gain an insight into the vehicle response behavior with relatively simple analysis.

The tire-terrain interactions have been characterized by different types of linear and nonlinear tire models. The tire models, reported in the literature, can be grouped in four categories based upon the characterization of the tire-road contact: point contact; rigid tread band; fixed foot print; and adaptive foot print models [29,30]. These models are conceived, to different degrees of complexity, to account for the tire deflection properties,

geometric filtering of the rolling wheel, and contact pattern with the road. In view of the complexities associated with adaptive foot print models, and the lack of knowledge of the tire properties, the wheel-terrain interactions in most heavy vehicle models are represented by a point contact. While some of the linear analytical models consider the force-deflection properties of the tire as bilinear and unbounded, others incorporated tire properties influenced by the wheel-hop motion [31].

1.2.2 Performance Measures and Passive Suspension Optimization

Design of a passive suspension for a heavy vehicle involves careful selection of the suspension parameters, namely the stiffness and damping properties, to achieve a compromise between the ride, handling and control performance characteristics. A rather extensive body of literature has been published on the ride quality and cargo safety aspects of tractor-semitrailers. The performance measures related to ride quality, suspension rattle space, handling, roll stability, and directional control characteristics pose conflicting requirements on passive suspension design. Enhancement of ride quality and cargo safety necessitates soft and lightly damped suspensions. The soft vehicle suspensions, however, result in poor roll stability and directional control performance. The suspension rattle space requirements also increase with soft suspensions. A passive vehicle suspension with constant parameters thus exhibit inherent limitations to meet all the conflicting requirements. The overall performance measures of a heavy vehicle suspension, however, must be formulated to address a design compromise among all aspects of desirable performance characteristics. Four primary concerns that evolve from suspension design formulate the objectives for the performance analysis: *(i)* the level of vibration perceived by the passenger/driver, which can be related to the acceleration response at the tractor driver/passenger seat or the acceleration response of the tractor sprung mass [32-34]; *(ii)* cargo safety, which can be related to the bounce and pitch accelerations at the semitrailer

center of gravity (*CG*); *(iii)* suspension deflections, which are indication of the working or rattle space requirements [35]; and *(iv)* tire deflections, which are an indication of the severity of forces transmitted to the roads [34,36].

The performance measure related to ride quality has been the subject of considerable analytical and experimental evaluations. Ride quality can be assessed in terms of preservation of health, comfort and performance. Proposed vibration tolerance criteria have related ride quality to driver's work station design, placement of controls, visual displays, cab temperature, driver seat, and cabin noise and vibration environment [37]. Although the ride quality related to work station design is frequently assessed using subjective rankings, subjective response data has been insufficient and inconsistent to derive a generally acceptable comfort criteria with respect to vibration levels. Many objective methods have been developed to assess the ride quality related to noise and vibration environment. Objective methods proposed to assess the ride vibrations are based upon directly measurable physical quantities, such as velocity, acceleration and jerk. A good correlation between the mean square jerk or acceleration and the subjective human response has been reported [38]. From various objective evaluations, it has been concluded that a seated human driver is most sensitive to vibrations in the 4 to 8 *Hz* frequency range [39]. The *International Organization for Standardization* (*ISO*) [40] has, therefore, suggested three exposure criteria as function of exposure time and frequency. The proposed exposure criteria are recommended for evaluation of health risks, comfort, and preservation of working efficiency under exposure to whole-body vibration.

Two *DOF*, quarter-vehicle models have been extensively used to gain a fundamental understanding of the effect of suspension parameters on the vehicle performance characteristics subjected to deterministic or random road disturbances. A study performed by *Chalasani* [41] presented a comprehensive attempt to evaluate the effects of suspension

stiffness and damping on the root mean square (*RMS*) values and frequency response characteristics of the vehicle. The author further presented the relative response characteristics of passive and ideal active suspensions using a seven *DOF*, three-dimensional car model, subjected to periodic excitations and transient excitations arising from a chuck-hole-type road disturbance. [42].

Vehicle ride vibrations and tire forces are strongly related to various vibrations of the vehicle. Vehicle vibrations and thus the dynamic tire loads are dependent on the restoring and dissipative properties of the suspension and tires. Extensive studies reported on ride dynamics of road vehicles, however, have concluded that suspension damping affects the vehicle vibration behavior in a significant manner [20,43,44]. The significance of suspension damping in reducing dynamic wheel loads has also been investigated through the response analysis of a nonlinear quarter-car model to identify the suspension damping properties most suited for tire forces reduction [45]. Vibration absorbers mounted on vehicle axles have been also suggested for reducing the dynamic pavement loads in the vicinity of wheel hop frequencies. The study concluded that adequately tuned vibration absorbers can yield 15 to 20% reduction in the dynamic load coefficient (*DLC*) [46].

The ride dynamics of heavy vehicles has been extensively addressed in numerous analytical and experimental studies. The analytical investigations using two- and three-dimensional vehicle models of diverse degrees of complexity have mostly employed numerical integration techniques to solve the differential equations of motion. The thrust of the work was basically in the validation of experimental measurements [19,47-51]. Design optimization in conjunction with time-domain analysis of vehicle models subjected to random road excitations pose considerable computational challenge, specifically when the performance index comprises several components. Alternatively, the frequency domain

analysis of linear or nonlinear equivalent vehicle models simplifies the design optimization tasks. The design optimization, however, necessitates well defined performance objective and the formulation of a performance index. A number of studies have employed optimization techniques and various forms of optimization criteria in the design of vehicle suspension systems [51,52-54]. The primary objective of these was to achieve an improved compromise between vibration isolation and suspension deflection, which have been identified as competing and contrary goals. Ride quality has by far been the major concern of heavy vehicle suspension design and optimization. In view of the excessive road damage caused by heavy vehicle tire forces transmitted to the pavement, it is desirable to integrate a measure of the tire forces within the performance index. There have been relatively few attempts to systematically address the tractor-semitrailer passive suspension optimization. *ElMadany* [55] identified this problem and presented an optimization method to minimize the acceleration and jerk transmitted to the driver position in an attempt to enhance the vehicle ride quality.

1.2.3 Active Suspensions

It has been established that passive suspension systems with fixed parameters exhibit inherent performance limitations to meet various design objectives related to ride, handling and directional control. Active suspension systems with parameters that can change with varying response and excitations offer considerable potentials to achieve an improved compromise among various conflicting design requirements. Although many designs of active suspensions have been proposed for passenger cars, light trucks and railway vehicles [10,32,56-61], their implementations have been severely limited due to associated high cost, poor reliability and high complexities. Recent relaxation in heavy vehicle weight and dimension regulations, however, have resulted in deterioration of directional stability and control performance, increased levels of ride vibration, and high levels of dynamic tire

forces transmitted to the pavements. A heavy vehicle driver is exposed to high levels of whole-body vehicular vibration for almost 10 hours a day. The dynamic tire forces transmitted to the roads have been associated with excessive maintenance costs for the highway infrastructure. The growing population of heavy vehicles on our highways, continued interests to further increase the weight and dimensions, the impact of vibration levels on driver performance and safety, and the road damage caused by heavy vehicles, have prompted a growing interest for development of active suspensions to enhance the driver- and road-friendliness performance of the vehicles. Recent advances in control technologies and hardware have further contributed to a renewed interest in the development of active vehicle suspensions. While, drivers of passenger cars can benefit greatly from the active suspensions, the potential and effectiveness of active suspensions can best be harnessed when used in heavy vehicles, since the ride vibration levels of heavy trucks are 9 to 16 times higher than those of the passenger cars [62]. In view of the prolonged exposure and high levels of ride vibrations, and significant dynamic tire forces known to accelerate pavement deterioration, the effectiveness of advanced suspensions need to be further investigated for use in heavy vehicles. Although considerable research effort has been mounted to develop effective active suspension systems, the majority of these efforts are either exploratory (based on one or two *DOF* vehicle models) or directed towards passenger cars. These studies provide considerable knowledge relevant to understanding the potential of the active suspension schemes. These suspension models, however, need to incorporate wheel base effects, dynamics due to articulation, etc. to study the performance enhancement potentials for heavy vehicles.

The design of an active suspension system involves the formulation of a feedback control scheme and a control optimization to determine the optimal control gains. Optimal control theory is the most widely used technique to achieve designs of active suspension systems [35,36,59,63,64]. Other control design techniques, such as pole placement or

classical techniques, where the gains are computed to obtain the desired natural frequencies and damping ratios for the sprung and the unsprung masses, can also be used [65,66]. Optimal control methodologies are very convenient for designing active suspensions based upon full-state feedback laws. The control theory requires that the performance index to be minimized is in a quadratic form, and all the state variables are measurable. The theory further requires that the system input must be a white noise [65,67]. Since the random road roughness can not be described by a white noise process, it is necessary to augment the suspension system model with an integrator causing the road elevation to become one of the system states rather than the input [36,68]. The requirement of full-state information then necessitates the measurement of the road elevations, which poses complexities in practical implementations of an active suspension. Alternatively, feedback control systems with limited-state measurements have been proposed. These methods employ a gradient descent method that results in limited-state feedback [36,60,63,69], or state estimation using *Kalman* filtering, which yields an estimate of the entire state vector [70,71].

The performance criteria of a tractor-semitrailer suspension contains a broad spectrum of objectives. Very little research exists on using active suspension specifically for tractor-semitrailers that targets all the performance criteria of the vehicle. Although some researchers have attempted to use active suspensions for tractor-semitrailers, most have stressed the improvement of ride quality alone [72]. A detailed investigation of a stochastic optimal suspension system for the cab of a tractor-semitrailer is reported in [73]. The vehicle is assumed to be traveling over a randomly profiled road and the control scheme includes both limited state measurements and corrupted signals. The study analyzed the ride performance of active actuators used to support the tractor cab only. The problem of limited-state measurement and corrupted signals can be formulated in a compact and elegant way by formulating the linear quadratic Gaussian (LQG) problem in

an equivalent H_2 control problem. *Kashani* et al [74] demonstrated the use of this methodology for the design of an active suspension based on a 2 *DOF* vehicle model.

1.2.4 Tire Generated Road Damage

High magnitude of static and dynamic tire loads in heavy vehicles are known to accelerate the pavement fatigue and rut formation. Various aspects of the road damage caused by heavy vehicles have been addressed in the literature.

A number of analytical and experimental studies have been carried out to assess the dynamic tire forces, road damage potentials of heavy vehicle tire loads, and to derive reliable pavement damage assessment tools. These studies have established that the magnitudes of dynamic tire loads are directly influenced by the vehicular vibration modes associated with the vertical and pitch motion of the sprung and unsprung masses. Many studies have concluded that the dynamic tire loads are strongly dependent upon vehicle and axle configurations, inertial and geometric properties of the vehicle, speed, road roughness, and suspension and tire properties.

Laboratory simulation of vehicle service stress was carried out by deriving synthesized random displacements based on the knowledge of road surface undulations. Laboratory evaluations of dynamic tire forces necessitate an accurate generation of road profile in the laboratory [81]. It has been shown that road displacement can be derived from the spectral density evaluated from a single traverse along the road [76]. *Hu* [75] stressed that correct regeneration of road undulation is significant for laboratory analyses of dynamic tire forces, and suggested that a standard vehicle configuration in conjunction with realistic and consistent levels of excitation must be established to determine the suspension performance related to the tire loads.

Misoi et al [14, 15] investigated the road corrugation problem in view of vehicle dynamics and wheel-soil interactions. The effect of a developing road corrugation on the dynamics of a single *DOF* tire model was discussed based on a sinusoidal corrugation profile, and the study suggested that poorly damped vehicles should be avoided. The study further described the corrugation creation and their relation to soil properties and environmental effects such as rainfall. Pavement types, the mechanisms related to pavement deterioration and the role of environmental factors have been described in a *US Department of Transportation* study by *Jackson* [77].

The design of pavement structures, the role of traffic loads, vehicle configuration and static loads have been described by *Mahoney* [78]. The study proposed that the pavement design should be based on the concept of *Equivalent Single Axle Loads* (*ESAL*) rather than on economics, and/or local practices and materials.

The dynamic load coefficient (*DLC*), defined as the ratio of the *RMS* tire force to the mean tire force, has been most widely used to assess the effect of tire loads on the pavement damage. Many studies have reported that the *DLC* increases with the increasing road roughness, speed, tire inflation pressure and suspension stiffness [19,79], while the influence of roll mass moment of inertia of sprung and unsprung masses, roll center height, auxiliary roll stiffness, lateral suspension spread, track width, and cornering and longitudinal stiffness of tires, on the *DLC* is found to be relatively insignificant [80].

The pavement-vehicle interactions have been investigated through road tests and analysis of various vehicle models. An experimental study conducted to evaluate the interactions between dynamic axle loads of heavy vehicles and pavement roughness, concluded that there is no unique pavement statistic providing the best fit between pavement roughness and the dynamic axle load variations over the range of test vehicle

speeds [81]. *Todd* et al [16] evaluated the vehicle ride quality and tire forces using a quarter truck (2 *DOF*), half single unit truck (4 *DOF*) and half tractor-semitrailer (9 *DOF*) models. The study investigated the correlation between the results obtained using the different models but did not address the influence of vehicle design parameters on the ride quality and tire dynamic forces.

A comprehensive study on tire generated road damage and its relation to vehicle design was reported in [17]. The effect of truck suspension on pavement response was evaluated using a truck simulation package *VESYM* [82] in conjunction with a flexible pavement simulation package *VESYS* [83]. The analysis dealt mostly with passive suspensions and the effects of variations in damping and stiffness properties. The analysis was carried out based on the dynamic load coefficient (*DLC*) and present serviceability index (*PSI*). The performance characteristics of an active suspension scheme, based upon feedback from the tire forces, were also compared to those of a passive suspension. The study further mentioned the difficulties, related to tire forces measurement, in practical implementation of the scheme. The effects of suspension systems on other performance aspects, such as suspensions rattle space requirements, ride quality and cargo safety were not addressed.

From the truck manufacturer's view point, suspensions and tires were identified as the most important elements in the design process, when pavement life is to be taken into account [84]. Experimental studies [85] have confirmed that heavy vehicle suspensions can impose high dynamic loads on road surfaces and that the magnitudes of these loads vary considerably from one type of suspension to another. A reliable methodology to assess the pavement failure, however, does not yet exist due to the complex dynamics associated with the wheel-road interactions and the pavement structures. Although, considerable efforts have been made to derive assessment tools, the agreement between

theory and experiment is often unsatisfactory [86]. Concerns on the validity of the *Fourth Power* law, variations in the vehicle configurations, and climatic effects are some of the complicating factors that can result in underestimating pavement fatigue lives by a factor of 100 [86-88]. The damage caused by dynamic wheel loads is thus considered to be an area of high uncertainty [19]. It has been proposed, therefore, that various vehicle configurations should be classified based on the magnitudes of tire forces, represented by the dynamic load coefficients to assess their road damage potentials.

1.3 SCOPE OF THE THESIS

The overall objective of this thesis research is to contribute towards enhancement of driver- and road-friendliness of articulated freight vehicles through design of optimal active and passive suspension systems. The specific objective of the thesis research is to carry out an analytical investigation of passive and active suspension systems for articulated freight vehicles to achieve an improved compromise among the various conflicting design requirements identified in the previous section. The suspension systems are analyzed and optimized in view of a performance criteria comprising ride quality, cargo safety, suspension rattle space, and dynamic tire forces. Active suspension systems are further formulated to achieve a fail-safe design based on limited-state measurements, to reduce their associated cost and complexity, and to enhance their reliability. The particular objectives of the study are:

1. To develop a comprehensive mathematical model, for the most commonly used heavy vehicle configuration, to investigate the performance characteristics of suspension systems through computer simulation.

2. To incorporate realistic stochastic road undulation and time delay in the model development.
3. To formulate a performance index to assess different conflicting design requirements, such as ride quality, cargo safety, rattle space and dynamic tire forces.
4. To investigate the influence of stiffness and damping properties of a passive suspension on the vehicle performance characteristics using covariance analysis and frequency domain techniques.
5. To select "optimal" passive suspension stiffness and damping parameters to ensure a compromise among all the design objectives.
6. To formulate an ideal fail-safe active suspension scheme for the heavy vehicles.
7. To investigate the effects of variations in the actuator power supply, and variations in the stiffness and damping properties of the active suspension on the performance characteristics of the vehicle.
8. To select controller feedback gains and passive suspension properties to ensure a fail-safe and optimum performance of the active suspension system.
9. To develop a realistic active suspension control scheme that incorporates limited-state measurements and sensor noise in the design.
10. To assess the effects of sensor noise and limited-state measurement on the performance characteristics of the actively suspended heavy vehicle.
11. To investigate the effects of passive and active suspension schemes and vehicle parameter variations on the tire dynamic forces.

1.3.1 Layout of the Thesis

In Chapter 2, the most commonly used vehicle configuration is identified from the

reported survey on heavy vehicle population. A representative ride dynamic model of an articulated freight vehicle is formulated with an objective to assess the suspension system performance criteria comprising: ride quality, cargo safety, rattle space requirements and dynamic tire forces. The randomly distributed road roughness is characterized, and the time delays between the consecutive wheel-road contact points are incorporated using *Padé* approximation.

In Chapter 3, an "optimum" passive suspension is developed for the heavy vehicle. A performance criteria is formulated to assess the performance characteristics related to ride quality, cargo safety, rattle space requirements and dynamic tire forces. The validity of the mathematical vehicle model is asserted by comparing the analytical frequency response with the road measured data. A sensitivity analysis, based upon the covariance matrix of the state vector, is performed to select optimal suspension parameters. The method is quite efficient and specifically well suited for multi-parameter design optimization. The covariance matrix is employed to yield mean square values of the various performance indices, such as tractor and semitrailer bounce and pitch accelerations, suspension deflections, and dynamic tire loads. The effects of varying the damping and stiffness properties of the suspension on the frequency response characteristics are further investigated to verify the conclusions drawn from the covariance analysis.

In Chapter 4, *Linear Quadratic Gaussian* (*LQG*) control technique is employed to design an ideal active suspension scheme based on full-state feedback. The ideal active suspension scheme is formulated to minimize a quadratic performance measure that includes ride quality, cargo safety, suspension and tire dynamic deflections, and power requirements. The active suspension suggested is a parallel combination of passive elements and a feedback controlled force generator. Although an active suspension is often designed without the passive elements, the presence of the passive components

yields a fail-safe active suspension design that reduces the power requirements and enhances the reliability. While the design aspects are briefly addressed, the performance characteristics of the ideal active suspension are compared to those of the "optimum" passive suspension to determine their potential performance benefits.

In view of the extensive hardware and signal processing requirements, high cost and poor reliability of a full-state feedback active suspension design, a thorough analysis of a more realistic active suspension scheme, based on H_2 synthesis, is undertaken in Chapter 5. The assumption of full and perfect measurement of the states is relaxed in the design of the H_2 active suspension. The proposed active suspension system is analytically formulated incorporating the sensor signal noise in the output equation. A *Kalman* filter is incorporated to derive an optimum estimate of all the state variables. Two suspension schemes based upon limited-state measurements are investigated and the relevant design aspects such as actuator size, measurement noise intensity and its effect on the performance are addressed. The performance characteristics of the proposed suspension designs are compared to those of the full-state active suspension and the "optimum" passive suspension systems.

Chapter 6 presents a comprehensive investigation of the effects of the passive and various active suspension schemes on the dynamic tire forces. Road friendliness of heavy vehicles is assessed in terms of the *DLC*. Effects of the restoring and dissipative properties of the suspensions, road roughness, vehicle velocity, tire stiffness, semitrailer axle spacing and loading patterns are also investigated in view of *DLC*.

Finally, the conclusions and recommendations for future work are presented in Chapter 7.

1.4 REFERENCES

1. T. D. Gillespie, "*Heavy Truck Ride,*" SAE, SP-607, 1985.

2. G. Hu, "*Simulation of Heavy Truck Ride Using a Desktop Computer,*" SAE Trans., Paper No. 871557, 1987.

3. P. Michelberger and D. Szoke, "*Speed Dependent Vertical Vibrations of Elastic Vehicle Bodies,*" Int. J. Vehicle Design, 8(1) pp. 8-95, 1985.

4. J. I. Ribarits, J. Aurell and E. Andersers, "*Ride Comfort Aspects of Heavy Truck Design,*" SAE Tran., 781064 pp. 4046-4069, 1978.

5. A. R. Smith, "*Frame Bending, Fifth Wheel Location -Special Body Mounting and Loading Problems,*" SAE Special Report SR260, 1965.

6. K. N. Norman Jr. and F. Giannopoulos, "*Recent Advances in Analytical and Computational Aspects of Modeling Active and Passive Vehicle Suspensions,*" Computational Methods in Ground Transportation Vehicles, AMD-Vol. 50, ASME, 1982, pp. 75-115

7. E. K. Bender, D. C. Karnopp and I. L. Paul, "*On the Optimization of Vehicle Suspensions Using Random Process Theory,*" ASME 67-TRANS-12.

8. J. K. Hedrick, G. F. Billington and D. A. Dreesbach, "*Analysis Design and Optimization of High Speed Vehicle Suspensions Using State Variable Technique,*" Journal of Dynamic Systems, Measurements and Control, June 1974, pp. 193-203.

9. A. G. Thompson, "*Design of Active Suspensions,*" Proceedings of the Institute of Mechanical Engineers, Automobile Division, Vol. 185, 1970-71, pp. 36-71.

10. J. K. Hedrick, "*Some Optimal Control Techniques Applied to Suspension System Design,*" ASME 73-ICT-55.

11. J. R. Ellis , "*The Ride and Handling of Semitrailer Articulated Vehicle,*" Automobile Engineering, Vol. 26, 1966, pp. 141-161.

12. W. D. Walter, D. Gossard and P. Fensel, "*Truck Ride: a Mathematical and Empirical Study,*" SAE paper No. 690099, January 13-17, 1969.

13. A. B. Allan M. M. ElMadany and M. A. Dokainish, "*Articulated Vehicle Models,*" SAE Paper No. 801420, 1980.

14. G. K. Misoi and R. M. Carson, *"Corrugation of Unmetalled Roads, Part 1: Vehicle Dynamics,"* proceedings of the IMechE Vol. 203, 1989, pp. 205-214.

15. G. K. Misoi, F. G. Gichaga and R. M. Carson, *"Corrugation of Unmetalled Roads, Part 2: Wheel-Soil Interaction,"* proceedings of the IMechE Vol. 203, 1989, pp. 215-220.

16. K. B. Todd, B. T. Kulakowski, *"Simple Computer Models for Predicting Ride Quality and Pavement Loading of Heavy trucks,"* Transportation Research Record 1215, pp. 137-149.

17. J. K. Hedrick, K. Yi, *"The Effect of Alternative Heavy Truck Suspensions on flexible Pavement Response,"* presented at the Second International Symposium on Heavy Vehicle Weights and Dimensions Vol. 1, June 18-22, 1989, Kelowna British Columbia, Canada.

18. D. J. Cole, D. Cebon, *"Simulation and Measurement of Dynamic Tire Forces,"* presented at the Second International Symposium on Heavy Vehicle Weights and Dimensions Vol. 2, June 18-22, 1989, Kelowna British Columbia, Canada.

19. D. Cebon, *"Vehicle Generated Road Damage: A Review,"* Vehicle System Dynamics Vol. 18, 1989, pp. 107-150.

20. S. Rakheja et al., *"Ride Vibrations of Articulated Vehicles and Significance of Secondary Suspension,"* SAE 1989 Noise and Vib. Conf., SAE Publ. No. P-222, May 16-18, pp. 139-147.

21. R. D. Ervin and G. Yoram, *"The Influence of Weights and Dimensions on the Stability and Control of Heavy Duty Trucks in Canada,"* University of Michigan Transportation Research Institute, Report No. 86-35, July 1986.

22. J. B. Roberts, *"Response of Nonlinear Mechanical Systems to Random Excitation-Part 1: Markov Methods,"* Shock and Vibration Digest, Vol. 13, No. 4, 1981, pp. 17-28.

23. S. H. Crandall, *"Perturbation Techniques for Random Vibration of Nonlinear Systems,"* The Journal of the Acoustical Society of America, Vol. 35, No. 11, 1963, pp. 1700-1705.

24. J. B. Roberts, *"Response of Nonlinear Mechanical Systems to Random Excitation-Part 2: Equivalent Linearization and Other Methods,"* Shock and Vibration Digest, Vol. 13, No. 11, 1981, pp. 15-29.

25. T. K. Caughy, *"Equivalent Linearization Techniques,"* The Journal of the Acoustical Society of America, Vol. 35, No. 11, 1963, pp. 1706-1711.

26. N. C. Nigam, *Introduction to Random Vibration,* The MIT Press, Cambridge, Massachusetts, 1983.

27. S. Rakheja, *Computer Aided Dynamic Analysis and Optimal Design of Suspension Systems for Off-Road Tractors,* Ph.D. Thesis, Mechanical Engineering Department, Concordia University, 1983.

28. S. Rakheja, M. Van Vliet and S. Sankar, *"A Discrete Harmonic Linearization Technique for Simulation of Nonlinear Mechanical Systems,"* Journal of Sound and Vibration, 100(4), 1985, pp. 511-526.

29. K. M. Captain, A. B. Boghani and D. M. Wormley, *"Analytical Tire Models for Dynamic Vehicle Simulation,"* Vehicle System Dynamics, Vol. 8, pp. 1-32, 1979.

30. D. C. Creighton, *"Revised Vehicle Dynamic Module: User's Guide for Computer Program VEHDYN II,"* Research Note No. SL-86-9, U.S. Army Engineer Waterways Experiment Station, Vicksburg, Miss., May 1986.

31. D. J. Cole and D. Cebon, *"Simulation and Measurement of Vehicle Response to Road Roughness,"* Proc. Inst. Acoustics, Vol. 10, Part 2, 1988.

32. A. Hac, "*Suspension Optimization of a 2-DOF Vehicle Model Using Stochastic Optimal Control Technique,*" Journal of Sound and Vibration, 100(3), 1985, pp. 343-357.

33. D. Bastow, "*Car Suspension and Handling,*" Pentech Press, London, 1987.

34. R. S. Sharp and D. A. Crolla, "*Road Vehicle Suspension Design-a Review,*" Vehicle System Dynamics, 16, 1987, pp. 167-192.

35. D. Hrovat M. Hubbard, "*Optimal Vehicle Suspensions Minimizing RMS Rattle Space, Sprung Mass Acceleration and Jerk,*" Trans. ASME Journal of Dynamic Systems, Measurement and Control, 103, September 1981, pp. 228-236.

36. D. A. Wilson R. S. Sharp and S. A. Hassan, "*The Application of Linear Optimal Control Theory to the Design of Active Automotive Suspension,*" Vehicle System Dynamics, 15, 1986, pp. 105-118.

37. Society of Automotive Engineers, *"Measurement of Whole Body Vibration of the Seated Operator of Agricultural Equipment,"* SAE Handbook, J1013.

38. D. B. Van Deussen, *"Human Response to Vehicle Vibration,"* SAE Trans., Vol. 77, No. 1, pp. 328-345, 1968.

39. D. E. Goldmann, *"A Review of Subjective Responses to Vibratory Motion of the Human Body in the Frequency Range 1 to 70 cps,"* Naval Med. Res. Institute, Report No. 4, March 1948.

40. International Organization for Standardization, "*Guide for Evaluation of Human Exposure to Whole Body Vibration,"* ISO 2631, 1974(E).

41. R. M. Chalasani, *"Ride Performance Potential of Active Suspension Systems-Part I: Simplified Analysis Based on a Quarter Car Model,"*. 1986 ASME Winter Annual Meeting, AMD-Vol. 80, pp. 187-204.

42. R. M. Chalasani, *"Ride Performance Potential of Active Suspension Systems-Part II: Comprehensive Analysis Based on a Full Car Model,"* 1986 ASME Winter Annual Meeting,, AMD-Vol. 80, pp. 205-234.

43. R. Karadayi and G. Y. Masada, *"A Nonlinear Shock Absorber Model,"* Proc. of the 1988 ASME Winter Annual Meeting.

44. E. Saibel and M. C. C. Tsao, "*Dynamics of Pneumatic Tire Vehicles with Connected Suspension Systems,"* Vehicle System Dynamics, Vol. 1, pp. 89-102, 1972.

45. S. Rakheja and J. Woodrooffe, *"Role of Suspension Damping in Enhancement of Road Friendliness of Heavy Vehicles,"* to be published in Heavy Vehicle Systems, Int. J. of Veh. Design, 1995.

46. S. Rakheja and J. Woodrooffe, *"Study of an Axle Vibration Absorber to Reduce the Dynamic Pavement Loads Caused by Heavy Vehicles,"* (Paper not yet published).

47. D. Cebon, *"Heavy Vehicle Vibration-a Case Study,"* Proc. 9th IAVSD symposium on The Dynamics of Vehicles on Roads and on Tracks, Linkoping, Swets and Zeitlinger, 1985.

48. D. J. Cole and D. Cebon, *"Validation of an Articulated Vehicle Simulation,"* Vehicle System Dynamics, 21, 1992, pp. 197-223.

49. G. Hu, *"Simulation of Heavy Truck Ride Using a Desktop Computer,"* SAE Trans. 1987, paper No. 871557.

50. N. Sakuma et al., *"Heavy Duty Truck Ride Comfort Analysis by Computer Simulation,"* Int. J. Veh. Des., 1986, pp. 279-290.

51. D. B. Van Deussen, *"Truck Suspension System Optimization,"* SAE Trans., 1971, paper No. 710222.

52. A. E. Duncan, *"Application of Model Modeling and Mount System Optimization to Light Duty Truck Ride Analysis,"* SAE paper No. 811313, 1981,

53. M. M. ElMadany and M. E. Samaha, *"Optimum Response of a Stochastic Model of a Tractor-Semitrailer Vehicle-Part 1: Linear and Nonlinear Models of a Passively Suspended Vehicle,"* The 1989 ASME Design Technical Conferences, 12th Biennial Conference on Mechanical Vibration and Noise, Montreal, Quebec, Canada. September 12-21, 1989, pp. 167-175.

54. R. E. Allen, *"Cab Isolation and Ride Quality,"* SAE. paper No. 750165, 1975

55. M. M. ElMadany, *" A Procedure for Optimization of Truck Suspensions,"* Vehicle System Dynamics, 16(1987), pp. 297-312.

56. A. G. Thompson, *"Quadratic Performance Indices and Optimal Suspensions Design,"* Proc. Inst. of Mechanical Engineers, Vol. 187, No. 4, 1973, pp. 129-139.

57. D. R. Guenther and C. T. Leondes, *"Synthesis of a High-Speed Tracked Vehicle Suspension System. Part I: Problem Statement, Suspension Structure and Decomposition, and Part 2: Definition and Solution of the Control Problem"* IEEE Trans. on Automatic Control, Vol. AC-22, No. 42, 1977, pp. 158-172.

58. P. K. Sinha, D . N. Wormley and J. K. Hedrick, *"Rail Passenger Vehicle Lateral Dynamic Performance Improvement Through Active Control,"* ASME Journal of Dynamic Systems, Measurement and Control, Vol. 100, Dec. 1978, pp. 270-283.

59. A. G. Thompson, *"Optimal and Suboptimal Linear Active Suspension for Road Vehicles,"* Vehicle System Dynamics, Vol. 13, No. 2, 1984, pp. 61-72.

60. F. Oueslati and S. Sankar, *"Performance of a Fail-Safe Active Suspension with Limited State Feedback for Improved Ride Quality and Reduced Pavement Loading in Heavy Vehicles,"* 1992 Truck & Bus Meeting & Exposition Toledo, Ohio.

61. F. Oueslati, S. Sankar and A. K. W. Ahmed, *"Limited-State Active Suspension for Improved Ride Quality in Rail Vehicles Subjected to Vertical Track Irregularities,"* The International Symposium on Technological Innovation in Guided Transportation, Sep. 28-30, 1993, Lille, France.

62. D. G. Stephens, *"Comparative Vibration Environment of Transportation Vehicles,"* Passenger Vibration in Transportation Vehicles, ASME AMD, Vol. 24, 1979, pp. 59-72.

63. A. Hac, *"Adaptive Control of Vehicle Suspension,"* Vehicle System Dynamic, Vol. 16, 1987, pp. 57-74.

64. A. G. Ulsoy, D. Hrovat, *"Stability Robustness of LQG Active Suspensions,"* ACC, San Diego, California, May 23-25, 1990, pp. 61-72.

65. C. Walvoord and J. K. Hedrick, *"Active Control of Vehicle Ride and Handling,"* ASME Transaction, Advanced Automotive Technologies, DE-Vol. 40, 1991, pp. 303-314.

66. L. Magnus, *"Dynamic Leveling for Ground Vehicles,"* Ph.D. Thesis, Department of Machine Elements, Royal Institute of Technology, S-100 Stockholm, Sweden, 1990, pp. 42-49.

67. H. Kwakernaak and R. Sivan, *"Linear Optimal Control Systems,"* Wiley-Interscience, 1972.

68. A. G. Thompson *"An Active Suspension With Optimal Linear State Feedback,"* Vehicle System Dynamic, Vol. 5, 1976, pp. 187-203.

69. A. G. Thompson, B. R. Davis and F. J. M. Salzborn, *"Active Suspensions with Vibration Absorbers and Optimal Output Feedback Control,"* SAE paper No. 841253, 1984.

70. T. Yoshimura, N. Ananthanarayana and D. Deepak, *"An Active Vertical Suspension for Track/Vehicle Systems,"* J. Sound and Vibration, Vol. 106, No. 2, 1986, pp. 103-1128.

71. D. Metz and J. Maddock, *"Optimal Ride Height Control for Championship Race Car,"* Automatica, Vol. 22, No. 5, 1986, pp. 509-520.

72. A. A. Alexandridis and T. R. Weber, *"Active Vibration Isolation of Truck Cabs,"* Proceedings of the American Control Conference, June 1984, pp. 1199-1208.

73. M. M. ElMadany, *"Stochastic Optimal Control of Highway Tractors With Active Suspensions,"* Vehicle System Dynamics, Vol. 17, 1988, pp. 193-210.

74. R. Kashani and S. Kiriczi, *"Robust Stability Analysis of LQG-Controlled Active Suspension With Model Uncertainty Using Structured Singular Value μ Method,"* Vehicle System Dynamics, Vol. 21 No. 6, 1992, pp. 361-384.

75. G. Hu, *"Use of Road Simulator for Measuring Dynamic Wheel Loads,"* SAE Special Publication SP-765, paper No. 881194, Nov. 1988.

76. C. J. Dodds, *"The Laboratory Simulation of Vehicle Service Stress,"* Journal of Engineering for Industry, May 1974, pp. 391-398.

77. N. C. Jackson, *"Pavement Performance-A State DOT Perspective,"* SAE Special Publication SP-765, paper number 881843 Nov. 1988.

78. J. P. Mahoney, *"The relationship Between Axle Configurations, Wheel Loads and Pavement Structure,"* SAE Special Publication SP-765, paper number 881844, Nov. 1988.

79. A. N. Heath and M. C. Good, *"Heavy Vehicle Design Parameters and Dynamic Pavement Loading,"* Australian Road research, 1985, 15(4).

80. Lin, Wn-Kan, Chen, Yen-Cheng, Kulakowski, T. Bohdan, A. Donald, *"Dynamic Wheel/Pavement Force Sensitivity to Variations in Heavy Vehicle Parameters, Speed and Road Roughness,"* Heavy Vehicle Systems, Special Series, Int. J. of Vehicle Design, 1994, 1(2), 139-155.

81. A. T. Papagiannakis and J. H. F. Woodrooffe, *"Suitability of Alternative Pavement Roughness Statistics to Describe Dynamic Axle Loads of Heavy Vehicles,"* Proceedings of the 2nd International Symposium of Heavy Vehicle Weights and Dimensions, June 18-22, 1989, Kelowna B. C.

82. J. K. Hedrick et al., *"The Simulation of Vehicle Dynamic Effects on Road Pavements,"* Final Report, USDOT office of University Research/FHWA, June 1989.

83. *"Predictive Design Procedures VESYS Users Manual,"* Federal Highway Administration, Project 5C, January 1978.

84. L. W. Orr, *"Truck Pavement Factors-The Truck Manufacturer's Viewpoint,"* SAE Special Publication SP-765, paper number 881842, Nov. 1988.

85. J. H. F. Woodrooffe, P. A. LeBlanc and A. T. Papagiannakis, *"Suspension Dynamics-Experimental Findings and Regulatory Implications,"* SAE paper No. 881847, 1988.

86. E. N. Thrower, *"A Parametric Study of a Fatigue Prediction Model for Bituminous Road Pavements,"* TRRL Report LR892, 1979.

87. K. R. Peattie, *"Flexible of Pavement Design Ch. 1. Development in Highway Pavement Engineering,"* Applied Science Publishers Ltd., London 1978.

88. P. Ulliditz and C. Busch, *"Mathematical Models for Predicting Pavement Performance,"* Transp. Res. Rec. 949. TRB, 1983, pp. 32-44

CHAPTER 2

VEHICLE MODEL AND ROAD CHARACTERIZATION

2.1 INTRODUCTION

A study of ride dynamics and pavement interaction of a freight vehicle involves development or selection of a representative dynamic model that closely describes the vehicle behavior. Many analytical and experimental studies on vehicle ride have been reported in the literature. The primary objectives of these studies, in general, include assessment of vehicle ride quality, performance of different vehicle suspensions, cargo vibrations, etc. Ride dynamic models of articulated freight vehicles, reported in the literature vary from a simple two-dimensional 3 degrees-of-freedom (*DOF*) to a comprehensive three-dimensional 19 *DOF* models [1-3]. In recent years, these analytical models have been further employed to study the dynamic wheel loads transmitted to the pavement [4-7]. Various studies on dynamic ride and vehicle-pavement interactions have concluded that contributions of the roll-plane dynamics of highway vehicles are insignificant [8]. The vehicle ride quality and the dynamic wheel loads are strongly related to the pitch and vertical deflection modes of the sprung and unsprung masses. An analogy between the vehicle ride and pavement interactions has been further derived based on their

strong dependence upon the vehicle vibration modes [9,10]. Results of these studies have demonstrated that in-plane models can predict the ride dynamic behavior reasonably well.

Although vehicle models with large number of *DOF* provide comprehensive insight into the dynamic behavior of the vehicle, in-plane vehicle models with reduced *DOF* are known to yield reasonably accurate estimate of dynamics associated with vehicle ride and vehicle-pavement interaction. Vehicle models of reduced size are particularly desirable when optimization studies need to be performed. In this study, an articulated freight vehicle is characterized by a 9 *DOF* dynamical system, while neglecting the contributions due to roll dynamics. Freight vehicle vibration primarily originate at the tire-road interface, and hence the ride behavior of the vehicle is greatly influenced by the highway profile. While a qualitative analysis of the ride performance of vehicle suspensions may be conveniently carried out using simplistic sinusoidal representation of the road profile, a comprehensive road characterization is necessary to closely predict the vehicle ride response to realistic road profiles. An analytical characterization of the randomly irregular road surface is, thus, undertaken to analyze the ride and pavement load response characteristics in a quantitative manner.

2.2 BASELINE MODEL OF A HEAVY VEHICLE

A large number of commercial vehicle configurations, such as straight trucks, tractor-semitrailers, tractor-trailers and B-trains are used in highway transportation of freight. The percentage population of various vehicle combinations used across Canada is summarized in Table 2.1 [11]. The results of the survey, presented in the table, reveal that approximately 77% of all heavy vehicles operating in Canada are tractor-semitrailers with a tandem or tri-axle semitrailer. In this study, a tractor-semitrailer is selected as the candidate vehicle for model development and analysis. The *DOF* of the analytical model

directly relate to its complexity and ability to predict the dynamic response. The *DOF* and thus the complexity of the model is further related to the objectives of the analysis. Four primary concerns that evolve from suspension design formulate the objectives for the performance analysis, which include: *(i)* the level of vibration perceived by the passenger/driver, which can be related to the acceleration response at the tractor center of gravity (*CG*) [12-14]; *(ii)* cargo safety, which can be related to the bounce and pitch accelerations at the semitrailer *CG*; *(iii)* suspension deflections, which are indication of the working or rattle space requirements [15]; and *(iv)* tire deflections, which are an indication of the severity of forces transmitted to the roads [14,16]. A tractor-semitrailer model that is not very complex but realistic enough to allow for the study of these aspects can be represented by an in-plane 9 *DOF* dynamic model, as shown in Figure 2.1. This model allows for the study of the tractor and semitrailer motions as well as the suspension and tire deflections, while neglecting contributions due to roll dynamics.

The model comprises the tractor and semitrailer sprung masses each with bounce and pitch *DOF*. Assuming rigid cab mounts, the cab and chassis of the tractor are lumped together and represented by the sprung mass m_{s1}. The tractor is, thus, represented by a planar rigid body supported by three axle suspensions, as shown. Assuming the cargo is rigidly attached, the semitrailer is modeled by a planar rigid body m_{s2} and is assumed to have two independent axles. The drive and semitrailer axles are represented by independent axle suspensions assuming that the couplings contribute primarily to the higher frequency vibration. Furthermore, the independent axle suspension representation closely relates to current tridem configurations of the semitrailer. Since the modern trends in freight transportation are inclined towards tridem and quad-axle semitrailers, the proposed analytical model can be effectively used to characterize these configurations. The lumped unsprung mass of each wheel and axle assembly is represented by m_{ui} with only vertical *DOF*. Each axle suspension is represented by a linear spring and a viscous damper

in parallel. These passive elements will be supplemented by active actuators when dealing with active suspensions. The vertical compliance of the fifth wheel is modeled as a parallel combination of a spring and a damper constrained to move along the vertical direction. The elastic property of each tire is characterized by a linear stiffness element, K_{ti}, assuming point contact with the road and negligible wheel hop motion. The suspension stiffness and damping elements as well as the tire stiffness coefficients are assumed to be linear. Although passive vehicle suspension, invariably, exhibit progressively hardening force-deflection and variable force-velocity properties, the linear suspension parameters yield significant insight into vehicle response behavior with relatively simple analysis. The tractor and semitrailer pitch motions are assumed to be small and hence first order approximations are considered for the derivation of the equations of motion. The numerical parameters for the baseline model, along with the range of values for the suspension stiffness and damping rates, are listed in Table 2.2 [6,11]. Freight vehicles employ different designs of vehicle suspension with varying values of equivalent stiffness and damping coefficients. Published studies on suspension parameters are reviewed to identify the ranges of suspension parameters listed in Table 2.2. The identified ranges of suspension parameters serve as a guideline for selection of optimal parameters presented in the following chapter.

The effects of the frame bending are neglected assuming that the corresponding motions imposed on the axles are quite small relative to motions caused by the sprung and unsprung mass rigid body vibration. Although the frame bending vibration of a semitrailer are known to be significant, the location of suspensions near the nodes diminishes their contributions [17-21].

Table 2.1 Percent population of the various heavy vehicle combinations present in various centers across Canada [11]

Vehicle Combination	*Vancouver*	*Calgary*	*Winnipeg*	*Toronto*	*Montreal*	*Monition*
Tractor-semitrailer	60	80	60	70	90	98
A-Doubles	32	8	25		8	1
B-Doubles	8	10	14	5	2	1
C-Doubles	0	< 2	< 1	< 1	< 1	0
Triples	0	< 1	< 1	0	< 1	0

Table 2.2 List of parameters for the baseline model along with ranges of suspension parameters [6,11].
(Based on half-a-vehicle)

Description of the Parameter	*Parameter Value/Range*
Tractor mass (m_{s1})	2,000.0 kg
Tractor pitch moment of inertia (I_{y1})	10,000.0 $kg.m^2$
Tractor front tire and axle assembly mass (m_{u1})	270.0 kg
Tractor leading rear tire and axle assembly mass (m_{u2})	520.0 kg
Tractor trailing rear tire and axle assembly mass (m_{u2})	520.0 kg
Semitrailer mass (m_{s2})	14,000.0 kg
Semitrailer pitch moment of inertia (I_{y2})	300,000.0 $kg.m^2$
Semitrailer leading tire and axle assembly mass (m_{u3})	340.0 kg
Semitrailer trailing tire and axle assembly mass (m_{u3})	340.0 kg
Tractor front suspension stiffness (K_1)	10,000.0 to 510,000.0 N/m
Tractor front suspension damping coefficient (C_1)	9,000.0 to 59,000 $N.s/m$
Tractor leading rear axle suspension stiffness (K_2)	10,000.0 to 510,000.0 N/m
Tractor leading rear axle suspension damping coefficient (C_2)	9,000.0 to 59,000 $N.s/m$
Tractor trailing rear axle suspension stiffness (K_2)	10,000.0 to 510,000.0 N/m
Tractor trailing rear axle suspension damping coefficient (C_2)	9,000.0 to 59,000 $N.s/m$
Semitrailer leading axle suspension stiffness (K_3)	10,000.0 to 510,000.0 N/m
Semitrailer leading axle suspension damping coefficient (C_3)	9,000.0 to 59,000.0 $N.s/m$
Semitrailer trailing axle suspension stiffness (K_3)	10,000.0 to 510,000.0 N/m
Semitrailer trailing axle suspension damping coefficient (C_3)	9,000.0 to 59,000.0 $N.s/m$

Table 2.2 Continued...

Description of the parameter	*Parameter Value/Range*
Tractor front tire stiffness (K_{t1})	788,000.0 *N/m*
Tractor leading rear axle tire stiffness (K_{t2})	1,576,000.0 *N/m*
Tractor trailing rear axle tire stiffness (K_{t2})	1,576,000.0 *N/m*
Semitrailer leading axle tire stiffness (K_{t3})	1,576,000.0 *N/m*
Semitrailer trailing axle tire stiffness (K_{t3})	1,576,000.0 *N/m*
Fifth wheel stiffness (K_5)	20,000,000.0 *N/m*
Fifth wheel damping coefficient (C_5)	200,000.0 *N.s/m*
Distance from tractor CG to tractor steer axle (A_1)	1.5 *m*
Distance from tractor CG to tractor first drive axle (B_1)	2.8 *m*
Distance from tractor CG to tractor second drive axle (B_2)	4.5 *m*
Distance from tractor CG to fifth wheel (B_5)	3.0 *m*
Distance from semitrailer CG to fifth wheel (A_2)	6.0 *m*
Distance from semitrailer CG to semitrailer first axle (B_3)	5.6 *m*
Distance from semitrailer CG to semitrailer second axle (B_4)	6.8 *m*

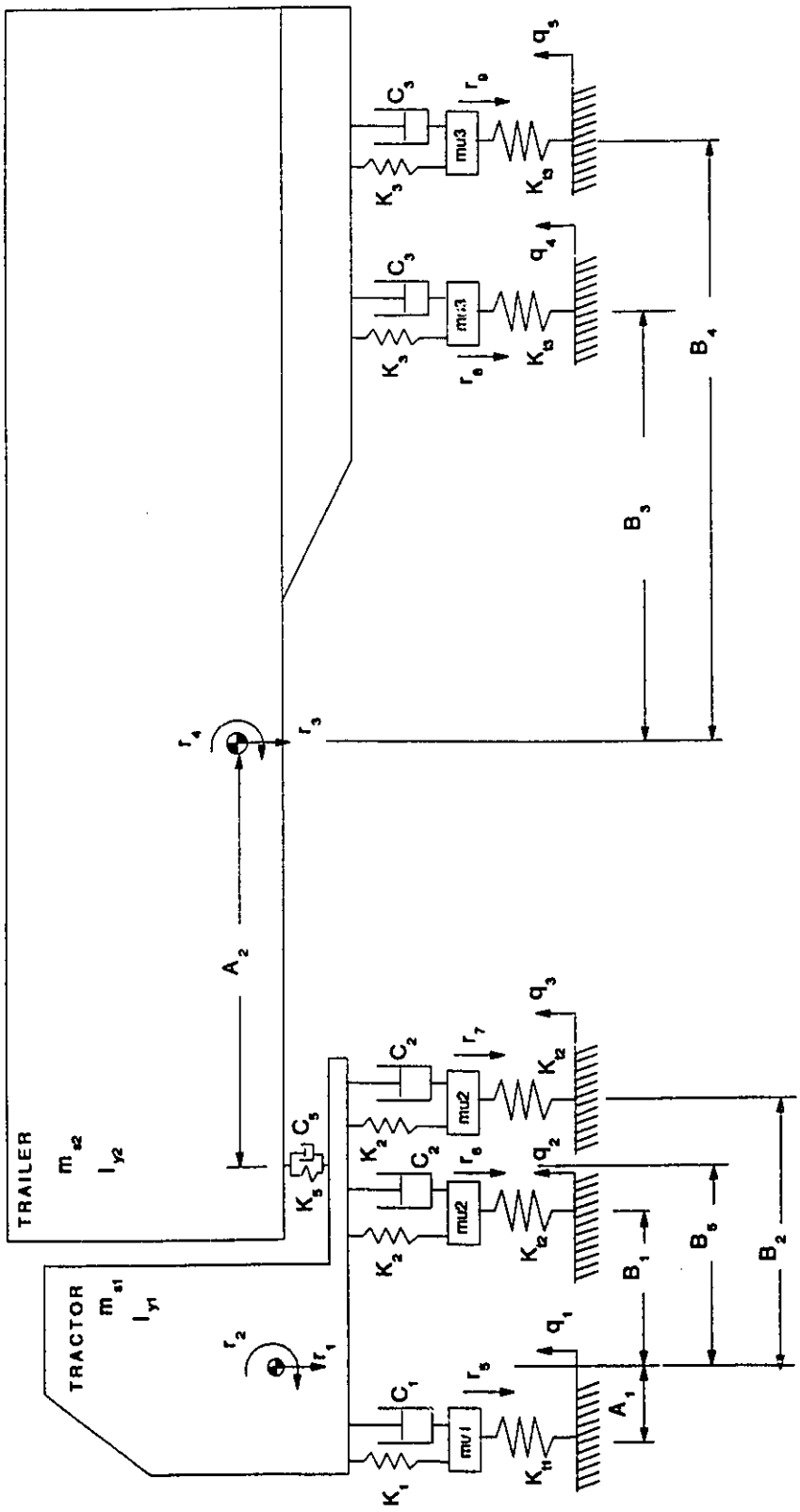

Figure 2.1 Baseline tractor-semitrailer model

2.2.1 Equations of Motion

Assuming linear behavior of all elements and small angular displacements, the following set of second order coupled differential equations characterizing the ride dynamics of the baseline vehicle model are obtained;

Vertical motion of the tractor sprung mass:

$$\begin{aligned} & m_{s1}\ddot{r}_1 + \\ & C_1(\dot{r}_1 + A_1\dot{r}_2 - \dot{r}_5) + C_2(2\dot{r}_1 - B_1\dot{r}_2 - \dot{r}_6 - B_2\dot{r}_2 - \dot{r}_7) + C_5(\dot{r}_1 - B_5\dot{r}_2 - \dot{r}_3 - A_2\dot{r}_4) + \\ & K_1(r_1 + A_1r_2 - r_5) + K_2(2r_1 - B_1r_2 - r_6 - B_2r_2 - r_7) + K_5(r_1 - B_5r_2 - r_3 - A_2r_4) \\ & = 0 \end{aligned} \tag{2.1a}$$

Pitch motion of the tractor sprung mass:

$$\begin{aligned} & I_{y1}\ddot{r}_2 + C_1A_1(\dot{r}_1 + A_1\dot{r}_2 - \dot{r}_5) + C_2[B_1(\dot{r}_1 - B_1\dot{r}_2 - \dot{r}_6) + \\ & B_2(\dot{r}_1 - B_2\dot{r}_2 - \dot{r}_7)] - C_5B_5(\dot{r}_1 - B_5\dot{r}_2 - \dot{r}_3 - A_2\dot{r}_4) + \\ & K_1A_1(r_1 + A_1r_2 - r_5) + K_2[B_1(r_1 - B_1r_2 - r_6) + \\ & B_2(r_1 - B_2r_2 - r_7)] - K_5B_5(r_1 - B_5r_2 - r_3 - A_2r_4) = 0 \end{aligned} \tag{2.1b}$$

Vertical motion of the semitrailer sprung mass:

$$\begin{aligned} & m_{s2}\ddot{r}_3 + \\ & C_3(\dot{r}_3 - B_3\dot{r}_4 - \dot{r}_8 + \dot{r}_3 - B_4\dot{r}_4 - \dot{r}_9) + C_5(\dot{r}_3 + A_2\dot{r}_4 - \dot{r}_1 + B_5\dot{r}_2) + \\ & K_3(r_3 - B_3r_4 - r_8 + r_3 - B_4r_4 - r_9) + K_5(r_3 + A_2r_4 - r_1 + B_5r_2) = 0 \end{aligned} \tag{2.1c}$$

Pitch motion of the semitrailer sprung mass:

$$\begin{aligned} & I_{y2}\ddot{r}_4 - C_3[B_3(\dot{r}_3 - B_3\dot{r}_4 - \dot{r}_8) + B_4(\dot{r}_3 - B_4\dot{r}_4 - \dot{r}_9)] + \\ & C_5A_2(\dot{r}_3 + A_2\dot{r}_4 - \dot{r}_1 + B_5\dot{r}_2) - K_3[B_3(r_3 - B_3r_4 - r_8) + \\ & B_4(r_3 - B_4r_4 - r_9)] + K_5A_2(r_3 + A_2r_4 - r_1 + B_5r_2) = 0 \end{aligned} \tag{2.1d}$$

Vertical motion of axle 1:

$$m_{u1}\ddot{r}_5 + C_1(\dot{r}_5 - \dot{r}_1 - A_1\dot{r}_2) + K_1(r_5 - r_1 - A_1 r_2) + K_{t1}r_5 = K_{t1}q_1 \qquad (2.1e)$$

Vertical motion of axle 2:

$$m_{u2}\ddot{r}_6 + C_2(\dot{r}_6 - \dot{r}_1 + B_1\dot{r}_2) + K_2(r_6 - r_1 + B_1 r_2) + K_{t2}r_6 = K_{t2}q_2 \qquad (2.1f)$$

Vertical motion of axle 3:

$$m_{u2}\ddot{r}_7 + C_2(\dot{r}_7 - \dot{r}_1 + B_2\dot{r}_2) + K_2(r_7 - r_1 + B_2 r_2) + K_{t2}r_7 = K_{t2}q_3 \qquad (2.1g)$$

Vertical motion of axle 4:

$$m_{u3}\ddot{r}_8 + C_3(\dot{r}_8 - \dot{r}_3 + B_3\dot{r}_4) + K_3(r_8 - r_3 + B_3 r_4) + K_{t3}r_8 = K_{t3}q_4 \qquad (2.1h)$$

Vertical motion of axle 5:

$$m_{u3}\ddot{r}_9 + C_3(\dot{r}_9 - \dot{r}_3 + B_4\dot{r}_4) + K_3(r_9 - r_3 + B_4 r_4) + K_{t3}r_9 = K_{t3}q_5 \qquad (2.1i)$$

2.3 DESCRIPTION OF ROAD UNDULATIONS

The ride vibrations of a road vehicle, primarily, originate from the random road undulations. The vehicle ride and dynamic wheel load response characteristics are directly related to the road roughness. The evaluation of the vehicle suspension performance thus necessitates a description of the road roughness.

Road roughness, characterizing the random deviations in road elevation resulting from practical limits on precision to which the road surface can be constructed and maintained, acts as a vertical displacement excitation to the wheel and tire assemblies, resulting in highly complex vibration of the vehicle. It has been established that road profiles, described by stationary *Gaussian* random functions with zero mean, can be mathematically characterized by their *PSD* [22]. These excitations are, evidently, dependent on the road roughness and the vehicle speed v. Road irregularities can be characterized in terms of the temporal angular frequency ω by a single sided power spectral density, Φ_q, of the form [23]:

$$\Phi_q(\omega) = \frac{2\alpha v\sigma^2}{\pi(\alpha^2 v^2 + \omega^2)} \tag{2.2}$$

where α is a coefficient that depends on the roughness of road irregularities and σ^2 is the variance of road irregularities. Table 2.3 illustrates the values of α and σ for asphalt and concrete highways [23].

Table 2.3 Roughness parameters for asphalt and concrete roads [23].

Type of road	α *(1/m)*	σ *(m)*
Asphalt *(smooth)*	0.15	0.0033
Concrete *(medium rough)*	0.20	0.0056
Concrete *(rough)*	0.40	0.0120

EQ (2.2) yields a reasonably good approximation of the actual road spectra as illustrated in Figure 2.2. The spatial displacement spectral densities, $\Phi_s(\Omega)$, of various measured road profiles [24] are compared to those derived from EQ (2.2). The spatial displacement *PSD* and spatial frequency Ω *(1/m)* are related to the temporal *PSD* and temporal frequency ω *(rad/s)* in the following manner:

$$\Phi_q(\omega) = \frac{\Phi_s(\Omega)}{v}, \quad \text{and} \quad \omega = \Omega v \tag{2.3}$$

The temporal *PSD* of the elevation of the three different roads are shown in Figure 2.3. The *PSD* of road elevation tends to increase with increase in vehicle speed beyond a certain frequency that depends on the road type. While the *PSD* of road profiles is strongly dependent upon road type and vehicle speed, the magnitude of the *PSD*, in general, decreases considerably at higher frequencies. The road profiles exhibit larger deviations corresponding to low frequencies or long wavelengths, and the magnitude of deviations decreases significantly corresponding to short wavelengths.

2.3.1 Synthesis of Road Roughness

While all the wheel-road contact points of a multiple wheeled vehicle are subject to identical road profile, the cross-correlation among the inputs is dependent upon the time lapses between the various tire-road contact points. The road roughness model is thus formulated with appropriate consideration of the time delays between the first and subsequent tire-road contact points. This can be accomplished by expressing the input at the first wheel in a state space format and representing the time delay between subsequent inputs by *Padé* approximation. The resulting first order state space format of the road excitation can be conveniently combined with the equations of motion of the vehicle.

The road roughness characterized by a stationary *Gaussian* random excitation, can be realized from a white noise signal passed through a first order filter. The *PSD* of the road excitation $\Phi_q(\omega)$ at the first wheel can be generated by passing a white noise process, ξ, with covariance $E[\xi(t)\xi(\tau)] = 2\alpha v\sigma^2\delta(t-\tau)$, through a first order filter of the form:

$$\dot{q}_1 = -\alpha v q_1 + \xi_1 \tag{2.4}$$

where $\delta(t-\tau)$ is the *Dirac delta function* and q_1 is the road elevation at the first wheel.

A vehicle traversing a road is subjected to random road input at all the wheel-road contact points. Assuming constant vehicle velocity and rigid pavement, the excitation at the second tire-road contact point is identical to that encountered at the first contact point with the exception of the time delay, which is related to the vehicle speed. The roughness excitation encountered at the subsequent contact points may thus be expressed as:

$$q_{n(s)} = e^{-s\Delta_n} q_1 \quad n = 2,\ldots,5 \tag{2.5}$$

where Δ_n is the time delay between the first and the n^{th} wheel. The time delay can be represented by a first order *Padé* approximation. The transfer function of the first order *Padé* approximation is given in the frequency domain by [25]:

$$\frac{q_n}{q_1} = e^{-s\Delta_n} \approx \frac{2-\Delta_n s}{2+\Delta_n s} \tag{2.6}$$

The road roughness encountered at the n^{th} tire-road contact point can, thus, be derived from the following:

$$\dot{q}_n = -\dot{q}_1 + \frac{2}{\Delta_n}(\dot{q}_1 - \dot{q}_n) \tag{2.7}$$

where $\dot{q}_1$ is given by EQ (2.4). For the five-wheeled vehicle considered in this study, the tire-road excitation can be expressed in the following matrix from:

$$\begin{bmatrix} \dot{q}_1 \\ \dot{q}_2 \\ \dot{q}_3 \\ \dot{q}_4 \\ \dot{q}_5 \end{bmatrix} = \begin{bmatrix} -\alpha v & 0 & 0 & 0 & 0 \\ \alpha v + 2/\Delta_2 & -2/\Delta_2 & 0 & 0 & 0 \\ \alpha v + 2/\Delta_3 & 0 & -2/\Delta_3 & 0 & 0 \\ \alpha v + 2/\Delta_4 & 0 & 0 & -2/\Delta_4 & 0 \\ \alpha v + 2/\Delta_5 & 0 & 0 & 0 & -2/\Delta_5 \end{bmatrix} \begin{bmatrix} q_1 \\ q_2 \\ q_3 \\ q_4 \\ q_5 \end{bmatrix} + \begin{bmatrix} 1 \\ -1 \\ -1 \\ -1 \\ -1 \end{bmatrix} \xi \tag{2.8}$$

or:

$$\dot{\boldsymbol{q}} = \boldsymbol{A}_q \boldsymbol{q} + \boldsymbol{B}_q \xi \tag{2.9}$$

where $\boldsymbol{A}_q \in \mathbb{R}^{5\times5}$, and $\boldsymbol{B}_q \in \mathbb{R}^{5\times1}$. In the absence of correlation between the road disturbance signals at the different tire-road contact points, the matrices $\boldsymbol{A}_q$ and $\boldsymbol{B}_q$ are

expressed as:

$$A_q = -\alpha \upsilon I, \text{ and } B_q = I \tag{2.10}$$

where I is the identity matrix. Moreover a vector of five time-delayed white noise inputs, ξ^*, will replace the single white noise input ξ:

$$\xi^* = \{\xi_1, \xi_2, \xi_3, \xi_4, \xi_5\}' \tag{2.11}$$

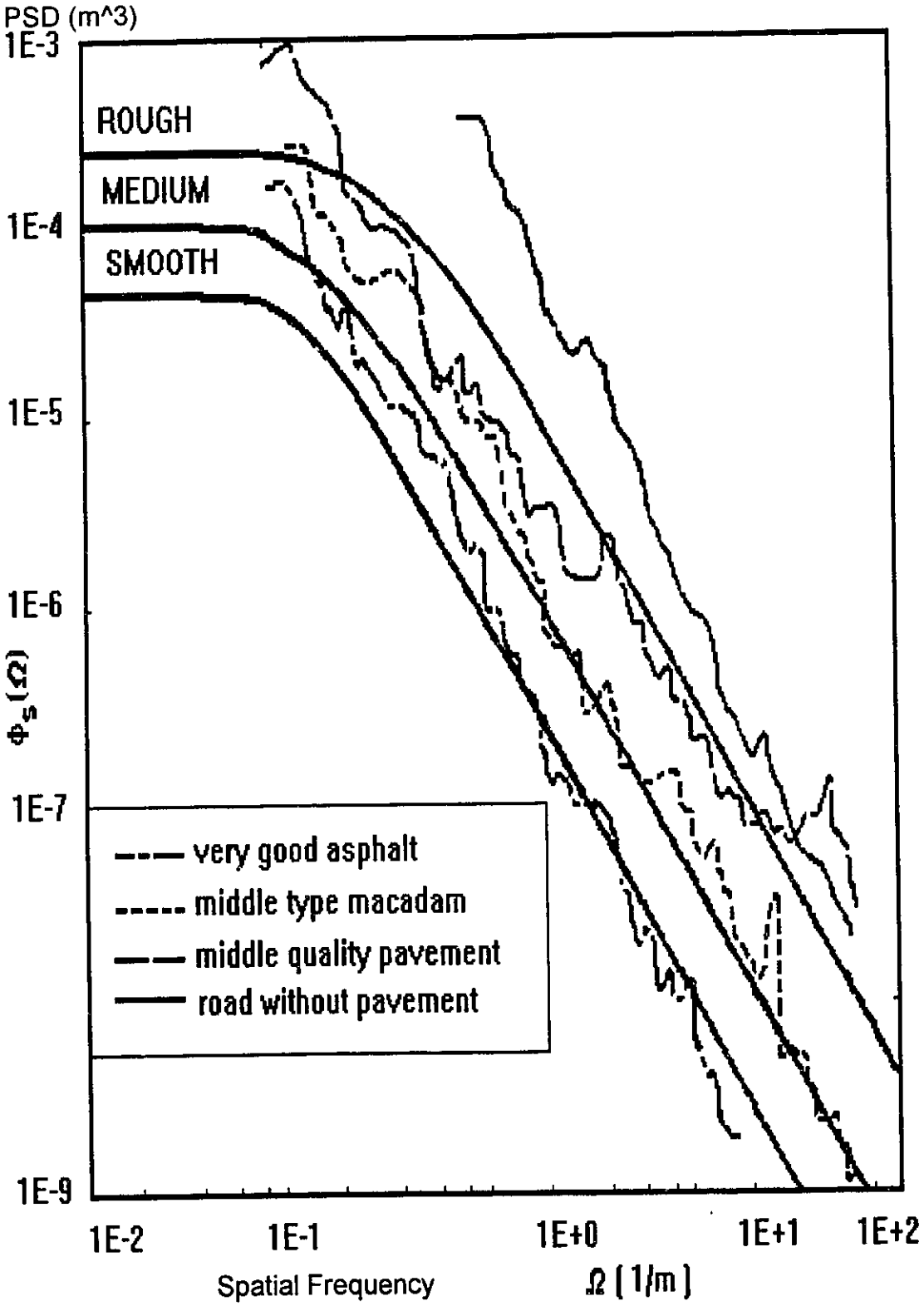

Figure 2.2 *PSD* of several types of roads and their approximation using EQ (2.2) [24]

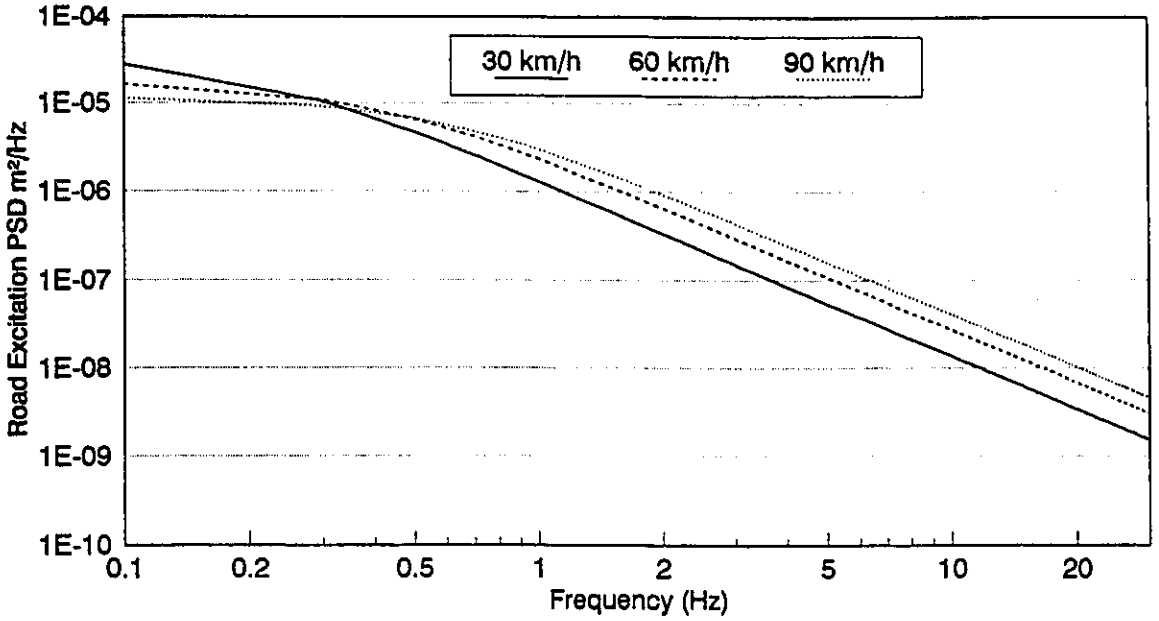

Figure 2.3a Power spectra for a smooth road at different speeds

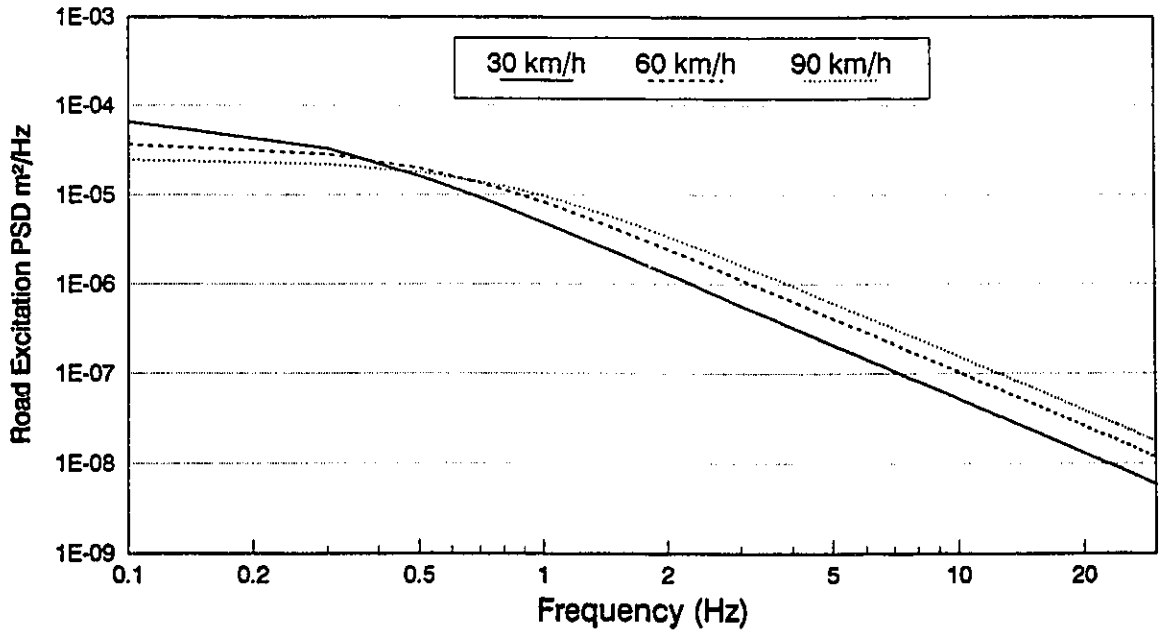

Figure 2.3b Power spectra for a medium rough road at different speeds

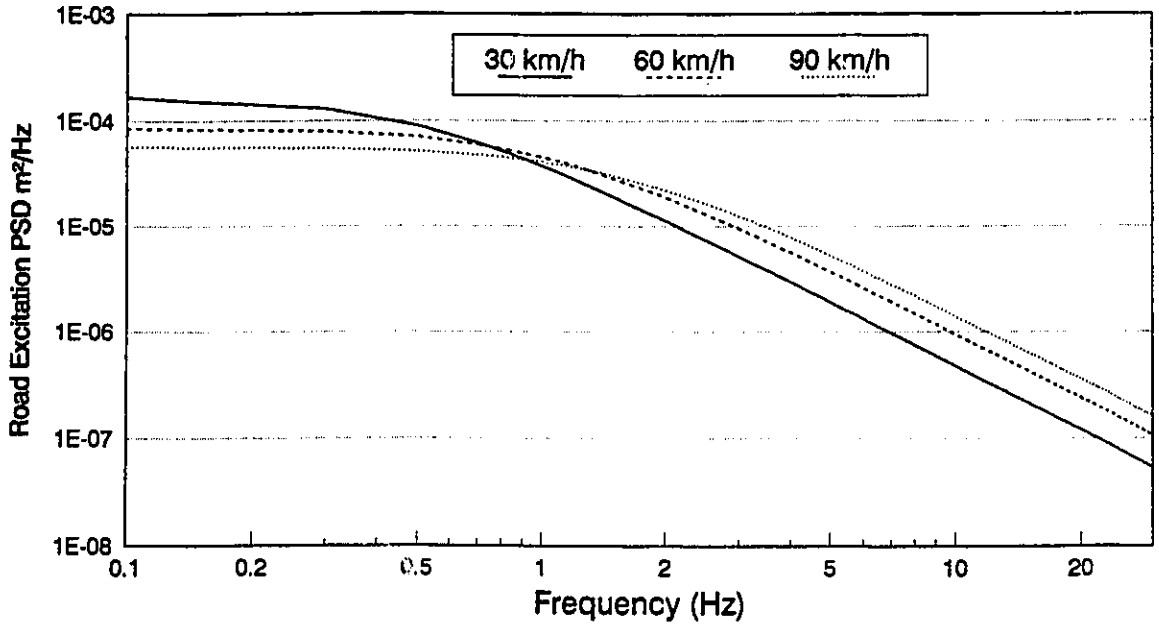

Figure 2.3c Power spectra for a rough road at different speeds

2.4 SUMMARY

The candidate vehicle, a tractor-semitrailer, is characterized by a 9 *DOF* dynamic model to investigate the ride behavior and road load performance characteristics of the suspension system. The baseline parameters for the vehicle model are proposed and the equations of motion are derived in the vertical-pitch plane. The road roughness is characterized by a white noise process passed through a first-order filter. The time delays between various tire-road contact points are accounted for by using a first order *Padé* approximation. The analytical model of the vehicle and the road roughness will be utilized to study the performance of passive and active suspensions in the following chapters.

2.5 REFERENCES

1. J. R. Ellis , "*The Ride and Handling of Semitrailer Articulated Vehicle,*" Automobile Engineering, Vol. 26, 1966, pp. 141-161.

2. W. D. Walter, D. Gossard and P. Fensel, "*Truck Ride: a Mathematical and Empirical Study,*" SAE paper No. 690099, January 13-17, 1969.

3. A. B. Allan M. M. ElMadany and M. A. Dokainish, "*Articulated Vehicle Models,*" SAE Paper No. 801420, 1980.

4. G. K. Misoi and R. M. Carson, *"Corrugation of Unmetalled Roads, Part 1: Vehicle Dynamics,"* proceedings of the IMechE Vol. 203, 1989, pp. 205-214.

5. G. K. Misoi, F. G. Gichaga and R. M. Carson, *"Corrugation of Unmetalled Roads, Part 2: Wheel-Soil Interaction,"* proceedings of the IMechE Vol. 203, 1989, pp. 215-220.

6. K. B. Todd, B. T. Kulakowski, *"Simple Computer Models for Predicting Ride Quality and Pavement Loading of Heavy trucks,"* Transportation Research Record 1215, 1990, pp. 137-149.

7. J. K. Hedrick, K. Yi, *"The Effect of Alternative Heavy Truck Suspensions on Flexible Pavement Response,"* presented at the Second International Symposium on Heavy Vehicle Weights and Dimensions Vol. 1, June 18-22, 1989, Kelowna British Columbia, Canada.

8. D. J. Cole, D. Cebon, *"Simulation and Measurement of Dynamic Tire Forces,"* presented at the Second International Symposium on Heavy Vehicle Weights and Dimensions Vol. 2, June 18-22, 1989, Kelowna British Columbia, Canada.

9. D. Cebon, *"Vehicle Generated Road Damage: A Review,"* Vehicle System Dynamics Vol. 18, 1989, pp. 107-150.

10. S. Rakheja et al., *"Ride Vibrations of Articulated Vehicles and Significance of Secondary Suspension,"* SAE 1989 Noise and Vib. Conf., SAE Publ. No. P-222, May 16-18, pp. 139-147.

11. R. D. Ervin and G. Yoram, "*The Influence of Weights and Dimensions on the Stability and Control of Heavy Duty Trucks in Canada,*" University of Michigan Transportation Research Institute, Report No. 86-35, July 1986.

12. A. Hac, "*Suspension Optimization of a 2-DOF Vehicle Model Using Stochastic Optimal Control Technique,*" Journal of Sound and Vibration, 100(3), 1985, pp. 343-357.

13. D. Bastow, "*Car Suspension and Handling,*" Pentech Press, London, 1987.

14. R. S. Sharp and D. A. Crolla, "*Road Vehicle Suspension Design-a Review,*" Vehicle System Dynamics, 16, 1987, pp. 167-192.

15. D. Hrovat M. Hubbard, "*Optimal Vehicle Suspensions Minimizing RMS Rattle Space, Sprung Mass Acceleration and Jerk,*" Trans. ASME Journal of Dynamic Systems, Measurement and Control, 103, September 1981, pp. 228-236.

16. D. A. Wilson R. S. Sharp and S. A. Hassan, "*The Application of Linear Optimal Control Theory to the Design of Active Automotive Suspension,*" Vehicle System Dynamics, 15, 1986, pp. 105-118.

17. T. D. Gillespie, "*Heavy Truck Ride,*" SAE, SP-607, 1985.

18. G. Hu, "*Simulation of Heavy Truck Ride Using a Desktop Computer,*" SAE Trans., 871557, 1987.

19. P. Michelberger and D Szoke, "*Speed Dependent Vertical Vibrations of Elastic Vehicle Bodies,*" Int. J. Vehicle Design, 8(1) pp. 8-95, 1985.

20. J. I. Ribarits, J Aurell and E. Andersers, "*Ride Comfort Aspects of Heavy Truck Design,*" SAE Tran., 781064 pp. 4046-4069, 1978.

21. A. R. Smith, "*Frame Bending, Fifth Wheel Location-Special Body Mounting and Loading Problems,*" SAE Special Report SR260, 1965.

22. M. M. ElMadany and M. E. Samaha, "*Optimum Response of a Stochastic Model of a Tractor Semitrailer Vehicle-Part II: Ride Control of an Actively Suspended Vehicle,*" ASME Vibration Conference, Proceedings on Vehicle Dynamics and Special Topics, Montreal, Sep. 17-21, 1989, pp. 177-184.

23. P. Michelberger, L. Palkovics and J. Bokor, "*Robust Design of Active Suspension System,*" Int. J. of Vehicle Design, vol. 14, No. 2/3, 1993.

24. M. Mitchke, "*Dynamik der Krafthafrzeuge,*" Springer Verlag, Berlin, 1972.

25. A. G. Baker Jr. "*Essentials of Padé Approximants,*" Academic Press, 1975.

CHAPTER 3

PASSIVE SUSPENSION DESIGN AND OPTIMIZATION

3.1 INTRODUCTION

Design of a passive suspension for a heavy vehicle requires careful choice of the suspension parameters, namely the stiffness and damping properties, to achieve a compromise between the ride, handling and control performance characteristics. A rather extensive body of literature has been published on the ride quality and cargo safety aspects of tractor-semitrailers. A soft and adequately damped suspension yields good ride quality with larger suspension deflection and reduced effective roll stiffness. Alternatively, a stiffer suspension, yields good roll stability and control performance with poor ride quality and reduced suspension deflection. The suspension design further influences the characteristics of the dynamic wheel loads transmitted to the pavement, which contribute to premature pavement fatigue and rut formation. Design of vehicle suspension, thus, involves a compromise among different conflicting requirements including good ride quality, suspension travel, good roll stability and low dynamic forces transmitted to the pavement. These performance characteristics are strongly related to vehicle configuration, vehicle weights and dimensions, road roughness, speed, and suspension and tire properties. Since

the vehicle weights and dimensions are selected based on the road laws and economic aspects of freight transportation, the suspension and tire properties have been the primary design focus to enhance the vehicle performance.

While the roll stability of a vehicle is related to its roll stiffness, the vehicle ride quality and dynamic wheel loads are related to the restoring and damping properties of the suspensions and tires. The roll dynamics of the vehicle yield only minimal contribution to the ride quality and wheel load performance of the vehicle. The performance characteristics related to vehicle ride quality, suspension deflection, and pavement loads are thus directly related to the vertical and pitch vibration modes of the vehicle. These vibration modes of the vehicle are strongly dependent upon the suspension design.

Suspension tuning to achieve an "optimum" performance can be accomplished through the study of the frequency response of each of the design criteria for varying suspension parameters. While such a design approach involves simple analyses, it tends to be extremely tedious and cumbersome, specifically when many design variables and performance requirements are considered. Alternatively, optimum suspension parameters may be selected from sensitivity analysis based upon the covariance matrix of the state vector. The method is quite efficient and is specifically well suited for multi-parameter design optimization. The covariance matrix is employed to yield mean square values of the various performance indices, such as tractor and semitrailer bounce and pitch accelerations, suspension deflections, and dynamic tire loads.

In this chapter, the covariance matrix of the state vector is formulated for the 9 *DOF* in-plane model of the tractor-semitrailer derived in the previous chapter. A range of suspension parameters is identified from the various database and published literature. The analyses are performed to derive the performance indices for variations in the suspension

parameters. The mean suspension performance, characterized by the mean square values of each component of the performance index is evaluated through the covariance matrix. The mean square values of the performance indices are presented in a graphical form for easy interpretation. The analytical vehicle model is validated using the road measured data and an extensive frequency response analysis is performed to validate the conclusions drawn from the covariance analysis.

3.2 STATE SPACE FORMULATION

The coupled differential equations of motion for the nine-*DOF* vehicle model, developed in Chapter 2, can be expressed in the matrix form:

$$\boldsymbol{M}\ddot{\boldsymbol{r}} + \boldsymbol{C}\dot{\boldsymbol{r}} + \boldsymbol{K}_s\boldsymbol{r} = \boldsymbol{K}_T\boldsymbol{q} \tag{3.1}$$

where $\boldsymbol{M}$, $\boldsymbol{C}$ and $\boldsymbol{K}_s$, are (9×9) mass, damping and stiffness matrices, respectively. $\boldsymbol{K}_T$ is a (9×5) tire stiffness matrix. $\boldsymbol{r}$ and $\boldsymbol{q}$ are (9×1) and (5×1) vectors of generalized coordinates and road excitations, respectively.

The equations of motion may be expressed in the first order state-space form by defining the new state vector y_y as:

$$y_y = \begin{Bmatrix} \dot{\boldsymbol{r}} \\ \boldsymbol{r} \end{Bmatrix} \tag{3.2}$$

The dynamics of the tractor-semitrailer can thus be described by the first order matrix equation:

$$\dot{y}_y(t) = A_y y_y + B_y q \tag{3.3}$$

where,

$$A_y = \begin{bmatrix} -M^{-1}C & -M^{-1}K_s \\ I & 0 \end{bmatrix} \text{ and } B_y = \begin{bmatrix} M^{-1}K_T \\ 0 \end{bmatrix} \tag{3.4}$$

and I is a (9×9) identity matrix.

Since q is a vector of stationary *Gaussian* random road excitation, derived from a white noise process with covariance $E[\xi_{(t)}\xi_{(\tau)}] = 2\alpha v\rho^2\delta_{(t-\tau)}$ and a first order filter, as described in Chapter 2:

$$\dot{q} = A_q q + B_q \xi \tag{3.5}$$

EQ (3.3) can be combined with the road excitation EQ (3.5) to yield the following augmented state-space form:

$$\dot{x} = Ax + B_1 \xi \tag{3.6}$$

where,

$$x = \begin{bmatrix} y_y \\ q \end{bmatrix},\ A = \begin{bmatrix} A_y & B_y \\ 0 & A_q \end{bmatrix},\ \text{and}\ B_1 = \begin{bmatrix} 0 \\ B_q \end{bmatrix} \tag{3.7}$$

where x is the (23×1) augmented state vector given by:

$$x = \left[\dot{r}_1, \dot{r}_2 \ldots, \dot{r}_9, r_1, r_2 \ldots, r_9, q_1, q_2, q_3, q_4, q_5\right]'$$

where " ' " designates the transpose. $A_j \in \mathbb{R}^{23\times23}$, is the system dynamics matrix and $B_j \in \mathbb{R}^{23\times1}$, is the excitation disturbance vector.

3.3 PERFORMANCE INDEX

The performance index, in general, is selected to reflect specific design objectives. For the candidate vehicle considered in this study, the suspension design objectives include: ride quality, cargo safety, rattle space requirements and dynamic tire forces. The vehicle ride quality is known to be a complex function of driver's work station design, placement of controls, visual displays, cab temperature, driver seat and cabin noise and vibration environment. While the ride quality related to work station design is frequently assessed using subjective rankings, many objective methods have been developed to assess the ride quality related to noise and vibration environment. Since the suspension design primarily determines the whole-body vibration environment of the driver's compartment, the ride quality related to vehicle vibration is addressed in this study. Although ride quality related to vehicle vibration is assessed using the weighting filters representing the human response to vibration [1], a relative measure of vehicle ride quality can be conveniently derived from the vertical (z_1) and pitch (z_2) acceleration responses.

The cargo safety is primarily related to the vibration levels transmitted to the cargo, while the cargo placement and attachment play a secondary role. The performance index related to cargo safety can thus be expressed in terms of vertical (z_3) and pitch (z_4) acceleration response of the semitrailer.

The relative deflections across the axle suspensions (z_5, z_6, z_7, z_8, z_9) determine the rattle space requirements for the suspension system. The relative deflections across the tire elements (z_{10}, z_{11}, z_{12}, z_{13}, z_{14}) directly relate to the dynamic forces transmitted to the pavements. The pavement fatigue and rut formation, attributed to heavy vehicle dynamic loads, is thus related to the tire deflections. The performance index, therefore, includes the square of the following response variable;

z_1 = Tractor bounce acceleration ($\ddot{r}_1$),

z_2 = Tractor pitch acceleration ($\ddot{r}_2$),

z_3 = Semitrailer bounce acceleration ($\ddot{r}_3$),

z_4 = Semitrailer pitch acceleration ($\ddot{r}_4$),

z_5 to z_9 = Suspension deflections,

z_{10} to z_{14} = Tire deflections.

From the equations of motion, EQ (2.1), these performance variables can be related to the components of the augmented state vector as follows:

$$\begin{aligned} z_1 = -\big[&C_1(x_1 + A_1x_2 - x_5) + C_2(2x_1 - B_1x_2 - x_6 - B_2x_2 - x_7) + \\ &C_5(x_1 - B_5x_2 - x_3 - A_2x_4) + K_1(x_{10} + A_1x_{11} - x_{14}) + \\ &K_2(2x_{10} - B_1x_{11} - x_{15} - B_2x_{11} - x_{16}) + K_5(x_{10} - B_5x_{11} - x_{12} - A_2x_{13})\big]/m_{s1} \end{aligned} \tag{3.8a}$$

$$\begin{aligned} z_2 = -\big[&C_1A_1(x_1 + A_1x_2 - x_5) + C_2[B_1(x_1 - B_1x_2 - x_6) + \\ &B_2(x_1 - B_2x_2 - x_7)] - C_5B_5(x_1 - B_5x_2 - x_3 - A_2x_4) + \\ &K_1A_1(x_{10} + A_1x_{11} - x_{14}) + K_2[B_1(x_{10} - B_1x_{11} - x_{15}) + \\ &B_2(x_{10} - B_2x_{11} - x_{16})] - K_5B_5(x_{10} - B_5x_{11} - x_{12} - A_2x_{13})\big]/I_{y1} \end{aligned} \tag{3.8b}$$

$$\begin{aligned} z_3 = -\big[&C_3(x_3 - B_3x_4 - x_8 + x_3 - B_4x_4 - x_9) + C_5(x_3 + A_2x_4 - x_1 + B_5x_2) + \\ &K_3(x_{12} - B_3x_{13} - x_{17} + x_{12} - B_4x_{13} - x_{18}) + K_5(x_{12} + A_2x_{13} - x_{10} + B_5x_{11})\big]/m_{s2} \end{aligned} \tag{3.8c}$$

$$z_4 = -[-C_3[B_3(x_3 - B_3x_4 - x_8) + B_4(x_3 - B_4x_4 - x_9)] + C_5A_2(x_3 + A_2x_4 - x_1 + B_5x_2) - K_3[B_3(x_{12} - B_3x_{13} - x_{17}) + B_4(x_{12} - B_4x_{13} - x_{18})] + K_5A_2(x_{12} + A_2x_{13} - x_{10} + B_5x_{11})]/I_{y2} \quad (3.8d)$$

$$z_5 = x_{10} + A_1x_{11} - x_{14} \quad (3.8e)$$

$$z_6 = x_{10} - B_1x_{11} - x_{15} \quad (3.8f)$$

$$z_7 = x_{10} - B_2x_{11} - x_{16} \quad (3.8g)$$

$$z_8 = x_{12} - B_3x_{13} - x_{17} \quad (3.8h)$$

$$z_9 = x_{12} - B_4x_{13} - x_{18} \quad (3.8i)$$

$$z_{10} = x_{14} - x_{19} \quad (3.8j)$$

$$z_{11} = x_{15} - x_{20} \quad (3.8k)$$

$$z_{12} = x_{16} - x_{21} \quad (3.8l)$$

$$z_{13} = x_{17} - x_{22} \quad (3.8m)$$

$$z_{14} = x_{18} - x_{23} \quad (3.8n)$$

The performance variables, z_i's, may be related to the state vector x in the following manner:

$$z = C_1x \quad (3.9)$$

where z is the vector of performance variables, and $C_1, \in \mathbb{R}^{14\times23}$, is the state-to-performance variables transformation matrix. The performance index can, thus, be written as:

$$J = \lim_{T\to\infty} E\left\{\int_0^T \left(\sum_{i=1}^{14} \mu_i z_i^2\right) dt\right\} \quad (3.10)$$

Alternatively,

$$J = \lim_{T\to\infty} E\left\{ \int_0^T \begin{bmatrix} z_1 & z_2 & \cdots & z_{14} \end{bmatrix} \begin{bmatrix} \mu_1 & 0 & \cdots & 0 \\ 0 & \mu_2 & \cdots & 0 \\ \vdots & \vdots & \ddots & \vdots \\ 0 & 0 & \cdots & \mu_{14} \end{bmatrix} \begin{bmatrix} z_1 \\ z_2 \\ \vdots \\ z_{14} \end{bmatrix} dt \right\} = \lim_{T\to\infty} E\left\{ \int_0^T z' \hat{Q} z dt \right\} \quad (3.11)$$

Where $\hat{Q} = Diag[\mu_1, \mu_2, \mu_3, \ldots \mu_{14}]$ and μ_i's are weighting factors. Upon substituting for z in terms of the state vector x, EQ (3.9), the performance index can be expressed as:

$$J = \lim_{T\to\infty} E\left\{ \int_0^T x' C_i' \hat{Q} C_i x dt \right\} \quad (3.12)$$

3.3.1 Evaluation of Performance Indices

EQ (3.6) is formulated to determine the vehicle response to random road excitations. The performance characteristics of the vehicle suspension are then examined using the performance index formulated in section 3.3. The resulting performance index J is strongly dependent upon the selected weighting factors μ_i's. The optimum solution necessitates selection of appropriate weighting factors for each performance variable. The selection of weighting factors, however, is quite complex due to excessive variations in the magnitudes of different performance variables. For instance, the mean square values of the tire deflections (z_{10} to z_{14}) are normally small when compared to those of the suspension deflections, and bounce and pitch accelerations of the vehicle. The performance variables representing the tire deflections thus need to be heavily weighted in order to reflect their contribution to the overall performance index J. The performance index, described by EQ (3.12), comprises the weighted mean square response of 14

performance variables, which represents the combined desired performance objectives of the suspension system. The overall performance index thus can not accurately describe the characteristics of each performance variable due to its dependence upon the selected weighting factors μ_i's. In view of the complexities associated with selection of appropriate weighting factors, it is desirable to examine each performance variable independent of the others to derive the optimum suspension parameters.

The influence of variations in suspension design variables on each of the performance variables can then be investigated, while eliminating the complexities associated with the selection of weighting factors. The weighting factors are thus selected to be unity and the overall performance index J is represented by its 14 variants (J_{zi}; *i=1 to 14*) characterizing the performance associated with each variable z_i.

3.4 COVARIANCE ANALYSIS

The steady-state mean square response of the passively suspended vehicle model can be described by the covariance matrix X of the state vector $x(t)$. The covariance matrix X depends on the system dynamic matrix A, the excitation vector B_j and the covariance of the disturbance ξ. The covariance matrix is derived from the solution of the following *Lyapunov* equation [2,3]:

$$AX + XA' + 2\alpha v\sigma^2 B_j B_j' = 0 \tag{3.13}$$

The performance index can then be expressed in terms of the covariance matrix X and the transformation matrix C_j, in the following manner [2]:

$$J = Tr(XC_j'\hat{Q}C_j) \tag{3.14}$$

Where *Tr* denotes the trace. The performance index J represents the weighted sum of mean square contributions of all the penalized variables. The contributions of each performance variable, however, can be determined from:

$$J_{zi} = \mu_i \, E\left(z_i^2\right) \tag{3.15}$$

Upon combining EQ (3.15) with the state-to-performance variables transformation, EQ (3.9), the contribution of the above penalized variable to the performance index is computed from:

$$J_{zi} = \mu_i E\left[\sum_{j=1}^{23} C_1(i,j)x_j\right]^2 \tag{3.16}$$

which can be rewritten as:

$$J_{zi} = \mu_i \sum_{m=1}^{23}\sum_{n=1}^{23}\left[C_1(i,m)C_1(i,n)\right]E(x(m)x(n)) \tag{3.17}$$

In the above equation, the expected value $E(x_{(m)}x_{(n)})$ is the element $X(m,n)$ of the covariance matrix X. The performance index can thus be described in terms of the elements of the covariance matrix:

$$J_{zi} = \mu_i \sum_{m=1}^{23}\sum_{n=1}^{23}\left[C_1(i,m)C_1(i,n)\right]X(m,n) \tag{3.18}$$

Once the covariance matrix X is determined, the above equation is used to evaluate the components of the performance index (J_{zi}; *i=1 to 14*). Since μ_i's are selected to be

unity, the elements of the performance index are simply unweighted mean squared values of the performance variables. The components of the performance index are evaluated for different suspension parameters to derive the optimum passive suspension design.

3.4.1 Ranges of Suspension Parameters

The passive vehicle suspensions employed in articulated freight vehicles exhibit excessive variations in their stiffness and damping properties. The leaf- and rubber-spring suspensions provide high stiffness, while the air-spring suspensions yield relatively low stiffness. The leaf-spring suspension provides energy dissipation through inter-layer friction and the air-spring suspension utilizes additional shock absorbers to damp the resonant oscillations. The range of stiffness and damping properties of different passive suspension systems is identified from the published data and summarized in Table 2.2. The suspension parameters are varied within this identified range, and EQ (3.18) is solved to examine the influence of variations on various components of the performance index, J_{zi}. A range of suspension parameters resulting in reduced mean square value is thus identified for each performance variable. The static deflection requirements of the suspension are also considered to arrive at a near optimum range of suspension parameters.

3.5 FREQUENCY DOMAIN ANALYSIS

The dynamic response characteristics of the linear vehicle model described in Chapter 2 can be conveniently derived using the frequency domain analysis. The frequency response characteristics of the passively suspended vehicle subjected to a random road excitation directly relates to the ride dynamics, suspension deflections and tire loads performance of the vehicle. Since the road excitations are assumed to be stationary and *Gaussian*, the vector of system response variables $\mathbf{z}$ is also stationary and *Gaussian* [4-6].

The power spectral density S_z of the response variables is related to the frequency response function and the *PSD* of the excitation [7]:

$$S_z(\omega) = H S_\xi H^* \tag{3.19}$$

where * denotes the complex conjugate transpose, and $H, \in \mathbb{C}^{14\times 1}$, is the frequency response function relating the excitation ξ to the vector of system response variables z. The frequency response function is evaluated from the *Laplace* transform of EQ (3.6) and (3.9) and is given by:

$$H = \left\{ C_l (sI - A)^{-1} B_l \right\} \tag{3.20}$$

C_l is the transformation matrix as described in EQ (3.9), and A and B_l are the system dynamic matrix and excitation disturbance vector, respectively, as defined in EQ (3.7). I is a (23×23) identity matrix and s is the *Laplace* operator.

S_ξ is the auto spectral density of the white noise input excitation given by:

$$S_\xi = \frac{2\alpha v \sigma^2}{\pi} \tag{3.21}$$

The diagonal elements of $S_z(\omega)$ ($S_z \in \mathbb{C}^{14\times 14}$) provide the spectral densities of the output state z_i described in section 3.3.

3.6 EXPERIMENTAL VALIDATION OF THE MATHEMATICAL MODEL

The validity of the mathematical vehicle model is asserted by comparing the analytical and experimental frequency response characteristics of the selected variables. The results of a road measurement study, undertaken by *CONCAVE Research Centre* [8], are examined to validate the analytical model of the passively suspended vehicle. The test vehicle consisted of a three-axle tractor and three-axle semitrailer, supplied by *Canadian Liquid Air Ltd.* The tractor consisted of a tandem rear axle and a tilt cab-over-engine configuration. The semitrailer was a *"FRUEHAUF"* box semitrailer with tandem axles at the rear, and a self-steering belly axle. The semitrailer was loaded with bottles up to half of the semitrailer height. The vehicle response data was acquired on major *Quebec* (20W and 40W) and *Ontario* (401W) highways at a constant forward speed of 90 km/h. The parameters of the test vehicle are summarized in Table 3.1 [8].

A number of accelerometers were mounted to measure the vertical acceleration response at the tractor axles, cab floor, and at the driver and passenger seat locations. A tri-axial seat accelerometer was mounted on the seat cushion to measure the vertical, lateral and longitudinal acceleration transmitted to the driver-seat interface.

The test vehicle is quite similar to that considered in this study with the exception of the belly axle. While the dynamics of the belly axle is expected to make definite contribution to the vehicle response, the analytical model can be validated in view of the general trends in the response characteristics. Since the statistical properties of the test road profiles are not known, the road undulations are derived from EQ (2.2) assuming medium rough roads. The constants α and σ, representing the road roughness, are thus selected as:

$\alpha = 0.2\ m^{-1}$ and $\sigma = .0056\ m$

In view of the different semitrailer and drive axle configurations, the measured vertical acceleration response of the front axle and the tractor's sprung masses are considered to examine the validity of the analytical model. Figure 3.1 illustrates a comparison of the *PSD* of the model and measured acceleration response characteristics of the unsprung mass of the front axle. The model and the measured response characteristics show similar trends in the unsprung mass frequency and the corresponding magnitude. While the simulation results reveal front axle resonance near 10.3 *Hz*, the measured data exhibits resonance in the 12-15 *Hz* range. The magnitudes of model and measured acceleration response characteristics corresponding to the resonant frequencies, however, are comparable. The discrepancies in the resonant frequencies can be attributed to the assumptions of linear stiffness and damping properties of the suspension, the lack of couplings present in the tandem axle suspension, and lack of accurate description of the road profile. The front axle suspension of the test vehicle was a leaf-spring type suspension, which yields progressively hardening spring characteristics, and non-linear hysteritic properties.

Figure 3.2 illustrates a comparison of the acceleration response characteristics derived at the tractor *CG* with those measured at the cab floor. The results reveal that the model response correlates well with the measured data. The model acceleration response reveals bounce and pitch resonance of the sprung mass near 1.9 and 2.5 *Hz*, respectively. The bounce and pitch frequencies of the test vehicle derived from the measured response are 2.0 and 3.1 *Hz*, respectively. The measured response also exhibits peaks near 7 and 10 *Hz*, which may be attributed to frame bending mode and axle resonance.

Table 3.1 Test vehicle parameters [8].

Description of vehicle parameter	*Parameter value*
Tractor mass (tractor, cab and seat)	4,825.0 *kg*
Tractor pitch mass moment of inertia	24,735.0 $kg.m^2$
Tractor front tire and axle assembly mass	544.0 *kg*
Tractor leading rear tire and axle assembly mass	1,136.0 *kg*
Tractor trailing rear tire and axle assembly mass	1,136.0 *kg*
Semitrailer mass	37,364.0 *kg*
Semitrailer pitch mass moment of inertia	741,525.0 $kg.m^2$
Semitrailer leading tire and axle assembly mass	1,032.0 *kg*
Semitrailer trailing tire and axle assembly mass	1,032.0 *kg*
Tractor front suspension stiffness	465,300.0 *N/m*
Tractor front suspension damping coefficient	14,980.0 *N.s/m*
Tractor leading rear axle suspension stiffness	1,970,100.0 *N/m*
Tractor leading rear axle suspension damping coefficient	27,600.0 *N.s/m*
Tractor trailing rear axle suspension stiffness	1,970,100.0 *N/m*
Tractor trailing rear axle suspension damping coefficient	27,600.0 *N.s/m*
Semitrailer leading axle suspension stiffness	2,604,750.0 *N/m*
Semitrailer leading axle suspension damping coefficient	27,240.0 *N.s/m*
Semitrailer trailing axle suspension stiffness	2,604,750.0 *N/m*
Semitrailer trailing axle suspension damping coefficient	27,240.0 *N.s/m*
Tractor front tire stiffness	1,970,000.0 *N/m*
Tractor leading rear axle tire stiffness	3,940,100.0 *N/m*
Tractor trailing rear axle tire stiffness	3,940,100.0 *N/m*
Semitrailer leading axle tire stiffness	5,910,200.0 *N/m*
Semitrailer trailing axle tire stiffness	5,910,200.0 *N/m*
Fifth wheel stiffness	20,000,000.0 *N/m*
Fifth wheel damping coefficient	200,000.0 *N.s/m*
Distance from tractor *CG* to tractor steer axle	2.00 *m*
Distance from tractor *CG* to first tractor drive axle	2.60 *m*
Distance from tractor *CG* to second tractor drive axle	2.60 *m*
Distance from tractor *CG* to fifth wheel	2.45 *m*
Distance from semitrailer *CG* to fifth wheel	5.93 *m*
Distance from semitrailer *CG* to first semitrailer axle	4.95 *m*
Distance from semitrailer *CG* to second semitrailer axle	4.95 *m*

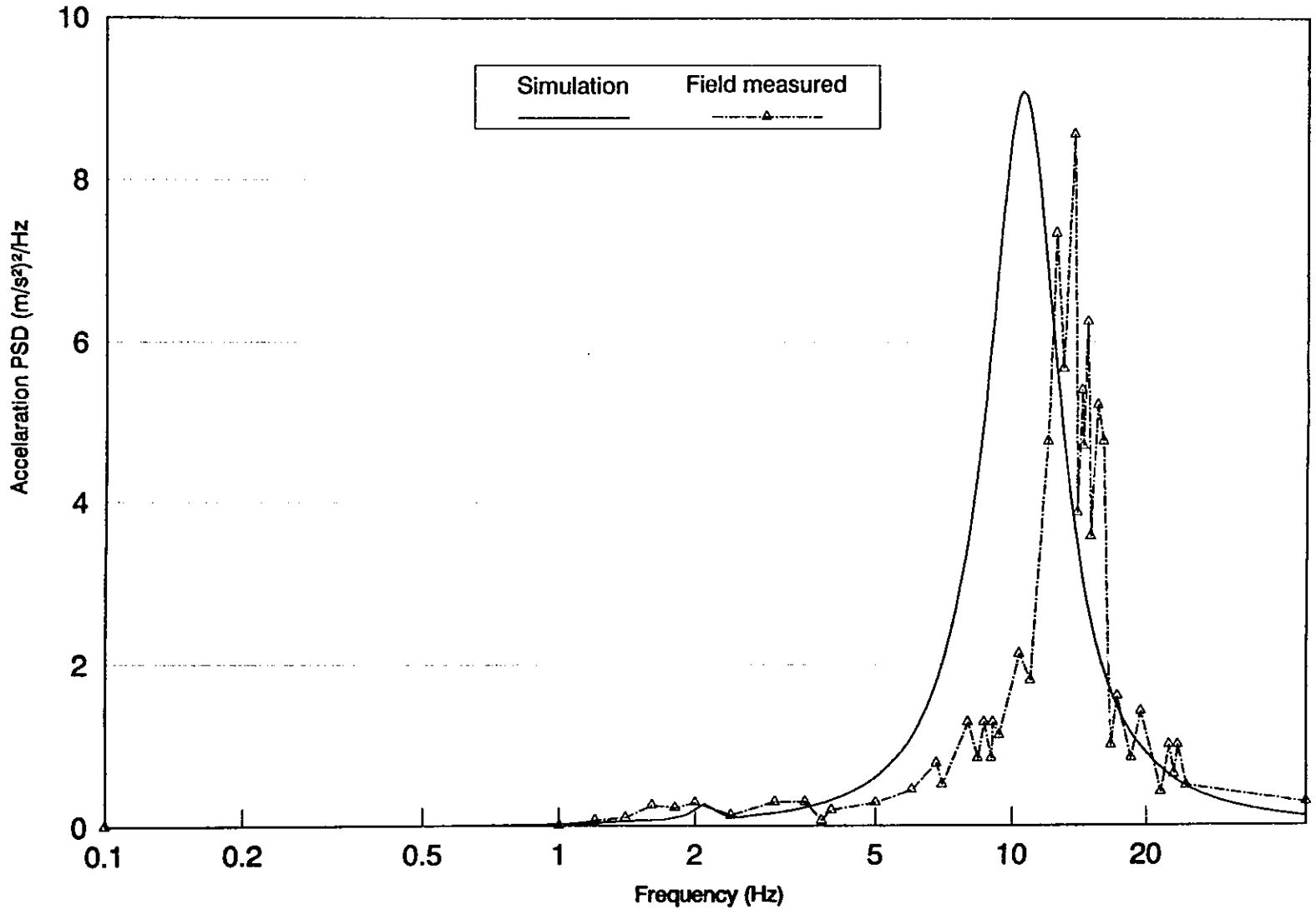

Figure 3.1 Comparison of field measured and simulation acceleration PSD of front axle bounce (medium rough road)

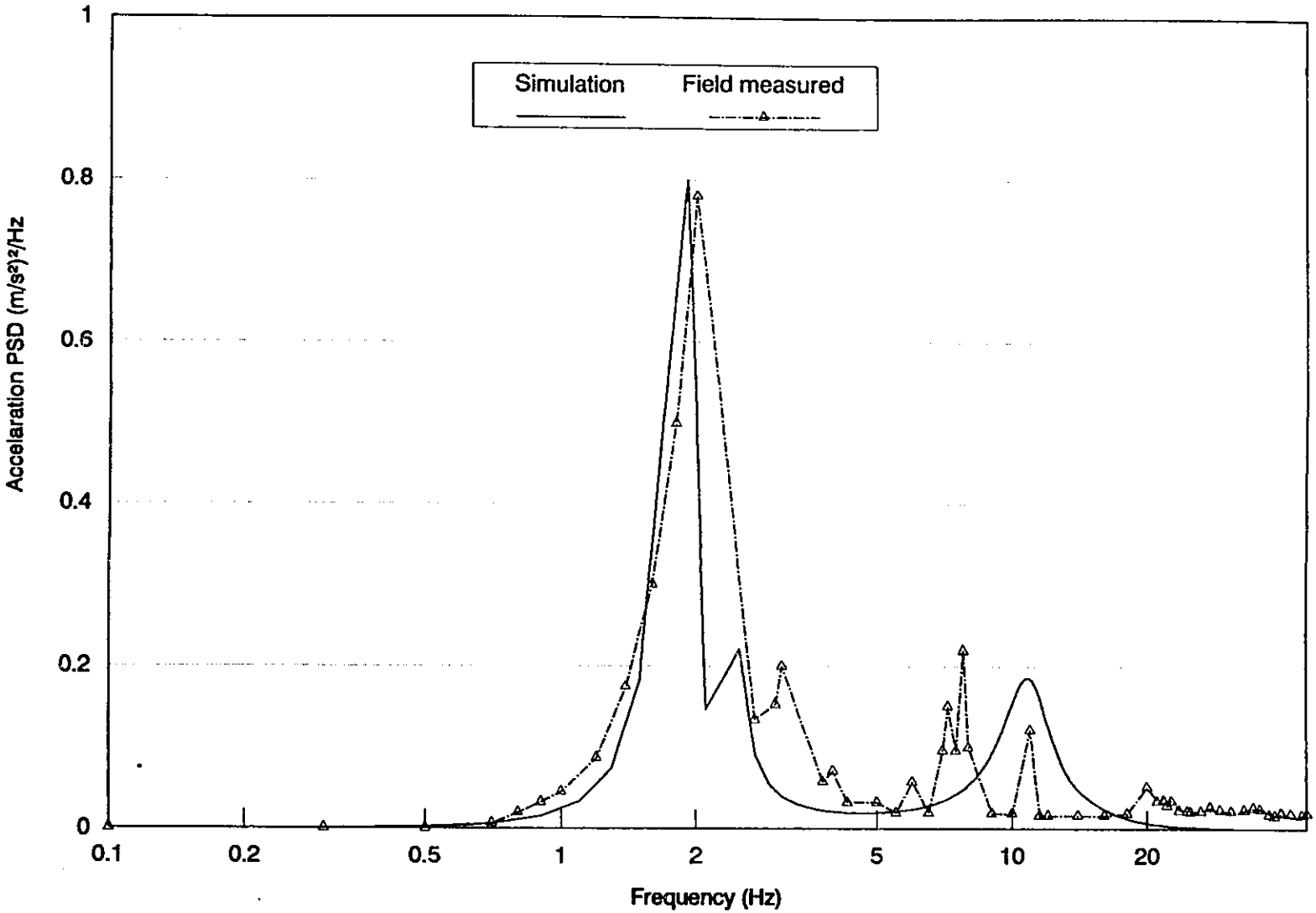

Figure 3.2 Comparison of field measured and simulation acceleration PSD of tractor bounce (medium rough road)

3.7 IDENTIFICATION OF OPTIMUM SUSPENSION PARAMETERS

Design of a passive vehicle suspension involves the study of the influence of variations in suspension parameters on the desired performance objectives, and necessary compromise when conflicting design requirements are considered. For the candidate vehicle model considered in this study, the influence of variations in the stiffness and damping properties of the passive suspension on the different performance variables is investigated to identify the optimum suspension parameters. The road excitation is formulated for excitation arising from a smooth road ($\alpha = 0.15\ m^{-1}$ and $\sigma = 0.0033\ m$), as described in Chapter 2. The vehicle and road parameters are used to formulate the system dynamic matrix A, defined in EQ (3.7). EQ (3.13) is solved to determine the covariance matrix X, and the mean square value of each component of the performance index is then evaluated using EQ (3.18). The stiffness and damping properties of all the five suspension systems are varied concurrently resulting in simultaneous changes in all the performance variables. The components of the performance index are computed for various suspension parameters within the identified range listed in Table 2.2. Unity weighting factors are selected to study the direct influence of suspension parameters on each component of the performance index.

3.7.1 Influence of Suspension Stiffness and Damping Parameters on the Performance Variables

The performance objective comprising vehicle ride quality, cargo safety, suspension deflections and tire deflections is strongly related to the vehicle suspension parameters. Different components of the objective function often pose conflicting design requirements. The effects of suspension parameters on the different components of the performance index is thus investigated to realize an acceptable design compromise.

Selection of passive suspension parameters involves the study of effects of stiffness and damping variations on the components of the performance index and realization of an acceptable compromise among the different performance objectives. EQ (3.7), (3.13) and (3.18) are solved to evaluate each component of the performance index, which is presented as a function of the suspension stiffness and damping parameters. The analysis is repeated for different values of suspension parameters within the identified range. Figures 3.3 to 3.6 illustrate the influence of variations in suspension parameters on various performance variables: vertical and pitch accelerations of the tractor sprung mass (z_1, z_2), a measure of ride quality; vertical and pitch accelerations of the semitrailer sprung mass (z_3, z_4), a measure of cargo safety; suspension deflections (z_5 to z_9), a measure of the rattle space requirements; and tire deflections (z_{10} to z_{14}), a measure of tire forces transmitted to the pavement.

Figures 3.3a and 3.3b illustrate the effect of varying the suspension parameters on the tractor bounce and pitch responses. The results are presented in terms of vertical and pitch acceleration derived at the *CG* of the tractor sprung mass. The results show that a soft suspension is required to improve the vehicle ride performance. The results further reveal the existence of an ideal damping value for a given suspension stiffness. The existence of the optimum suspension damping is quite apparent with stiff suspension. Very light damping, in conjunction with a stiff suspension, yields high bounce and pitch acceleration response of the tractor sprung mass. High suspension damping also results in large bounce and pitch acceleration of the tractor, irrespective of the suspension stiffness. Although lightly damped soft suspensions yield enhanced ride quality, the associated rattle space and roll stiffness of the suspension may be unsatisfactory.

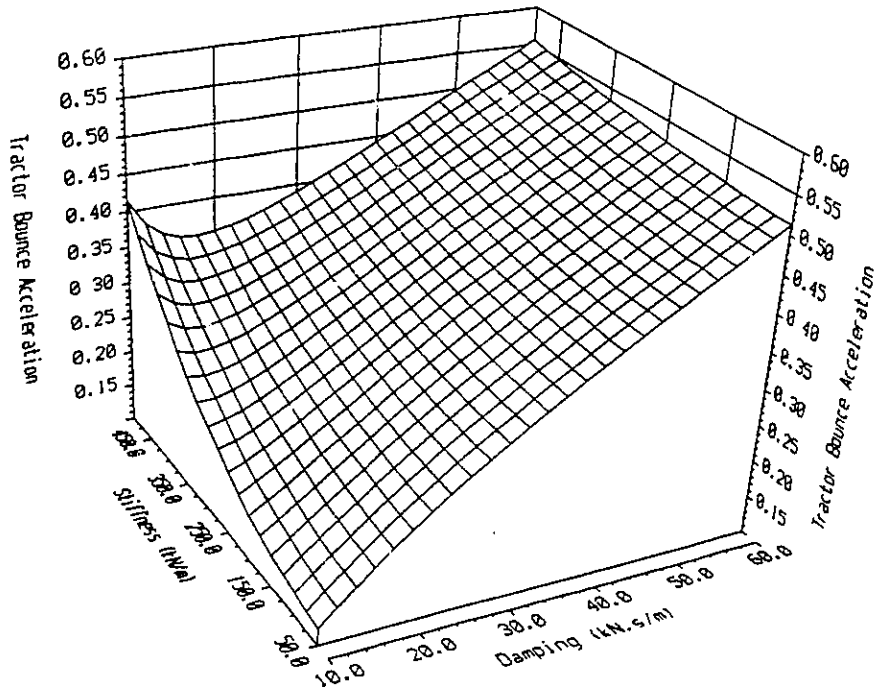

Figure 3.3a Mean square acceleration of the tractor bounce for varying suspension stiffness and damping.

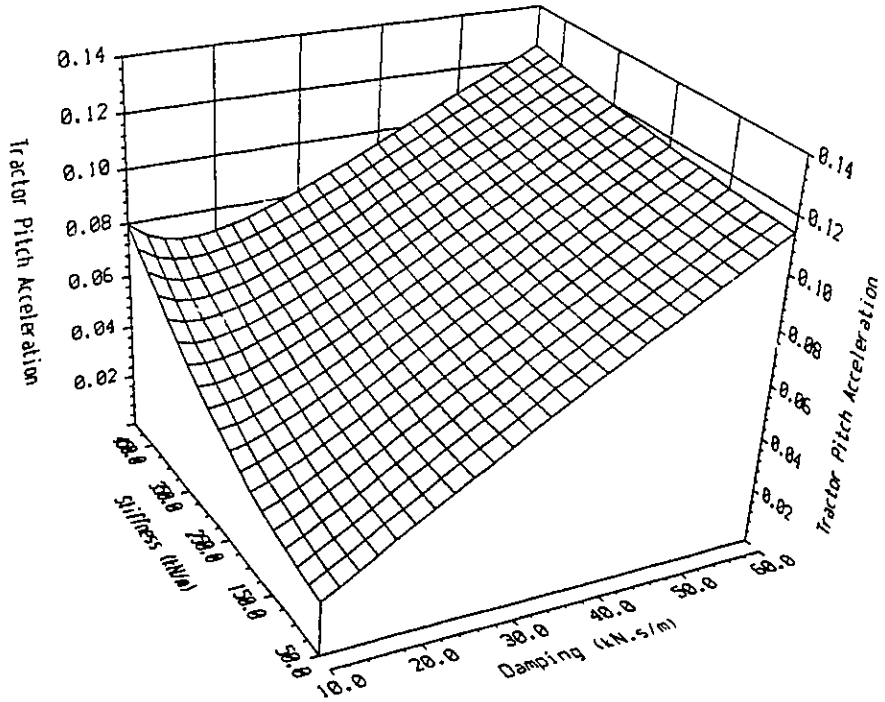

Figure 3.3b Mean square acceleration of the tractor pitch for varying suspension stiffness and damping.

The influence of suspension parameters on the bounce and pitch acceleration response of the semitrailer is illustrated in Figures 3.4a and 3.4b, respectively. The influence of suspension parameters on the semitrailer response is quite similar to that observed for the tractor response. The semitrailer pitch response is relatively insensitive to variations in suspension damping, when soft suspensions are used. The dependence of pitch response on the damping value, however, increases rapidly with increase in the suspension stiffness. From the vertical and pitch acceleration response characteristics of the tractor and semitrailer sprung masses, it can be concluded that an optimum suspension damping value exists to achieve improved ride and cargo safety. A soft suspension, while desirable to achieve good ride quality and cargo safety, contradicts the handling and roll stability as well as the static suspension deflection requirements. A heavily damped suspension is desirable to reduce the suspension deflections, as illustrated in Figures 3.5a to 3.5e. The results reveal the existence of an optimum suspension stiffness value for a given value of damping for the tractor axle suspensions. The existence of the optimum value is specifically apparent for lightly damped suspensions. The deflection response of a heavily damped suspension, however, is relatively insensitive to variations in suspension stiffness. Contrary to the tractor axle suspensions, the deflection response characteristics of the semitrailer axle suspension do not reveal an optimum value in the range of suspension parameters considered in this study. The results clearly illustrates the conflicting requirements of suspension design to achieve improved ride quality and rattle space. The deflection response of the drive axle suspensions is illustrated in Figures 3.5b and 3.5c. The deflection response of the trailing drive axle is considerably larger than that of the leading axle. The deflection response of the trailing semitrailer axle is also observed to be larger than that of the leading semitrailer axle (Figures 3.5d and 3.5e). Although the two axles are closely spaced, the larger deflection of the trailing axle suspension is attributed to increased pitch oscillations of tractor and semitrailer sprung masses with increased suspension stiffness, as demonstrated in Figures 3.3b and 3.4b.

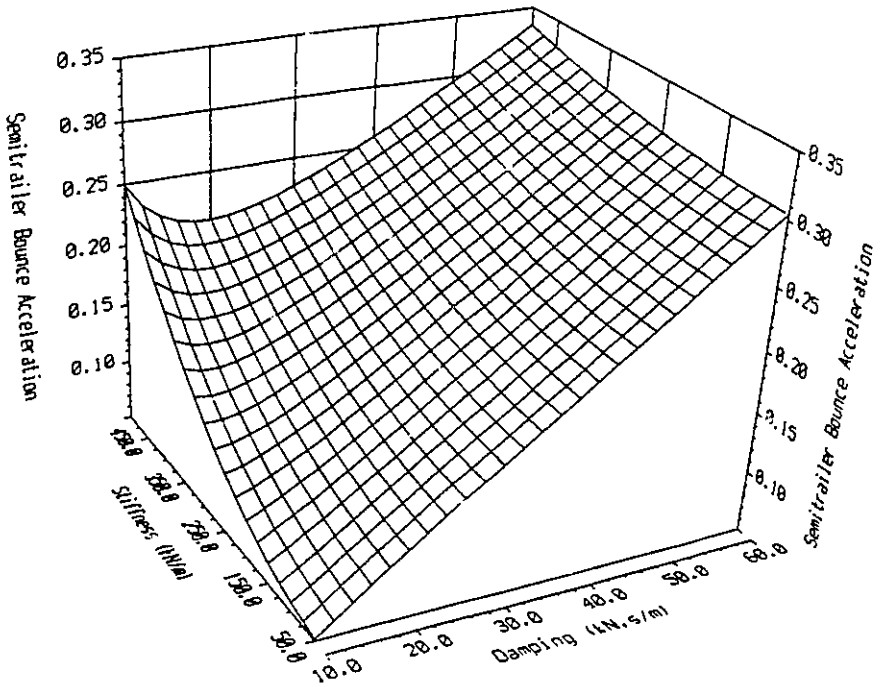

Figure 3.4a Mean square acceleration of the semitrailer bounce for varying suspension stiffness and damping.

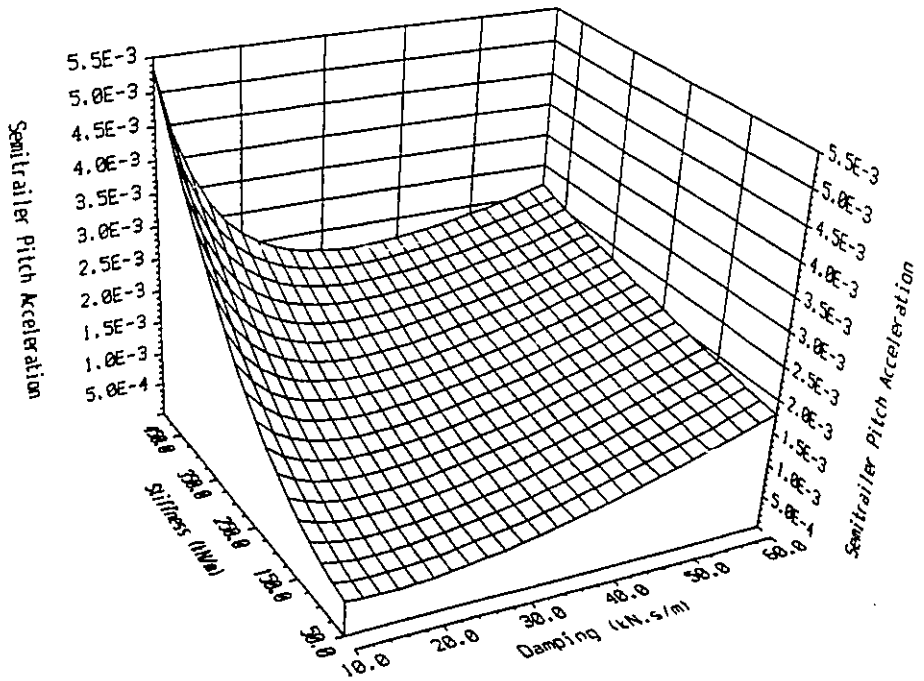

Figure 3.4b Mean square acceleration of the semitrailer pitch for varying suspension stiffness and damping.

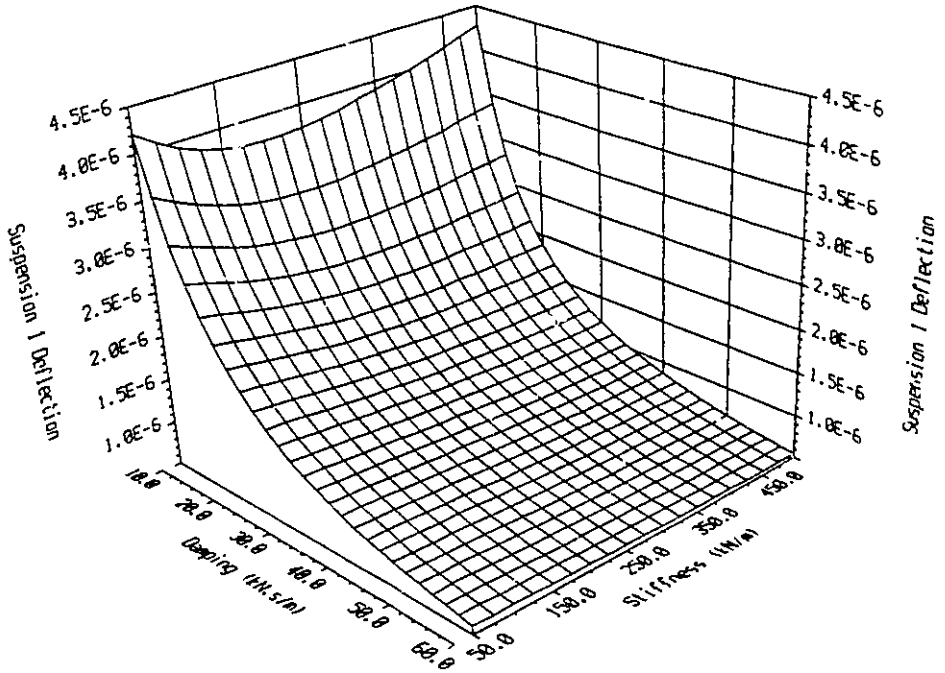

Figure 3.5a Dynamic mean square deflection of the first suspension for varying stiffness and damping.

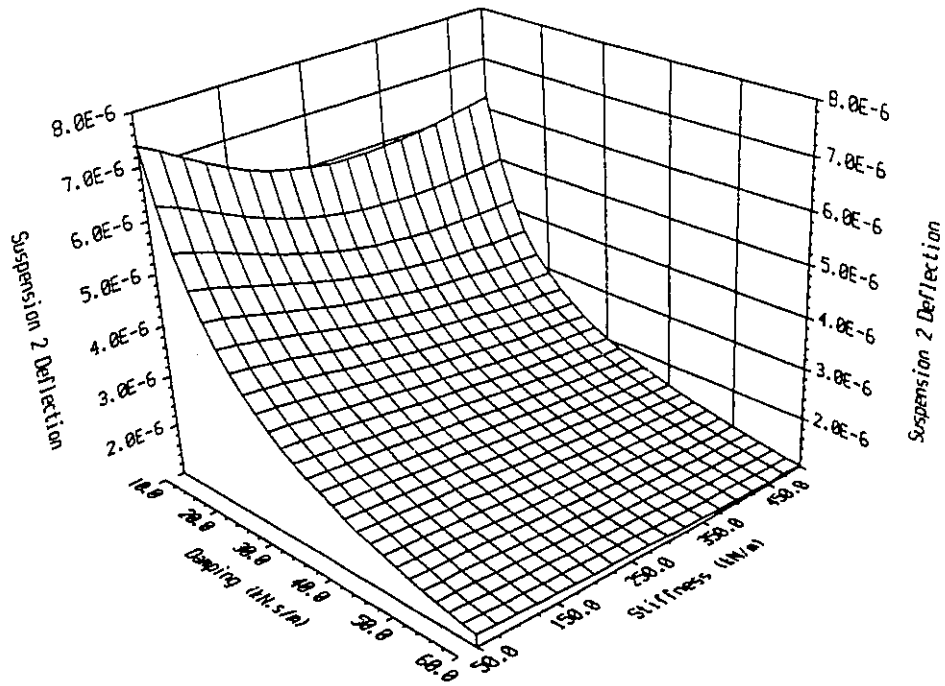

Figure 3.5b Dynamic mean square deflection of the second suspension for varying stiffness and damping.

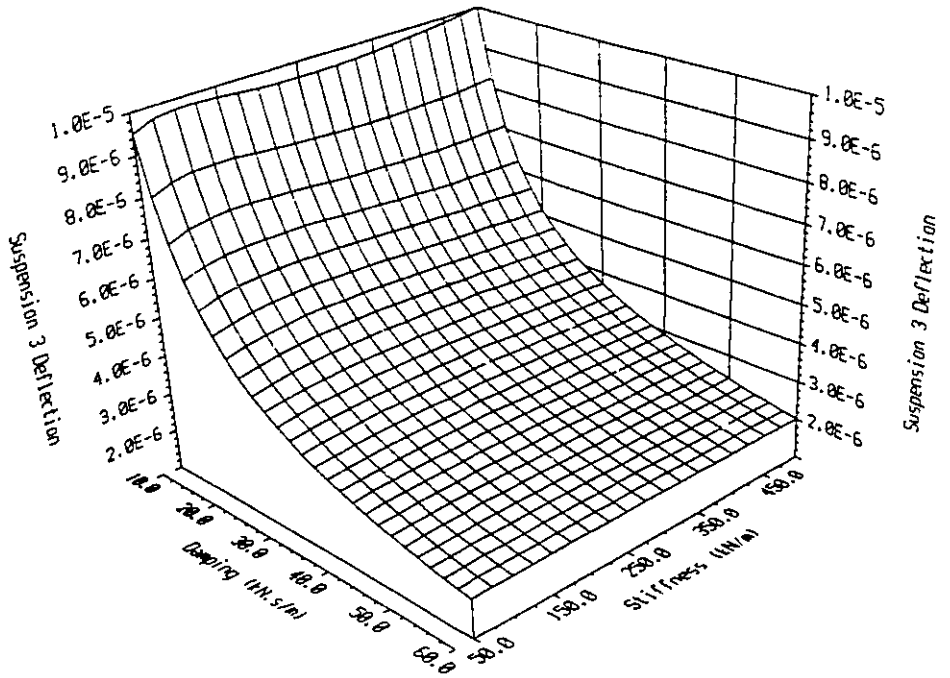

Figure 3.5c Dynamic mean square deflection of the third suspension for varying stiffness and damping.

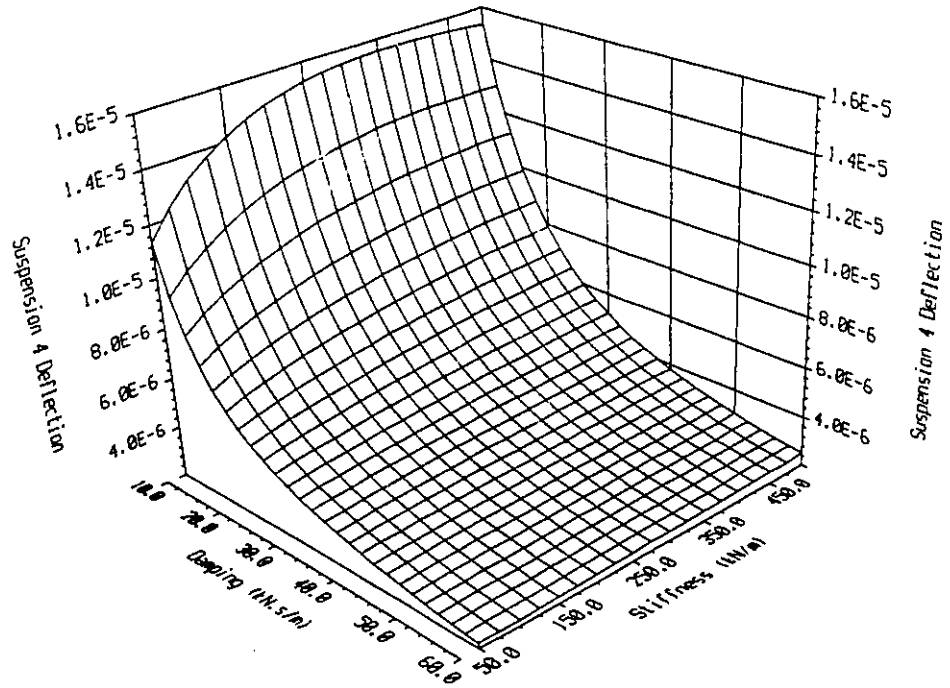

Figure 3.5d Dynamic mean square deflection of the fourth suspension for varying stiffness and damping.

Figures 3.6a to 3.6e illustrate the influence of suspension parameters on the dynamic deflection response of the tires. The figures clearly illustrate the existence of an optimum suspension damping and stiffness to achieve low dynamic deflection of all the axle tires. The tire deflection response of a lightly damped suspension is strongly influenced by the suspension stiffness. The influence of stiffness of a heavily damped suspension on the dynamic tire deflection, however is relatively insignificant. The tire deflection tends to increase for extremely low and high damping values, irrespective of the suspension stiffness. The deflections of tires on the trailing axle of the drive and semitrailer axles are observed to be larger than those of leading axle tires due to pitch motions of the respective sprung weights. The difference in magnitudes of mean square deflections of the leading and trailing axle tires tends to increase with increased damping. This increase in deflection is attributed to increase in tractor and semitrailer pitch motions with increase in suspension damping, as illustrated in Figures 3.3b and 3.4b.

In an attempt to identify optimum suspension parameters leading to minimal tire deflections and thus minimum dynamic tire loads, the results of the covariance analysis are presented in terms of contour plots. Figures 3.7a to 3.7e illustrate the constant tire deflection curves as functions of the suspension stiffness and damping parameters. Each curve represents a constant value of the mean square tire deflection, and different combinations of suspension parameters can yield identical tire deflections as shown in the figures. The damping and stiffness values corresponding to the center-most iso-value curves would result in the minimal dynamic tire deflection. The contour plots clearly illustrate that the front axle suspension with light damping and stiffness value around 180 *kN/m* yields minimal dynamic tire deflection. The drive and semitrailer axle suspension with slightly higher damping values in the 20-30 *kNs/m* range yields low dynamic deflections of the respective tires.

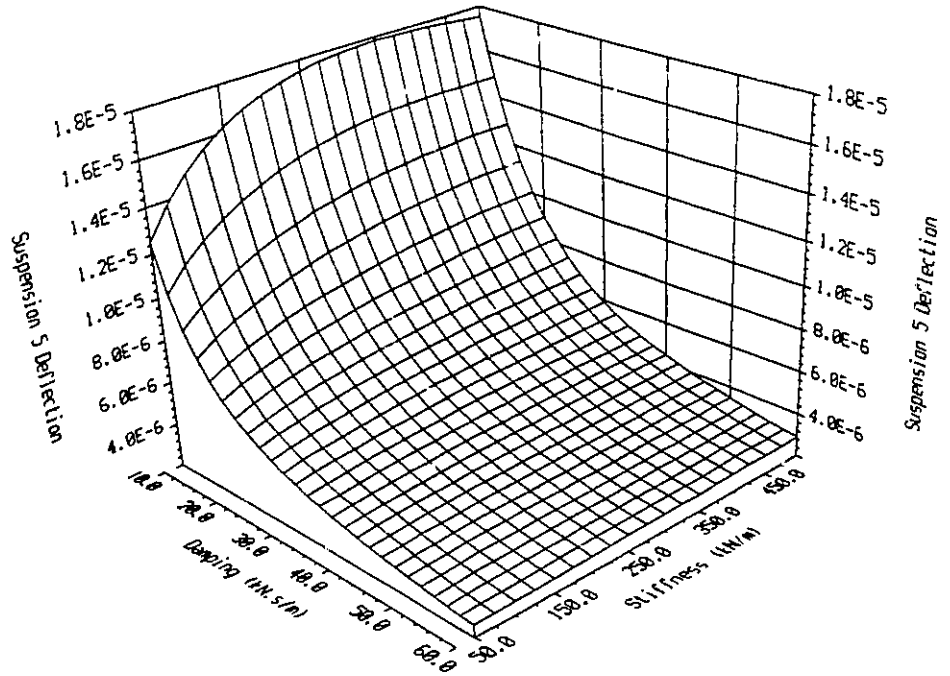

Figure 3.5e Dynamic mean square deflection of the fifth suspension for varying stiffness and damping.

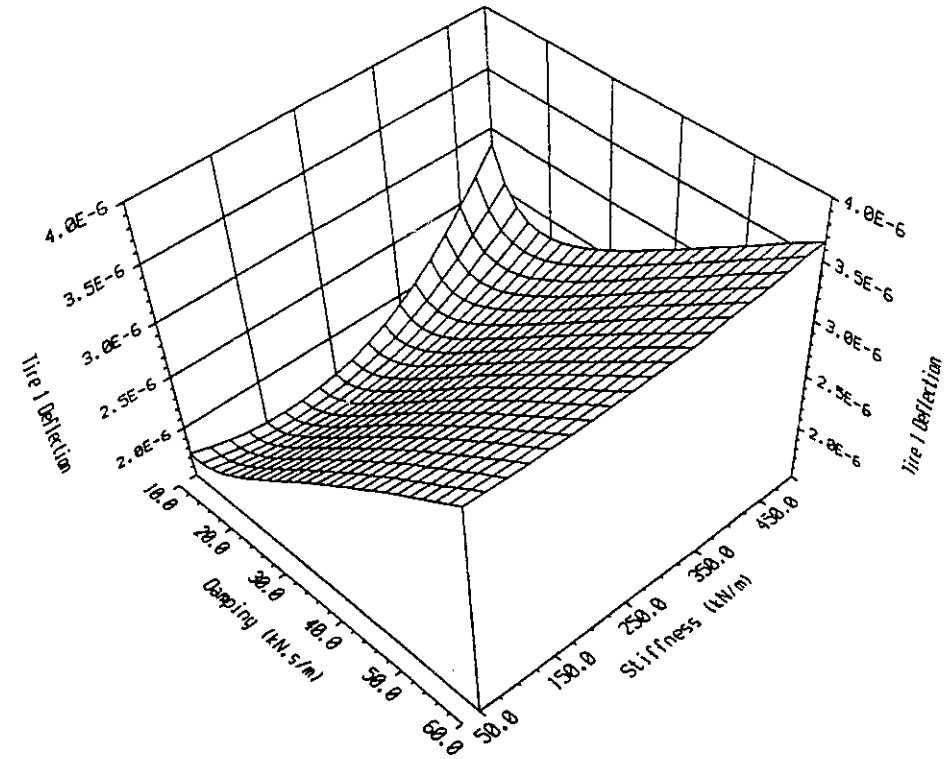

Figure 3.6a Dynamic mean square deflection of the first tire for varying suspension stiffness and damping.

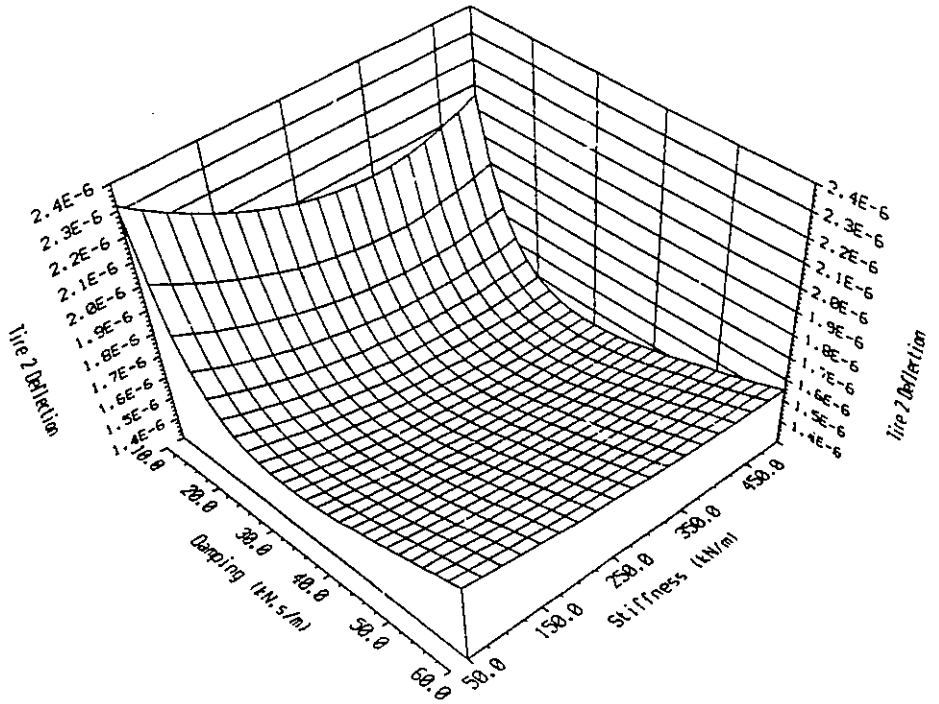

Figure 3.6b Dynamic mean square deflection of the second tire for varying suspension stiffness and damping.

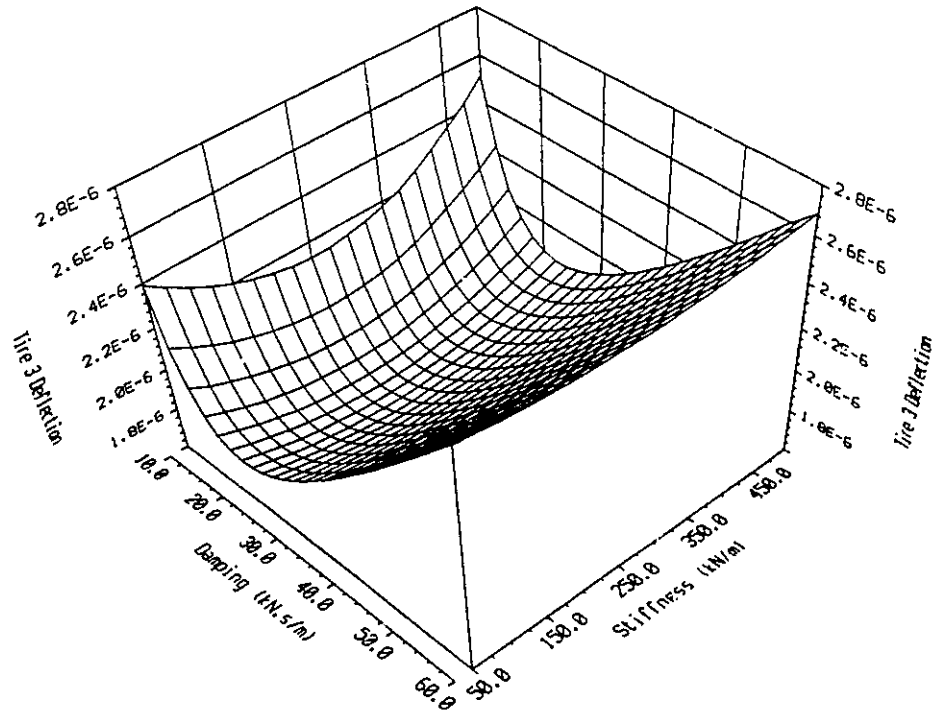

Figure 3.6c Dynamic mean square deflection of the third tire for varying suspension stiffness and damping.

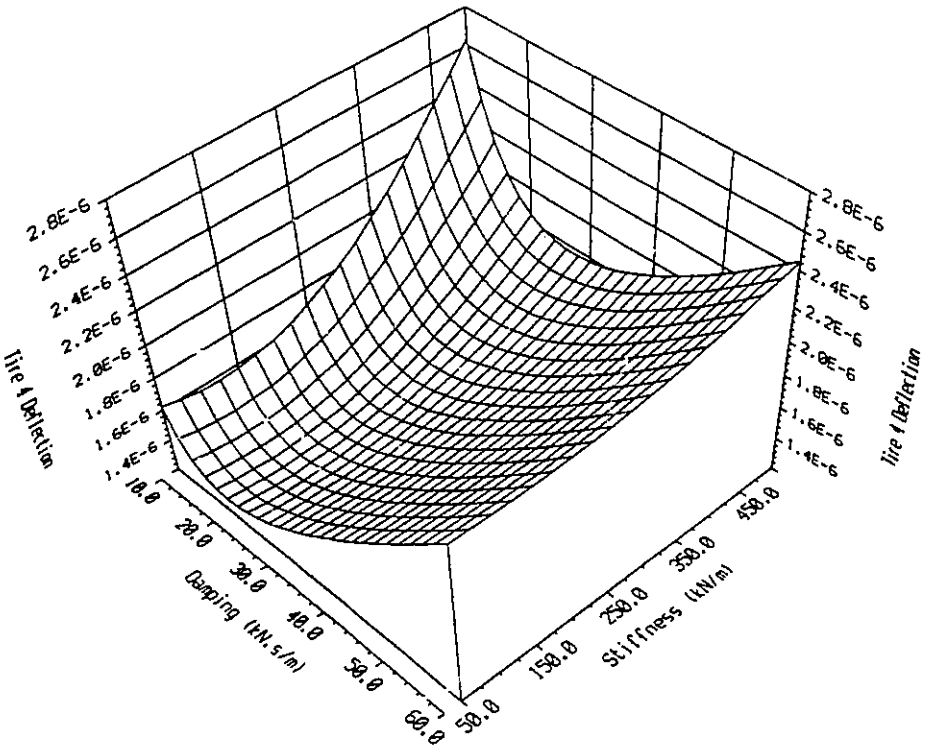

Figure 3.6d Dynamic mean square deflection of the fourth tire for varying suspension stiffness and damping.

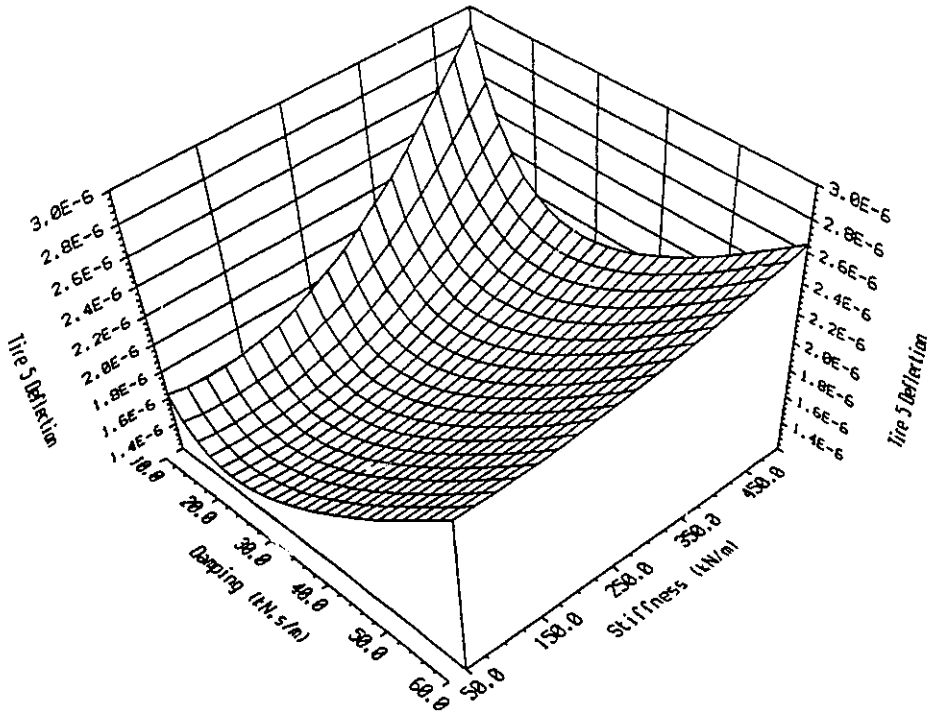

Figure 3.6e Dynamic mean square deflection of the fifth tire for varying suspension stiffness and damping.

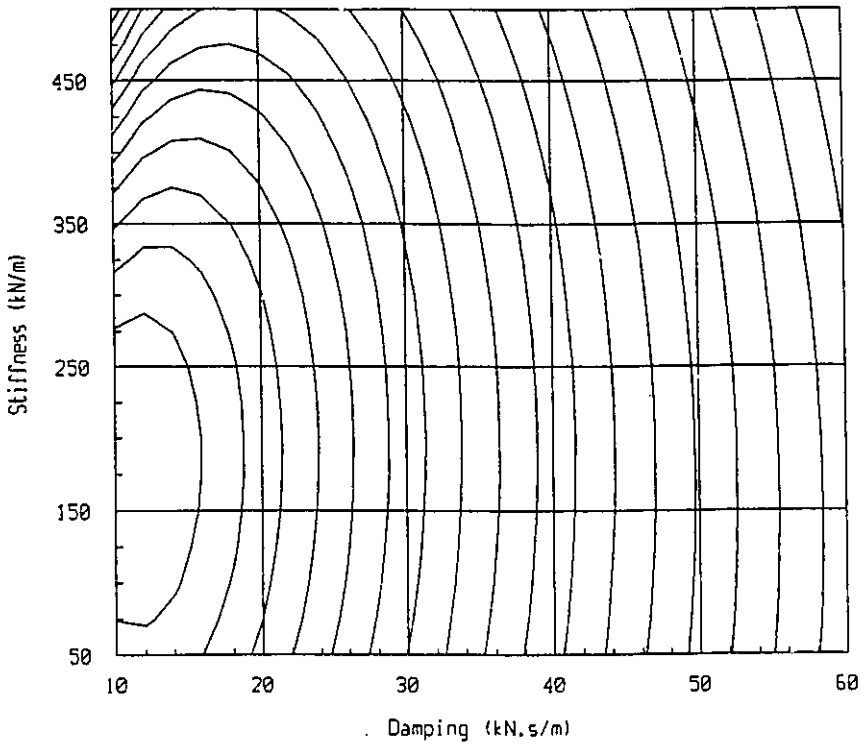

(3.7a Tire 1)

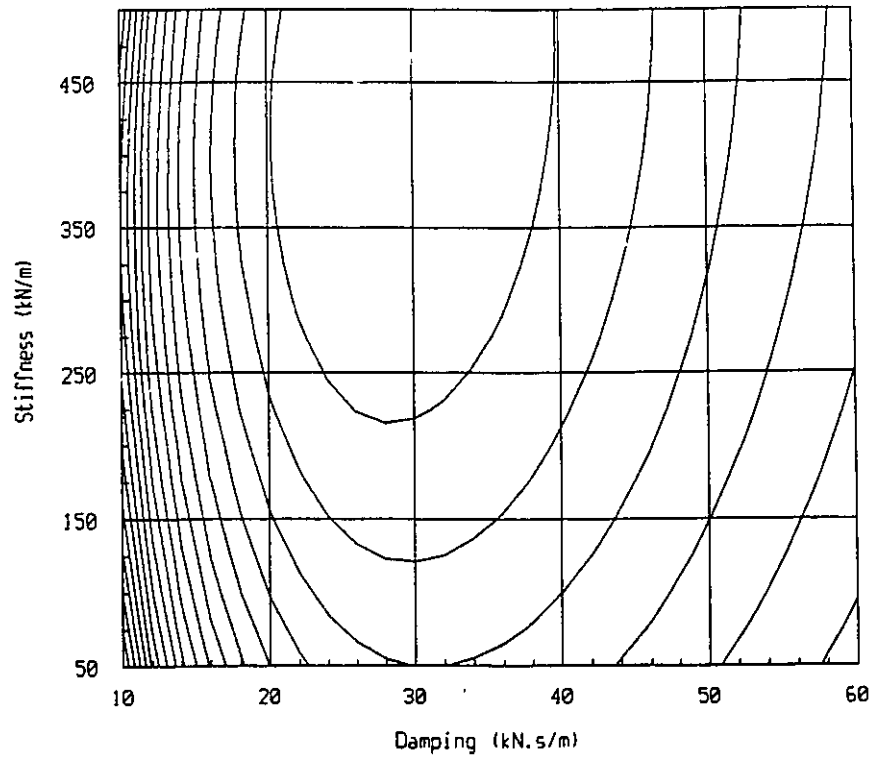

(3.7b Tire 2)

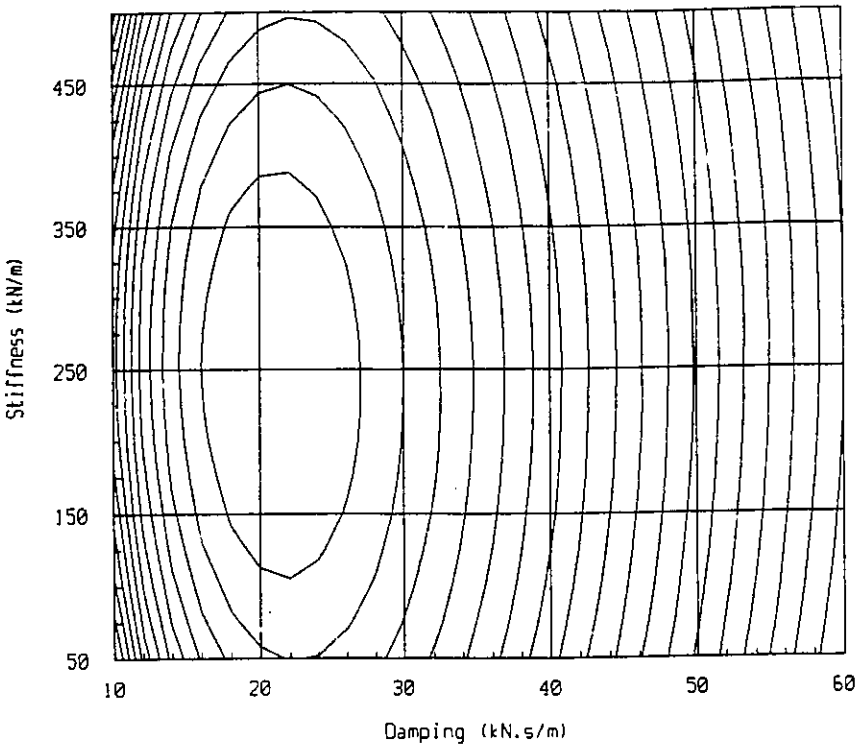

(3.7c Tire 3)

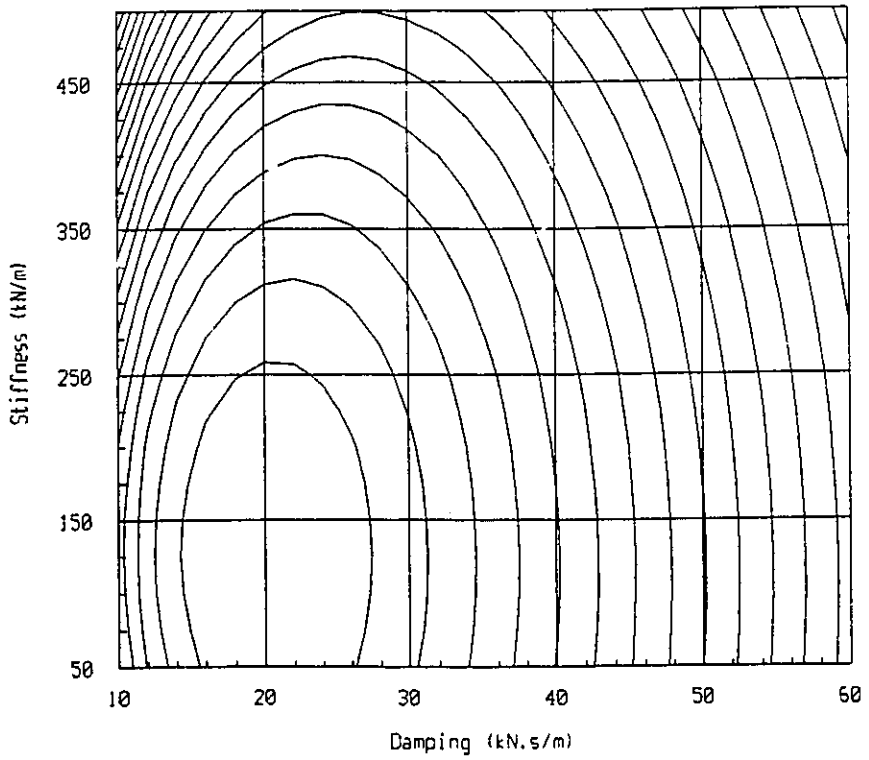

(3.7d Tire 4)

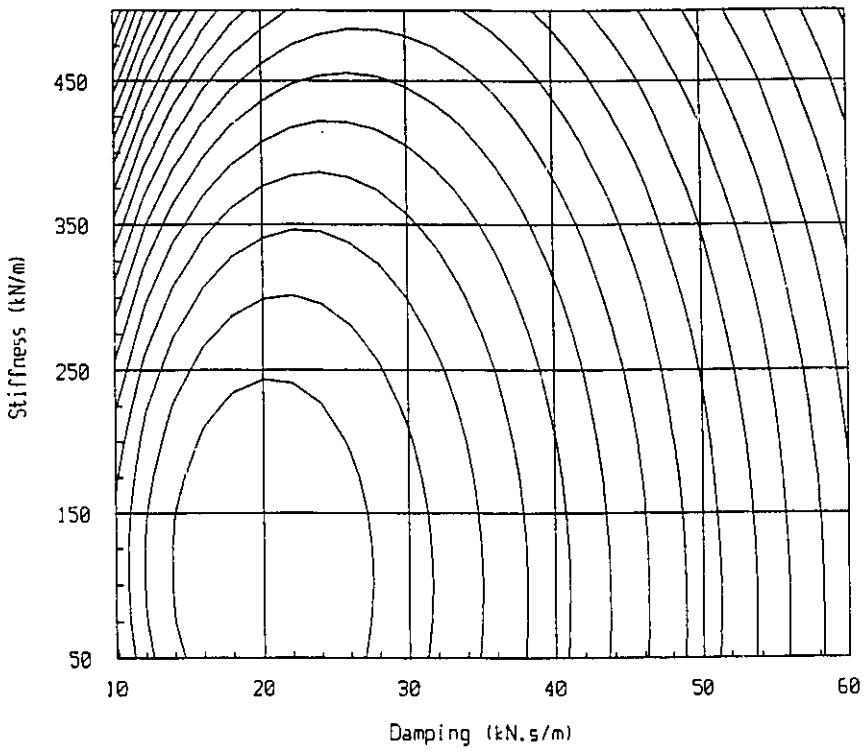

(3.7e Tire 5)

Figure 3.7 Iso-value curves of mean square tire deflections.

The results presented in Figures 3.3 to 3.7 are examined to identify a range of suspension parameters that can provide best compromise among the different components of the performance index. Although attempts are made to identify a single optimum parameter value to meet all the design objectives, a range of optimum parameters is identified in certain cases when conflicting design requirements exist. The optimum suspension parameters derived from the results of the covariance analysis are summarized in Table 3.2. The table describes the ideal suspension parameters required to achieve five design objectives including: static suspension deflection, ride quality, cargo safety, dynamic suspension deflection, and dynamic tire deflection.

The range of suspension stiffness parameters is identified based upon static deflections in the 0.05 to 0.15 *m* range, assuming static load equalization between he tandem axles. Since the design objectives related to ride quality, cargo safety and dynamic suspension and tire deflections pose conflicting requirements on the suspension design, optimum parameters can not be identified to meet all the design objectives. Although soft and lightly damped suspensions yield enhanced ride quality and cargo safety, soft suspensions are not desirable to meet the design objectives related to dynamic suspension deflection. The desirable values of suspension stiffness and damping for realization of improved ride quality and cargo safety are thus indicated as *"low"* in the table. The suspension damping parameters required to meet the suspension deflection objective are indicated as *"high"* in a similar manner. Using the contour plots of the dynamic tire deflections, optimum suspension parameters are identified to achieve minimal tire deflection and thus minimal dynamic tire loads transmitted to the pavement. After setting up the ranges of suspension parameters that would best satisfy each of the design requirements, an initial selection of the nominal suspension stiffness and damping is made. When selecting the nominal suspension parameters conflicting design requirements have to

be carefully considered to achieve a compromise. The resulting suspension should not jeopardize any of the design requirements. A set of nominal suspension parameters is derived to achieve a compromise among the different components of the performance index. This initial set of nominal parameters is presented in Table 3.2.

Table 3.2 Ranges of suspension stiffness and damping parameters required for each design objective.

Design objective →	*Static deflection requirement: 0.15 to 0.05 m*	*Ride quality/cargo safety*	*Low suspension deflections*	*Low tire deflections*	*1st Selection of nominal suspension parameters*
Stiffnesses 1.	154K to 432K	Low	Optimum exists depending on damping	180 K	180 K
2.	226K to 680K			410 K	300 K
3.	226K to 680K			250 K	300 K
4.	230K to 688K			110 K	300 K
5.	230K to 688K			110 K	300 K
Damping 1.	—	Low	High	11 K	11 K
2.	—			31 K	22 K
3.	—			22 K	22 K
4.	—			21 K	22 K
5.	—			21 K	22 K

3.7.2 Frequency Response Characteristics of the Passively Suspended Vehicle

The covariance analysis represents a first step in choosing the "optimum" passive suspension parameters. The results obtained from the covariance analysis, however, are based on the mean square values of the penalized variables and thus yield an overall measure of the performance. A study of the resonant behavior and frequency components of the response characteristics necessitates the frequency response analysis. While the nominal suspension parameters obtained from the covariance analysis (last column of Table 3.2) are used to obtain the frequency response characteristics, the suspension parameters are varied to further tune the suspension design and to achieve better

compromise among the different performance objectives. The power spectral density of the bounce and pitch acceleration response of the tractor and semitrailer sprung weights, suspension deflections and tire forces are derived using EQ (3.19) for suspension values variations around the nominal parameters. A preliminary examination of the frequency response characteristics revealed that the only adjustment deemed necessary was the increase in the damping coefficients of the fourth and fifth suspensions. This adjustment was carried out in an attempt to reduce the deflection response of the fourth and fifth axle suspensions and tires. The resulting final, referred to as "optimum", passive suspension parameter values are shown in Table 3.3.

Table 3.3 "Optimum" suspension parameters

	Nominal suspension parameters
Stiffnesses 1.	180 K
2.	300 K
3.	300 K
4.	300 K
5.	300 K
Damping 1.	11 K
2.	22 K
3.	22 K
4.	33 K
5.	33 K

The effects of varying the damping and stiffness properties of the suspension on the frequency response characteristics are further investigated to verify the conclusions drawn from the covariance analysis. While the performance index comprises 14 variants, the bounce and pitch acceleration response of the tractor and semitrailer and the deflection response of the second and fifth axle suspensions and tires are presented to demonstrate the effectiveness of the covariance analysis. Although the covariance analysis was performed using the disturbance vector based upon a smooth road, the frequency response

analyses are performed for excitations arising from smooth, medium rough, and rough roads to further demonstrate the validity of the analysis for varying road conditions.

Figures 3.8a and 3.8b illustrate the influence of road roughness and variations in suspension parameters on the bounce acceleration *PSD* of the tractor sprung mass. While the magnitude of the acceleration response increases considerably in the entire frequency range with increase in the road roughness, the response characteristics reveal identical dependency upon variations in the suspension parameters. Soft suspension yield improved ride response, irrespective of the road roughness. An increase or decrease in the suspension damping tends to increase the acceleration response in specific frequency ranges, irrespective of the road roughness. These observations support the conclusions drawn from the covariance analysis and demonstrate the validity of the covariance analysis for varying road conditions.

The covariance analysis was performed to derive the mean square values of different performance variables under excitations arising from rough and medium rough roads for the "optimum" suspension parameters. The resulting mean square values are compared to those derived for the smooth road, as illustrated in Table 3.4.

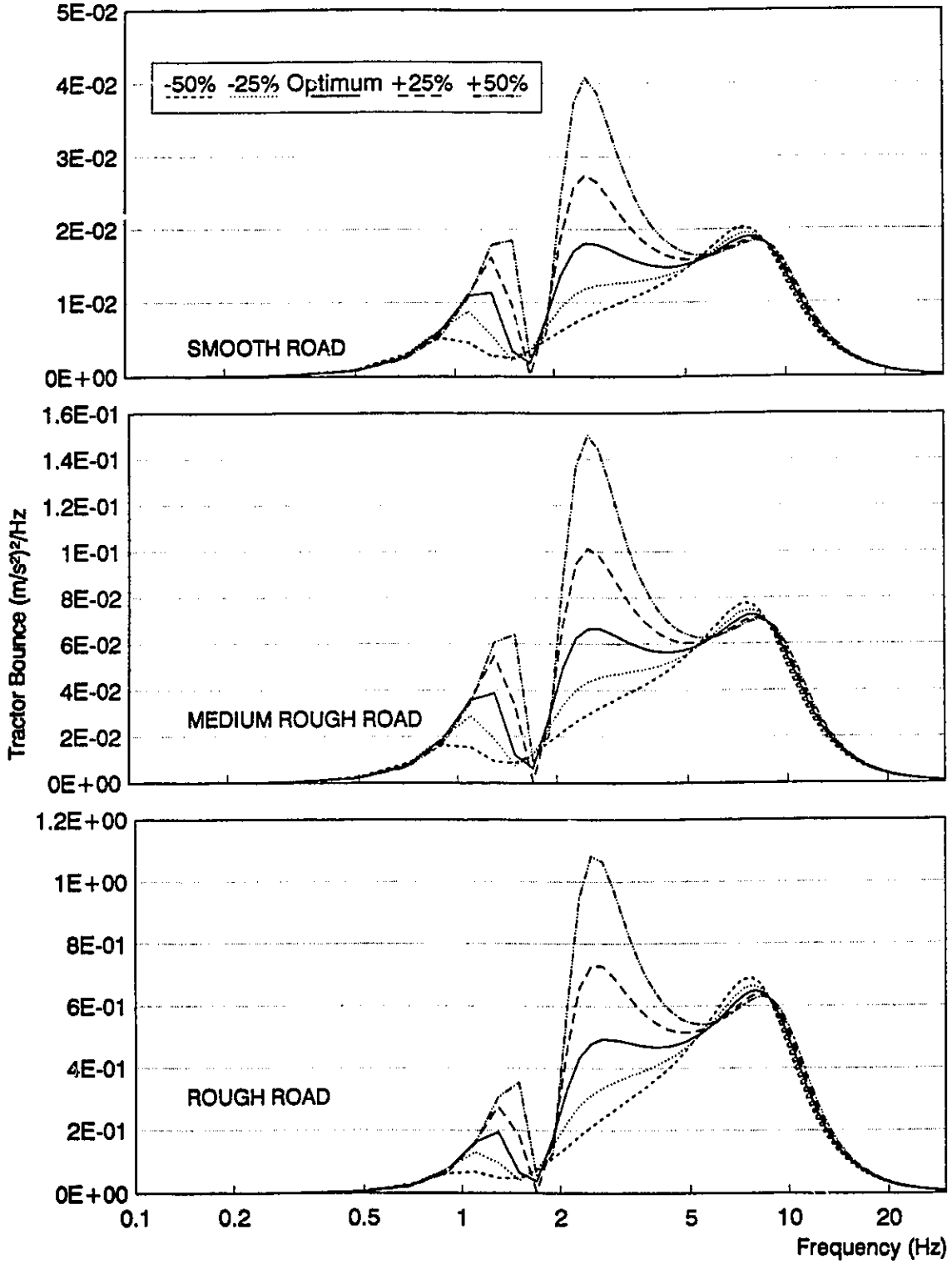

Figure 3.8a Effect of varying suspension stiffness on tractor bounce acceleration for smooth, medium rough, and rough roads.

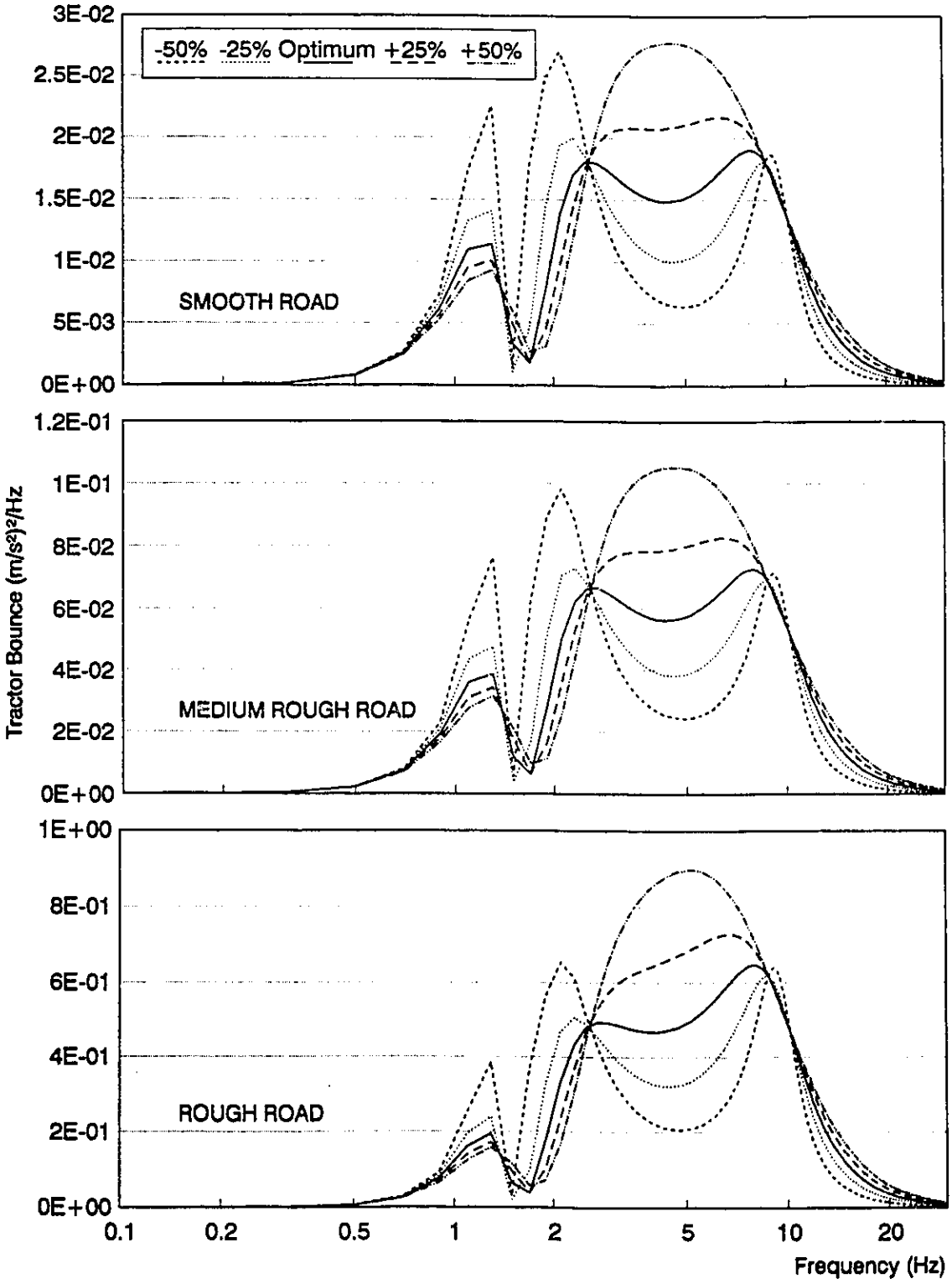

Figure 3.8b Effect of varying suspension damping on tractor bounce acceleration for smooth, medium rough, and rough roads.

Table 3.4 Mean square value of the output variables for different roads
(v = 90 km/h and "optimum" suspension parameters).

Performance variable	*Smooth road*	*Medium rough road*	*Rough road*
Tractor bounce acceleration	1.976e-1	7.473e-1	6.369e+0
Tractor pitch acceleration	3.563e-2	1.343e-1	1.120e+0
Semitrailer bounce acceleration	1.762e-1	6.581e-1	5.306e+0
Semitrailer pitch acceleration	9.585e-4	3.553e-3	2.784e-2
Suspension 1 deflection	3.206e-6	1.152e-5	8.159e-5
Suspension 2 deflection	3.581e-6	1.287e-5	8.831e-5
Suspension 3 deflection	5.212e-6	1.866e-5	1.256e-4
Suspension 4 deflection	4.410e-6	1.581e-5	1.057e-4
Suspension 5 deflection	4.936e-6	1.761e-5	1.158e-4
Tire 1 deflection	1.573e-6	5.962e-6	5.157e-5
Tire 2 deflection	1.401e-6	5.313e-6	4.608e-5
Tire 3 deflection	1.652e-6	6.239e-6	5.308e-5
Tire 4 deflection	1.511e-6	5.677e-6	4.705e-5
Tire 5 deflection	1.570e-6	5.890e-6	4.845e-5

Figures 3.9 to 3.16 present the effect of variations in suspension parameters on the frequency response characteristics of the vehicle subjected to excitations arising from a rough road. Figures 3.9 and 3.10 reveal that for a given damping value, an increase in suspension stiffness yields an increase in tractor and semitrailer bounce and pitch acceleration response in the entire frequency range. A soft suspension may be desirable to achieve improved ride quality and cargo safety. Reduction in the suspension spring rate further yields small reduction in the peak suspension deflection as illustrated in Figures 3.11a and 3.11b. The dynamic tire forces at low frequencies also decrease with soft suspension as shown in Figures 3.12a and 3.12b. The tire forces beyond 4 *Hz*, however, increase with decrease in suspension spring rate. The "optimum" suspension stiffness values presented in Table 3.3 may thus be considered to provide an overall good performance without compromising the static suspension deflection requirements.

The selection of adequate suspension damping (once the stiffness is fixed) involves a compromise between low and high frequency performance. For a given stiffness, an increase in the suspension damping results in improved ride quality, cargo safety and tire forces only at low frequencies (below 2.5 *Hz*). The ride quality, cargo safety and tire forces, however, deteriorate at frequencies above 2.5 *Hz*, as shown in Figures 3.13, 3.14 and 3.16. The rattle space requirements, however, decrease throughout the frequency range with increase in suspension damping, as shown in Figure 3.15. The "optimum" damping parameters are thus considered to provide an adequate compromise among the different performance objectives.

The "optimum" suspension parameters thus result in suspension static deflections that are within the acceptable limits, as shown in Table 3.5.

Table 3.5 Static deflections of the "optimum" suspension

Axle suspension	*Deflection (m)*
Suspension 1	.1286
Suspension 2	.1133
Suspension 3	.1133
Suspension 4	.1148
Suspension 5	.1148

The eigen values, natural frequencies (*Hz*) and damping ratios associated with different deflection modes of the tractor-semitrailer with "optimum" passive suspension are derived as follows:

$-4.55 \pm 10.53i$ $f_n = 1.82$, $\zeta_d = 0.396$; tractor bounce

$-2.41 \pm 08.59i$ $f_n = 1.42$, $\zeta_d = 0.270$; semitrailer bounce

$-5.61 \pm 11.91i$ $f_n = 2.09$, $\zeta_d = 0.426$; tractor pitch and semitrailer pitch

$-22.10 \pm 53.16i$ $f_n = 9.62$, $\zeta_d = 0.365$; axle 1 bounce

$-21.05 \pm 56.21i$ $f_n = 9.55$, $\zeta_d = 0.350$; axle 2 bounce

$-21.50 \pm 56.29i$ $f_n = 9.59$, $\zeta_d = 0.356$; axle 3 bounce

$-49.42 \pm 44.06i$ $f_n = 10.53$, $\zeta_d = 0.746$; axle 4 bounce

$-48.52 \pm 56.21i$ $f_n = 11.81$, $\zeta_d = 0.653$; axle 5 bounce

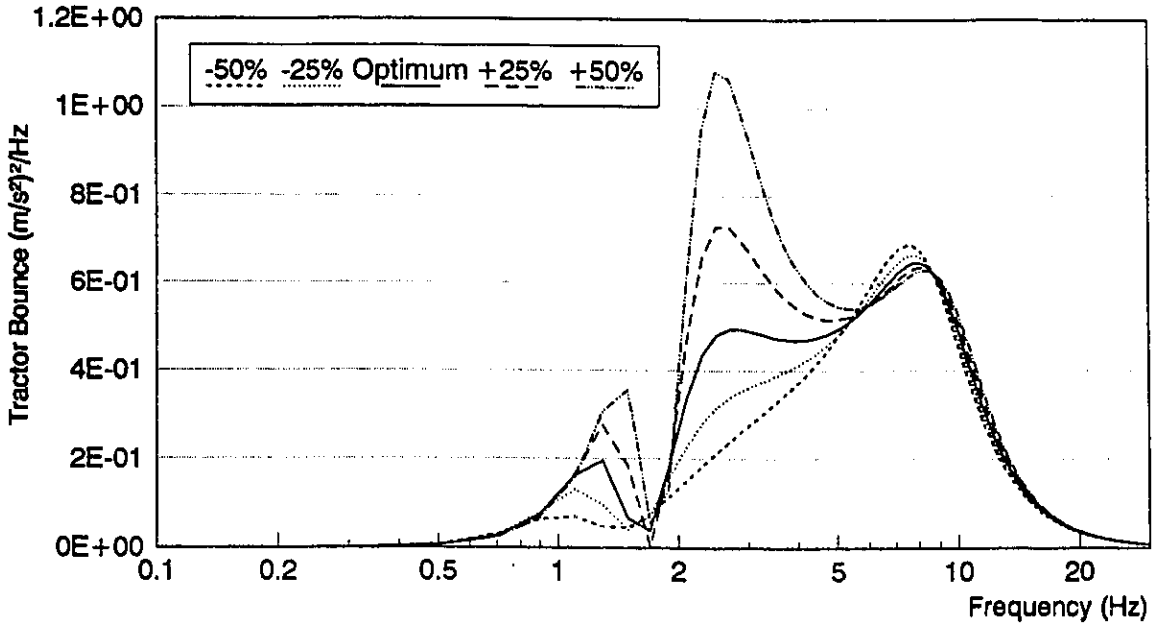

Figure 3.9a Effect of varying suspension stiffness on tractor bounce acceleration

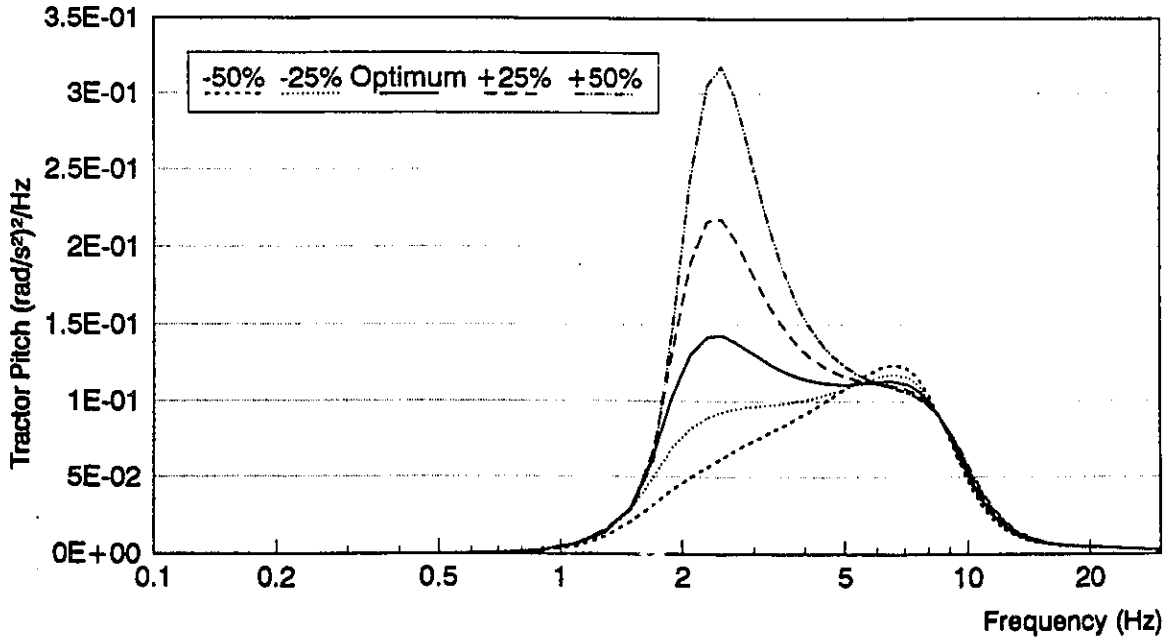

Figure 3.9b Effect of varying suspension stiffness on tractor pitch acceleration

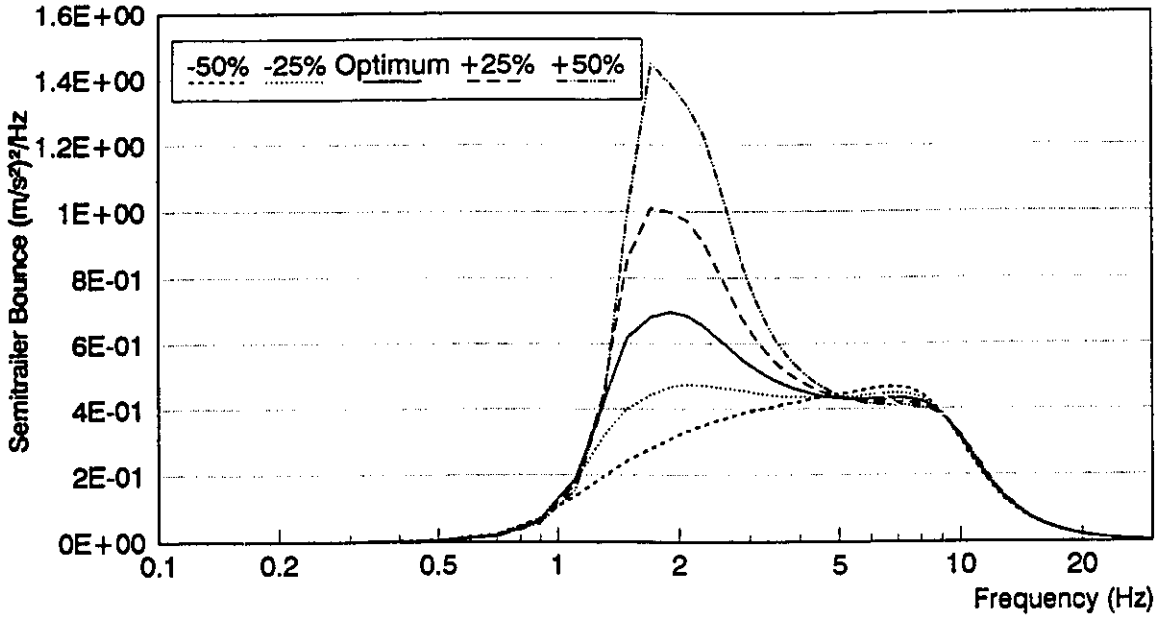

Figure 3.10a Effect of varying suspension stiffness on semitrailer bounce acceleration

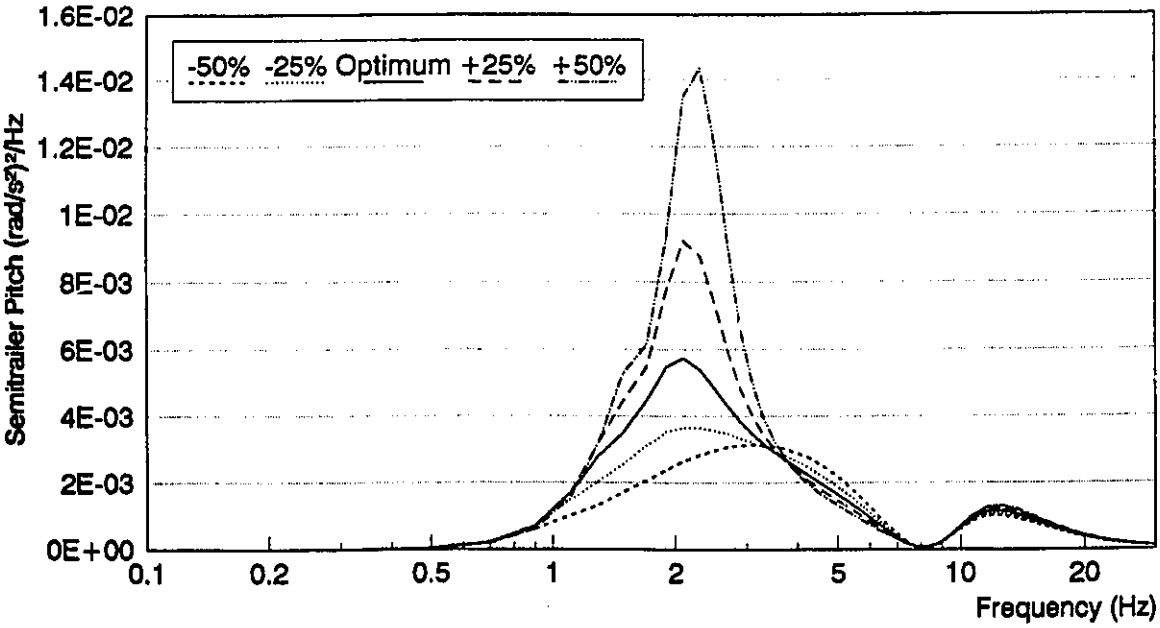

Figure 3.10b Effect of varying suspension stiffness on semitrailer pitch acceleration

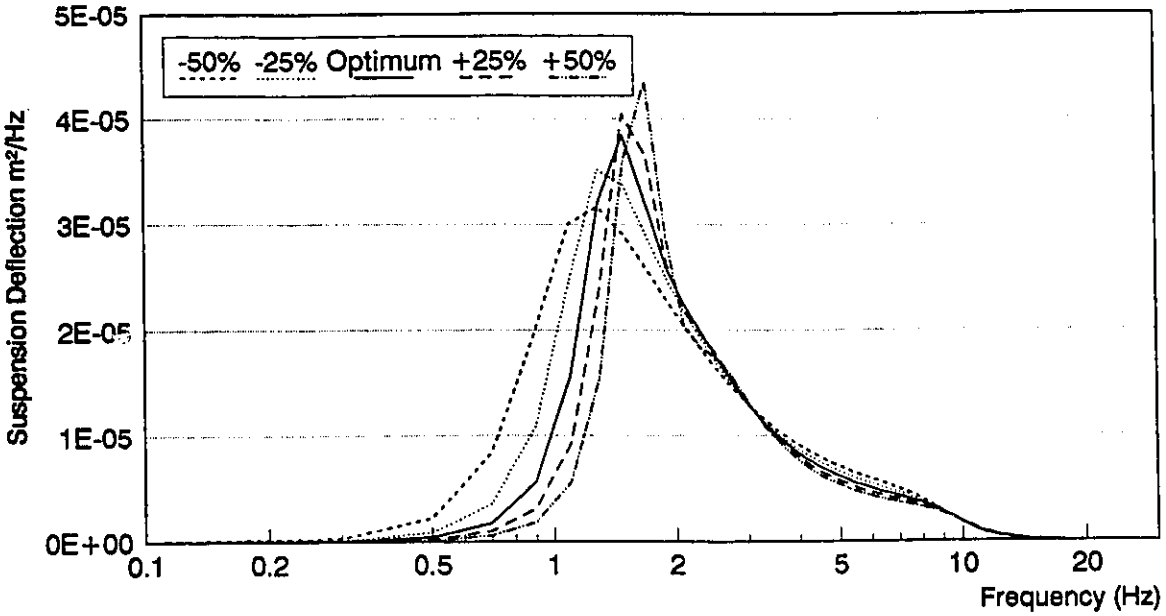

Figure 3.11a Effect of varying stiffness on second suspension deflection

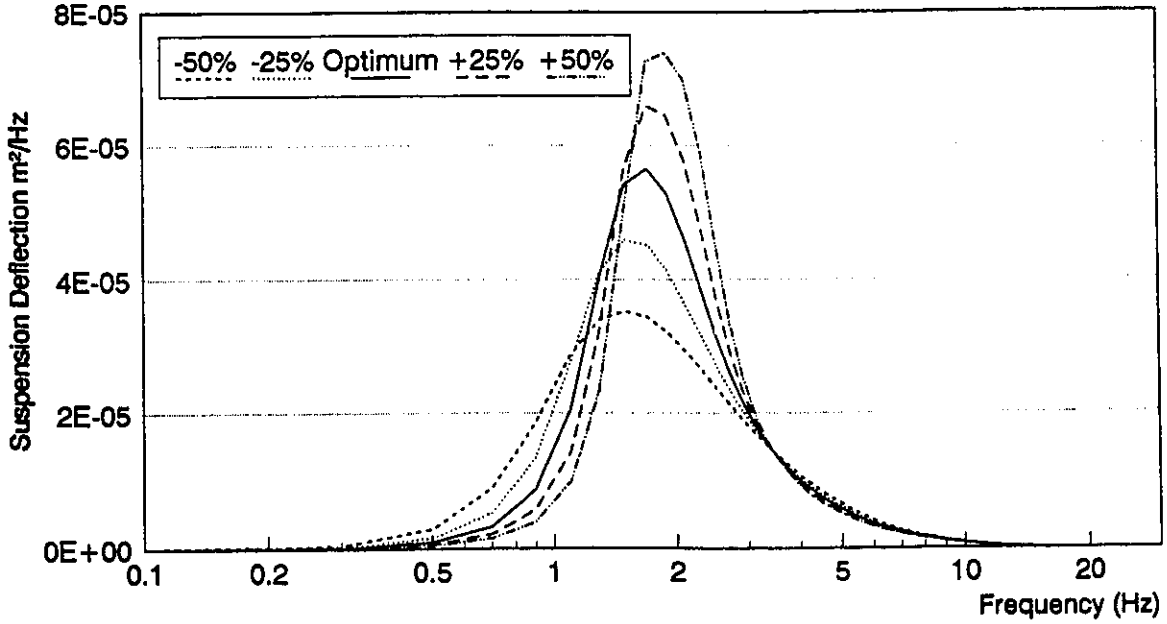

Figure 3.11b Effect of varying stiffness on fifth suspension deflection

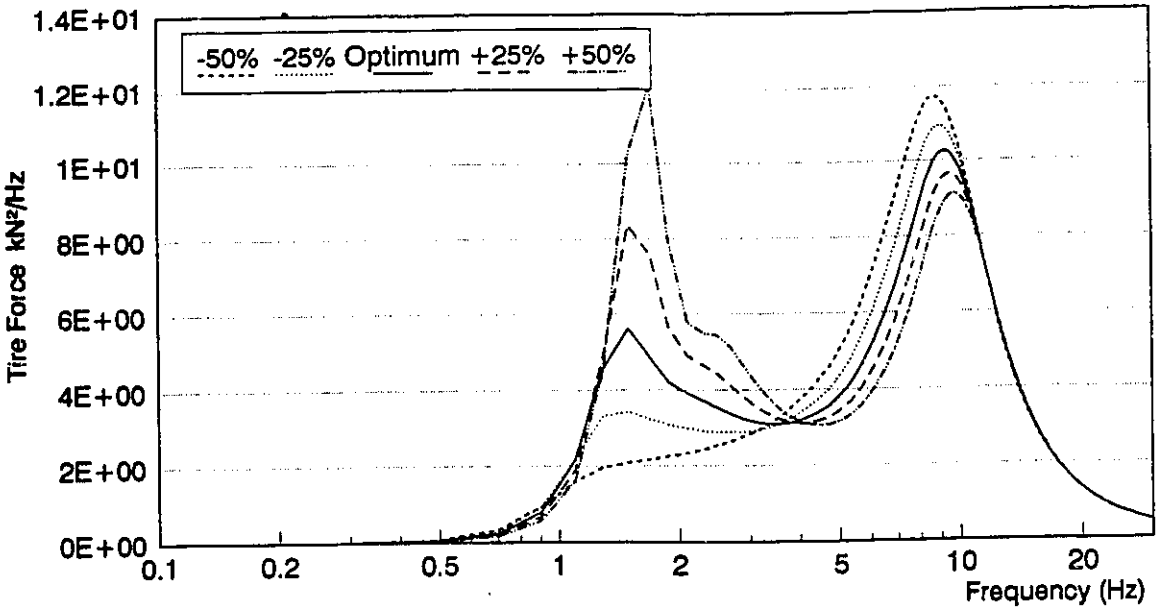

Figure 3.12a Effect of varying suspension stiffness on second tire force

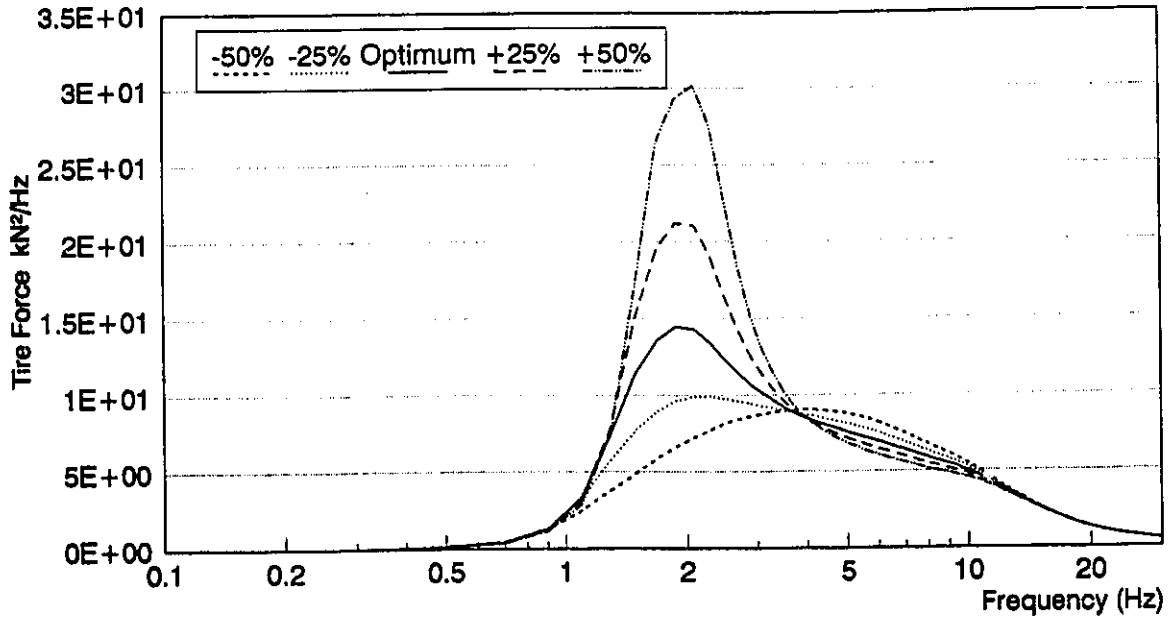

Figure 3.12b Effect of varying suspension stiffness on fifth tire force

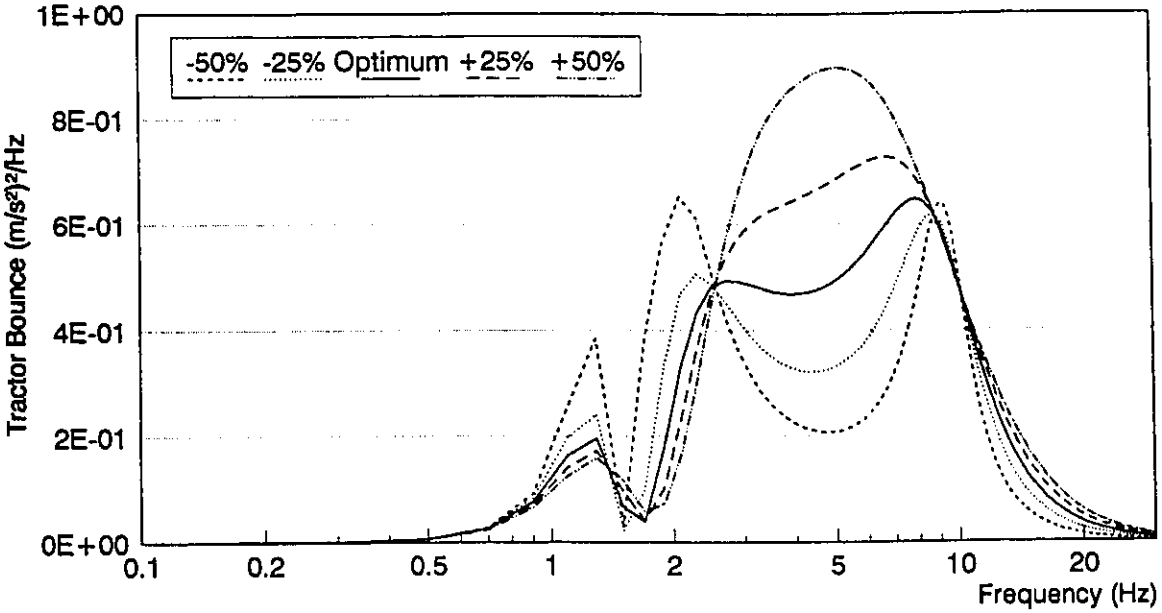

Figure 3.13a Effect of varying suspension damping on tractor bounce acceleration

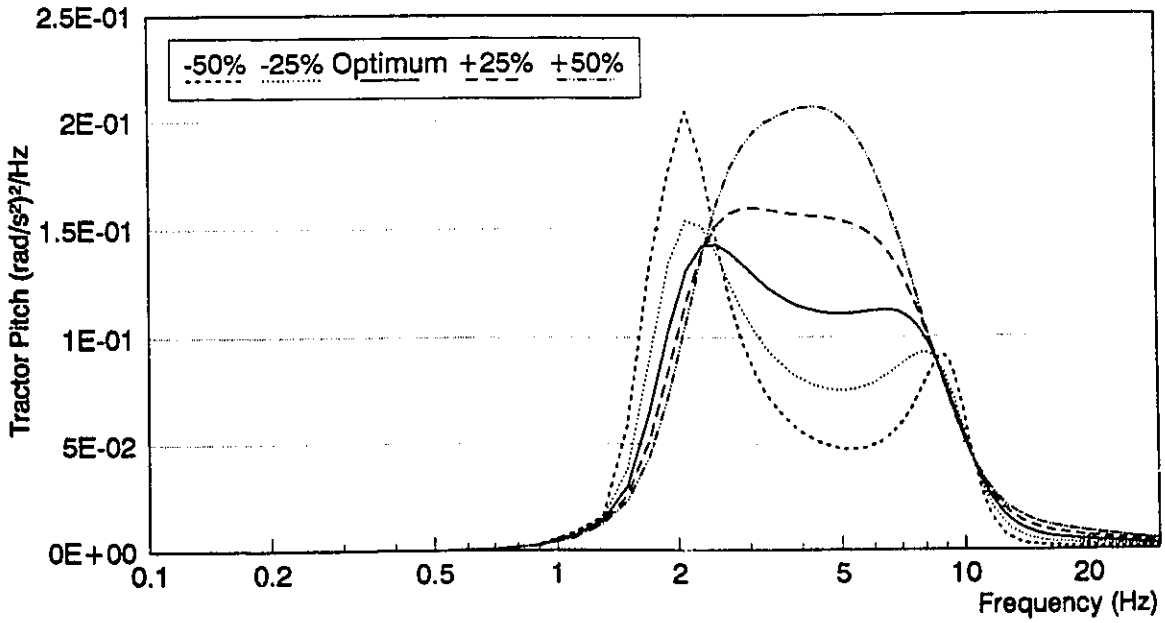

Figure 3.13b Effect of varying suspension damping on tractor pitch acceleration

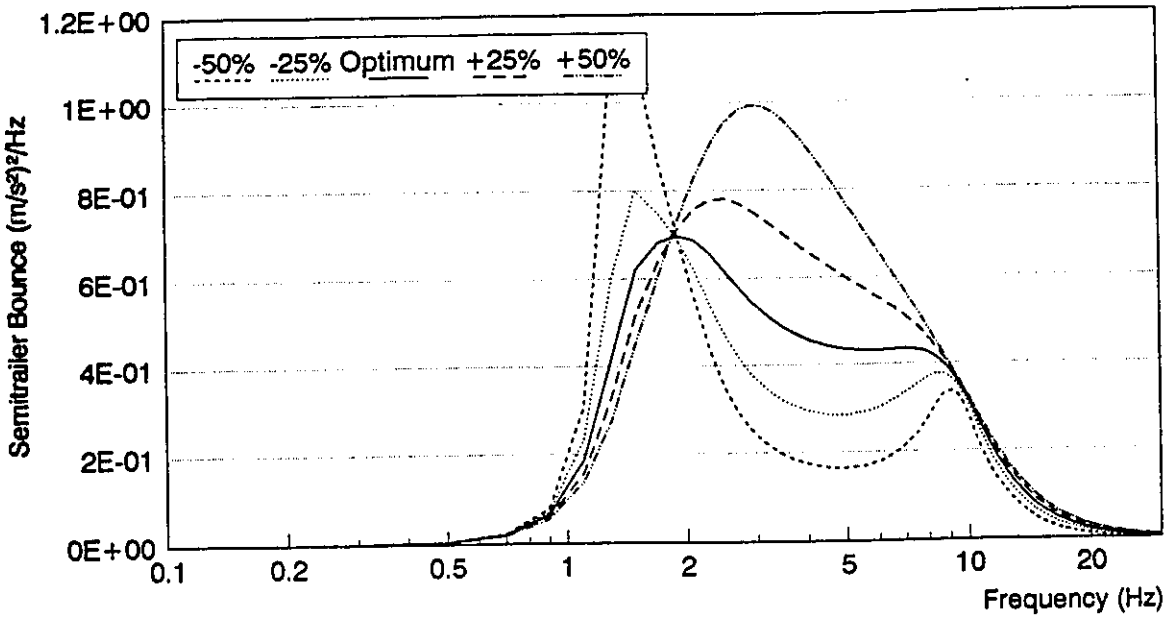

Figure 3.14a Effect of varying suspension damping on semitrailer bounce acceleration

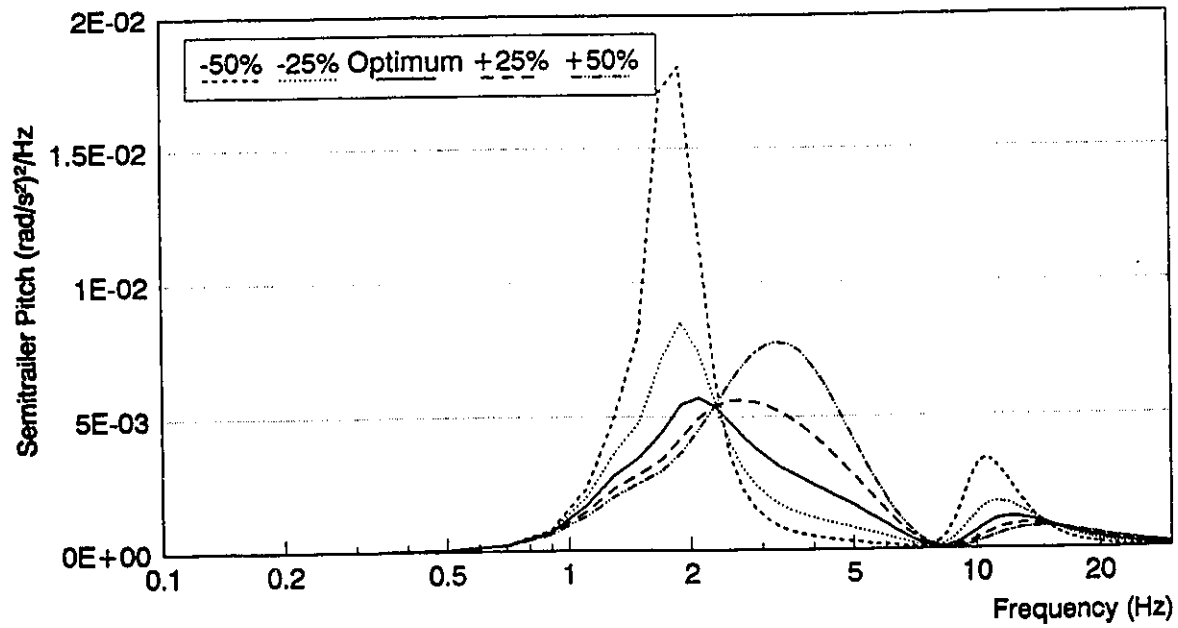

Figure 3.14b Effect of varying suspension damping on semitrailer pitch acceleration

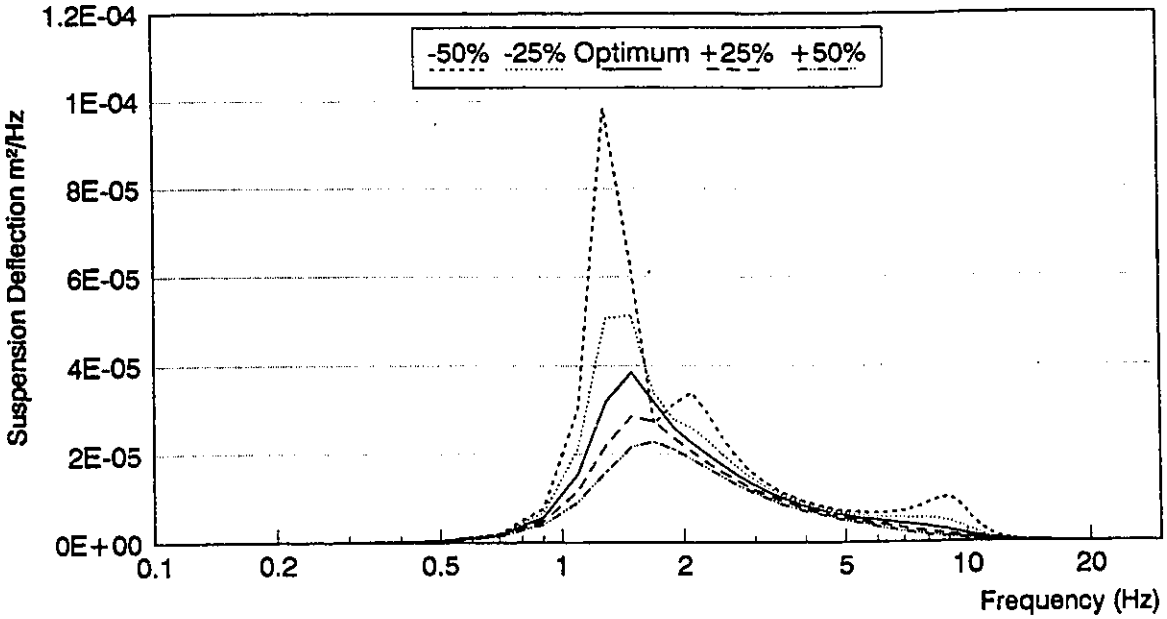

Figure 3.15a Effect of varying damping on second suspension deflection

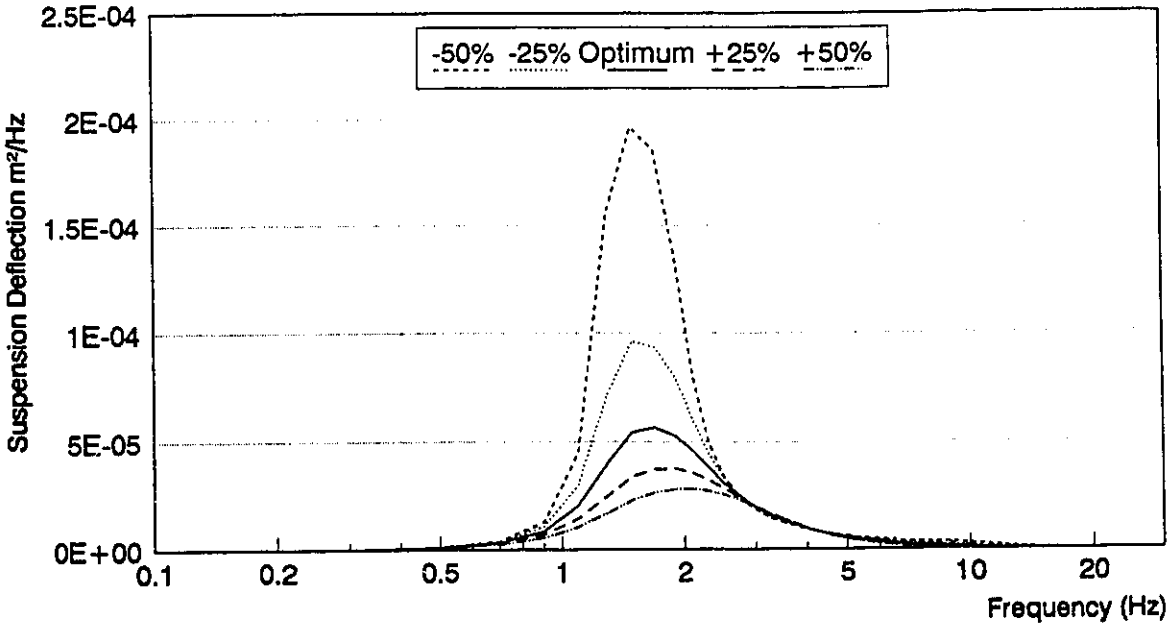

Figure 3.15b Effect of varying damping on fifth suspension deflection

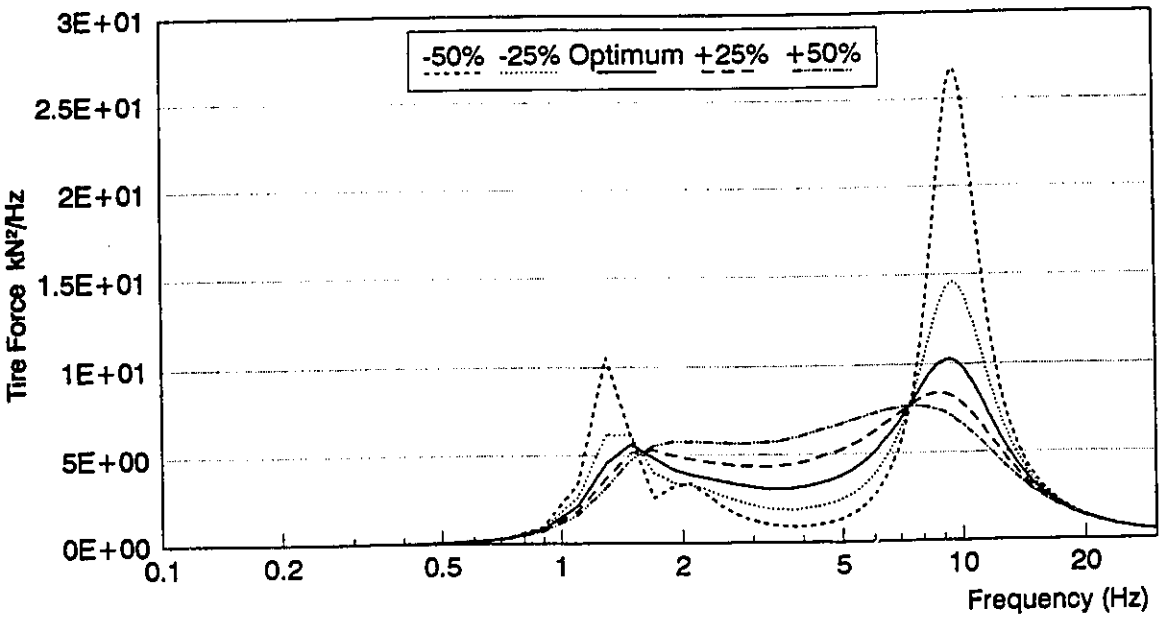

Figure 3.16a Effect of varying suspension damping on second tire force

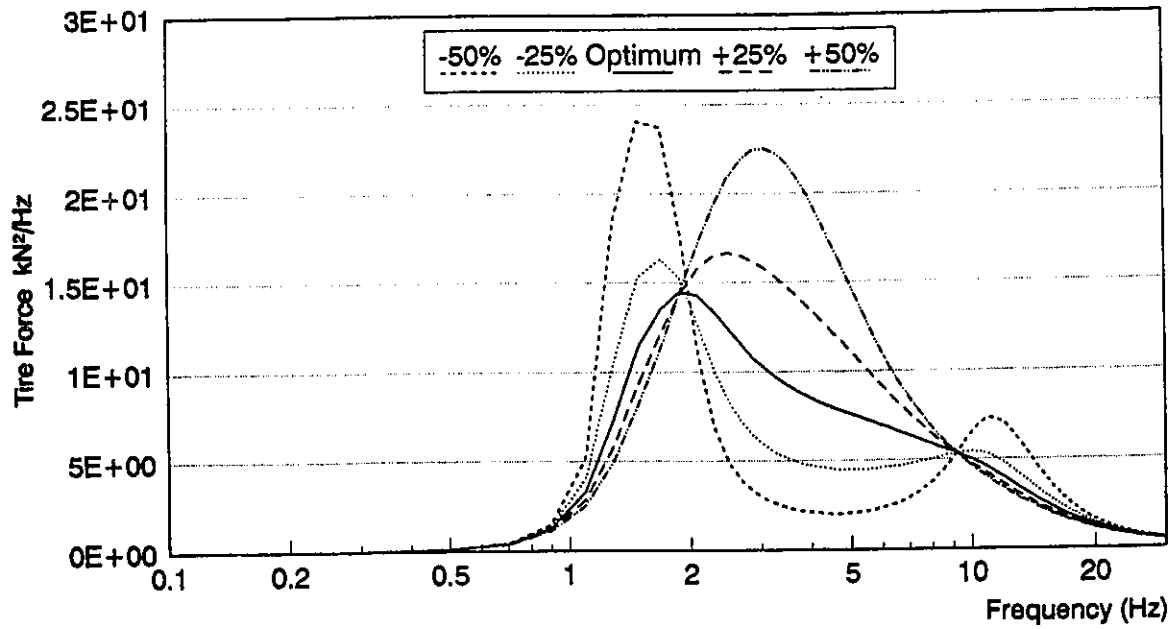

Figure 3.16b Effect of varying suspension damping on fifth tire force

3.8 SUMMARY

A method based on covariance analysis was demonstrated for the selection of an "optimum" passive suspension for the tractor-semitrailer. The second order coupled differential equations of motion of the 9 *DOF* planar vehicle model reduced to the first order state-space form were augmented with the road excitation. The objectives of the suspension design are expressed in a matrix form as a function of the augmented state vector comprising tractor and semitrailer bounce and pitch acceleration, suspension deflections and tire deflections. The performance index is then formulated and each of its components is determined separately. The validity of the mathematical freight vehicle model is examined using the data obtained from the road tests conducted by *CONCAVE Research Centre*. The effects of variations in suspension parameter on the penalized variables are investigated to achieve a better compromise among different performance objectives. The results demonstrate the effectiveness and convenience of the covariance technique in selecting the nominal suspension.

3.9 REFERENCES

1. International Organization for Standardization, "*Guide for Evaluation of Human Exposure to Whole Body Vibration,*" ISO 2631, 1974(E).

2. A. E. Bryson and Y. C. Ho, " *Applied Optimal Control. Optimization, Estimation, and Control,*" New York, John Wiley and Sons, 1975.

3. W. D. Hoskins, D. S. Meek and D. J. Walton, " *The Numerical Solution of* $AQ+QA=-C$," IEEE Transactions of Automatic Control, Vol. AC-22, No. 5, October 1977, pp. 882-883.

4. C J. Dodds, *"The Laboratory Simulation of Vehicle Service Stress,"* Journal of Engineering for Industry, ASME Transactions, May 1974, Vol. 96, No. 2, pp. 391-398.

5. C. J. Dodds, and J. D. Robson, *"The Description of Road Surface Roughness,"* Journal of Sound and Vibration, 1973, Vol. 31, No. 2, pp. 175-184.

6. J. D. Robson, *"Road Surface Description and Vehicle Response,"* International Journal of Vehicle Design, 1979, Vol. 1, No. 1, pp. 25-35.

7. J. S. Bendat and A. G. Piersol, *"Random Data: Analysis and Measurement Procedures,"* Whiley-Interscience, 1971, Toronto, Ontario, Canada.

8. *"Ride Vibration Levels at the Driver-Seat Interface, Part 1: Measuremeni, Analysis and Assessment of Heavy Vehicle Ride Vibrations,"* prepared by Concave Research Centre, Department of Mechanical Engineering, Concordia University Montreal, Canada for Transportation Development Centre, Transport Canada, Report No. CONCAVE-02-87.

CHAPTER 4

IDEAL *LQG* ACTIVE SUSPENSION DESIGN

4.1 INTRODUCTION

Design of a passive vehicle suspension involves a careful compromise among the various conflicting design requirements, such as ride, handling and directional control. Results presented in Chapter 3 further illustrate the complexities associated with conflicting design requirements posed by the ride quality, suspension deflections and tire forces. In view of the inherent performance limitations of passive suspensions, a number of active suspension concepts have been proposed to strike a better compromise among different design requirements. Although various active suspension designs have been developed for cars, light trucks and railway vehicles [1-8], their general implementation has been severely limited due to high cost, poor reliability and high complexity. The demand for improved working conditions, cargo safety, low dynamic pavement loads, handling and stability performance of heavy vehicles, however, has been growing steadily. This, coupled with availability of more economical and reliable hardware, has resulted in renewed interest in active suspensions as feasible alternative to passive suspensions. While, drivers of passenger cars can benefit greatly from active suspensions, the potential and effectiveness of active suspensions can best be harnessed to enhance the performance of

heavy vehicles. Heavy trucks and articulated vehicles exhibit complex ride behavior and significant dynamic tire forces when compared to passenger cars. A review of measured ride vibration data at the driver's seat revealed that the ride vibration levels of heavy trucks are 9 to 16 times higher than those of the passenger cars [9]. Moreover, most heavy vehicle drivers are exposed to ride vibrations for 10 to 20 hours a day. The ride vibrations of heavy freight vehicles have a significant influence on the driver fatigue and safety. In view of driver health and safety risks associated with prolonged exposure to high levels of ride vibrations, and significant dynamic tire forces resulting in accelerated pavement deterioration, the effectiveness of advanced suspensions need to be further investigated for use in heavy vehicles.

In this chapter, an ideal active suspension scheme based on full-state feedback is investigated to evaluate its performance potentials for freight vehicles. While the design aspects are briefly addressed, the performance characteristics of the ideal active suspension are compared to those of the "optimum" passive suspension to determine their potential performance benefits.

4.2 MATHEMATICAL FORMULATION

An articulated freight vehicle is analytically modeled as illustrated in Figure 4.1 and described in Chapter 2. The vehicle model comprises the tractor and semitrailer sprung masses each with bounce and pitch *DOF*. The tractor is represented by a planar rigid body, m_{s1}, supported by three axle suspensions. The semitrailer is modeled by a planar rigid body m_{s2}, and is assumed to have two independent axles. The drive and semitrailer axles are represented by independent axle suspensions. The lumped unsprung mass of each wheel and axle assembly is represented by m_{ui} with only vertical *DOF*. The elastic property of each tire is characterized by a linear stiffness element, K_{ti}, assuming point contact with

the road and negligible wheel hop motion. The suspension stiffness and damping elements as well as the tire stiffness coefficients are assumed to be linear. Each axle suspension is represented by a linear spring and a viscous damper in parallel as seen in Figure 4.1, these passive elements are supplemented by active force generators. The control forces u_1 to u_5 are generated using a control scheme and the feedback from road excitations and vehicle response variables to reduce a given cost function or performance index. An active suspension thus hereafter refers to a parallel combination of passive elements and an active force generator. Such a parallel arrangement reduces the power requirements of an active force generator, and permits the study of influence of variations in the passive element rates on the suspension performance and the actuators power requirement. Furthermore, a parallel combination of active-passive elements yields a fail-safe suspension design.

Assuming linear behavior for all elements and small angular displacements, a set of second order coupled differential equations characterizing the ride dynamics of the baseline actively suspended vehicle are derived as follows;

Vertical displacement of the tractor:

$$\begin{aligned} & m_{s1}\ddot{r}_1 + \\ & C_1(\dot{r}_1 + A_1\dot{r}_2 - \dot{r}_5) + C_2(2\dot{r}_1 - B_1\dot{r}_2 - \dot{r}_6 - B_2\dot{r}_2 - \dot{r}_7) + C_5(\dot{r}_1 - B_5\dot{r}_2 - \dot{r}_3 - A_2\dot{r}_4) + \\ & K_1(r_1 + A_1r_2 - r_5) + K_2(2r_1 - B_1r_2 - r_6 - B_2r_2 - r_7) + K_5(r_1 - B_5r_2 - r_3 - A_2r_4) + \\ & u_1 + u_2 + u_3 = 0 \end{aligned} \tag{4.1a}$$

Pitch displacement of the tractor:

$$\begin{aligned} & I_{y1}\ddot{r}_2 + C_1A_1(\dot{r}_1 + A_1\dot{r}_2 - \dot{r}_5) + C_2[B_1(\dot{r}_1 - B_1\dot{r}_2 - \dot{r}_6) + \\ & B_2(\dot{r}_1 - B_2\dot{r}_2 - \dot{r}_7)] - C_5B_5(\dot{r}_1 - B_5\dot{r}_2 - \dot{r}_3 - A_2\dot{r}_4) + \\ & K_1A_1(r_1 + A_1r_2 - r_5) + K_2[B_1(r_1 - B_1r_2 - r_6) + \\ & B_2(r_1 - B_2r_2 - r_7)] - K_5B_5(r_1 - B_5r_2 - r_3 - A_2r_4) + A_1u_1 - B_1u_2 - B_2u_3 = 0 \end{aligned} \tag{4.1b}$$

Vertical displacement of the semitrailer:

$$
\begin{aligned}
&m_{s2}\ddot{r}_3 + \\
&C_3(\dot{r}_3 - B_3\dot{r}_4 - \dot{r}_8 + \dot{r}_3 - B_4\dot{r}_4 - \dot{r}_9) + C_5(\dot{r}_3 + A_2\dot{r}_4 - \dot{r}_1 + B_5\dot{r}_2) + \\
&K_3(r_3 - B_3r_4 - r_8 + r_3 - B_4r_4 - r_9) + K_5(r_3 + A_2r_4 - r_1 + B_5r_2) + \\
&u_4 + u_5 = 0
\end{aligned}
\tag{4.1c}
$$

Pitch displacement of the semitrailer:

$$
\begin{aligned}
&I_{y2}\ddot{r}_4 - C_3[B_3(\dot{r}_3 - B_3\dot{r}_4 - \dot{r}_8) + B_4(\dot{r}_3 - B_4\dot{r}_4 - \dot{r}_9)] + \\
&C_5A_2(\dot{r}_3 + A_2\dot{r}_4 - \dot{r}_1 + B_5\dot{r}_2) - K_3[B_3(r_3 - B_3r_4 - r_8) + \\
&B_4(r_3 - B_4r_4 - r_9)] + K_5A_2(r_3 + A_2r_4 - r_1 + B_5r_2) - \\
&B_3u_4 - B_4u_5 = 0
\end{aligned}
\tag{4.1d}
$$

Vertical displacement of axle 1:

$$
m_{u1}\ddot{r}_5 + C_1(\dot{r}_5 - \dot{r}_1 - A_1\dot{r}_2) + K_1(r_5 - r_1 - A_1r_2) + K_{t1}r_5 - u_1 = K_{t1}q_1 \tag{4.1e}
$$

Vertical displacement of axle 2:

$$
m_{u2}\ddot{r}_6 + C_2(\dot{r}_6 - \dot{r}_1 + B_1\dot{r}_2) + K_2(r_6 - r_1 + B_1r_2) + K_{t2}r_6 - u_2 = K_{t2}q_2 \tag{4.1f}
$$

Vertical displacement of axle 3:

$$
m_{u2}\ddot{r}_7 + C_2(\dot{r}_7 - \dot{r}_1 + B_2\dot{r}_2) + K_2(r_7 - r_1 + B_2r_2) + K_{t2}r_7 - u_3 = K_{t2}q_3 \tag{4.1g}
$$

Vertical displacement of axle 4:

$$m_{u2}\ddot{r}_8 + C_3(\dot{r}_8 - \dot{r}_3 + B_3\dot{r}_4) + K_3(r_8 - r_3 + B_3 r_4) + K_{13}r_8 - u_4 = K_{13}q_4 \qquad (4.1h)$$

Vertical displacement of axle 5:

$$m_{u3}\ddot{r}_9 + C_3(\dot{r}_9 - \dot{r}_3 + B_4\dot{r}_4) + K_3(r_9 - r_3 + B_4 r_4) + K_{13}r_9 - u_5 = K_{13}q_5 \qquad (4.1i)$$

The coupled differential equations of motion for the vehicle are represented in the following matrix form:

$$\boldsymbol{M}\ddot{\boldsymbol{r}} + \boldsymbol{C}\dot{\boldsymbol{r}} + \boldsymbol{K}_s\boldsymbol{r} + \boldsymbol{F}\boldsymbol{u} = \boldsymbol{K}_T\boldsymbol{q} \qquad (4.2)$$

where;

$\boldsymbol{M} \in \mathbb{R}^{9\times 9}$, is the mass matrix,

$\boldsymbol{C} \in \mathbb{R}^{9\times 9}$, is the damping matrix,

$\boldsymbol{K}_s \in \mathbb{R}^{9\times 9}$, is the stiffness matrix,

$\boldsymbol{F} \in \mathbb{R}^{9\times 5}$, is the matrix of control forces,

$\boldsymbol{K}_T \in \mathbb{R}^{9\times 5}$, is the tire stiffness matrix,

$\boldsymbol{r} \in \mathbb{R}^{9\times 1}$, is the vector of generalized coordinates,

$\boldsymbol{u} \in \mathbb{R}^{5\times 1}$, is the control forces vector,

and $\boldsymbol{q} \in \mathbb{R}^{5\times 1}$, is the road disturbance vector (defined in Chapter 2).

The presence of the damping matrix $\boldsymbol{C}$ and the stiffness matrix $\boldsymbol{K}_s$ in the ride dynamics equation (EQ (4.2)), arises from the fact that the suspension comprises an active actuator in parallel with passive stiffness and damping.

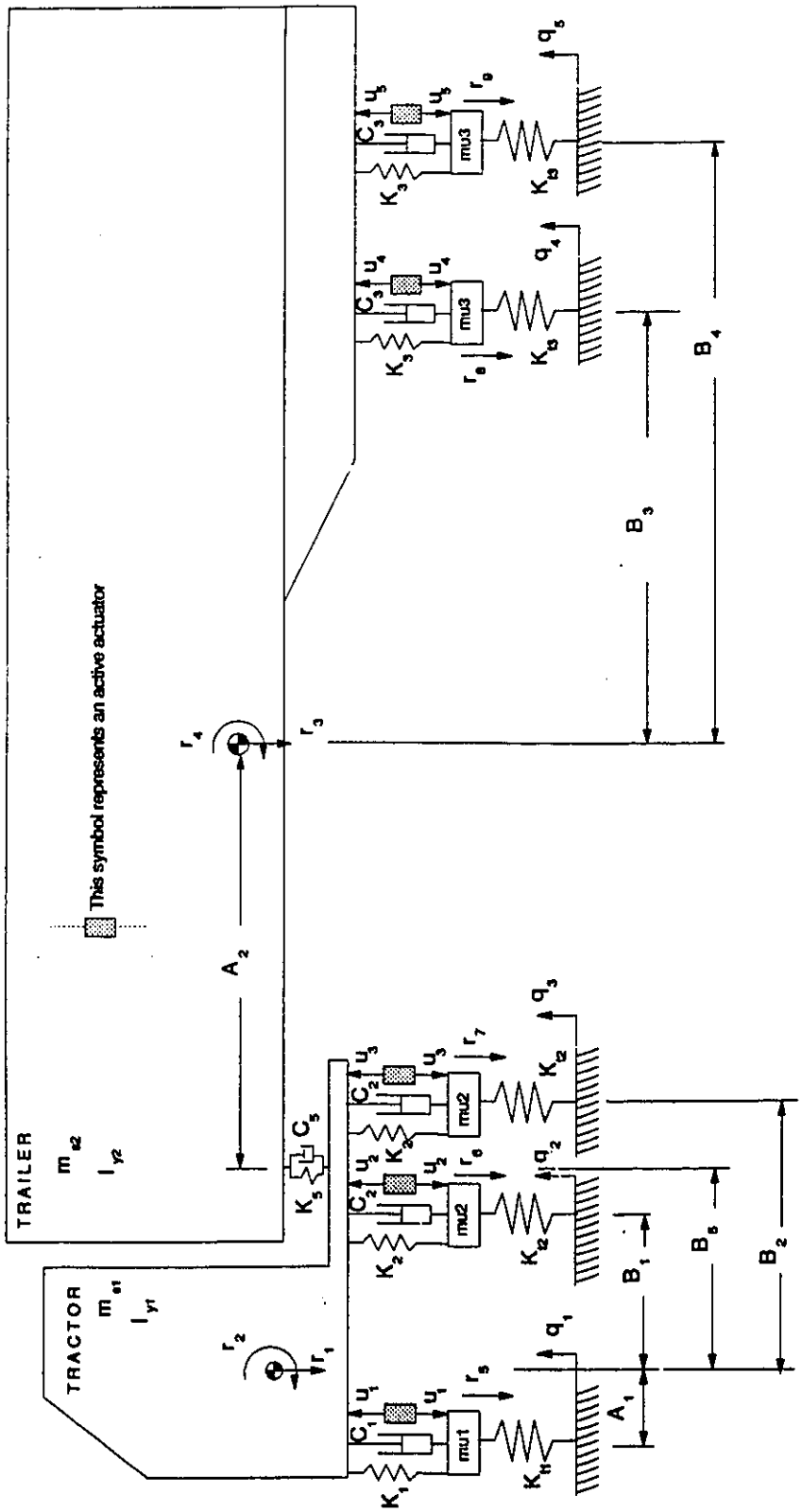

Figure 4.1 Baseline tractor-semitrailer model with active suspensions

Defining the new state vector y_y as:

$$y_y = \begin{Bmatrix} \dot{r} \\ r \end{Bmatrix}$$

The dynamics of the actively suspended tractor-semitrailer can be described by the first order matrix equation:

$$\dot{y}_y(t) = A_y y_y + B_y q + F_y u \tag{4.3}$$

where:

$$A_y = \begin{bmatrix} -M^{-1}C & -M^{-1}K_s \\ I & 0 \end{bmatrix}, \quad B_y = \begin{bmatrix} M^{-1}K_T \\ 0 \end{bmatrix} \text{ and } F_y = \begin{bmatrix} -M^{-1}F \\ 0 \end{bmatrix} \tag{4.4}$$

where $A_y \in \mathbb{R}^{18\times18}$, $B_y \in \mathbb{R}^{18\times5}$, and $F_y \in \mathbb{R}^{18\times5}$ are matrices of vehicle and road constants. $I \in \mathbb{R}^{9\times9}$, is an identity matrix and $y_y \in \mathbb{R}^{18\times1}$ is the state vector.

The design of an active suspension for the tractor-semitrailer, in principle, poses an optimization problem involving various performance measures related to ride quality, cargo safety, pavement loads etc. *LQG (Linear Quadratic Gaussian)* optimal control technique can be conveniently implemented for the design and analysis of the proposed active suspension system. *LQG* optimal control theory, however, requires the disturbance acting on the system to be white noise [11]. Since this condition is not explicitly satisfied here, a plant augmentation can be carried out as illustrated in Figure 4.2. The stationary *Gaussian* random excitation vector q is obtained by passing a white noise process with

covariance $E[\xi(t)\xi(\tau)] = 2\alpha v\sigma^2\delta(t-\tau)$ through a first order filter, as shown in Chapter 2:

$$\dot{q} = A_q q + B_q \xi \tag{4.5}$$

EQ (4.4) can be rearranged along with the road excitation EQ (4.5) in the following augmented state-space form:

$$\dot{x} = Ax + B_1\xi + B_2 u \tag{4.6}$$

where:

$$x = \begin{bmatrix} y_v \\ q \end{bmatrix},\ A = \begin{bmatrix} A_v & B_v \\ 0 & A_q \end{bmatrix},\quad B_1 = \begin{bmatrix} 0 \\ B_q \end{bmatrix} \text{ and } B_2 = \begin{bmatrix} F_v \\ 0 \end{bmatrix} \tag{4.7}$$

where x is the 23×1 augmented state vector given by:

$$x = [\dot{r}_1\ \dot{r}_2 \cdots \dot{r}_9\ r_1\ r_2 \cdots r_9\ q_1\ q_2\ q_3\ q_4\ q_5]'$$

and " $'$ " designates the transpose. $A \in \mathbb{R}^{23\times 23}$, is the system dynamics matrix; and $B_1 \in \mathbb{R}^{23\times 1}$, is the excitation disturbance vector, and $B_2 \in \mathbb{R}^{23\times 5}$, is the control force matrix. The plant augmentation results in a system that is disturbed by a white noise ξ, and hence is well suited for the *LQG* optimal control technique.

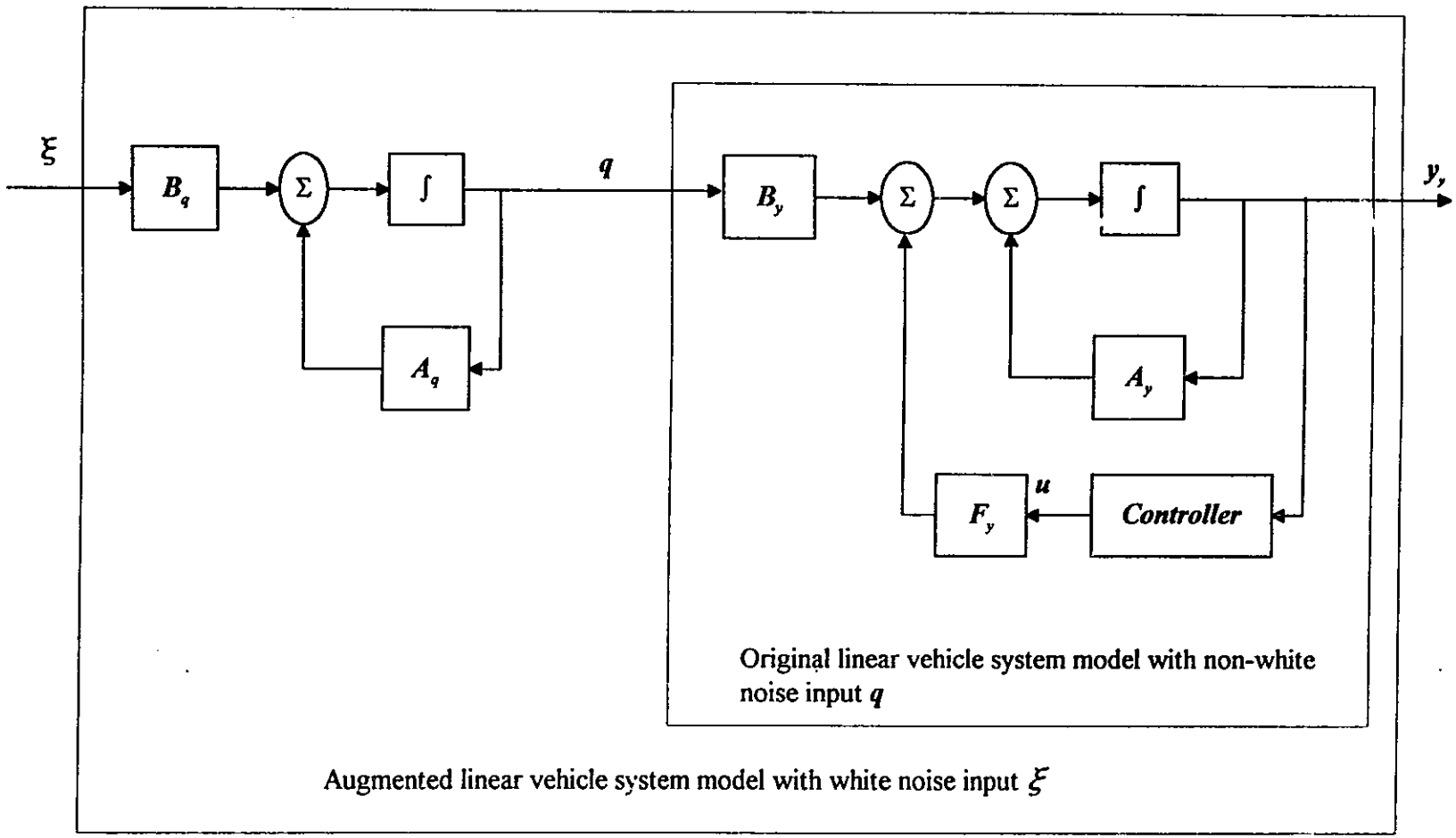

Figure 4.2 Realization of vehicle model augmentation.

4.3 THE PERFORMANCE INDEX

The performance index, in general, is selected to reflect specific design objectives. As in the case of a passive suspension, these design objectives include: ride quality, cargo safety, rattle space requirements and dynamic tire forces. While the ride quality related to work station design is frequently assessed using subjective rankings, many objective methods have been developed to assess the ride quality related to noise and vibration environment. Since the suspension design primarily determines the whole-body vibration environment of the driver's compartment, the ride quality related to vehicle vibration is addressed in this study. A relative measure of vehicle ride quality can be conveniently derived from the vertical (z_1) and pitch (z_2) acceleration responses. The cargo safety is primarily related to the vibration levels transmitted to the cargo, and the performance index related to cargo safety can thus be expressed in terms of vertical (z_3) and pitch (z_4) acceleration responses of the semitrailer. The relative deflections across the axle suspensions (z_5, z_6, z_7, z_8, z_9) determine the rattle space requirements for the suspension system. Similarly, the relative deflections across the tire elements (z_{10}, z_{11}, z_{12}, z_{13}, z_{14}) directly relate to the dynamic forces transmitted to the pavements. The performance index also encompasses the control forces (u_1 to u_5), in addition to the above penalized variables to minimize the power requirements of the suspension systems. The performance index, therefore, includes the square of the following response variables ;

z_1 = Tractor bounce acceleration ($\ddot{r}_1$),

z_2 = Tractor pitch acceleration ($\ddot{r}_2$),

z_3 = Semitrailer bounce acceleration ($\ddot{r}_3$),

z_4 = Semitrailer pitch acceleration ($\ddot{r}_4$),

z_5 to z_9 = Suspension deflections,

z_{10} to z_{14} = Tire deflections,

u_1 to u_5 = Actuator forces.

The performance variables z_1 to z_{14} can be related to the components of the augmented state vector and the actuator forces as follows:

$$\begin{aligned} z_1 = -\big[&C_1(x_1 + A_1x_2 - x_5) + C_2(2x_1 - B_1x_2 - x_6 - B_2x_2 - x_7) + \\ &C_5(x_1 - B_5x_2 - x_3 - A_2x_4) + K_1(x_{10} + A_1x_{11} - x_{14}) + \\ &K_2(2x_{10} - B_1x_{11} - x_{15} - B_2x_{11} - x_{16}) + K_5(x_{10} - B_5x_{11} - x_{12} - A_2x_{13}) + \\ &u_1 + u_2 + u_3\big] / m_{s1} \end{aligned} \tag{4.8a}$$

$$\begin{aligned} z_2 = -\big[&C_1A_1(x_1 + A_1x_2 - x_5) + C_2[B_1(x_1 - B_1x_2 - x_6) + \\ &B_2(x_1 - B_2x_2 - x_7)] - C_5B_5(x_1 - B_5x_2 - x_3 - A_2x_4) + \\ &K_1A_1(x_{10} + A_1x_{11} - x_{14}) + K_2[B_1(x_{10} - B_1x_{11} - x_{15}) + \\ &B_2(x_{10} - B_2x_{11} - x_{16})] - K_5B_5(x_{10} - B_5x_{11} - x_{12} - A_2x_{13}) + \\ &A_1u_1 - B_1u_2 - B_2u_3)\big] / I_{y1} \end{aligned} \tag{4.8b}$$

$$\begin{aligned} z_3 = -\big[&C_3(x_3 - B_3x_4 - x_8 + x_3 - B_4x_4 - x_9) + C_5(x_3 + A_2x_4 - x_1 + B_5x_2) + \\ &K_3(x_{12} - B_3x_{13} - x_{17} + x_{12} - B_4x_{13} - x_{18}) + K_5(x_{12} + A_2x_{13} - x_1 + B_5x_{11}) + \\ &u_4 + u_5\big] / m_{s2} \end{aligned} \tag{4.8c}$$

$$\begin{aligned} z_4 = -\big[&-C_3[B_3(x_3 - B_3x_4 - x_8) + B_4(x_3 - B_4x_4 - x_9)] + \\ &C_5A_2(x_3 + A_2x_4 - x_1 + B_5x_2) - K_3[B_3(x_{12} - B_3x_{13} - x_{17}) + \\ &B_4(x_{12} - B_4x_{13} - x_{18})] + K_5A_2(x_{12} + A_2x_{13} - x_{10} + B_5x_{11}) - \\ &B_3u_4 - B_4u_5\big] / I_{y2} \end{aligned} \tag{4.8d}$$

$$z_5 = x_{10} + A_1x_{11} - x_{14} \tag{4.8e}$$

$$z_6 = x_{10} - B_1x_{11} - x_{15} \tag{4.8f}$$

$$z_7 = x_{10} - B_2x_{11} - x_{16} \tag{4.8g}$$

$$z_8 = x_{12} - B_3 x_{13} - x_{17} \tag{4.8h}$$

$$z_9 = x_{12} - B_4 x_{13} - x_{18} \tag{4.8i}$$

$$z_{10} = x_{14} - x_{19} \tag{4.8j}$$

$$z_{11} = x_{15} - x_{20} \tag{4.8k}$$

$$z_{12} = x_{16} - x_{21} \tag{4.8l}$$

$$z_{13} = x_{17} - x_{22} \tag{4.8m}$$

$$z_{14} = x_{18} - x_{23} \tag{4.8n}$$

Assuming rigid articulation, the tractor bounce response (x_{10}) can be related to the tractor pitch (x_{11}), the semitrailer bounce (x_{12}) and the semitrailer pitch (x_{12}) using the following constraint equation :

$$x_{10} \approx B_5 x_{11} + x_{12} + A_2 x_{13} \tag{4.9}$$

The tractor bounce acceleration thus need not be incorporated in the performance index. Accordingly, penalizing the tractor pitch, and the semitrailer bounce and pitch accelerations (z_2, z_3 and z_4), implicitly results in penalizing the tractor bounce acceleration (z_1).

EQ (4.8), describing the performance variables z_i's relationship with the state vector $\boldsymbol{x}$ and control force $\boldsymbol{u}$, can be expressed in the following form :

$$\boldsymbol{z} = \boldsymbol{C}_1 \boldsymbol{x} + \boldsymbol{D}_{12} \boldsymbol{u} \tag{4.10}$$

where $C_1 \in \mathbb{R}^{14\times 23}$, is the state-to-performance variables transformation matrix and $D_{12} \in \mathbb{R}^{14x5}$, is the control forces-to performance variables transformation matrix.

The performance index can be written as the weighted mean square sum of the performance variables and the control forces :

$$J = \lim_{T\to\infty} E\left\{\int_0^T \left(\sum_{i=1}^{14}\mu_i z_i^{\,2} + \sum_{j=1}^{5}\rho_j u_j^{\,2}\right) dt\right\} \tag{4.11}$$

where μ_i's and ρ_i's are weighting factors associated with the penalized response variables and the penalized actuator forces respectively.

EQ (4.11) can be rearranged in the following format:

$$J = \lim_{T\to\infty} E\left\{\int_0^T \begin{bmatrix} z_1 & \cdots & z_{14}\end{bmatrix}\begin{bmatrix}\mu_1 & \cdots & 0\\ \vdots & \ddots & \vdots\\ 0 & \cdots & \mu_{14}\end{bmatrix}\begin{bmatrix} z_1\\ \vdots\\ z_{14}\end{bmatrix} + \begin{bmatrix} u_1 & \cdots & u_5\end{bmatrix}\begin{bmatrix}\rho_1 & \cdots & 0\\ \vdots & \ddots & \vdots\\ 0 & \cdots & \rho_{15}\end{bmatrix}\begin{bmatrix} u_1\\ \vdots\\ u_5\end{bmatrix} dt\right\} \tag{4.12}$$

Upon combining EQ (4.10) and EQ (4.12), the performance index can expressed as:

$$J = \lim_{T\to\infty} E\left\{\int_0^T (C_1\boldsymbol{x} + D_{12}\boldsymbol{u})'\,\hat{Q}(C_1\boldsymbol{x} + D_{12}\boldsymbol{u}) + \boldsymbol{u}'\hat{R}\,\boldsymbol{u}dt\right\} \tag{4.13}$$

where:

$$\begin{aligned}\hat{Q} &= diag\ [\mu_1, \mu_2, \ldots \mu_{14}]\ ; \quad \mu_i > 0\\ \hat{R} &= diag\ [\rho_1, \rho_2, \ldots \rho_5]\ ; \quad \rho_i > 0\end{aligned} \tag{4.14}$$

Expanding and grouping the terms of EQ (4.13) results in:

$$J = \lim_{T\to\infty} E\left\{\int_0^T \left[x'C_1'\hat{Q}C_1x + u'(\hat{R} + D_{12}'\hat{Q}D_{12})u + x'C_1'\hat{Q}D_{12}u + u'D_{12}'\hat{Q}C_1x\right] dt\right\} \quad (4.15)$$

Defining:

$$\begin{aligned} R &= \hat{R} + D_{12}'\,\hat{Q}D_{12} \\ Q &= C_1'\hat{Q}C_1 \\ N &= C'_1\hat{Q}D_{12} \end{aligned} \quad (4.16)$$

EQ (4.15) can be rearranged in the following standard quadratic cost criterion:

$$J = \lim_{T\to\infty} E\left\{\int_0^T \begin{bmatrix} x' & u' \end{bmatrix}\begin{bmatrix} Q & N \\ N' & R \end{bmatrix}\begin{bmatrix} x \\ u \end{bmatrix} dt\right\} \quad (4.17)$$

4.3.1 Solution of the Standard *LQG* Problem

Design of an optimal controller for the multivariable active suspension system primarily involves the determination of the optimal control force vector $\boldsymbol{u}$ and its relation to the state vector $\boldsymbol{x}$ in the presence of a white noise input ξ. The control force vector $\boldsymbol{u}$ is optimum in the sense that it minimizes a quadratic cost function. This problem is well suited for the *LQG* technique, which is a well developed method for state-space design of multivariable systems. The advantage of the *LQG* design technique is that it reduces the problem of design to the choice of suitable weighting coefficients in the quadratic performance index J. The coefficients can be specified, to some extent, from the information available concerning the magnitude of the system states. Although the system

states are not known beforehand, an approximation is performed to formulate the coefficients in the first iteration. Alternatively, the weighting coefficients can be conveniently selected through the covariance analysis performed in Chapter 3.

The *LQG* problem is thus formulated to determine the optimal control force vector $\boldsymbol{u}$ for the multivariable system governed by EQ (4.6), while minimizing the quadratic performance index $\boldsymbol{J}$ described by EQ (4.17). This is a *Linear Quadratic Gaussian* optimization control problem leading to an optimal control which is a linear algebraic function of the state vector [10,11] :

$$\boldsymbol{u} = -\boldsymbol{K}\boldsymbol{x} \tag{4.18}$$

where the constant control gain matrix $\boldsymbol{K}$ is given by:

$$\boldsymbol{K} = \boldsymbol{R}^{-1}(\boldsymbol{N}' + \boldsymbol{B}_2'\boldsymbol{P}) \tag{4.19}$$

and $\boldsymbol{P}$ is a symmetric, positive-definite solution of the matrix *Riccati* equation:

$$\boldsymbol{P}(\boldsymbol{A} - \boldsymbol{B}_2\boldsymbol{R}^{-1}\boldsymbol{N}') + (\boldsymbol{A} - \boldsymbol{B}_2\boldsymbol{R}^{-1}\boldsymbol{N}')'\boldsymbol{P} + \boldsymbol{P}(-\boldsymbol{B}_2\boldsymbol{R}^{-1}\boldsymbol{B}_2')\boldsymbol{P} - (-\boldsymbol{Q} + \boldsymbol{N}\boldsymbol{R}^{-1}\boldsymbol{N}') = 0 \tag{4.20}$$

The fundamental idea behind the theory leading to the solution of $\boldsymbol{K}$ (EQ (4.19)) is based on constraining the control force vector $\boldsymbol{u}$ to be of the form of EQ (4.18). Upon substituting EQ (4.18) in the system dynamic equation, EQ (4.6), the closed loop system can be described by:

$$\dot{\boldsymbol{x}} = (\boldsymbol{A} - \boldsymbol{B}_2\boldsymbol{K})\boldsymbol{x} + \boldsymbol{B}_1\boldsymbol{\xi} \tag{4.21}$$

Similarly, replacing $\boldsymbol{u}$ by $-\boldsymbol{Kx}$ in the performance index (EQ (4.15)), results $\boldsymbol{J}$ being a function of $\boldsymbol{x}$ only :

$$\boldsymbol{J} = \lim_{T\to\infty} E\left\{\int_0^T \boldsymbol{x}'\left[C_1'\,\hat{Q}C_1 + K'\left(\hat{R} + D_{12}'\,\hat{Q}D_{12}\right)K - C'_1\hat{Q}D_{12}K - K'D_{12}'\,\hat{Q}C_1'\right]\boldsymbol{x}\,dt\right\} \quad (4.22)$$

The performance index $\boldsymbol{J}$ is minimized with respect to $\boldsymbol{K}$, resulting in the *Riccati* equation, EQ (4.20), which is then solved for $\boldsymbol{P}$ [10,11].

The steady-state, mean square response of the actively suspended vehicle can, therefore, be described by the covariance matrix $\boldsymbol{X}$ of the state vector $\boldsymbol{x(t)}$. The covariance matrix $\boldsymbol{X}$ depends on the closed loop system dynamic matrix $\boldsymbol{A-B_2K}$, the excitation disturbance vector $\boldsymbol{B_1}$, and the covariance of the disturbance ξ and is a solution of the following *Lyapunov* equation [11]:

$$(A - B_2K)X + X(A - B_2K)' + 2\alpha v\sigma^2 B_1B_1' = 0 \quad (4.23)$$

The performance index can be computed using the covariance matrix $\boldsymbol{X}$. Replacing $\boldsymbol{u}$ by $-\boldsymbol{Kx}$ in EQ (4.15), the following expression for the performance index $\boldsymbol{J}$ is obtained:

$$\boldsymbol{J} = \lim_{T\to\infty} E\left\{\int_0^T \boldsymbol{x}'(Q + K'RK - NK - K'N')\boldsymbol{x}\;dt\right\} \quad (4.25)$$

which can be expressed in terms of the covariance matrix $\boldsymbol{X}$ as :

$$\boldsymbol{J} = Tr\left(X(Q + K'RK - NK - K'N')\right) \quad (4.26)$$

where *Tr* denotes the trace. Upon substituting for $\boldsymbol{K}$ from EQ (4.19), EQ (4.26) can be

simplified as:

$$J = Tr\left(X\left(Q - NR^{-1}N' + PB_2R^{-1}B_2'P\right)\right) \tag{4.27}$$

The *Riccati* equation, EQ(4.20), however, yields the following:

$$Q - NR^{-1}N' = -P(A - B_2R^{-1}N') - (A - B_2R^{-1}N')'P + PB_2R^{-1}B_2'P \tag{4.28}$$

Combining EQ (4.27) and EQ (4.28), and, upon substituting for $R^{-1}(N' + B_2'P) = K$, the performance index can be expressed as:

$$J = Tr\left(P\left(-(A - B_2K)X - X(A - B_2K)'\right)\right) \tag{4.29}$$

Recalling from EQ (4.23):

$$-P\left((A - B_2K)X + X(A - B_2K)'\right) = 2\alpha v\sigma^2 PB_1B_1' \tag{4.30}$$

The performance index can thus be given by the simplified expression:

$$J = Tr\left(2\alpha v\sigma^2 PB_1B_1'\right) \tag{4.31}$$

In order to study the effects of variations in the suspension parameters on each performance measure (tractor and semitrailer bounce and pitch accelerations, suspension deflections and tire deflections), each of the components of the performance index is determined separately. Upon replacing u by $-Kx$ in EQ (4.10), the i^{th} performance

variable can be derived from :

$$z_i = \sum_{j=1}^{23} \left[C_1(i,j) - (D_{12}K)(i,j) \right] x(j) \qquad i = 1,\cdots,14 \tag{4.32}$$

The contribution of the each performance variable to the performance index can be computed from:

$$J_{zi} = \mu_i E(z_i^2) = \mu_i E\left\{ \left[\sum_{j=1}^{23} \left[C_1(i,j) - (D_{12}K)(i,j) \right] x(j) \right]^2 \right\} \tag{4.33}$$

Alternatively, the components of the performance index may be expressed as:

$$J_{zi} = \mu_i \sum_{m=1}^{23} \sum_{n=1}^{23} \left[C_1(i,m) - (D_{12}K)(i,m) \right] \left[C_1(i,n) - (D_{12}K)(i,n) \right] E\left[x(m)x(n) \right] \tag{4.34}$$

In the above equation, the expected value $E[x(m)x(n)]$ is the element $X(m,n)$ of the covariance matrix X obtained from EQ (4.23). The contribution of J_{zi} to the performance index is, thus, described in terms of the elements of the covariance matrix:

$$J_{zi} = \mu_i \sum_{m=1}^{23} \sum_{n=1}^{23} \left[C_1(i,m) - (D_{12}K)(i,m) \right] \left[C_1(i,n) - (D_{12}K)(i,n) \right] X(m,n); \; i = 1,..,14 \tag{4.35}$$

The contribution of the actuator control forces to the performance index can be similarly expressed as :

$$J_{uj} = \rho_j \sum_{m=1}^{23} \sum_{n=1}^{23} \left[K(j,m) \right] \left[K(j,n) \right] X(m,n) ; \qquad j = 1,...,5 \tag{4.36}$$

4.3.2 Solution of the *Riccati* Equation: Special Consideration

The optimal control gain matrix $\boldsymbol{K}$ as described in EQ (4.19), is a function of the weighting matrices $\boldsymbol{R}$ and $\boldsymbol{N}$, the control forces matrix $\boldsymbol{B}_2$, and the matrix $\boldsymbol{P}$. Computation of the control gain matrix $\boldsymbol{K}$ thus necessitates the solution of the *Riccati* equation for the matrix $\boldsymbol{P}$. The solution of the *Riccati* equation, EQ (4.20), for the matrix $\boldsymbol{P}$, however, requires the system to be completely controllable. Since the state vector $\boldsymbol{x}$ also comprises the road excitations, which can not be changed by the control force vector $\boldsymbol{u}$, the system of equations describing the dynamics of the tractor-semitrailer is not completely controllable. The controllability requirement can be verified mathematically by setting the controllability matrix C_m as [10]:

$$C_m = \left[B_2 \middle| AB_2 \middle| A^2 B_2 \ldots A^{22} B_2 \right] \tag{4.37}$$

The system given by EQ (4.6) is said to be completely controllable if and only if the matrix C_m has a rank of 23 (i.e. full rank). It can be verified that the rank deficit here is 5 corresponding to the 5 uncontrollable states (road excitations). To overcome this, the matrices $\boldsymbol{Q}$ and $\boldsymbol{P}$ are each subdivided into four sub-matrices as follows [11,12]:

$$\boldsymbol{Q} = \begin{bmatrix} \underset{(18\times18)}{\boldsymbol{Q}_{xx}} & \underset{(18\times5)}{\boldsymbol{Q}_{xw}} \\ \underset{(5\times18)}{\boldsymbol{Q}'_{xw}} & \underset{(5\times5)}{\boldsymbol{Q}_{ww}} \end{bmatrix}, \text{ and } \boldsymbol{P} = \begin{bmatrix} \underset{(18\times18)}{\boldsymbol{P}_{xx}} & \underset{(18\times5)}{\boldsymbol{P}_{xw}} \\ \underset{(5\times18)}{\boldsymbol{P}'_{xw}} & \underset{(5\times5)}{\boldsymbol{P}_{ww}} \end{bmatrix} \tag{4.38}$$

Similarly the matrix $\boldsymbol{N}$ is partitioned as:

$$N = \begin{bmatrix} N_x \\ {\scriptstyle (18\times 5)} \\ \\ 0 \\ {\scriptstyle (5\times 5)} \end{bmatrix} \tag{4.39}$$

Upon substituting for A, B_1 and B_2 from EQ (4.7), and the above partitioned matrices in EQ (4.20), the *Riccati* equation can be expressed as.

$$\begin{bmatrix} P_{xx} & P_{xw} \\ P'_{xw} & P_{ww} \end{bmatrix}\left(\begin{bmatrix} A_y & B_y \\ 0 & A_q \end{bmatrix} - \begin{bmatrix} F_y \\ 0 \end{bmatrix} R^{-1}\begin{bmatrix} N'_x & .0 \end{bmatrix}\right) +$$
$$\left(\begin{bmatrix} A_y & B_y \\ 0 & A_q \end{bmatrix} - \begin{bmatrix} F_y \\ 0 \end{bmatrix} R^{-1}\begin{bmatrix} N'_x & 0 \end{bmatrix}\right)' \begin{bmatrix} P_{xx} & P_{xw} \\ P'_{xw} & P_{ww} \end{bmatrix} +$$
$$\begin{bmatrix} P_{xx} & P_{xw} \\ P'_{xw} & P_{ww} \end{bmatrix}\left(-\begin{bmatrix} F_y \\ 0 \end{bmatrix} R^{-1}\begin{bmatrix} F'_y & 0 \end{bmatrix}\right)\begin{bmatrix} P_{xx} & P_{xw} \\ P'_{xw} & P_{ww} \end{bmatrix} -$$
$$\left(-\begin{bmatrix} Q_{xx} & Q_{xw} \\ Q'_{xw} & Q_{ww} \end{bmatrix} + \begin{bmatrix} N_x \\ 0 \end{bmatrix} R^{-1}\begin{bmatrix} N'_x & 0 \end{bmatrix}\right) = 0 \tag{4.40}$$

EQ (4.40) is rearranged to yield:

$$\begin{bmatrix} P_{xx} & P_{xw} \\ P'_{xw} & P_{ww} \end{bmatrix}\left(\begin{bmatrix} A_y - F_y R^{-1} N'_x & B_y \\ 0 & A_q \end{bmatrix}\right) + \left(\begin{bmatrix} A_y - F_y R^{-1} N'_x & B_y \\ 0 & A_q \end{bmatrix}\right)' \begin{bmatrix} P_{xx} & P_{xw} \\ P'_{xw} & P_{ww} \end{bmatrix} +$$
$$\begin{bmatrix} P_{xx} & P_{xw} \\ P'_{xw} & P_{ww} \end{bmatrix}\left(-\begin{bmatrix} F_y R^{-1} F'_y & 0 \\ 0 & 0 \end{bmatrix}\right)\begin{bmatrix} P_{xx} & P_{xw} \\ P'_{xw} & P_{ww} \end{bmatrix} - \left(-\begin{bmatrix} Q_{xx} - N_x R^{-1} N'_x & Q_{xw} \\ Q'_{xw} & Q_{ww} \end{bmatrix}\right) = 0 \tag{4.41}$$

EQ (4.41) can be expressed by the following two equations for the P_{xx} and P_{xw} components:

$$P_{xx}(A_y - F_y R^{-1} N_x') + (A_y - F_y R^{-1} N_u')' P_{xx} + P_{xx}(-F_y R^{-1} F_y') P_{xx} - (-Q_{xx} + N_x R^{-1} N_x') = 0 \quad (4.42)$$

$$P_{xw} A_q + \left[(A_y - F_y R^{-1} F_y')' - P_{xx} F_y R^{-1} B_y'\right] P_{xw} + P_{xx} B_y + Q_{xw} = 0 \quad (4.43)$$

The above equations are solved consecutively for P_{xx} and P_{xw}, and the control gain matrix can be derived using EQ (4.19) in conjunction with EQ (4.7), EQ (4.38) and EQ (4.39):

$$K = R^{-1}\left(\begin{bmatrix} N_x' & 0 \end{bmatrix} + \begin{bmatrix} F_y' & 0 \end{bmatrix} \begin{bmatrix} P_{xx} & P_{xw} \\ P_{xw}' & P_{ww} \end{bmatrix} \right) \quad (4.44)$$

Upon multiplying and rearranging, the following expression for control gain matrix is obtained:

$$K = R^{-1}\left[(N_x' + F_y' P_{xx}) \;\middle|\; F_y' P_{xw} \right] \quad (4.45)$$

4.3.3 Selection of the Weighting Factors

The *LQG* technique reduces the problem of designing the optimum active suspension for the tractor-semitrailer to the selection of appropriate weighting coefficients in the quadratic performance index J. Once the weighting coefficients are selected, the control gain matrix K is obtained and the performance characteristics of the actively suspended vehicle can be assessed. Referring to EQ (4.19), it can be seen that the control gain matrix K, and therefore the active suspension performance, is strongly dependent on the selected weighting factors.

The selection of weighting factors, however, is quite complex due to excessive variations in the magnitudes of different performance variables. For instance, the mean square values of the tire deflections (z_{10} to z_{14}) are normally small when compared to those of the suspension deflections, and bounce and pitch accelerations of the vehicle. The performance variables representing the tire deflections thus need to be heavily weighted in order to reflect their contribution to the overall performance index J. Since all the design objectives formulated in terms of the penalized variables z_i's are of comparable importance in the design of the tractor-semitrailer active suspension, the weighting factors have to be carefully selected. The weighting factors may be initially selected from the performance indices of the passive suspension (the unweighted mean square values of the performance variables) presented in Chapter 3, specifically Figures 3.3 to 3.6.

Recalling that each of the variants of the performance index J is given by :

$$J_{zi} = \mu_i E(z_i^2) \tag{4.46}$$

An equal importance of all the components of the performance index in the design of the active suspension implies that :

$$J_{z1} \approx J_{z2} \approx \cdots \approx J_{z14} \tag{4.47}$$

The weighting coefficients are thus computed from :

$$\mu_i \approx \frac{1}{E(z_i^2)} \qquad i = 1,\ldots,14 \tag{4.48}$$

To determine the appropriate weighting coefficients thus necessitates a prior

knowledge of the mean square response. The mean square values $E(z_i^2)$ can, however, be approximated from the response characteristics of the passive suspension system presented in Figures 3.3 to 3.6. Although these are the weighting coefficients correspond to the mean square values of the performance variables for a passively suspended vehicle, they can be used as an approximation of the relative contribution of each of the performance index components.

Figures 3.3 to 3.6 reveal that the mean square values $E(z_i^2)$ vary considerably with variations in the stiffness and damping parameters of the passive suspensions. The mean square values corresponding to mid-points of the stiffness and damping axes (stiffness = 275 *kN/m* and damping = 35 *kN.s/m*) are extracted from Figures 3.3 to 3.6 to estimate the corresponding weighting coefficients. An initial set of weighting coefficients obtained using EQ (4.48) is listed in Table 4.1. The control gain matrix $\boldsymbol{K}$ is then evaluated from EQ (4.19) and (4.20). EQ (4.35) is solved to determine each variant of the performance index, which are presented in Table 4.1. The results show that the variants of the performance index $\boldsymbol{J}_{zi}$ are not equal due to the presence of the actuator control forces. The variations between the different variants, however, are not as significant.

The weighting coefficients, μ_i, can be varied to emphasize certain specific performance aspects of the actively suspended vehicle. The analysis also requires careful selection of the weighting factors for the control forces (ρ_i). ρ_i must be selected to ensure that sufficient power is available for the control. In this study, the weighting factors ρ_i are initially selected arbitrarily, and are gradually reduced until no further changes in the performance index are observed. This minimum value signifies that adequate control effort is available and additional power is not needed. A preliminary study revealed that the choice of $\rho_i = 10^{-14}$ ensures that enough power is available for control and reducing ρ_i any further would have no impact on the performance characteristics of the vehicle. In the case

when not enough control effort is available the performance of the suspension will simply be governed by the passive elements in the suspension.

Table 4.1 Weighting coefficients and corresponding active suspension performance indices

i	μ_i	J_{zi}
1	2.8752e+0	0.6362
2	1.4144e+1	0.6054
3	5.3734e+0	0.8590
4	8.3333e+2	0.4241
5	8.7958e+5	0.9311
6	4.6004e+5	0.5719
7	2.8156e+5	1.0567
8	2.3527e+5	0.5971
9	2.0381e+5	0.5846
10	4.1293e+5	0.5989
11	7.2632e+5	0.4148
12	5.3905e+5	1.6865
13	6.7549e+5	0.7495
14	6.4716e+5	0.9909

4.4 FREQUENCY DOMAIN ANALYSIS

The frequency domain response of the actively suspended vehicle subjected to a random road excitation is evaluated. Since the road excitations are assumed to be stationary and *Gaussian*, the vector of system response variables, z, is also stationary and *Gaussian* [13-15]. Combining EQ (4.6) and EQ (4.10), and substituting for $\boldsymbol{u} = -\boldsymbol{K}\boldsymbol{x}$, in yields the frequency response function matrix $\boldsymbol{H}(j\omega)$, $\in \mathbb{C}^{4\times 1}$:

$$\boldsymbol{H} = \left\{(C_1 - D_{12}\boldsymbol{K})(s\boldsymbol{I} - \boldsymbol{A} + \boldsymbol{B}_2\boldsymbol{K})^{-1}\boldsymbol{B}_1\right\} \tag{4.49}$$

The power spectral density of the response variables can be derived from [16]:

$$\boldsymbol{S}_z(\omega) = \boldsymbol{H}\boldsymbol{S}_\xi\boldsymbol{H}^* \tag{4.50}$$

where, * denotes the complex conjugate transpose, $\boldsymbol{S}_z(\omega) \in \mathbb{C}^{14\times 14}$ is the matrix of *PSD* of the response variables, and $\boldsymbol{S}_\xi$ is the spectral density of the white noise input excitation given by:

$$\boldsymbol{S}_\xi = \frac{2\alpha v\sigma^2}{\pi} \tag{4.51}$$

The diagonal elements of $\boldsymbol{S}_z(\omega)$ provide the spectral densities of the output states z_i's.

4.5 PERFORMANCE CHARACTERISTICS OF THE ACTIVE SUSPENSION

An active suspension refers to a parallel combination of passive elements (springs and dampers) and a feedback controlled force generator. Although an active suspension is often designed without the passive elements, the presence of passive components yields a fail-safe active suspension design with reduced power requirement. Power requirement of an active suspension is the primary criteria for its implementation in heavy vehicles due to associated high axle loads. The fail-safe suspension concept reduces the load carrying capacity and thus the power requirement of an active force generator. Furthermore, the fail-safe suspension design enhances the reliability of the active suspension. The presence of the passive elements in the active suspension tends to affect the power requirements of the active suspension in a significant manner. The role of passive elements within a fail-safe arrangement thus needs to be assessed through a study of the influence of passive suspension parameters on the response characteristics. EQ (4.35) is solved using the weighting coefficients given in Table 4.1 to determine the influence of the suspension parameters on each component of the performance index. The damping and stiffness elements that are present in parallel with the force actuators are varied and the new control gain matrix $\boldsymbol{K}$ is evaluated accordingly. The results are examined to derive the passive elements that will best enhance the function of the active suspension. The influence of the passive parameters on each component of the performance index is presented and discussed in the following section.

4.5.1 Influence of Suspension Parameters on Vehicle Ride Quality

Figures 4.3a to 4.3d present the influence of varying the damping and stiffness properties of the passive elements on four performance variables: tractor bounce, semitrailer bounce, suspension deflection and tire deflection, respectively. Since the control force gain matrix $\boldsymbol{K}$ is determined to minimize the performance index, variations in the passive damping and stiffness do not affect the performance indices, as shown in the figures. While only four of the penalized variables are shown here for conciseness, identical behavior is also observed for all the other 10 performance variables. The results clearly illustrate that passive elements do not affect the suspension performance, provided the actuator gains are selected to account for the presence of the passive elements.

Although optimal control forces are derived to minimize the performance index for varying properties of the passive elements, the actuator forces are strongly dependent upon the passive damping and stiffness properties. Passive suspension elements can be selected to minimize the power requirements of the active suspension. The effect of varying the passive suspension parameters on the actuator forces is thus determined using EQ (4.36). Figures 4.4a to 4.4e illustrate the influence of passive suspension parameters on the weighted magnitude of required control forces. The results clearly show the existence of an ideal range of passive suspension stiffness and damping values to realize the active suspension with minimum actuator forces magnitude. While any passive element can be placed in parallel with the active actuators without effecting the performance as shown in Figures 4.3a to 4.3d, Figures 4.4a to 4.4e clearly indicate that these elements directly affect the actuators effort. The actuator control force requirement for tractor axle suspension tends to decrease when the passive suspension stiffness is increased. The reduction of the control force is attributed to reduced deflection and increased load carrying capacity of the stiff suspension spring. The control force requirements of the

semitrailer axle suspension increase with increase in the passive suspension stiffness. The variations in the power requirements are, however, quite small. The actuator force requirements are strongly affected by the dissipative properties of the passive components. An increase in the suspension damping properties, in general, results in a large increase in the power demand for the tractor axle suspensions. The semitrailer axle suspensions, however, exhibit an optimal value of suspension damping for minimal power requirements, as illustrated in Figures 4.4d and 4.4e.

Figures 4.5a to 4.5e illustrate the contour plots of the control forces as a function of the restoring and dissipative properties of the passive elements. The damping and stiffness values corresponding to the center-most curve will yield minimum control force requirements. The damping and stiffness values of passive elements, derived from the analysis of the passive suspension in Chapter 3 are used to realize the fail-safe active suspension. The corresponding control force requirements of the active suspension are indicated in the contour plots. Although the selected passive suspension components do not yield minimal power requirements, the power demand is quite close to the optimal as evident from Figures 4.4a and 4.4e. Such configuration yields a true fail-safe active suspension design for the heavy vehicle.

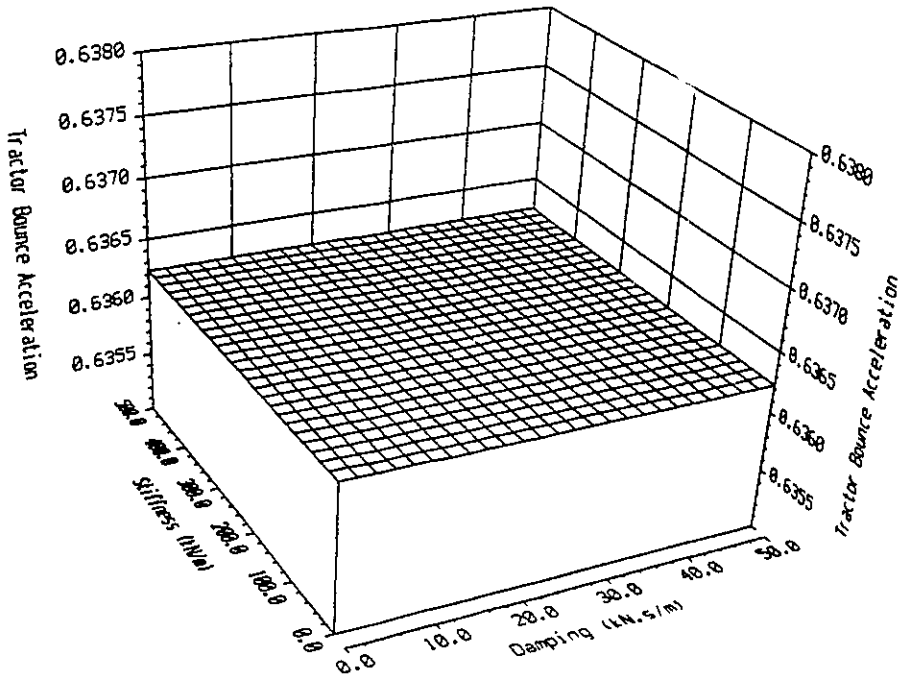

Figure 4.3a Weighted mean square acceleration of the tractor bounce for varying suspension stiffness and damping.

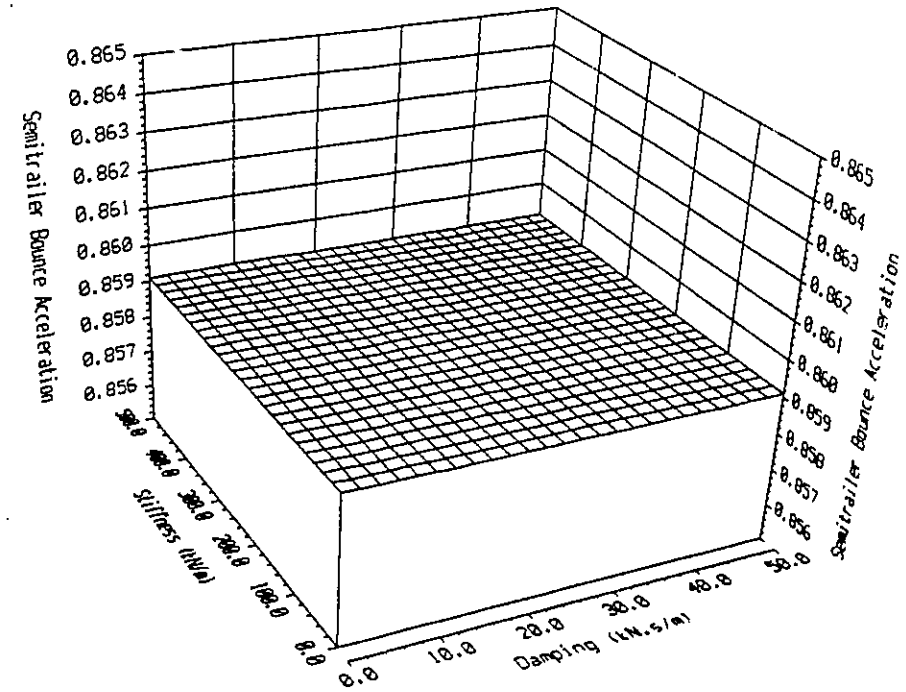

Figure 4.3b Weighted mean square acceleration of the semitrailer bounce for varying suspension stiffness and damping.

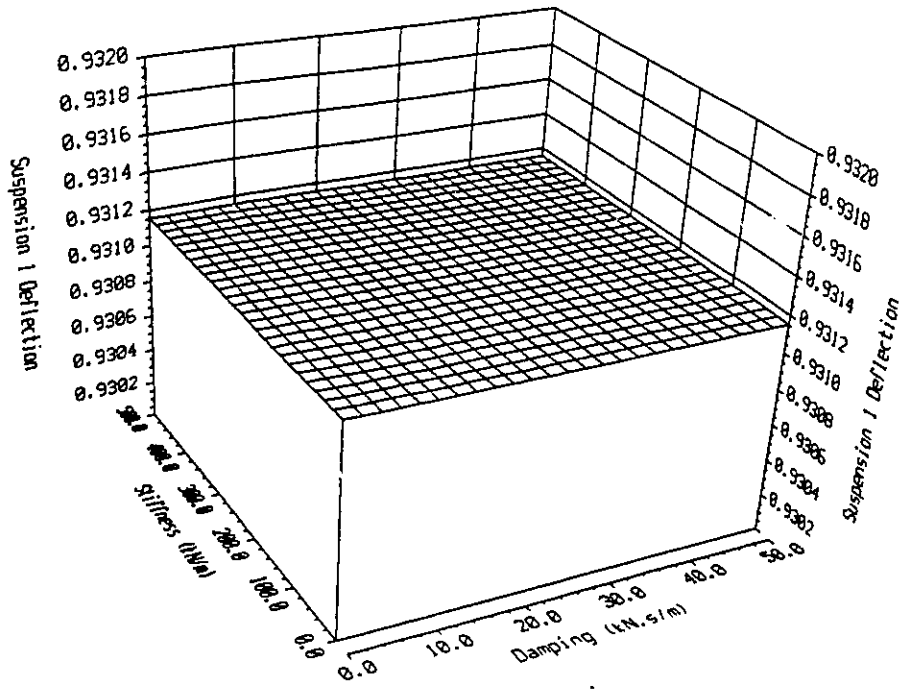

Figure 4.3c Weighted mean square deflection of suspension 1 for varying stiffness and damping.

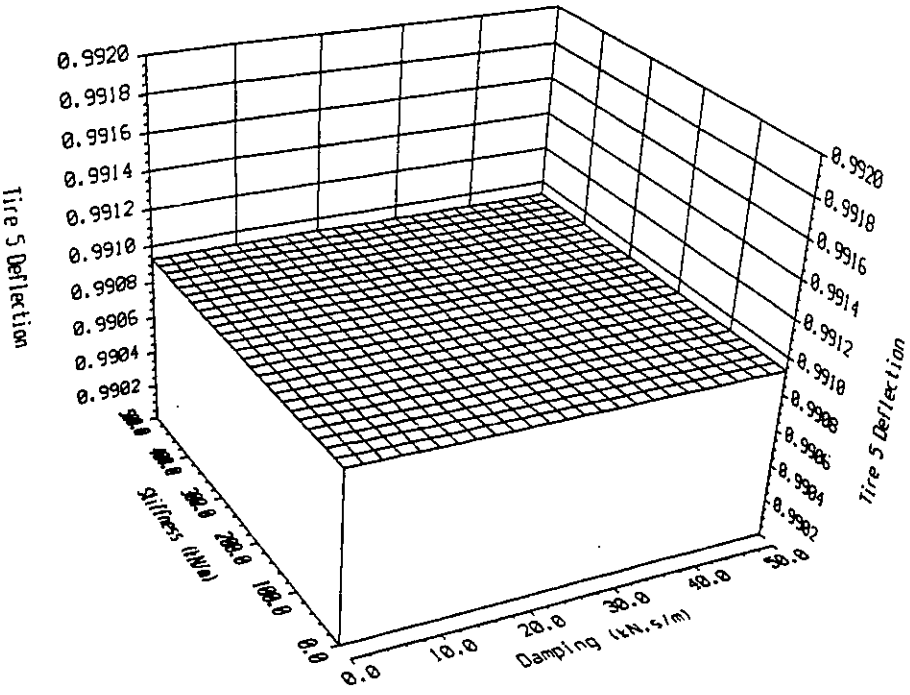

Figure 4.3d Weighted mean square deflection of tire 5 for varying supension stiffness and damping.

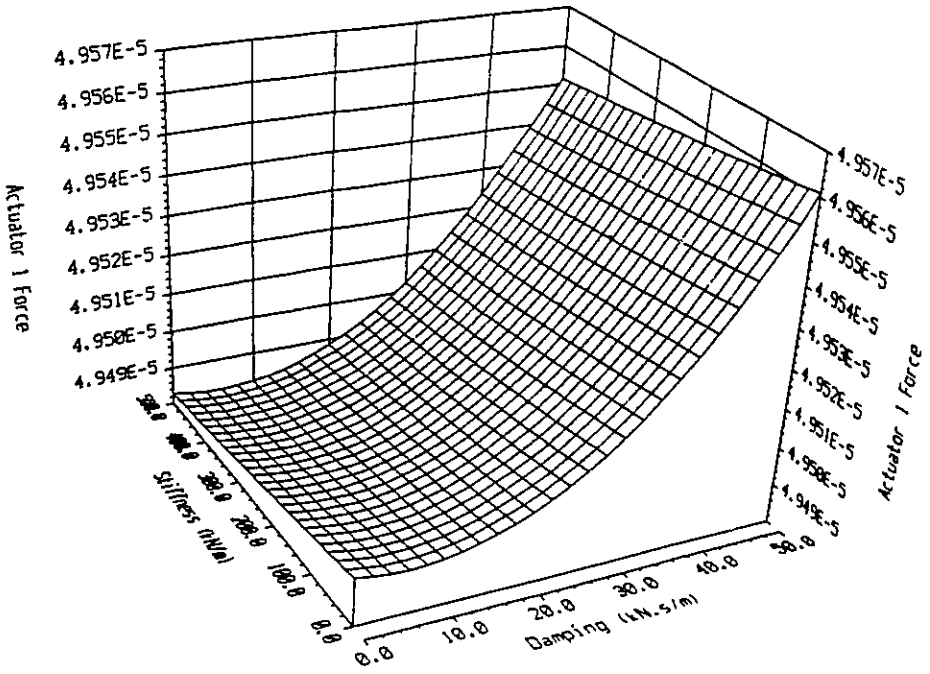

Figure 4.4a Weighted mean square force of actuator 1 for varying stiffness and damping.

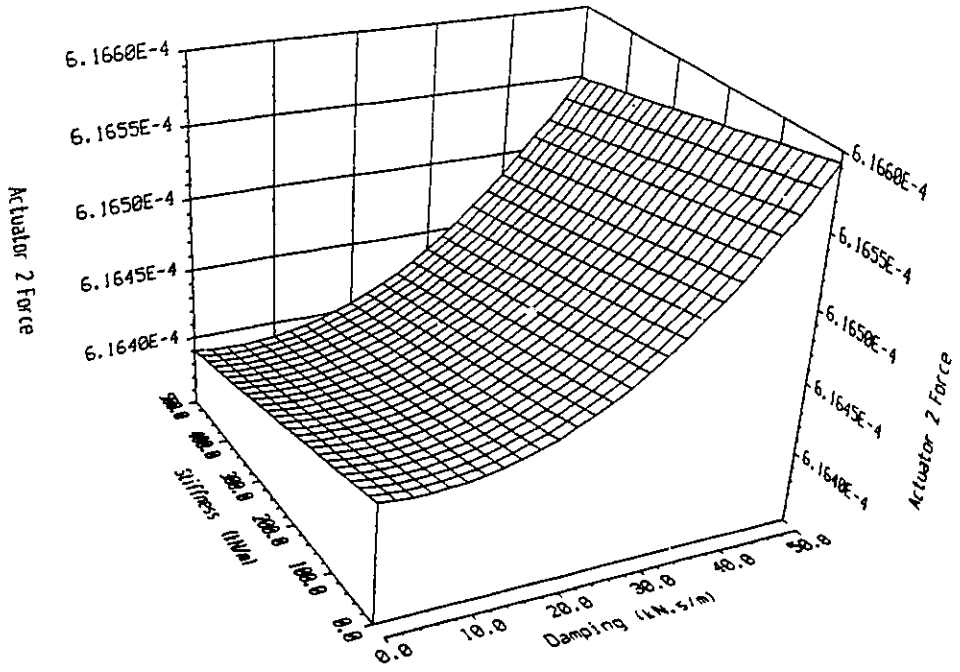

Figure 4.4b Weighted mean square force of actuator 2 for varying stiffness and damping.

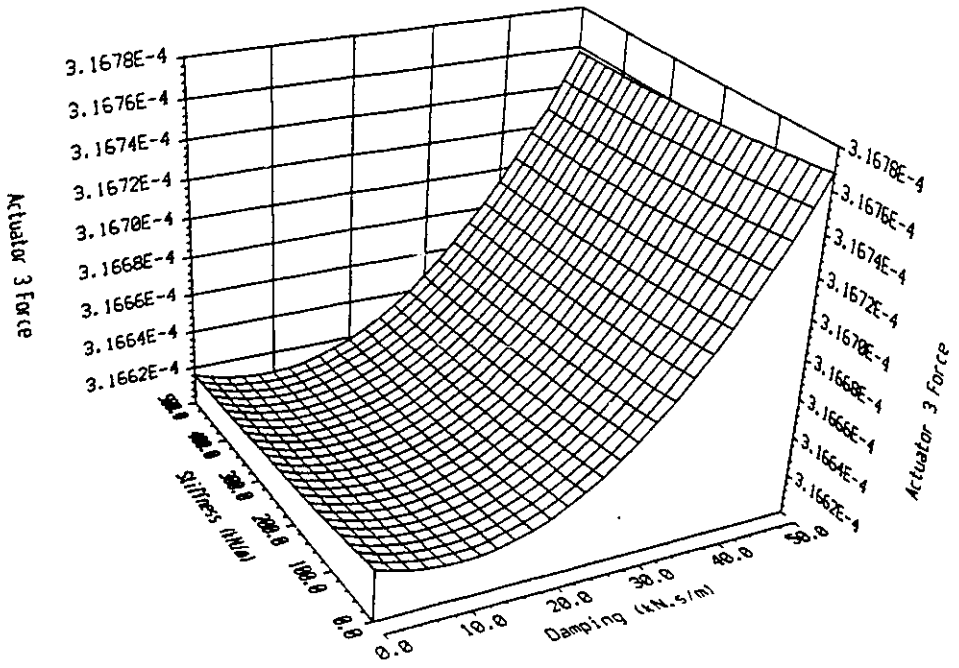

Figure 4.4c Weighted mean square force of actuator 3 for varying stiffness and damping.

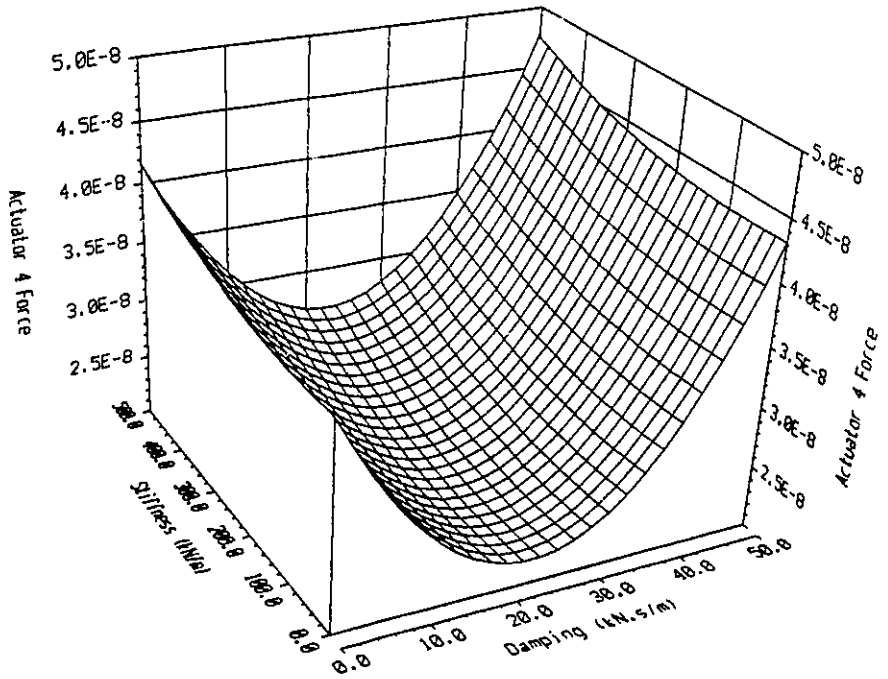

Figure 4.4d Weighted mean square force of actuator 4 for varying stiffness and damping.

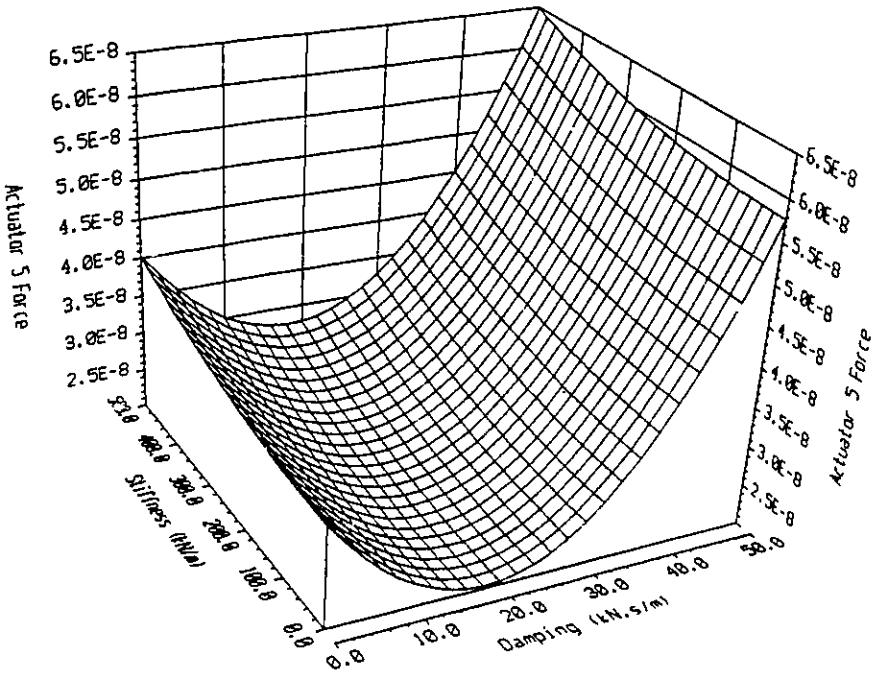

Figure 4.4e Weighted mean square force of actuator 5 for varying stiffness and damping.

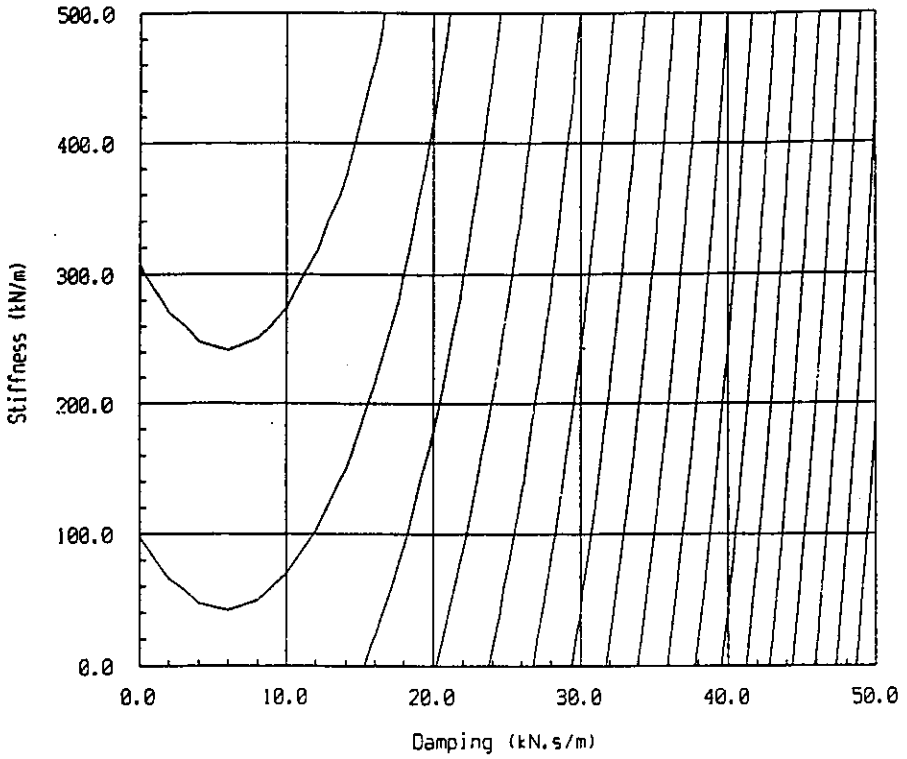

(4.5a Actuator 1 force)

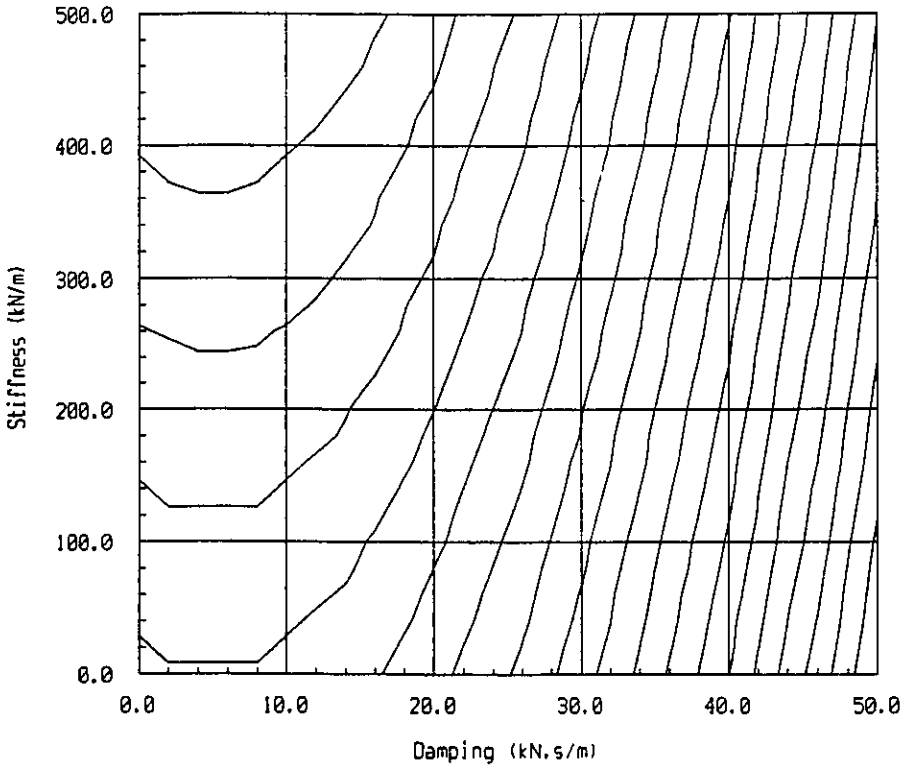

(4.5b Actuator 2 force)

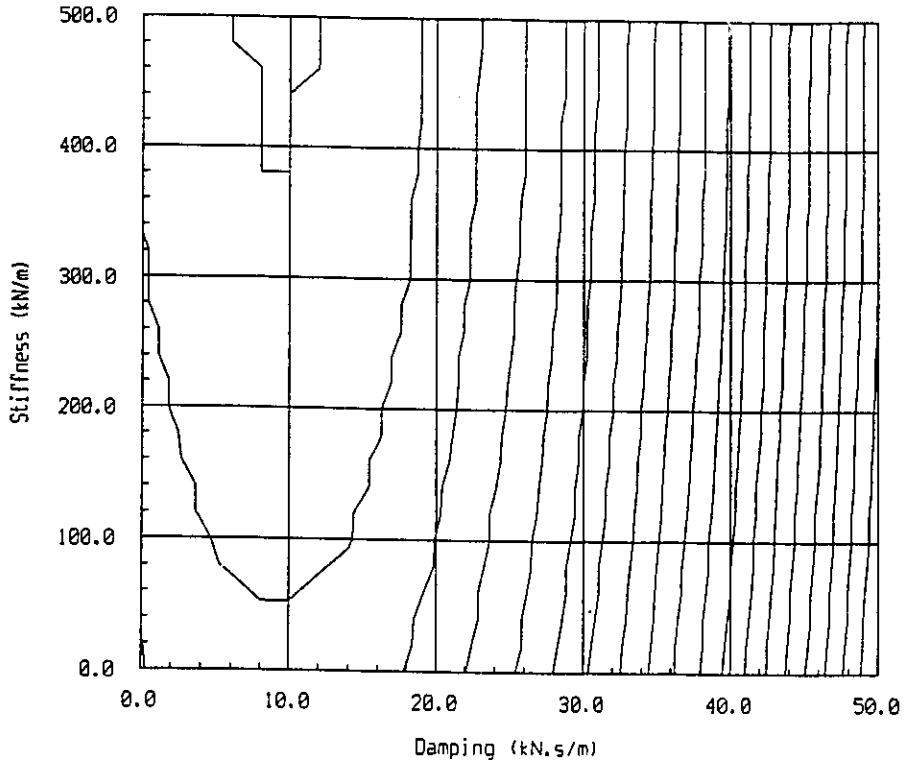

(4.5c Actuator 3 force)

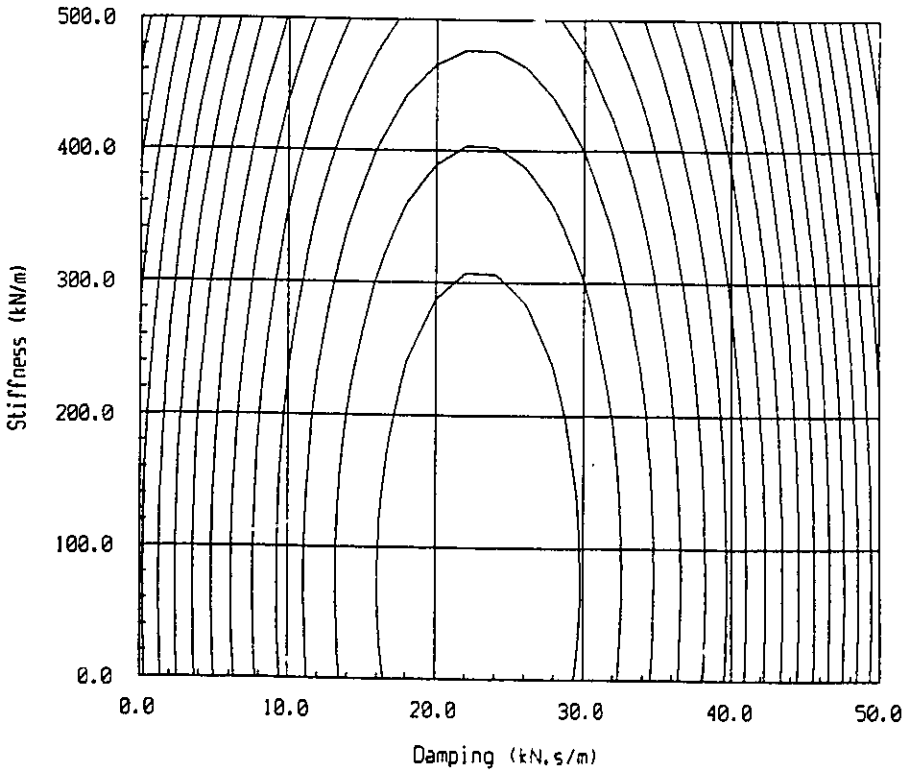

(4.5d Actuator 4 force)

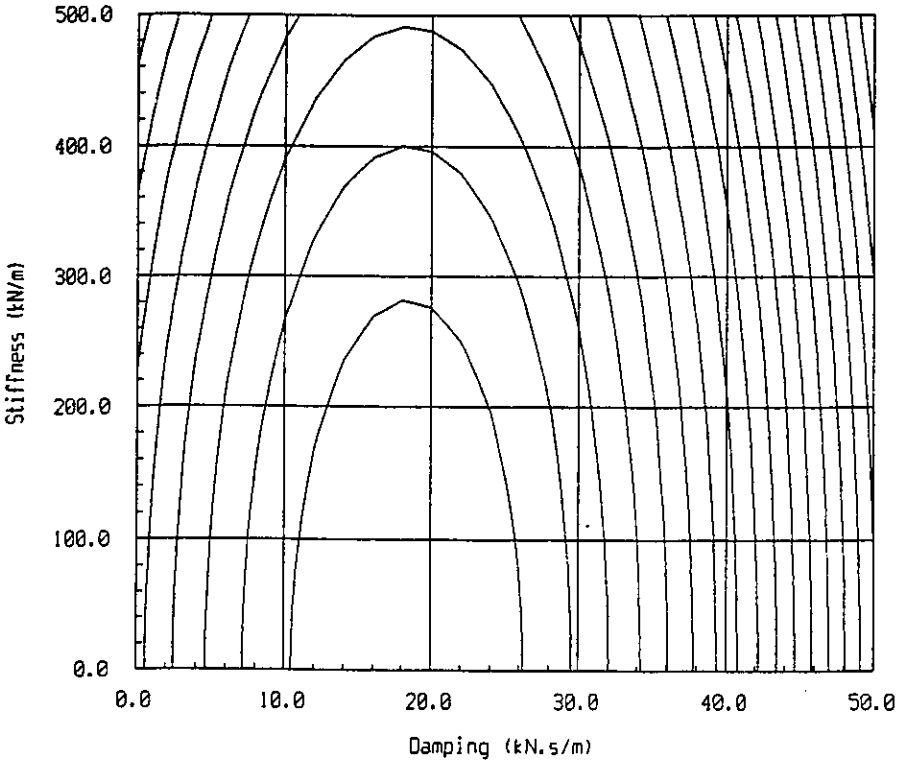

(4.5e Actuator 5 force)

Figure 4.5 Iso-value curves of mean square actuator forces

4.5.2 Influence of Weighting Coefficient Variations on the Suspension Performance

The performance of an active suspension is strongly dependent on the choice of the weighting coefficients in the performance index J. Using the covariance study of a passive suspension undertaken in Chapter 3, an initial set of weighting coefficients was selected in section 4.3.3. Any variation in these weighting coefficients may cause changes in the performance characteristics of the actively suspended vehicle. The influence of variations in the weighting coefficients on the different components of the performance index are investigated using EQ (4.35). The variations in the weighting coefficients are realized by introducing multiplication factors, Mt and Mf, with baseline coefficients listed in Table 4.1, and $\rho_i = 10^{+4}$.

The influence of weighting coefficients, μ_1 and μ_2, associated with tractor bounce and pitch acceleration response, on the components of the performance index is investigated to identify appropriate values of weighting coefficients. The coefficients μ_1 and μ_2 are varied simultaneously by varying the multiplication factor, Mi, in the range 1E-3 to 1E+2. The weighting factors, ρ_i ($i=1, \ldots,5$). are also varied by varying the corresponding multiplication factor, Mf, in the range 1E-20 to 1.00. The effect of varying these weighting coefficients on the performance variables is shown in Figures 4.6 to 4.9. An increase in μ_1 and μ_2 tends to emphasize the contribution of the tractor bounce and pitch acceleration response in the performance index J. The tractor bounce and pitch acceleration responses thus decrease, as shown in Figures 4.6a and 4.6b. This, however, necessitates penalyzation of the actuator forces to ensure availability of adequate control force. The suspension performance approaches that of the passive suspension when the weighting factors ρ_i are increased due to insufficient control forces developed by the

active force actuators. The influence of weighting coefficients on the suspension performance then becomes insignificant as reflected by the flat areas in the figures. An increase in μ_1 and μ_2 also results in improved semitrailer bounce acceleration response that may be attributed to the constraints posed by the articulation. However, increasing μ_1 and μ_2 beyond certain limit results in high semitrailer pitch acceleration, and suspensions and tires deflection, as shown in Figures 4.7b, 4.8 and 4.9. The expected values of these penalized variables, in extreme cases, exceed those derived for the passive suspension. A comprehensive parameteric study was carried out to study the influence of variations in other weighting coefficients on the performance index. While the results are not presented here, the following general observations were made: increasing a weighting coefficient, coupled with availability of sufficient actuating force, reduces the corresponding penalized variable and, generally, increases the other penalized variables.

Figures 4.6 to 4.9 clearly illustrate the strong dependency of the active suspension performance on the weighting coefficients, and the need to realize a compromise among the different components of the performance index. A set of weighting coefficients thus must be identified to realize an optimal suspension. It is desirable to design an active suspension to improve ride quality, cargo safety and reduce tires forces, while a reasonable increase in the suspension deflection can be considered acceptable. The weighting coefficients in the performance index are thus selected using an iterative procedure to attain the above design compromise. The weighting coefficients given in Table 4.1 are initially employed to determine the variants of the performance index (J_{zi}). The resulting variants are compared to those derived for the passive suspension. If any of the 14 variants exceeds the corresponding value derived for the passive suspension, the associated weighting coefficient is increased to emphasize the contribution of the particular variant in the performance index. The performance indices are then reevaluated and the process is repeated until an improvement in all the 14 variants of the performance index is achieved.

The procedure resulted in a number of weighting coefficients that satisfy the desired design compromise. A total of 5 sets of weighting coefficients are selected and are presented in Table 4.2. The suspension schemes based on these weighting coefficients are designated as *AS1* to *AS5*. The corresponding reduction or increase in the expected value of the penalized variables relative to those derived for the "optimum" passive suspension are listed in Table 4.3. All the five active suspension schemes, in general, yield improved performance when compared to the passive suspension. Each of these schemes, however, accentuates certain particular aspects of the performance index. The suspension schemes *AS1*, *AS2* and *AS3* emphasize, to different extents, ride quality, cargo safety and tire forces. While the schemes *AS4* and *AS5* mostly emphasize the tire deflection response. The *AS2* scheme yields best ride quality, while best cargo safety is achieved using *AS3*. A comparison of *AS4* and *AS5* schemes reveals that further improvements in the ride quality, cargo safety and tire deflection can be achieved by relaxing the suspension deflection requirements.

Table 4.2 Weighting coefficients for each of the penalized variables for the 5 differently weighted active suspensions

Suspension → *Penalized variable i* ↓	*AS1* μ_i	*AS2* μ_i	*AS3* μ_i	*AS4* μ_i	*AS5* μ_i
1	4.29e+0	6.86e+0	5.50e+3	2.98e+1	2.69e+1
2	2.28e+1	3.76e+1	3.18e+4	1.19e+2	1.51e+2
3	6.09e+0	8.52e+0	2.66e+3	7.70e+0	1.99e+1
4	8.33e+2	8.33e+2	1.38e+5	8.33e+2	8.33e+2
5	1.99e+5	3.01e+5	3.73e+8	1.00e+6	8.79e+5
6	8.75e+4	1.46e+5	1.21e+8	2.49e+5	4.60e+5
7	6.37e+4	1.49e+5	9.14e+7	8.23e+4	2.81e+5
8	1.54e+4	7.92e+4	4.62e+7	3.80e+4	2.35e+5
9	2.81e+3	5.10e+4	1.69e+7	1.84e+0	2.03e+5
10	4.98e+5	1.07e+6	1.00e+9	3.23e+6	3.41e+6
11	3.45e+5	1.30e+6	8.09e+8	5.73e+5	2.29e+6
12	9.12e+5	2.57e+6	1.93e+9	3.59e+6	5.85e+6
13	1.24e+5	9.07e+5	2.08e+8	6.32e+4	6.75e+5
14	1.55e+5	1.06e+6	2.42e+8	1.18e+5	7.13e+5

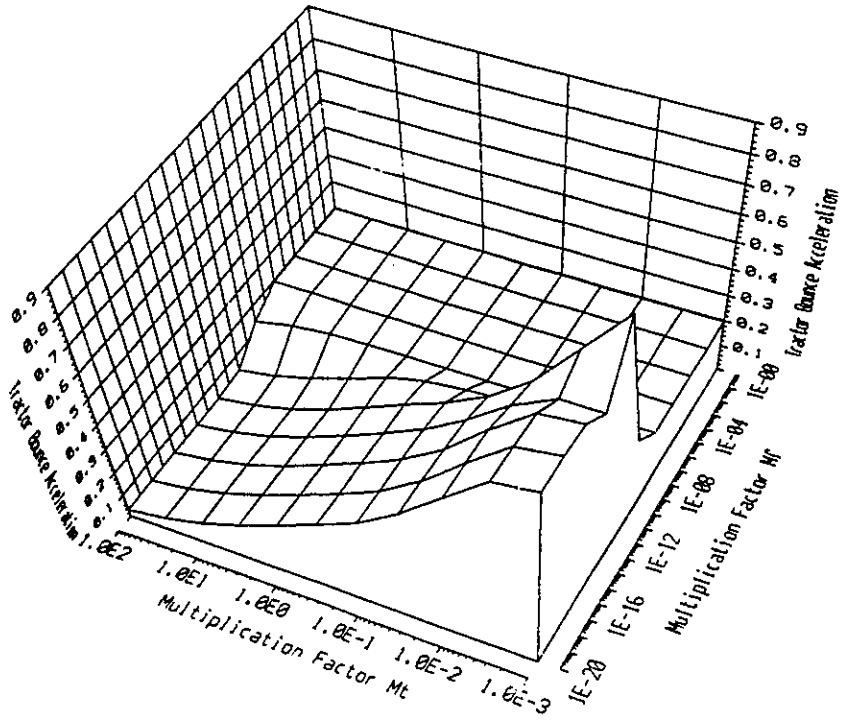

Figure 4.6a Mean square acceleration of the tractor bounce for varying weighting coefficients

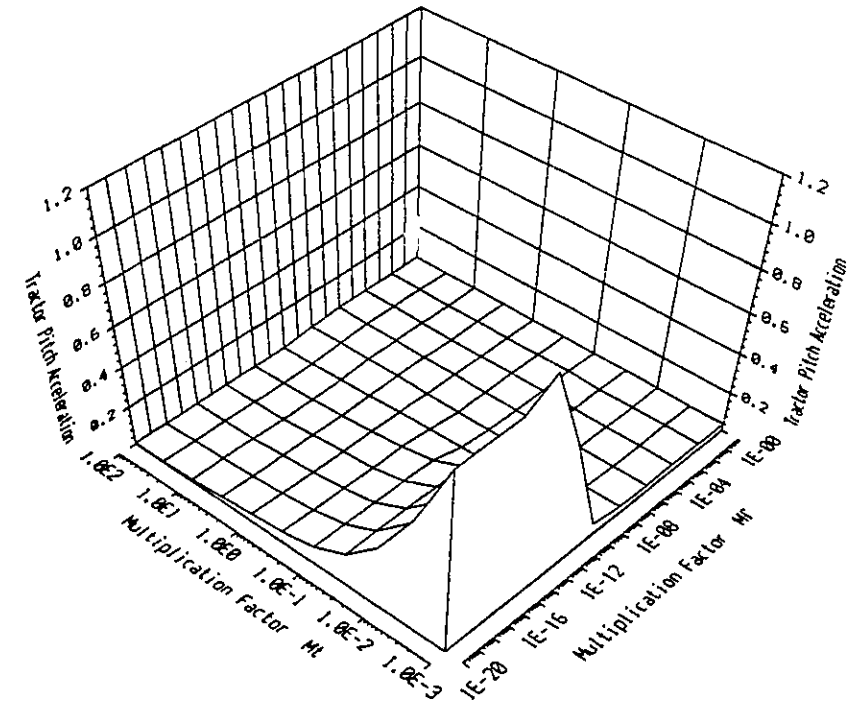

Figure 4.6b Mean square acceleration of the tractor pitch for varying weighting coefficients

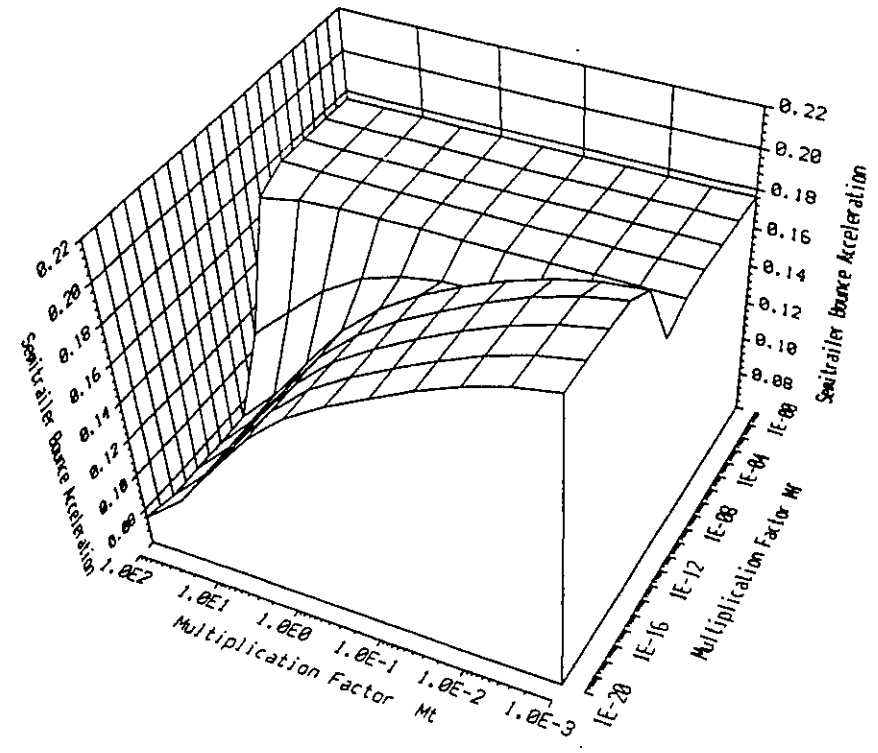

Figure 4.7a Mean square acceleration of the semitrailer bounce for varying weighting coefficients

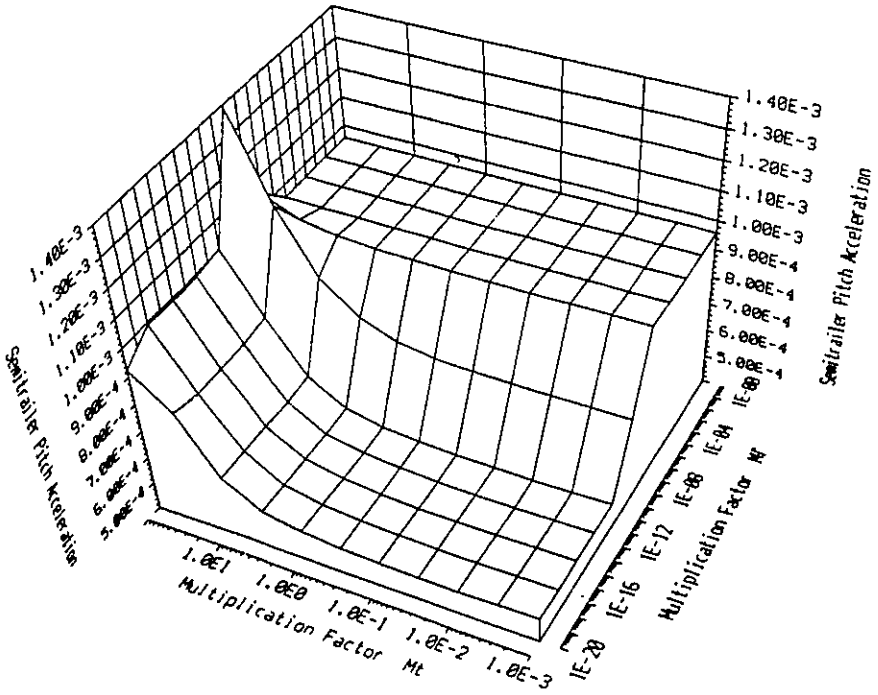

Figure 4.7b Mean square acceleration of the semitrailer pitch for varying weighting coefficients

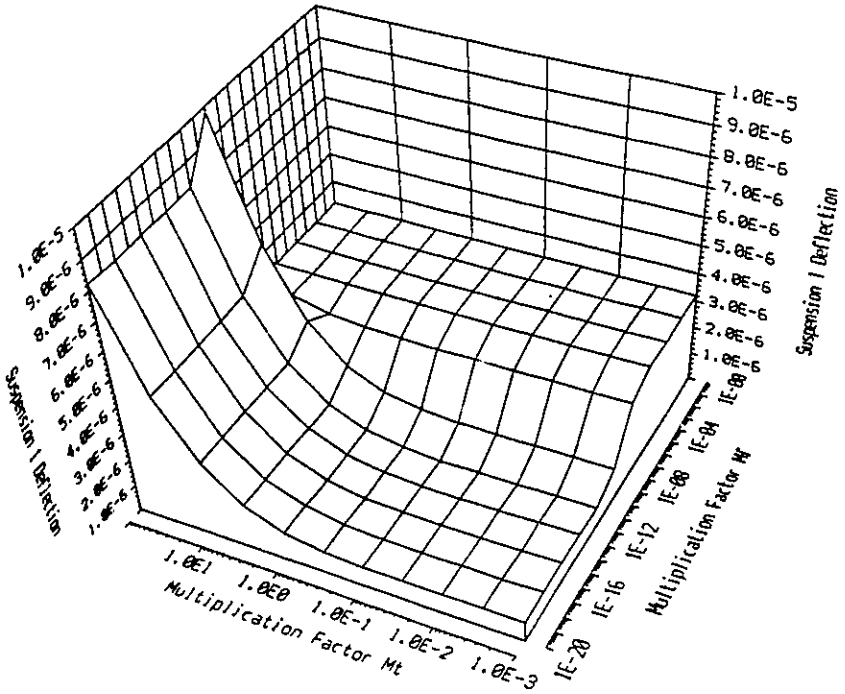

Figure 4.8a Mean square deflection of suspension 1 for varying weighting coefficients

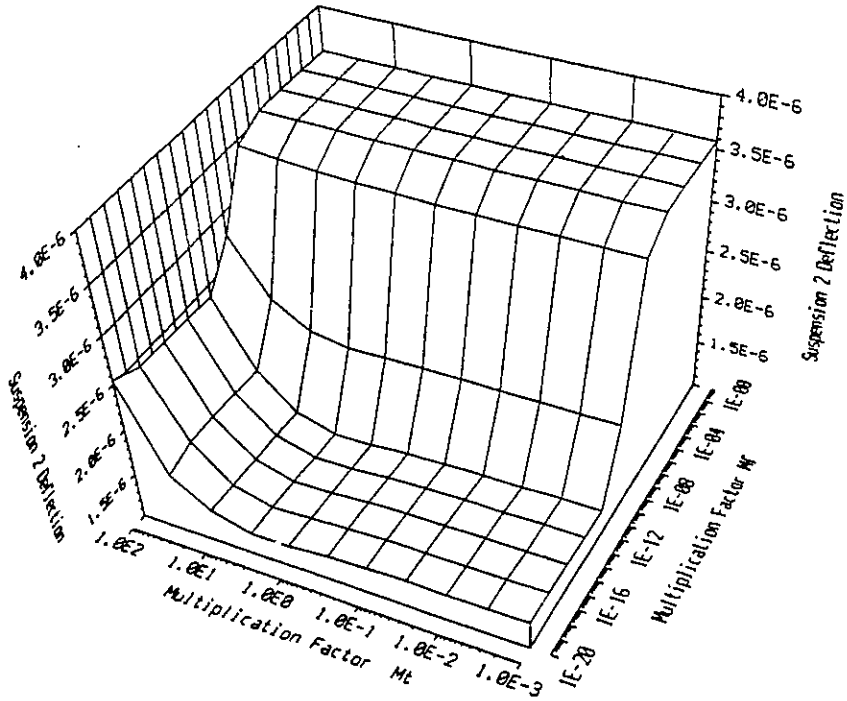

Figure 4.8b Mean square deflection of suspension 2 for varying weighting coefficients

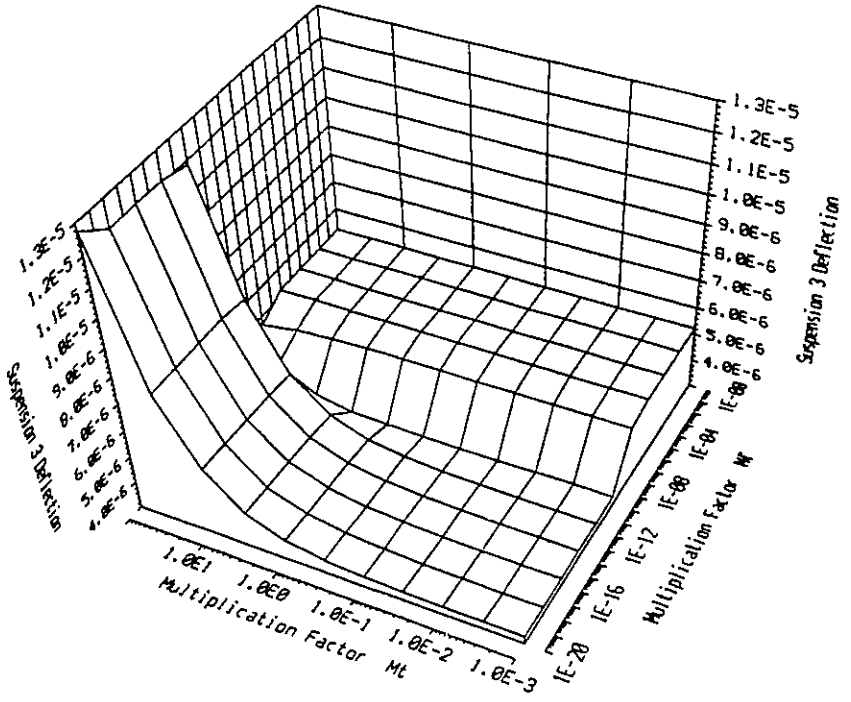

Figure 4.8c Mean square deflection of suspension 3 for varying weighting coefficients

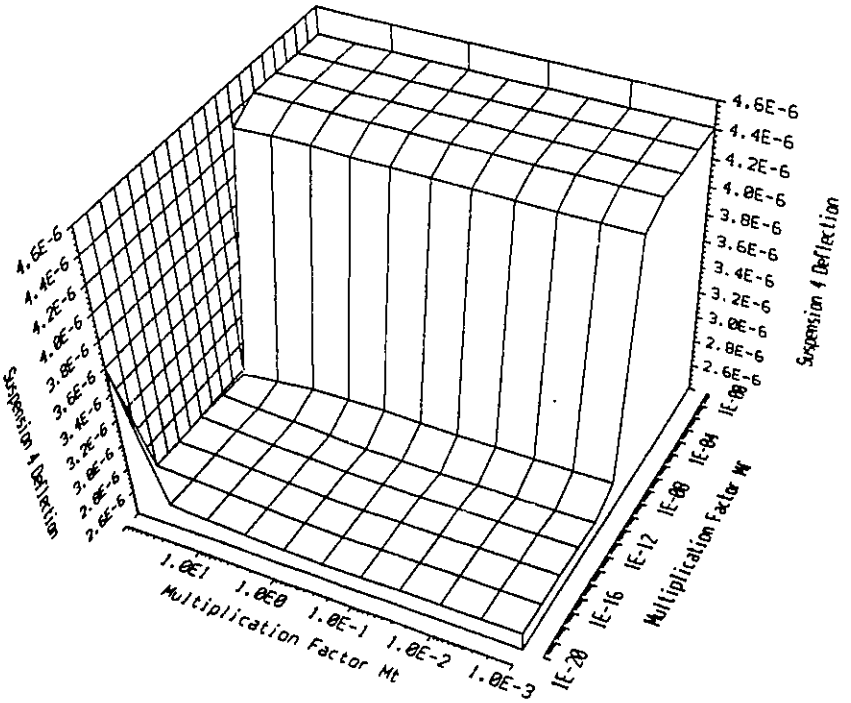

Figure 4.8d Mean square deflection of suspension 3 for varying weighting coefficients

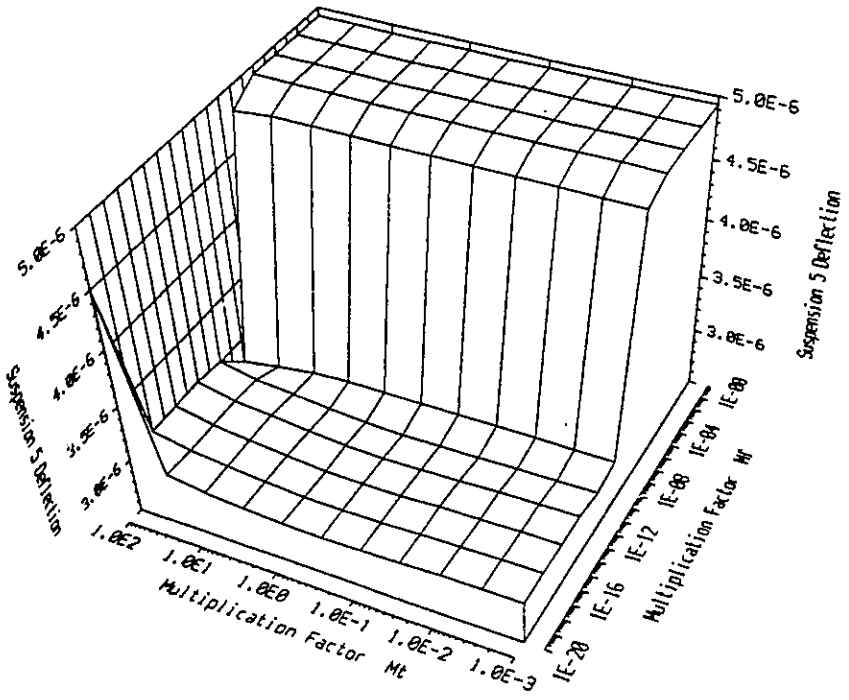

Figure 4.8e Mean square deflection of suspension 5 for varying weighting coefficients

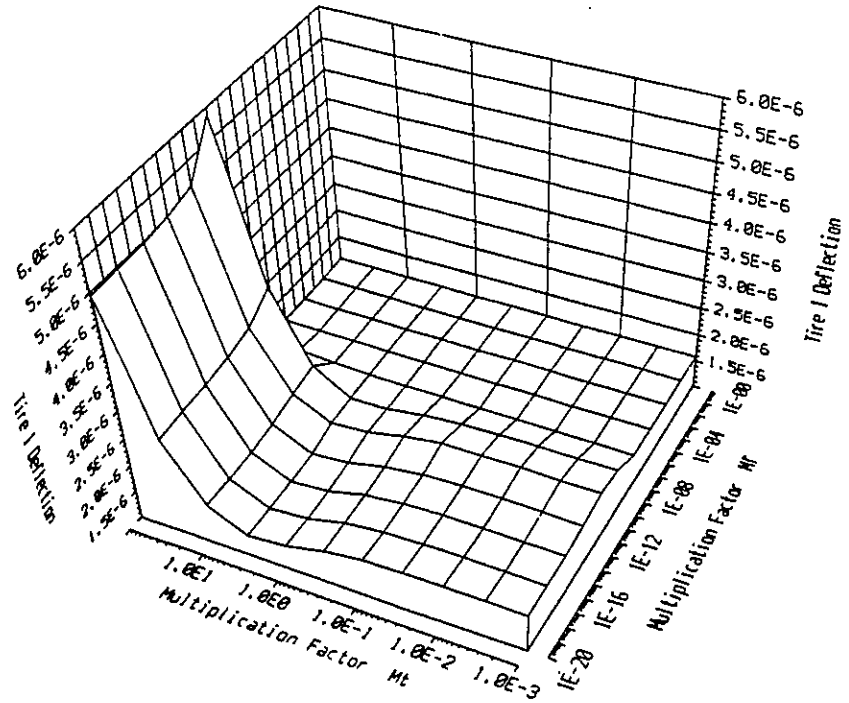

Figure 4.9a Mean square deflection of tire 1 for varying weighting coefficients

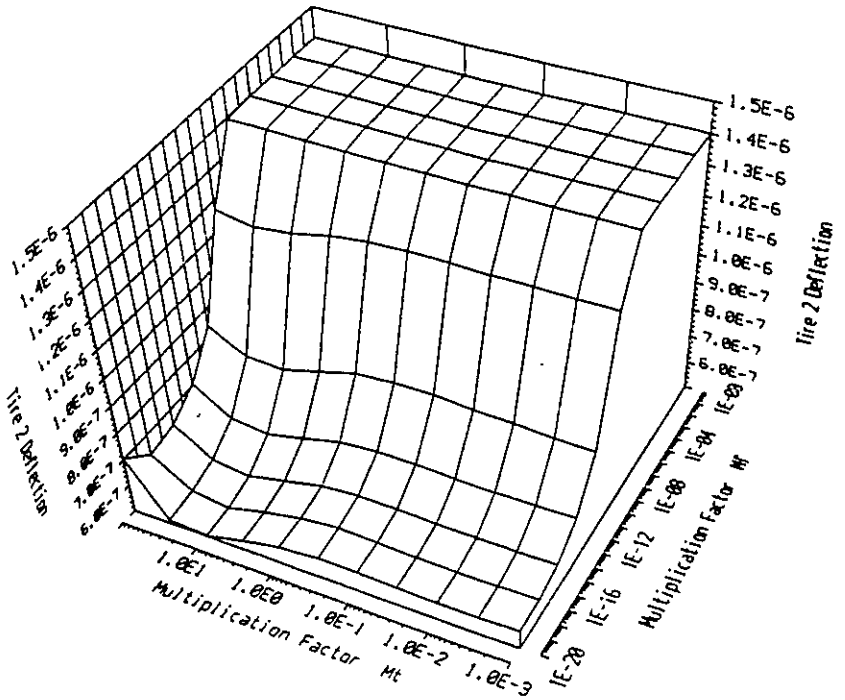

Figure 4.9b Mean square deflection of tire 2 for varying weighting coefficients

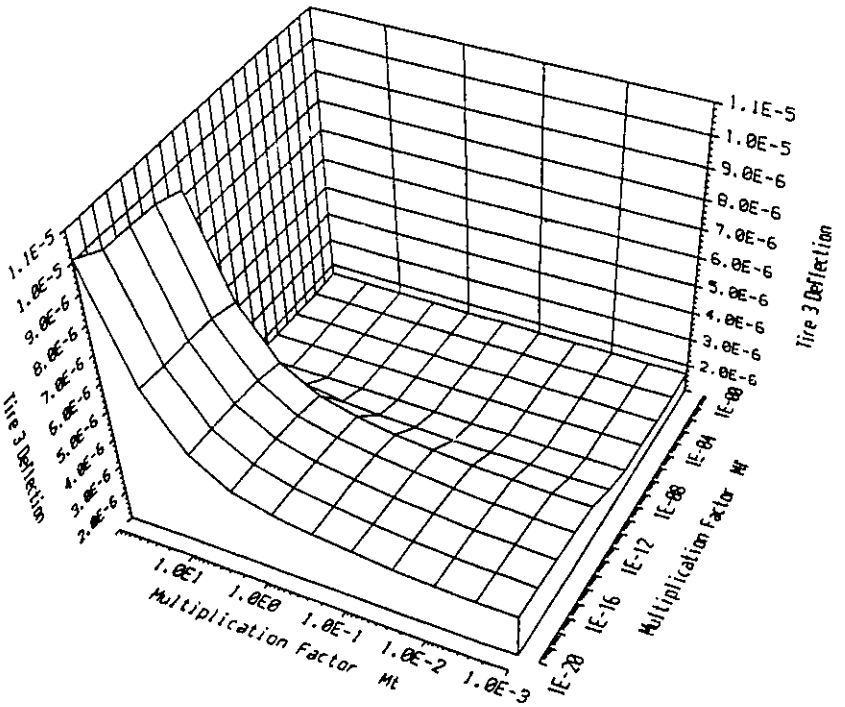

Figure 4.9c Mean square deflection of tire 3 for varying weighting coefficients

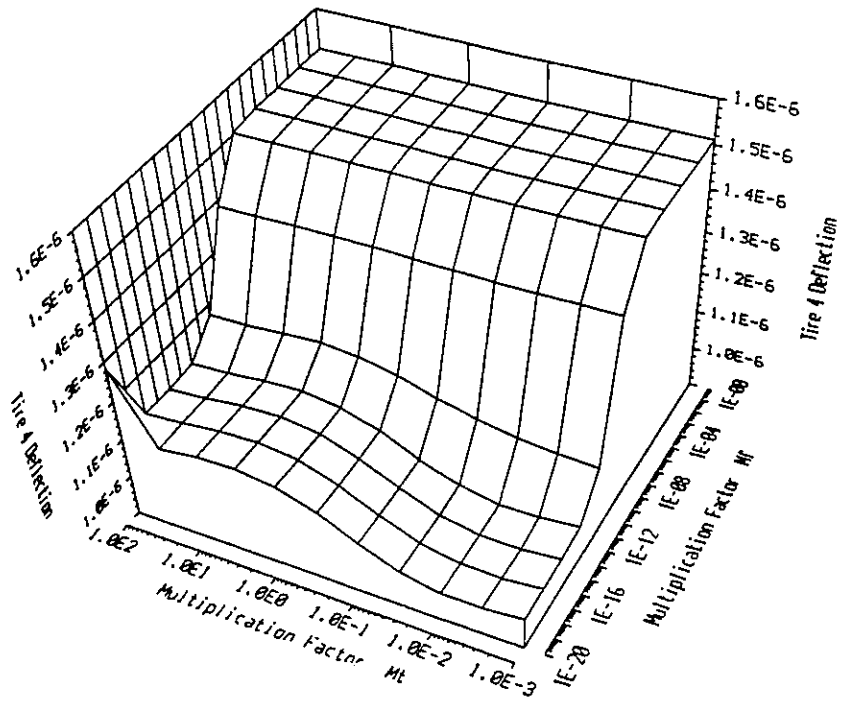

Figure 4.9d Mean square deflection of tire 4 for varying weighting coefficients

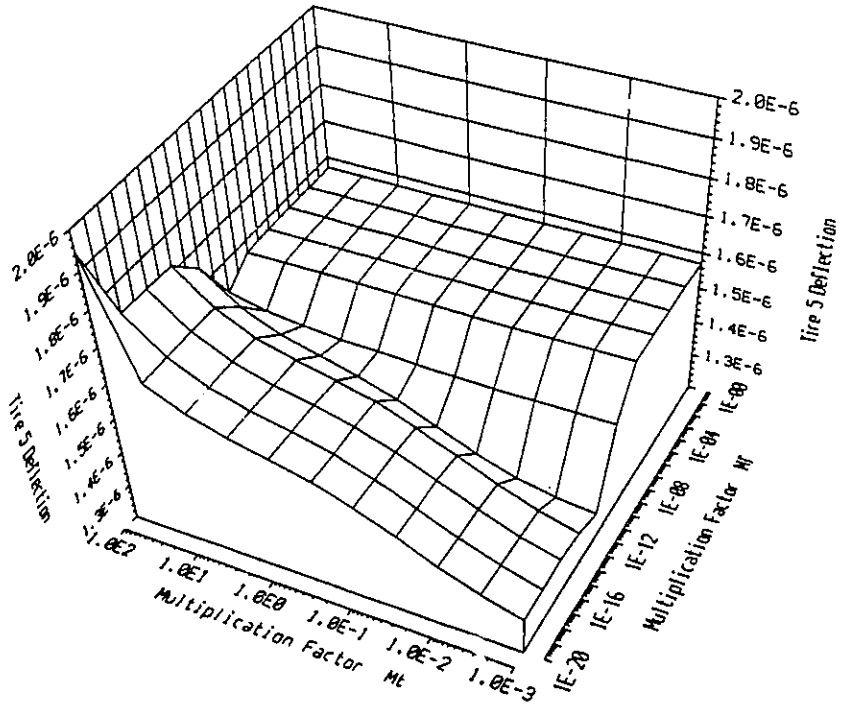

Figure 4.9e Mean square deflection of tire 5 for varying weighting coefficients

Table 4.3 Percent reduction(+)/increase(-) in the expected value of each of the penalized variables for 5 differently weighted active suspensions (compared to "optimum" passive)

Performance variable	*AS1* %	*AS2* %	*AS3* %	*AS4* %	*AS5* %
Tractor bounce acceleration	2.36e+1	2.17e+1	2.71e+1	1.30e+1	8.48e+0
Tractor pitch acceleration	2.65e+1	2.53e+1	2.71e+1	1.41e+1	9.24e+0
Semitrailer bounce acceleration	2.86e+1	3.63e+1	3.77e+1	2.52e+1	2.03e+1
Semitrailer pitch acceleration	4.82e+1	7.80e+1	6.29e+1	5.66e+1	1.76e+1
Suspension 1 Deflection	-6.92e+0	2.06e+0	1.04e-1	-2.64e+0	9.31e+0
Suspension 2 Deflection	8.35e+0	5.27e-1	1.39e+0	-7.54e+0	1.34e+1
Suspension 3 Deflection	1.18e+1	3.65e+0	3.60e+0	-6.49e-1	1.54e+1
Suspension 4 Deflection	2.40e+1	7.55e+0	1.58e+0	1.64e+1	1.58e+1
Suspension 5 Deflection	4.26e+1	2.83e+1	3.35e+1	2.78e+1	2.47e+1
Tire 1 force	2.76e-1	3.92e-2	8.39e-3	5.02e+0	7.45e+0
Tire 2 force	7.38e+0	2.73e+0	2.95e+0	1.51e+1	1.14e+1
Tire 3 force	4.80e+0	1.14e+0	6.40e-1	1.09e+1	1.09e+1
Tire 4 force	2.14e+1	1.08e+1	5.36e+0	2.50e+1	2.36e+1
Tire 5 force	1.29e+1	1.03e+1	3.78e+0	2.62e+1	2.36e+1

4.5.3 Frequency Response Characteristics of the Actively Suspended Vehicle

The results presented in the previous sections describe an overall measure of the different variants of the performance index obtained through the solution of EQ (4.35). A study of the resonant behavior and the ride quality necessitates the analysis of frequency spectra of the response characteristics of the different active suspension schemes. EQ (4.50) is thus solved to obtain the frequency response characteristics of the 5 active suspensions schemes (*AS1* to *AS5*) subjected to excitations arising from a rough road. The response characteristics are compared to the frequency response characteristics of the "optimum" passive suspension developed in Chapter 3.

Figures 4.10 to 4.13 present the *PSD* of the penalized variables for the five active and the "optimum" passive suspensions. All the five active suspension schemes offer improved ride quality and better cargo safety almost in the entire frequency range, as shown in Figures 4.10 and 4.11. Substantial benefits can be observed with all of the 5 active suspension schemes especially at low frequencies, which is a critical frequency region in ride quality evaluations. At higher frequencies, near the axles resonant frequencies around 10 *Hz*, the performance characteristics of the active suspensions are similar to those of the "optimum" passive suspension. The active suspensions, irrespective of the weighting coefficients, do not provide a significant improvement in the vertical and pitch responses of the tractor and semitrailer sprung masses near the wheel hop frequencies. This behavior of the active suspension is also supported by the studies reported in [17,18], which were based on a 2 *DOF* vehicle model. It has been shown that a single point, corresponding to the wheel hop frequency, exists on the sprung mass body acceleration response. This point is known as the invariant point and can not be changed regardless of the suspension scheme used [17,18].

The magnitude of relative deflection response across all the five axle suspensions also reduces considerably when proposed active suspensions are employed, as shown in Figure 4.12. The active suspensions, however, yield high suspension deflection at low frequencies, especially below 0.9 *Hz*, as illustrated in Figures 4.12a to 4.12c. The actuators are constantly trying to correct for any changes in the tractor, semitrailer and wheel motions using feedback signals related to all the states of the vehicle. The actuator forces are thus continuously adjusted to correct for the changes in the motion. Mathematically, the transfer functions for the active suspension deflections do not necessarily reach zero at low frequencies as in the case of a passive suspension. This limitation of active suspensions is also reported in the literature [17,19-22]. Figures 4.13a to 4.13e illustrate the frequency response spectra of the tire forces due to active and passive suspensions. Active suspension systems yield significant reduction in dynamic tire forces at low frequencies. The reduction of the dynamic tire forces, however, is not evident near wheel hop frequencies (near 10 *Hz*). The suspension scheme *AS5* yields the most significant reduction in the dynamic tire forces in the entire frequency range. This active suspension scheme is thus desirable when the design objectives involve a specific emphasis on the pavement fatigue caused by dynamic tire loads transmitted to the road.

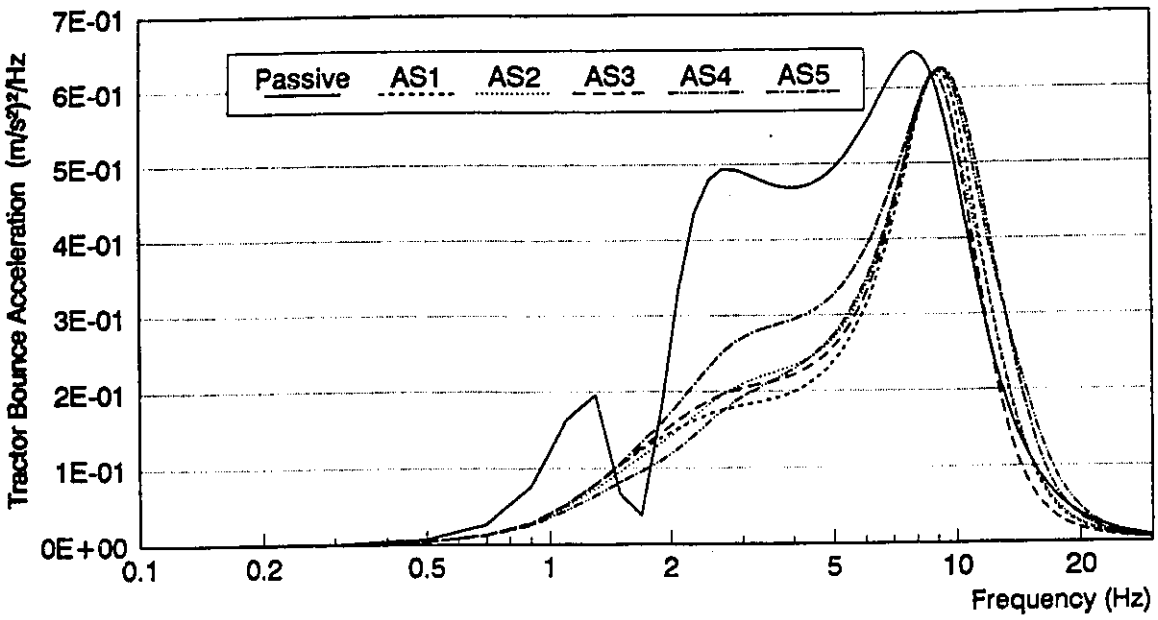

Figure 4.10a PSD of tractor bounce acceleration for passive and active systems

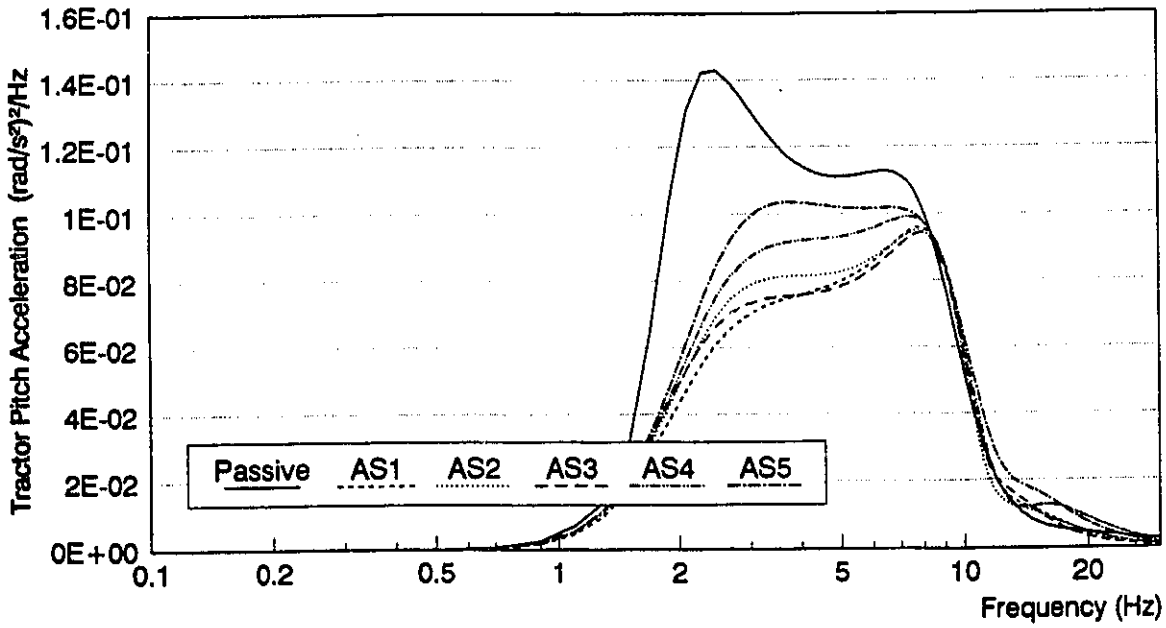

Figure 4.10b PSD of tractor pitch acceleration for passive and active systems

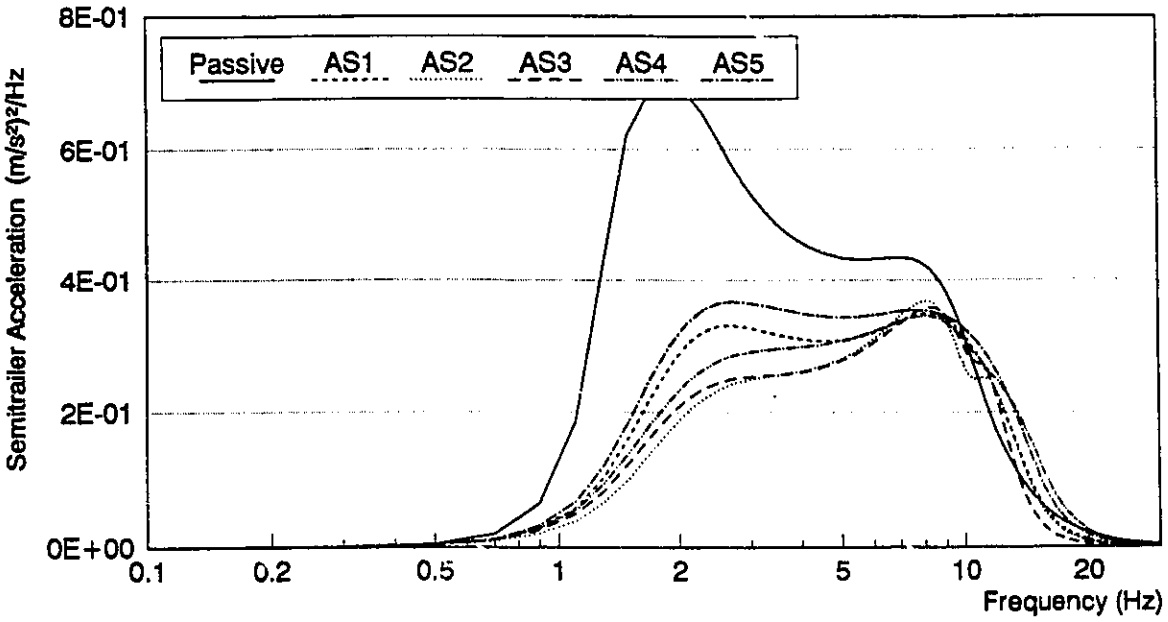

Figure 4.11a PSD of semitrailer bounce acceleration for passive and active systems

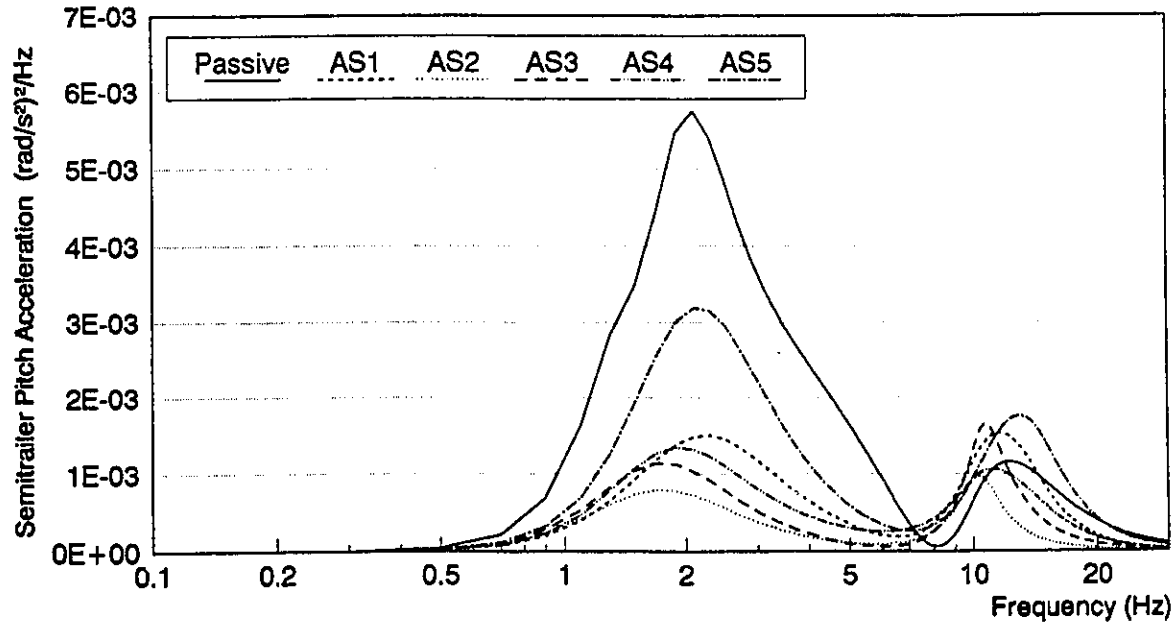

Figure 4.11b PSD of semitrailer pitch acceleration for passive and active systems

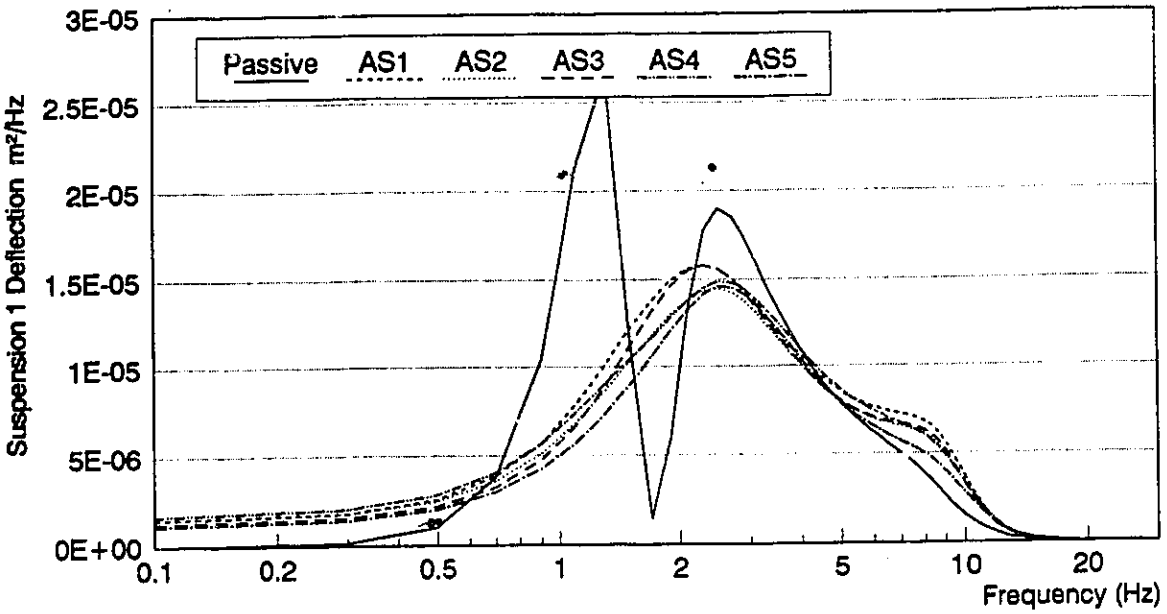

Figure 4.12a PSD of suspension 1 deflection for passive and active systems

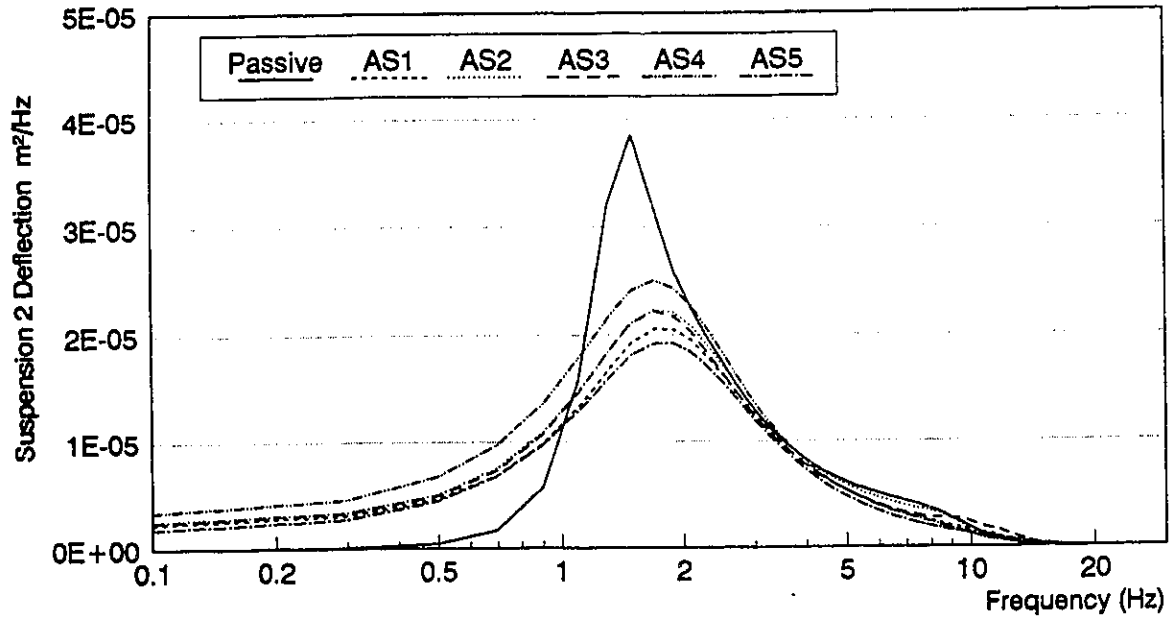

Figure 4.12b PSD of suspension 2 deflection for passive and active systems

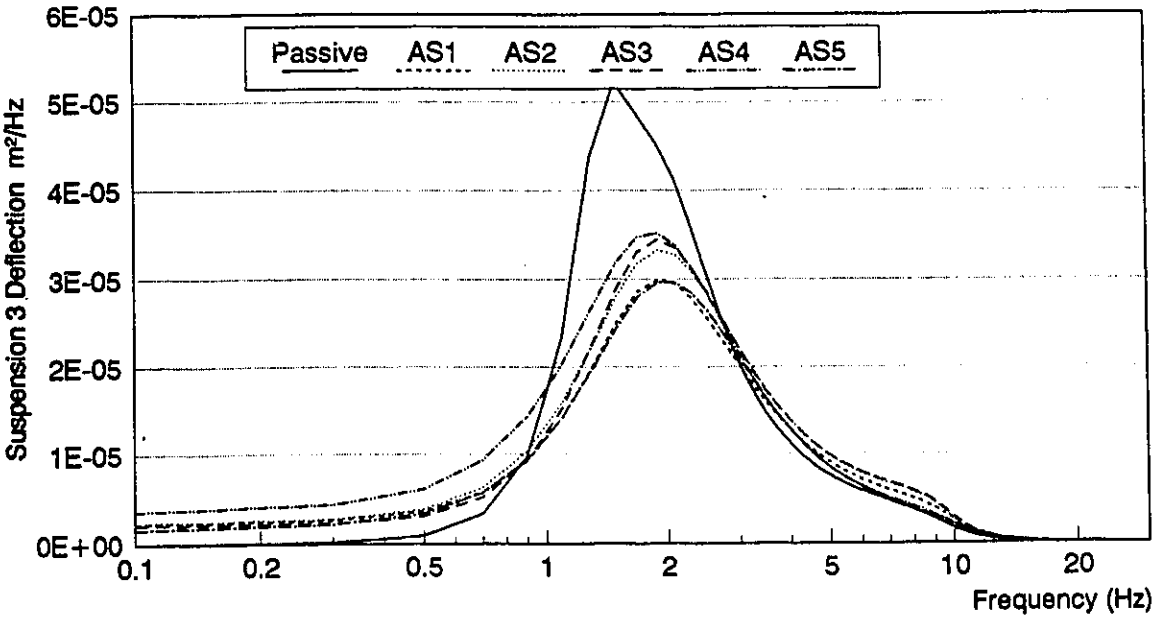

Figure 4.12c PSD of suspension 3 deflection for passive and active systems

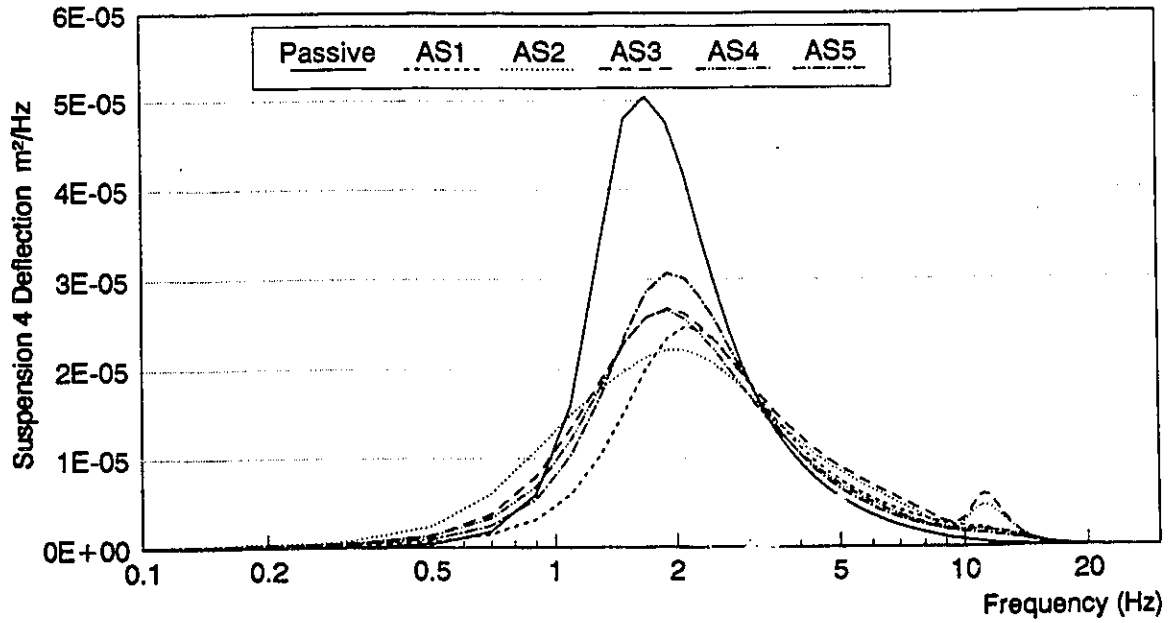

Figure 4.12d PSD of suspension 4 deflection for passive and active systems

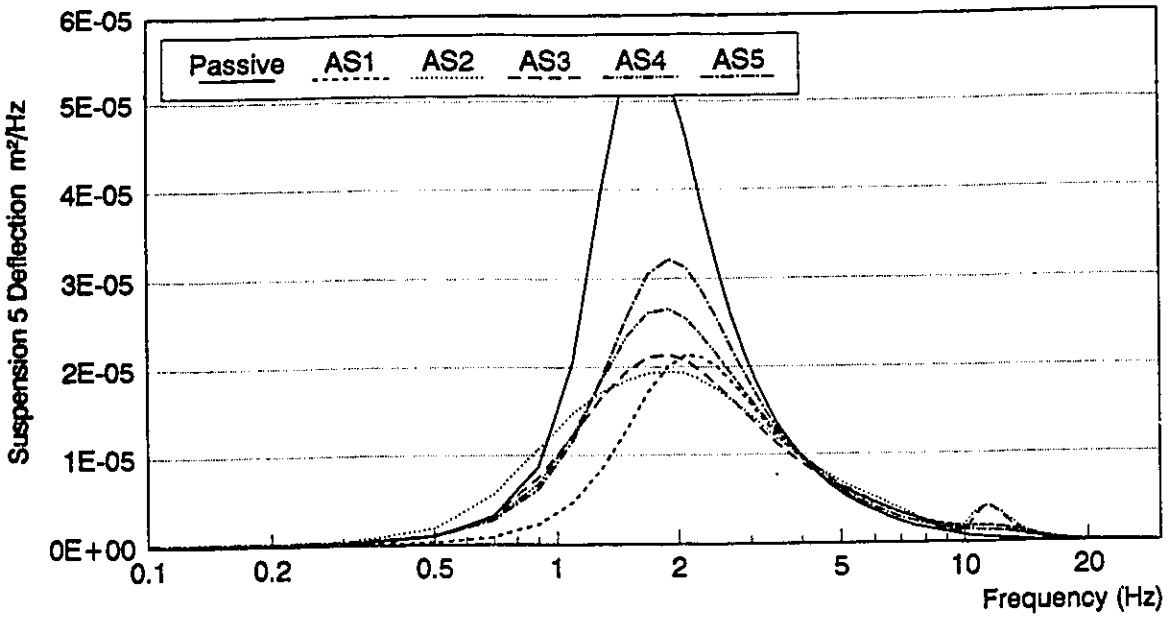

Figure 4.12e PSD of suspension 5 deflection for passive and active systems

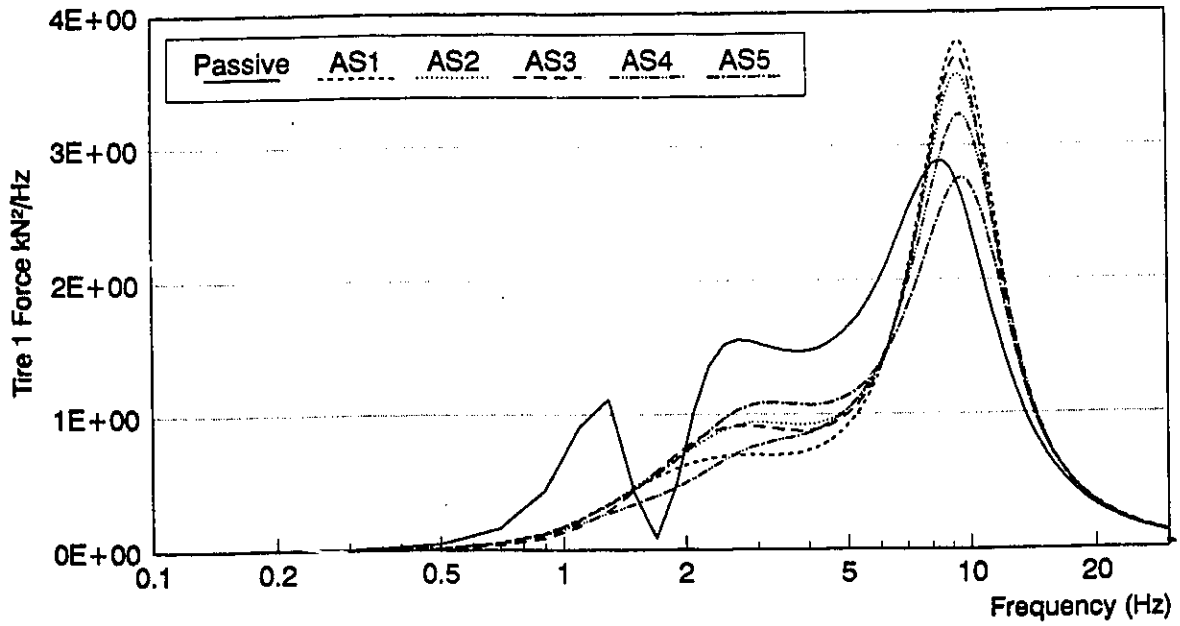

Figure 4.13a PSD of tire 1 force for passive and active systems

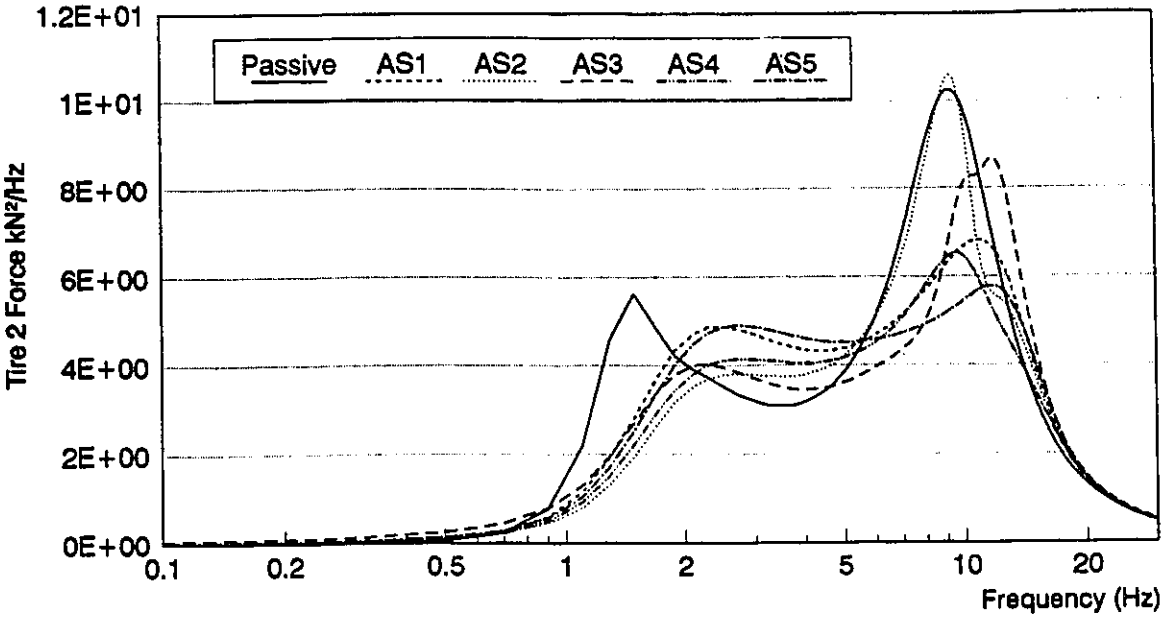

Figure 4.13b PSD of tire 2 force for passive and active systems

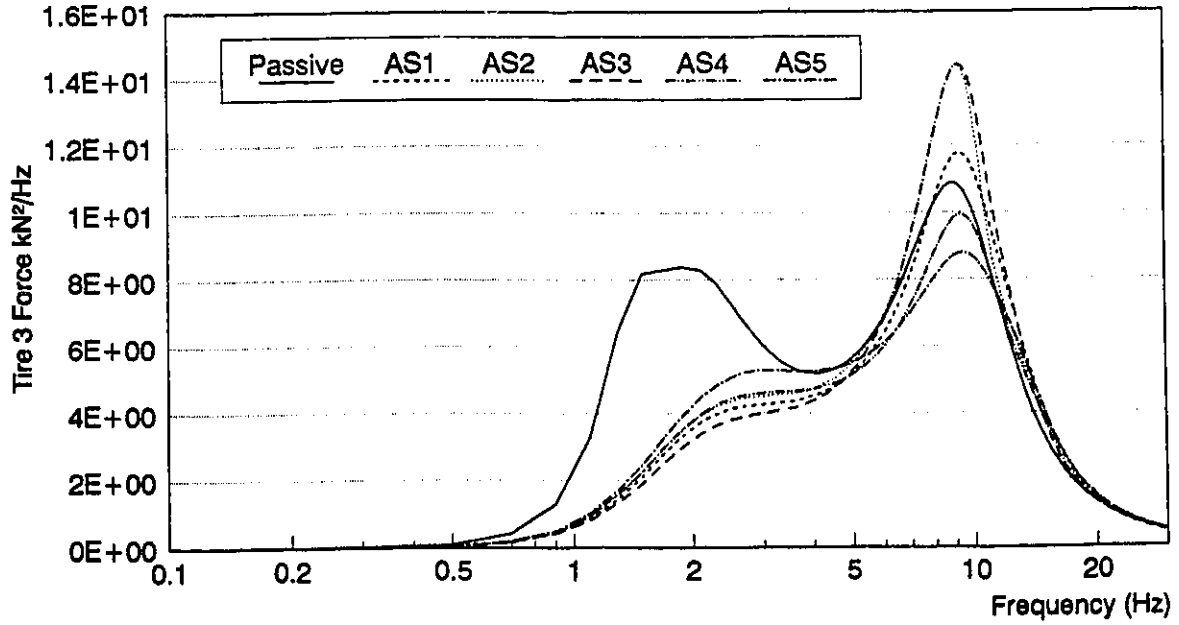

Figure 4.13c PSD of tire 3 force for passive and active systems

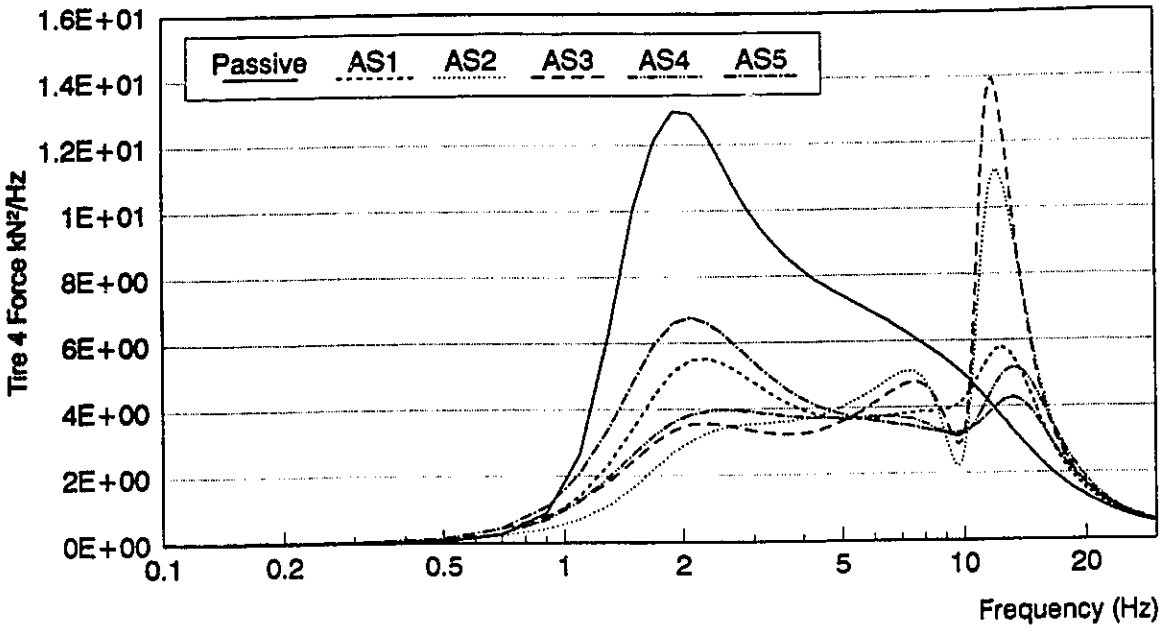

Figure 4.13d PSD of tire 4 force for passive and active systems

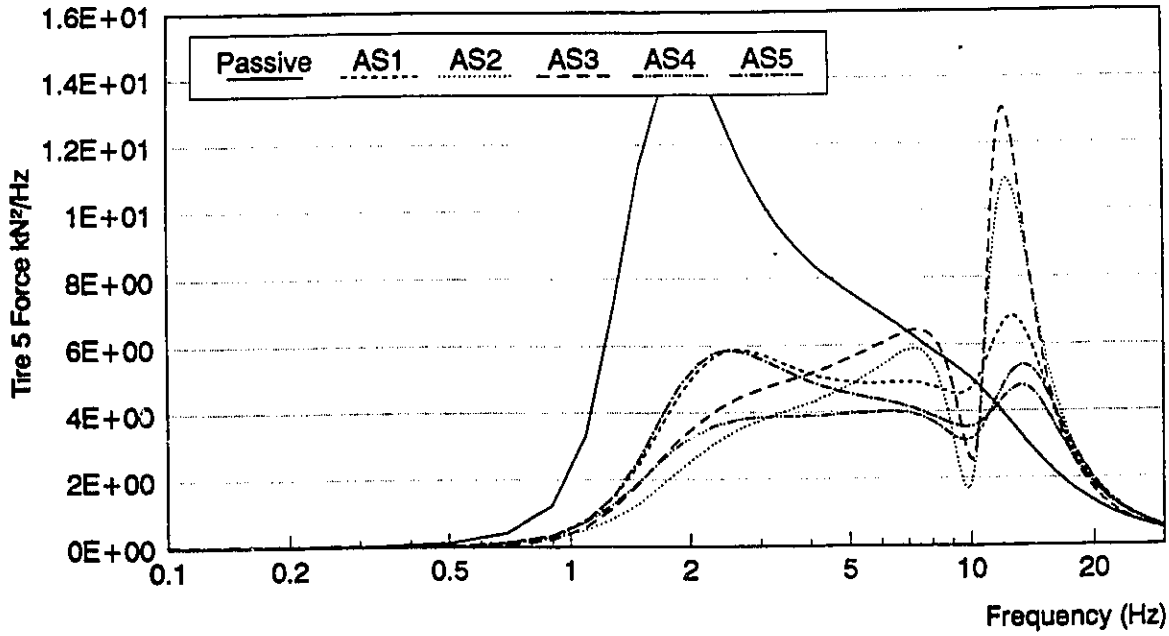

Figure 4.13e PSD of tire 5 force for passive and active systems

4.5.4 Influence of Vehicle Speed on Active Suspension Performance

The control gain matrices $\boldsymbol{K}$ in the analysis of the five active suspension configurations, *AS1* to *AS5*, were obtained for constant forward speed of 90 *km/h*. The performance characteristics of the active suspension systems is known to be dependent upon vehicle speed and the road roughness conditions. The performance characteristics are thus evaluated for variations in the vehicle speed to study the effectiveness of the active suspensions. Figures 4.14 to 4.17 show the effect of varying vehicle speed on the different penalized variables. The control gain for the active suspensions *AS1* to *AS5*, selected for a vehicle speed of 90 *km/h*, are used to evaluate the response characteristics in the 10-120 *km/h* speed range. Figures 4.14 and 4.15 clearly illustrate that the active suspensions provide significant improvement in the ride quality and cargo safety, irrespective of the vehicle speed and the active suspension scheme. The suspension scheme *AS3*, however, yields the most significant improvement in the ride quality and cargo safety performance of the vehicle. The relative deflection responses of the active suspensions are comparable to those of the passive suspension and thus no extra rattle space requirements is necessary for the active systems. However, if rattle space is a major factor, *AS3* and *AS4* have to be avoided since they result in large suspension deflection as shown in Figures 4.16b, 4.16c and 4.16d. The active suspension *AS1* yields considerable reduction in the rattle space requirements of the drive and semitrailer axles at highway speeds. Figures 4.17a to 4.17e illustrate the tire deflection response characteristics of the active and passive suspension systems. Except for *AS3*, all the active systems show lower tire deflections throughout the speed range (Figure 4.17). The performance of the active suspensions, in general, is enhanced as the vehicle speed increases, as illustrated in Figures 4.14 to 4.17. Since freight vehicles operate mostly at high speeds, the performance potentials of the active systems becomes more significant.

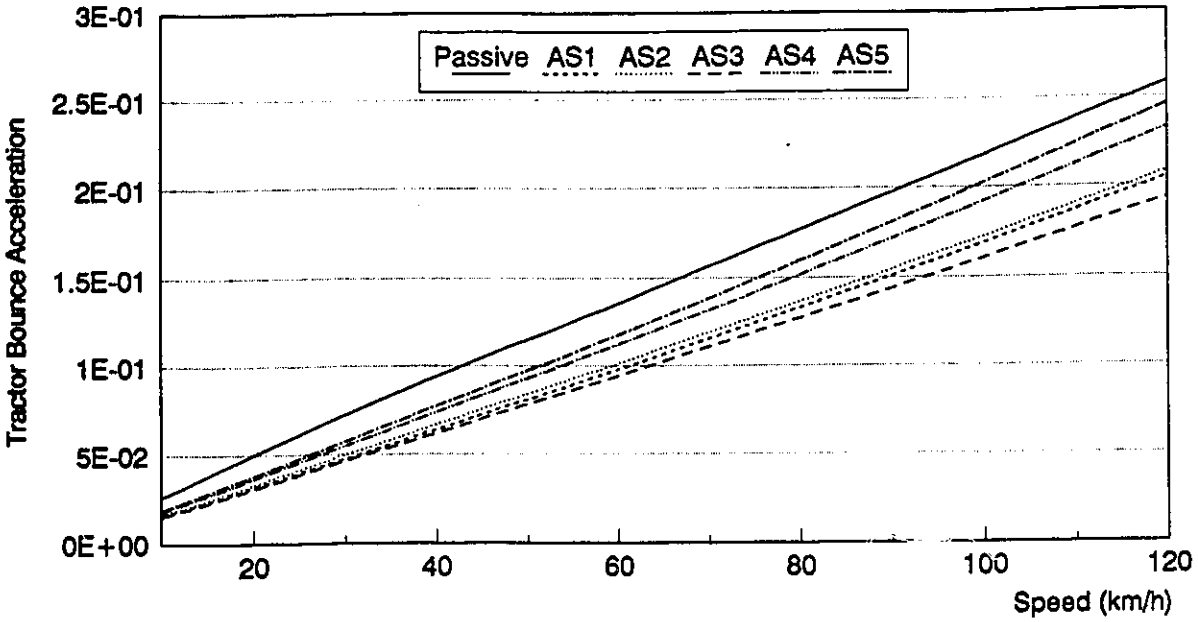

Figure 4.14a Effect of vehicle speed on mean square acceleration of tractor bounce for passive and active systems

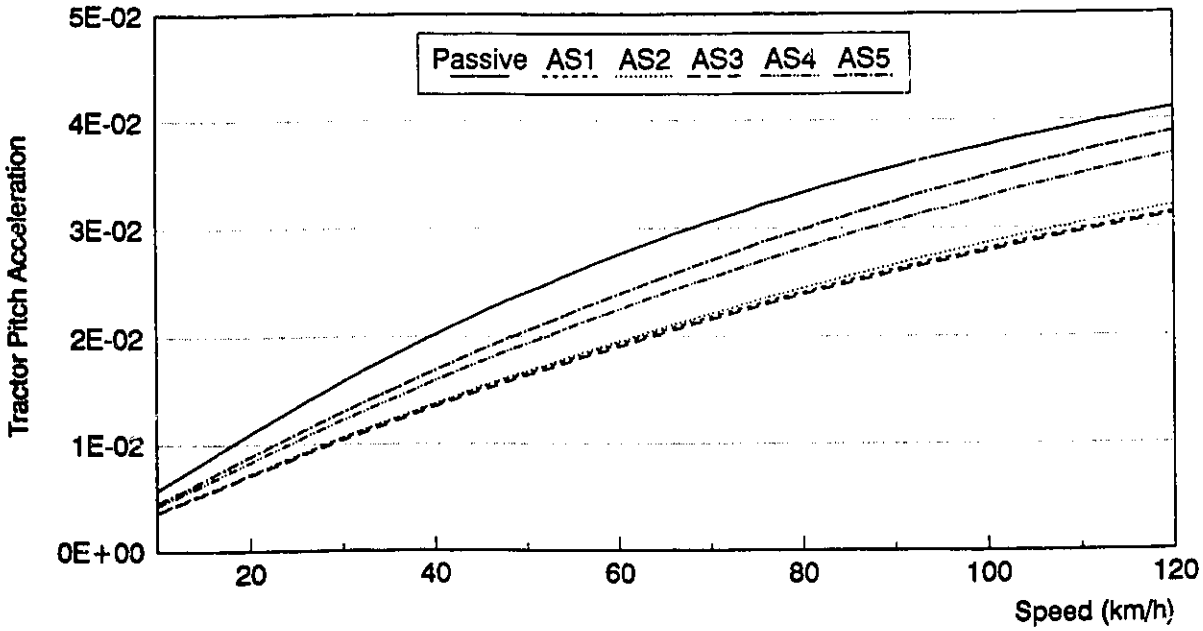

Figure 4.14b Effect of vehicle speed on mean square acceleration of tractor pitch for passive and active systems

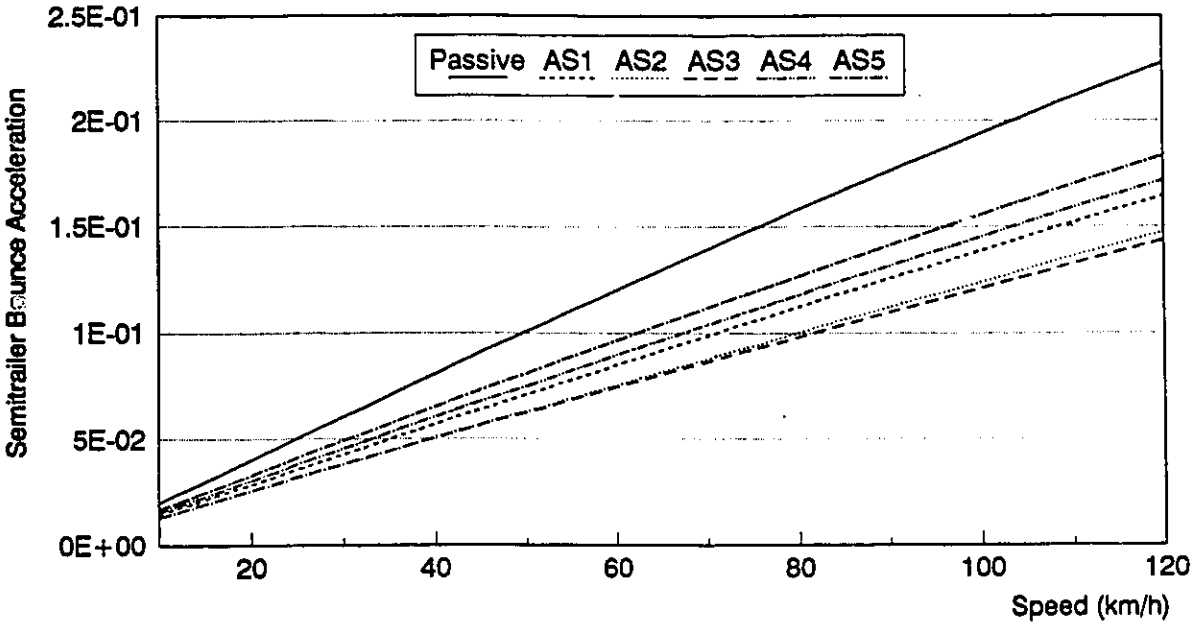

Figure 4.15a Effect of vehicle speed on mean square acceleration of semitrailer bounce for passive and active systems

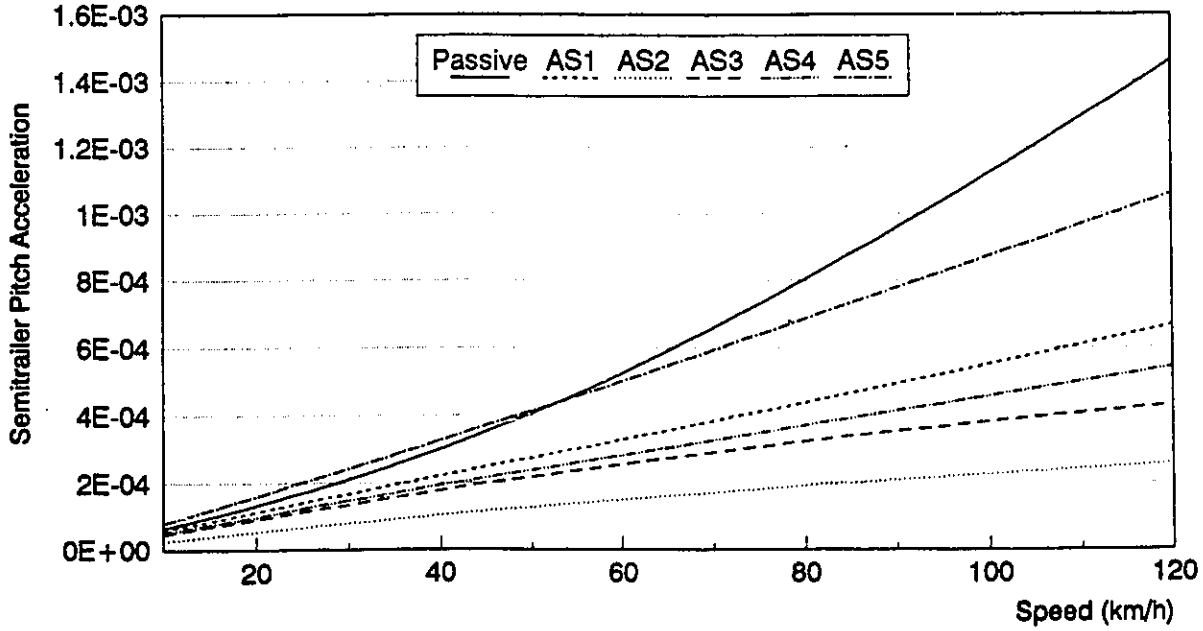

Figure 4.15b Effect of vehicle speed on mean square acceleration of semtrailer pitch for passive and active systems

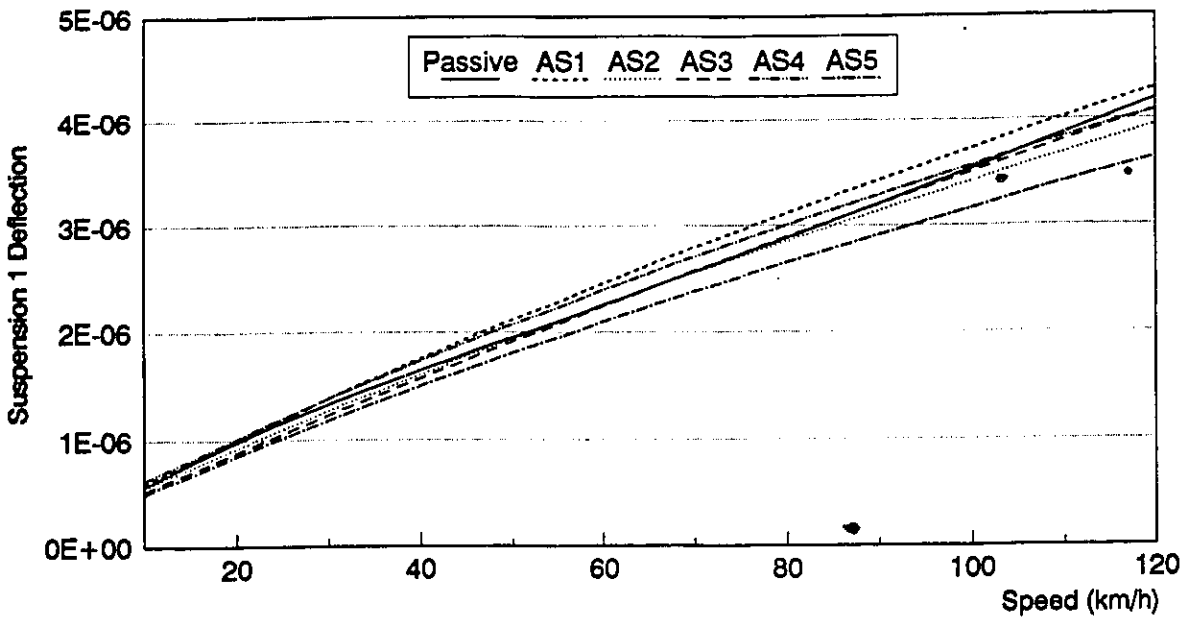

Figure 4.16a Effect of vehicle speed on mean square deflection of suspension 1 for passive and active systems

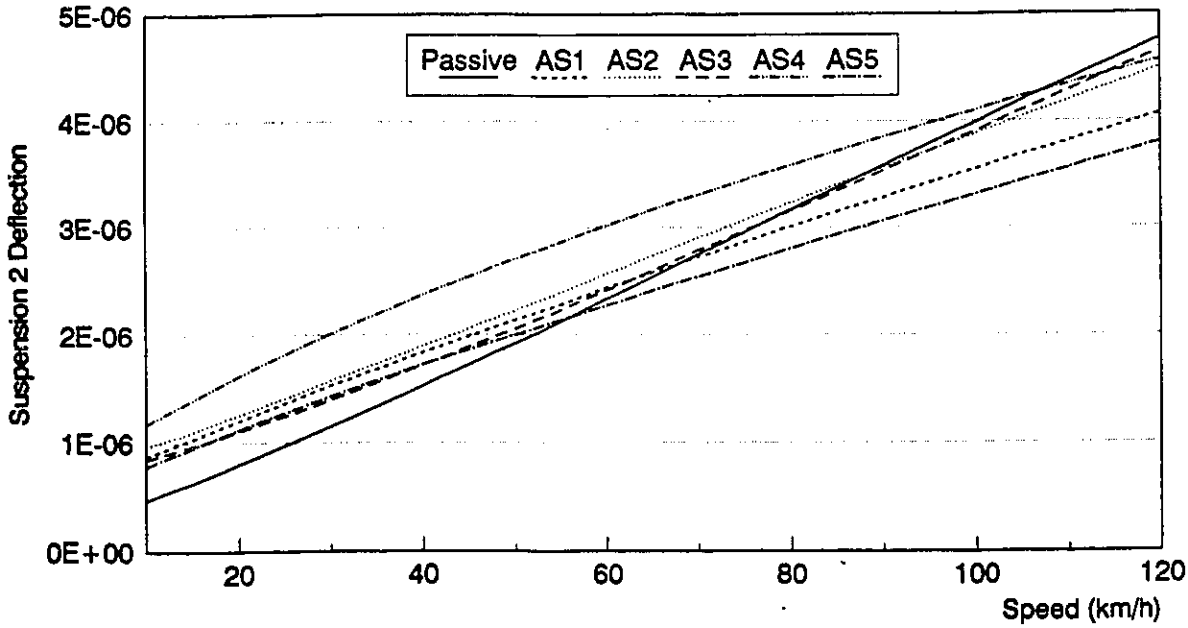

Figure 4.16b Effect of vehicle speed on mean square deflection of suspension 2 for passive and active systems

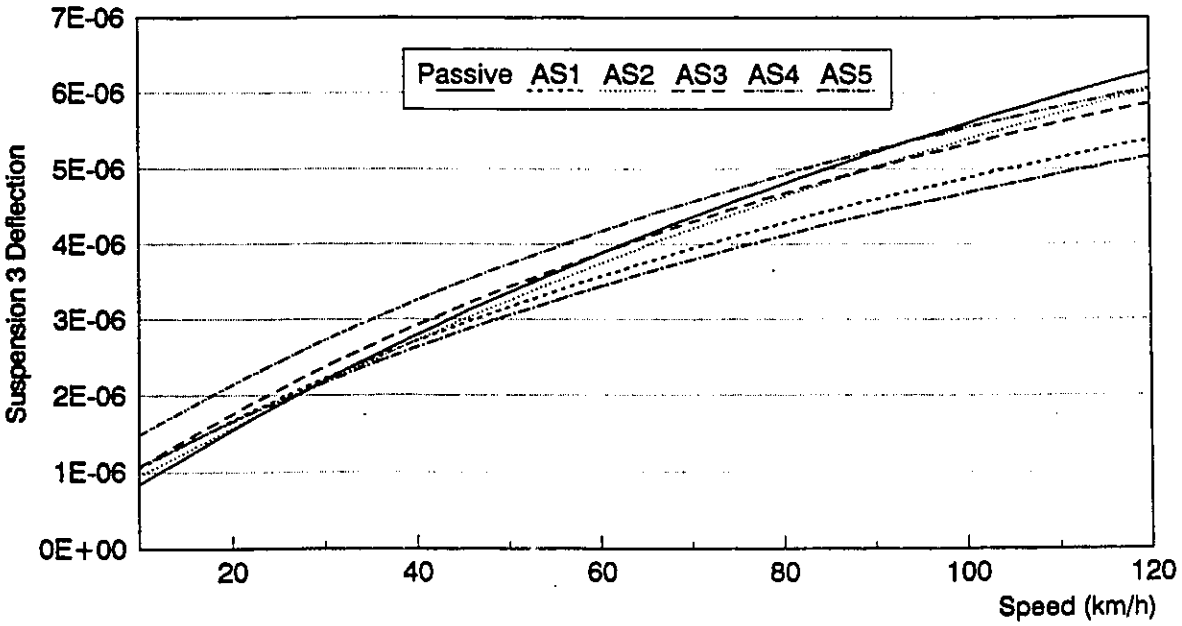

Figure 4.16c Effect of vehicle speed on mean square deflection of suspension 3 for passive and active systems

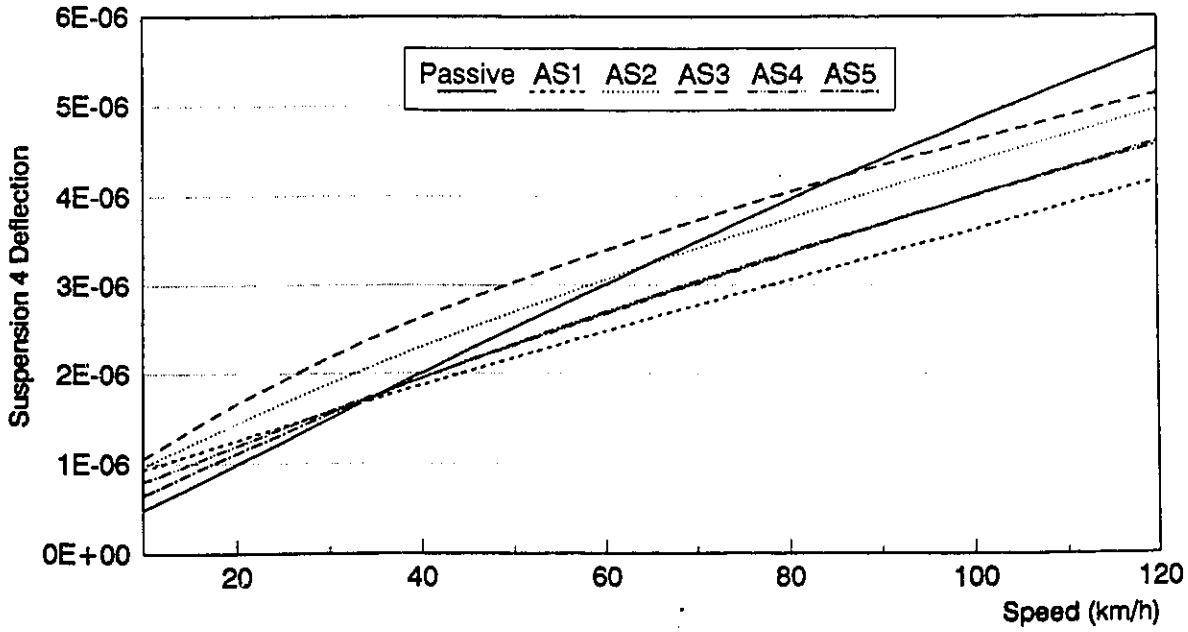

Figure 4.16d Effect of vehicle speed on mean square deflection of suspension 4 for passive and active systems

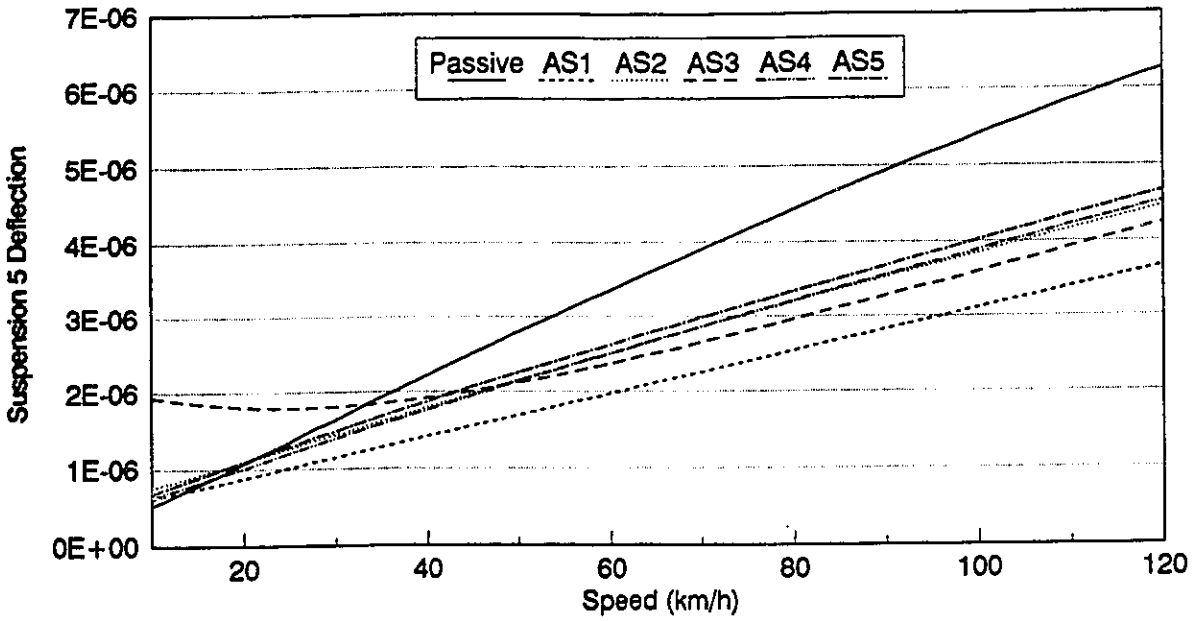

Figure 4.16e Effect of vehicle speed on mean square deflection of suspension 5 for passive and active systems

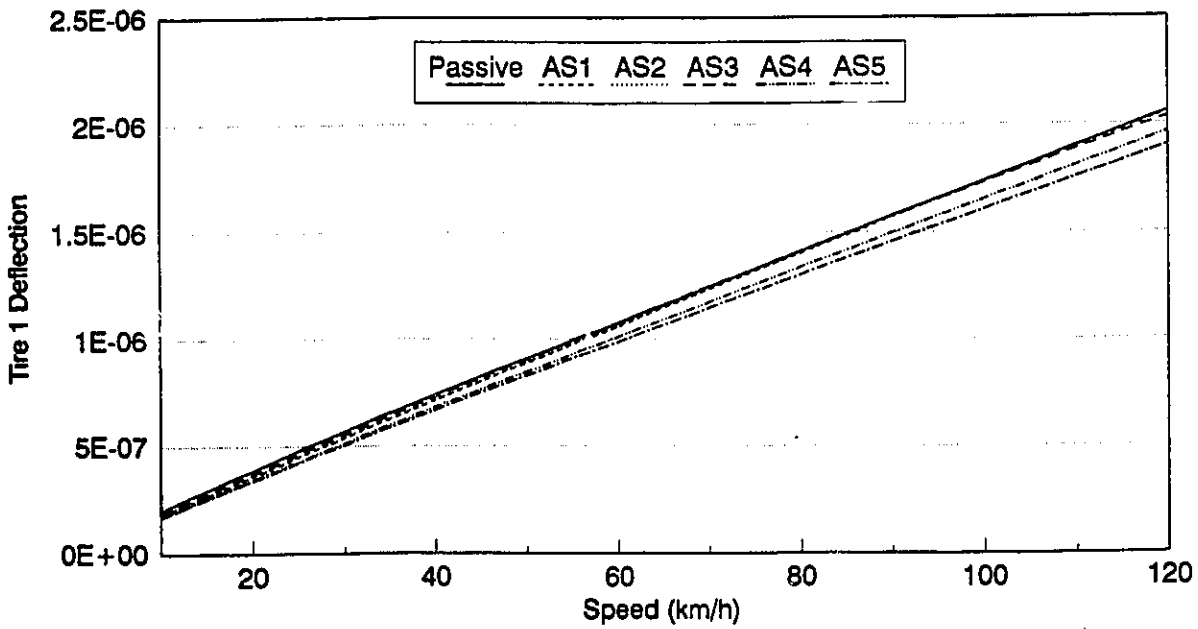

Figure 4.17a Effect of vehicle speed on mean square deflection of tire 1 for passive and active systems

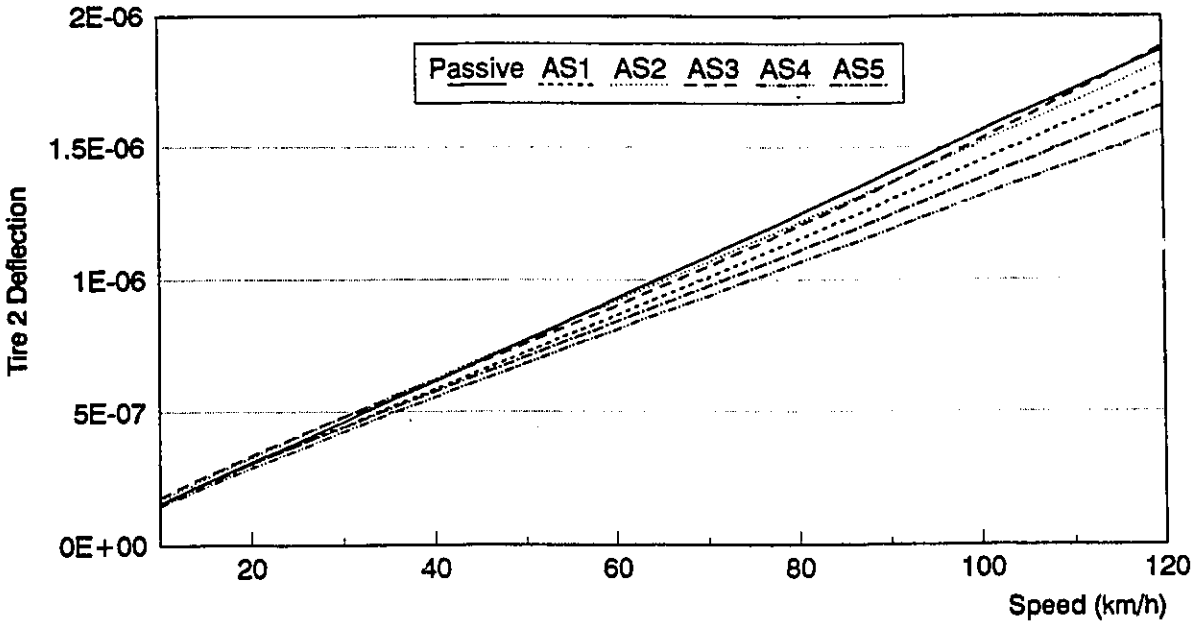

Figure 4.17b Effect of vehicle speed on mean square deflection of tire 2 for passive and active systems

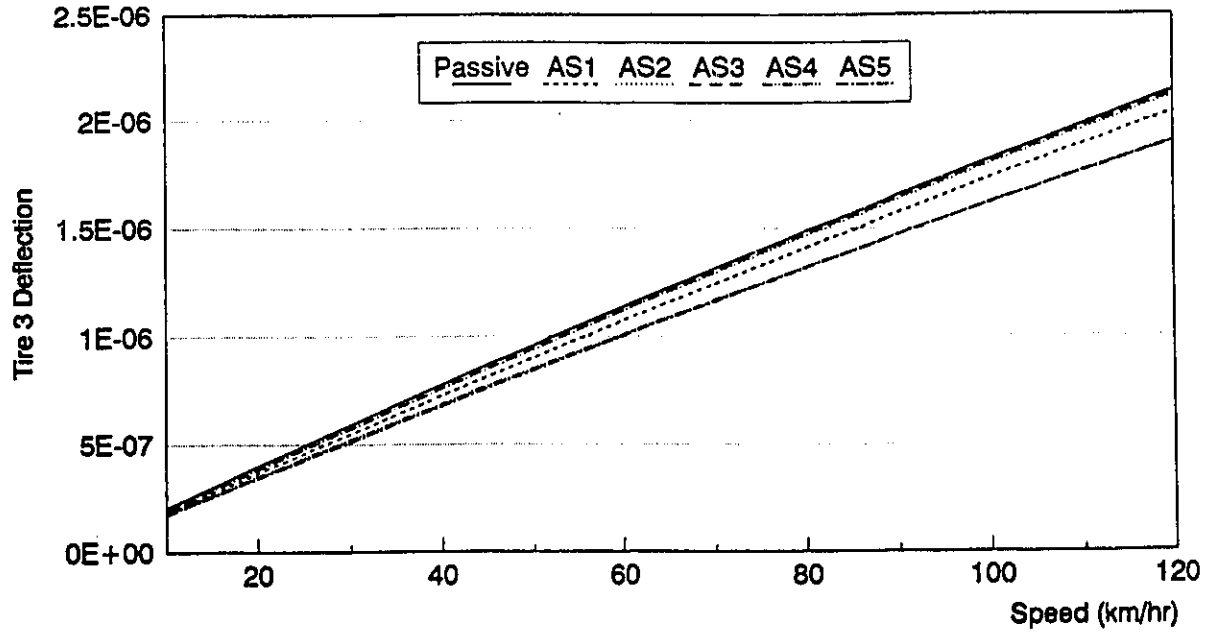

Figure 4.17c Effect of vehicle speed on mean square deflection of tire 3 for passive and active systems

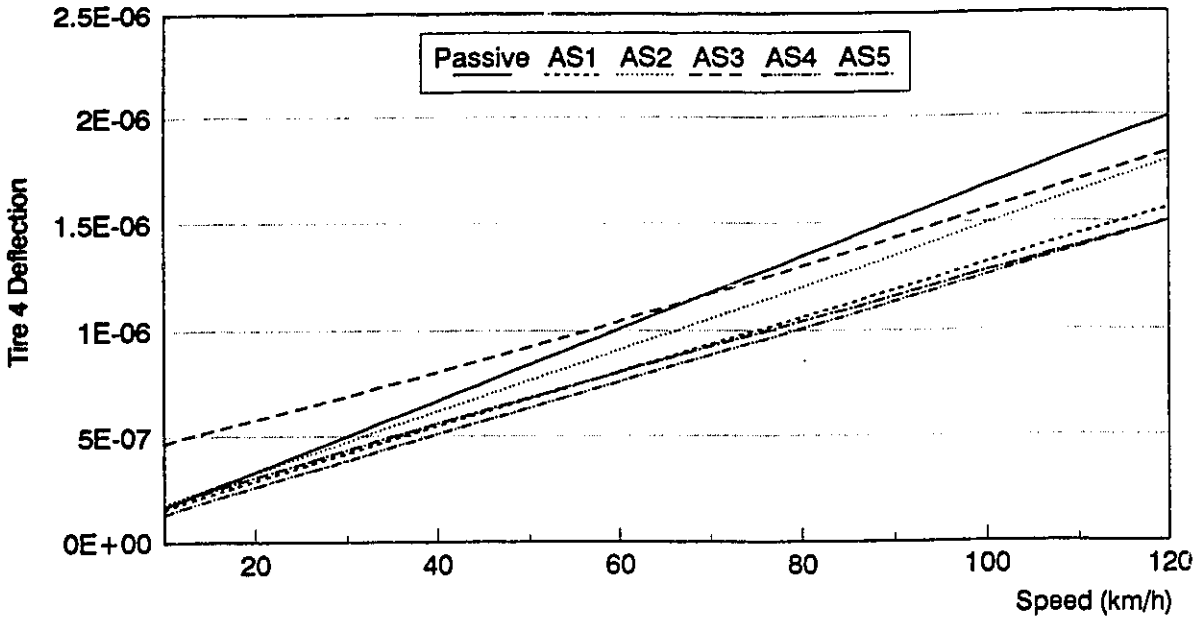

Figure 4.17d Effect of vehicle speed on mean square deflection of tire 4 for passive and active systems

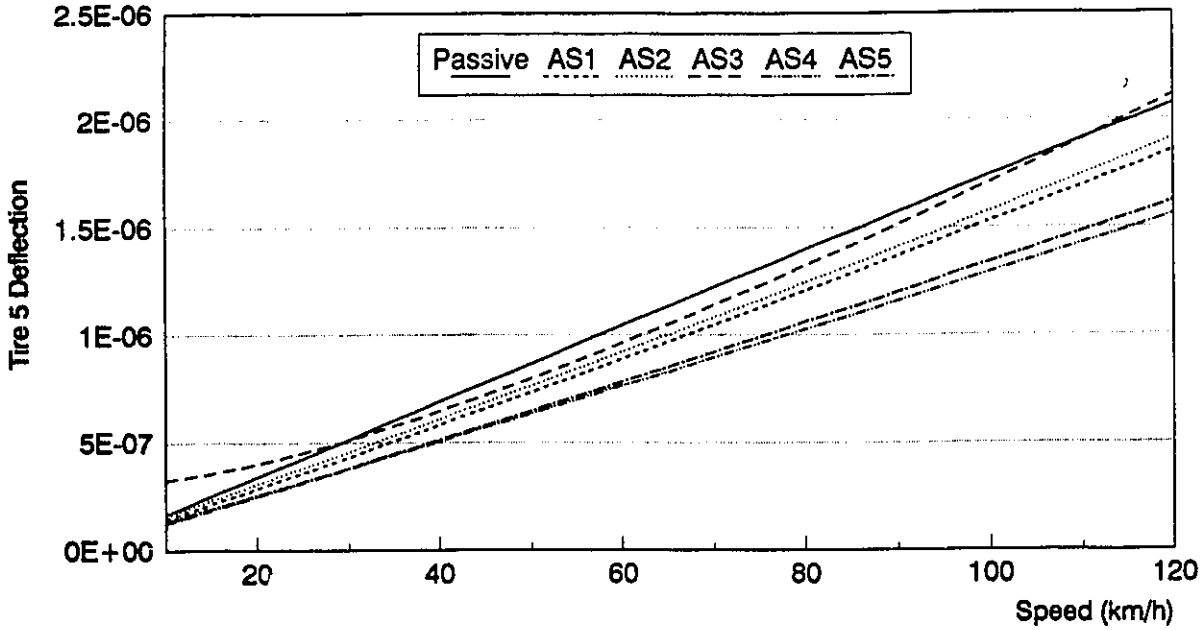

Figure 4.17e Effect of vehicle speed on mean square deflection of tire 5 for passive and active systems

4.5.5 Influence of Road Roughness on Suspensions Performance

The performance of an active suspension on three types of roads is compared to that of the passive suspension operated on the same road. Table 4.4 shows the percent improvement in the mean square values of the penalized variables for the *AS5* active suspension. The active suspension remains superior to the passive suspension for the three different roads. However, the improvement percentage is slightly reduced for rougher roads.

Table 4.4 Percent reduction(+)/increase(-) in the mean square value of each of the penalized variables for 3 types of roads (*AS5* compared to passive)

Performance variable	*Asphalt Road* %	*Concrete Road* %	*Rough Road* %
Tractor bounce acceleration	8.48e+0	8.01e+0	6.06e+0
Tractor pitch acceleration	9.24e+0	8.54e+0	6.65e+0
Semitrailer bounce acceleration	2.03e+1	1.89e+1	1.51e+1
Semitrailer pitch acceleration	1.76e+1	1.76e+1	1.30e+1
Suspension 1 Deflection	9.31e+0	8.66e+0	3.57e+0
Suspension 2 Deflection	1.34e+1	1.76e+1	2.12e+1
Suspension 3 Deflection	1.54e+1	1.59e+1	1.32e+1
Suspension 4 Deflection	1.58e+1	1.53e+1	1.01e+1
Suspension 5 Deflection	2.47e+1	2.44e+1	1.97e+1
Tire 1 force	7.45e+0	7.11e+0	5.56e+0
Tire 2 force	1.14e+1	1.12e+1	1.10e+1
Tire 3 force	1.09e+1	1.04e+1	8.09e+0
Tire 4 force	2.36e+1	2.29e+1	2.08e+1
Tire 5 force	2.36e+1	2.26e+1	1.84e+1

4.6 SUMMARY

A method based on *LQG* technique was used to design the active suspensions for the tractor-semitrailer vehicle. The second order coupled differential equations of motion of the actively suspended vehicle reduced to first order state-space form are augmented with the road excitation to satisfy the white noise input requirement of the *LQG* design. The performance objectives of the suspensions comprising the tractor and semitrailer bounce and pitch accelerations and the suspension and tire deflections are expressed in the matrix form as a function of the augmented state vector and the actuator forces. The performance index is then formulated, and each of its components is determined separately. While the passive elements do not affect the overall performance of the active suspension, the properties of the passive components are chosen to ensure minimum actuator force requirements. Five different sets of weighting coefficients are derived to achieve the design compromise for the active suspension, and the corresponding reduction/increase in the expected values of the penalized variables are investigated. The results clearly illustrate that the active suspensions yield improved performance related to all the design objectives. The suspension performance related to ride quality, cargo safety and tire forces can be further improved by relaxing the rattle space requirements.

4.7 REFERENCES

1. A. G. Thompson, *"Quadratic Performance Indices and Optimal Suspensions Design,"* Proc. Inst. of Mechanical Engineers, Vol. 187, No. 4, 1973, pp. 129-139.

2. J. K. Hedrick, *"Some Optimal Control Techniques Applicable to Suspension System Design,"* ASME Publication, 73-ICT-55, 1973.

3. D. R. Guenther and C. T. Leondes, *"Synthesis of a High-Speed Tracked Vehicle Suspension System. Part I: Problem statement, suspension structure and decomposition, and Part II: Definition and solution of the control problem"* IEEE Trans. on Automatic Control, Vol. AC-22, No. 42, 1977, pp. 158-172.

4. P. K. Sinha, D . N. Wormley and J. K. Hedrick, *"Rail Passenger Vehicle Lateral Dynamic Performance Improvement Through Active Control,"* ASME Journal of Dynamic Systems, Measurement and Control, Vol. 100, Dec. 1978, pp. 270-283.

5. A. G. Thompson, *"Optimal and Suboptimal Linear Active Suspension for Road Vehicles,"* Vehicle System Dynamics, Vol. 13, No. 2, 1984, pp. 61-72.

6. A. Hac, *"Suspension Optimization of a 2 DOF Vehicle Model Using Stochastic Optimal Control Technique,"* Journal of sound and vibration, Vol. 100, No. 33, 1985, pp. 343-357.

7. F. Oueslati and S. Sankar, *"Performance of a Fail-Safe Active Suspension with Limited State Feedback for Improved Ride Quality and Reduced Pavement Loading in Heavy Vehicles,"* 1992 Truck & Bus Meeting & Exposition Toledo, Ohio.

8. F. Oueslati and S. Sankar, A. K. W. Ahmed, *"Limited-State Active Suspension for Improved Ride Quality in Rail Vehicles Subjected to Vertical Track Irregularities,"* The International Symposium on Technological Innovation in Guided Transportation, Sep. 28-30, 1993, Lille, France.

9. D. G. Stephens, *"Comparative Vibration Environment of Transportation Vehicles,"* Passenger Vibration in Transportation Vehicles, ASME AMD, Vol. 24, 1979, pp. 59-72.

10. V. Rajnikant Patel and N. Munro, *"Multivariable System Theory and Design,"* International Series on Systems and Control, Vol. 4. 1st ed. Oxford, Eng. New York: Pergamon Press, 1982.

11. A. E. Bryson and Y. C. Ho, *"APplied Optimal Control, Optimization, Estimation and Control,"* New York: John Wiley and Sons, 1975.

12. A. Hac, *"Suspension Optimization of 2-DOF Vehicle Model Using a Stochastic Optimal Control Technique,"* Journal of Sound and Vibration, Vol. 100, No. 3, 1985, pp. 343-357.

13. C. J. Dodds, *"The Laboratory Simulation of Vehicle Service Stress,"* Journal of Engineering for Industry, ASME Transactions, Vol. 96, No. 2, May 1974, pp. 391-398

14. C. J. Dodds and J. D. Robson, *"The Description of Road Surface Roughness,"* Journal of Sound and Vibration, Vol. 31, No. 2, 1973, pp. 175-184.

15. J. D. Robson, *"Road Surface Description and Vehicle Response,"* International Journal of Vehicle Design, Vol. 1, No. 1, 1979, pp. 25-35.

16. J. S. Bendat and A. G. Piersol, *"Random Data: Analysis and Measurement Procedures,"* Whiley-Interscience, 1971, Toronto, Ontario, Canada.

17. A. Hac and I. Youn, *"Optimal Semi-Active Suspension with Preview Based on a Quarter Car Model,"* Transactions of the ASME, Journal of Vibration and Acoustics, Vol. 114, 1992 pp. 84-92.

18. J. K. Hedrick and T. Butsuen, *"Invariant Properties of Automotive Suspensions,"* Proc. International Conference on Advanced suspensions, London Oct. 24-25 1988, pp. 35-42.

19. R. M. Chalasani, *"Ride Performance Potential of Active Suspension Systems-Part I: Simplified Analysis Based on a Quarter Car Model,"*. 1986 ASME Winter Annual Meeting, AMD-Vol. 80, pp. 187-204.

20. R. M. Chalasani, *"Ride Performance Potential of Active Suspension Systems-Part II: Comprehensive Analysis Based on a Full Car Model,"* 1986 ASME Winter Annual Meeting,, AMD-Vol. 80, pp. 205-234.

21. A. Hac, *"Optimal Linear Preview Control of Active Vehicle Suspension,"* Vehicle System Dynamics, Vol. 21, 1992 pp. 167-195.

22. T. Butsuen and J. K. Hedrick, *"Optimal Semi-Active Suspensions for Automotive Vehicles: The 1/4 Car Model,"* 1989 ASME Winter Annual Meeting,, Vol. 13, pp. 305-316.

CHAPTER 5

ANALYSIS AND DESIGN OF AN ACTIVE SUSPENSION USING H_2 SYNTHESIS

5.1 INTRODUCTION

The active suspension design conceived in the previous chapter, using *LQG* optimal control method, requires perfect and complete measurement of the states. The suspension design for the tractor-semitrailer requires measurements of absolute velocities and displacements of all the sprung and unsprung masses of the vehicle. The control algorithm further necessitates a continuous measurement of the road elevations at all the tire-road contact points. Although absolute velocities and displacements can theoretically be obtained by integrating directly measurable acceleration signals, the signal integration poses various formidable tasks associated with filter design and phase variations. Similarly, the measurement of road elevation necessitates body mounted road height sensors. Although sonar sensors may be used, the reliability of these devices is yet to be assessed especially in the relatively severe road environment. The implementation of such active suspension is thus limited by its high costs and complexities associated with measurement of all the states of the vehicle. Furthermore, the measurement of certain directly measurable states is frequently corrupted with noise. In view of hardware and signal

processing requirements, high cost and poor reliability of a full-state feedback active suspension design, a thorough analysis of a more realistic active suspension scheme, based on H_2 synthesis, is undertaken to evaluate its suitability for the freight vehicles. The assumption of full and perfect measurement of the states is relaxed in the design of the H_2 active suspension. The proposed active suspension system is analytically formulated incorporating the sensor signals noise in the output equation. A *Kalman* filter is incorporated to derive an optimum estimate of all the state variables. Two suspension schemes based upon limited-state measurement are investigated and the relevant design aspects such as actuator size, measurement noise intensity and its effect on the performance are addressed. The performance characteristics of the proposed suspension designs are compared to those of the full-state measurement active, and the "optimum" passive suspension systems.

5.2 MATHEMATICAL FORMULATION OF AN *LQG*-EQUIVALENT H_2 CONTROL PROBLEM

In recent years, the search for new approaches to the design of stable and robust feedback controllers have gained momentum. As a result, the H_2 and H_∞ design methodologies have become widely accepted in multivariable control [1]. One of the most important recent mathematical advances in the theory of H_2 and H_∞ is the solution of the optimization problem using state space methods, in particular through the solution of two *Riccati* equations. The H_2 optimal control theory is developed to design stable feedback controllers that minimize the so called H_2 performance measure. This performance measure, however, can be formulated to be equivalent to the *LQG* quadratic performance index discussed in Chapter 4. The H_2 optimal control problem is then conveniently solved using the state-space method. The H_2 optimal control theory can be formulated to require

only limited-state measurements. Moreover the sensor noises can be easily incorporated in the formulation. The H_2 design method also offers the possibility of frequency-weighted performance measure through plant augmentation. The suspension design can thus be realized to yield frequency-dependent performance characteristics, which is perhaps most desirable for ride quality enhancement of the vehicle.

In order to be consistent and to be able to compare the performance behavior of an H_2 suspension with that using full-state measurement, presented in Chapter 4, the H_2 control problem is formulated to be equivalent to the classical LQG problem. The vehicle model can, in the most general case, be described by the following system of equations:

$$\begin{aligned} \dot{x} &= \tilde{A}x + \tilde{B}_1\tilde{w} + \tilde{B}_2u \\ z &= \tilde{C}_1x + \tilde{D}_{11}\tilde{w} + \tilde{D}_{12}u \\ y &= \tilde{C}_2x + \tilde{D}_{21}\tilde{w} + \tilde{D}_{22}u \end{aligned} \tag{5.1}$$

where;

u is the control forces vector to be determined,

x is the augmented state vector as defined in Chapter 4,

z is the error vector (or penalized variables) to be minimized,

y is the observation vector (or vector of measurable/accessible variables),

and $\tilde{w}$ is the exogenous signal and includes both the road disturbance and sensors noise ζ_i ($i = 1$ to n; where n is the number of observed, or available, signals). The road disturbance, ξ, is a filtered white noise process with covariance $E[\xi(t)\,.\,\xi'(\tau)] = W\delta(t-\tau) = 2\alpha v\rho^2\delta(t-\tau)$, as defined in Chapter 2. In the most general case, sensors noise do not fall in any specific frequency range, accordingly they are taken as white noise. The measurement error vector, ζ, is thus assumed to be white noise with covariance:

$$E[\zeta(t)\,.\,\zeta'(\tau)] = V\delta(t-\tau) \tag{5.2}$$

where $V = diag\ [\ V_1,\ V_2,\ ...,\ V_n\ ]$ is the matrix of mean square amplitude of the n signal noises. The matrices $\tilde{A}$, $\tilde{B}_1$, $\tilde{B}_2$, $\tilde{C}_1$, $\tilde{D}_{11}$, $\tilde{D}_{12}$, $\tilde{C}_2$, $\tilde{D}_{21}$, and $\tilde{D}_{22}$, representing the state space description of the tractor-semitrailer, are to be defined such that the resulting H_2 optimization problem is equivalent to the standard LQG optimization problem derived in Chapter 4. Since the measurement errors were considered negligible in the formulation presented in Chapter 4, the only exogenous signal considered was the road disturbance. The exogenous signal vector $\tilde{w}$ was thus represented by the filtered white noise ξ, as described in EQ (4.6). In the present formulation, however, $\tilde{w}$ would includes both the road disturbance and the sensors noise, such that:

$$\tilde{w} = \{\xi, \zeta_1, \zeta_2 \cdots \zeta_n\}'$$

where n is the size of the observation vector y, or the number of measurable variables.

In the case of the full-state feedback control presented in Chapter 4, the observation vector y was equal to the state vector x, such that $D_{21} = D_{22} = 0$. In this case, however, only accessible or directly measurable variables will be included, and will be defined later.

Let $\mathcal{P}$ be the transfer function matrix of the tractor-semitrailer mapping the input vectors $\tilde{w}$ and u to the output vectors z and y :

$$\begin{bmatrix} z \\ y \end{bmatrix} = \mathcal{P} \begin{bmatrix} \tilde{w} \\ u \end{bmatrix} \tag{5.3}$$

The transfer function matrix $\mathcal{P}$ can be derived from EQ (5.1) and represented in the standard 2×2 block transfer matrix as:

$$\mathcal{P} = \begin{bmatrix} P_{11} & P_{12} \\ P_{21} & P_{22} \end{bmatrix} = \left[\begin{array}{c|cc} \tilde{A} & \tilde{B}_1 & \tilde{B}_2 \\ \hline \tilde{C}_1 & \tilde{D}_{11} & \tilde{D}_{12} \\ \tilde{C}_2 & \tilde{D}_{21} & \tilde{D}_{22} \end{array}\right] \tag{5.4}$$

EQ (5.1) can be solved to derive the augmented state vector x, as:

$$x = \left(sI - \tilde{A}\right)^{-1}\begin{bmatrix} \tilde{B}_1 & \tilde{B}_2 \end{bmatrix}\begin{bmatrix} \tilde{w} \\ u \end{bmatrix}$$

upon substituting for x, the transfer function matrix $\mathcal{P}$ can be expressed as:

$$\mathcal{P} = \begin{bmatrix} \tilde{D}_{11} & \tilde{D}_{12} \\ \tilde{D}_{21} & \tilde{D}_{22} \end{bmatrix} + \begin{bmatrix} \tilde{C}_1 \\ \tilde{C}_2 \end{bmatrix}\left(sI - \tilde{A}\right)^{-1}\begin{bmatrix} \tilde{B}_1 & \tilde{B}_2 \end{bmatrix} \tag{5.5}$$

EQ (5.6) and (5.7) yield:

$$\begin{aligned} z &= P_{11}\tilde{w} + P_{12}u \\ y &= P_{21}\tilde{w} + P_{22}u \end{aligned} \tag{5.6}$$

Let K be the transfer function matrix relating the observation vector y to the control force u, such that:

$$u = Ky \tag{5.7}$$

EQ (5.3) and (5.8) yield the following expressions for the performance variable and the

observation vectors:

$$z = P_{11}\tilde{w} + P_{12}Ky \tag{5.8}$$

$$y = P_{21}\tilde{w} + P_{22}Ky \tag{5.9}$$

Alternatively, EQ (5.8) and (5.9) can be rewritten as:

$$y = (I - P_{22}K)^{-1}P_{21}\tilde{w} \tag{5.10}$$

$$z = \left[P_{11} + P_{12}K(I - P_{22}K)^{-1}P_{21}\right]\tilde{w} \tag{5.11}$$

The closed loop transfer function $T_{\tilde{w}z}$ relating the disturbance $\tilde{w}$ to the penalized variables vector z can thus be expressed as:

$$T_{\tilde{w}z} = P_{11} + P_{12}K(I - P_{22}K)^{-1}P_{21} \tag{5.12}$$

The H_2 control strategy is based upon minimizing the 2-norm of $T_{\tilde{w}z}$; i.e. finding a controller K such that; $\|T_{\tilde{w}z}\|_2 = \left\|P_{11} + P_{12}K(I - P_{22}K)^{-1}P_{21}\right\|_2$ is minimum [1]. Minimizing the 2-norm of $T_{\tilde{w}z}$ implies minimizing the effects of the road disturbance and sensors noise $\tilde{w}$ on the penalized variables z. The performance measure of the H_2 control scheme is thus formulated as the 2-norm of the transfer function $T_{\tilde{w}z}$ function, defined by:

$$J_{H_2} = \|T_{\tilde{w}z}\|_2^2 = \frac{1}{\pi}\int_0^{\infty} Tr\left(T_{\tilde{w}z}^{*}(j\omega)T_{\tilde{w}z}(j\omega)\right)d\omega \tag{5.13}$$

The H_2 multivariable control methodology involves determination of an optimal control force vector u for the multivariable system governed by EQ (5.1), such that the

performance index J_{H_2} described in EQ (5.13), is minimized. The H_2 performance index appears quite different from the quadratic LQG performance index described in EQ (4.17). The resulting control scheme is thus expected to be different from that derived using LQG design. A relationship between the H_2 and LQG design methodologies, however, can be established to compare the performance characteristics of the two designs. This can be accomplished by formulating the H_2 control problem to be equivalent to a conventional LQG optimal control problem.

Integrating the sum of the squared elements of the frequency response as implied by the H_2 optimization criteria in EQ (5.13), corresponds to the time integrating the sum of the squared elements z_i [2], such that:

$$J_{H_2} = \frac{1}{\pi}\int_0^{\infty} Tr\left(T_{\tilde{w}z}^{*}(j\omega)T_{\tilde{w}z}(j\omega)\right)d\omega = \lim_{T\to\infty} E\left[\int_0^T z'\,z dt\right] \tag{5.14}$$

Since the performance vector z does not depend on the plant disturbance $\tilde{w}$, $\tilde{D}_{11}$ in EQ (5.1) would simply be a null matrix. The H_2 performance criteria can thus be expressed as:

$$J_{H_2} = \lim_{T\to\infty} E\left[\int_0^T \left(\tilde{C}_1 x + \tilde{D}_{12}u\right)' \left(\tilde{C}_1 x + \tilde{D}_{12}u\right)dt\right] \tag{5.15}$$

or:

$$J_{H_2} = \lim_{T\to\infty} E\left[\int_0^T \left(x'\tilde{C}_1' + u'\tilde{D}_{12}'\right)\left(\tilde{C}_1 x + \tilde{D}_{12}u\right)dt\right] \tag{5.16}$$

Upon rearranging and multiplying, the following final expression for the performance index J_{H_2} is obtained:

$$J_{H_2} = \lim_{T\to\infty} E\left[\int_0^T \begin{bmatrix} x' & u' \end{bmatrix} \begin{bmatrix} \tilde{C}_1' \\ \tilde{D}_{12}' \end{bmatrix} \begin{bmatrix} \tilde{C}_1 & \tilde{D}_{12} \end{bmatrix} \begin{bmatrix} x \\ u \end{bmatrix} dt\right]$$
$$= \lim_{T\to\infty} E\left[\int_0^T \begin{bmatrix} x' & u' \end{bmatrix} \begin{bmatrix} \tilde{C}_1'\tilde{C}_1 & \tilde{C}_1'\tilde{D}_{12} \\ \tilde{D}_{12}'\tilde{C}_1 & \tilde{D}_{12}'\tilde{D}_{12} \end{bmatrix} \begin{bmatrix} x \\ u \end{bmatrix} dt\right] \tag{5.17}$$

The corresponding performance index based on the *LQG* formulation, however, is given by:

$$J = \lim_{T\to\infty} E\left[\int_0^T \begin{bmatrix} x' & u' \end{bmatrix} \begin{bmatrix} C_1'\hat{Q}C_1 & C_1'\hat{Q}D_{12} \\ (C_1'\hat{Q}D_{12})' & \hat{R} + D_{12}'\hat{Q}D_{12} \end{bmatrix} \begin{bmatrix} x \\ u \end{bmatrix} dt\right] \tag{5.18}$$

where $\hat{Q}$ and $\hat{R}$ are described in EQ (4.14). Consequently, if the formulation of the H_2 performance index, given by EQ (5.17), is to be equivalent to the *LQG* formulation, given by EQ (5.18), the following must be satisfied:

$$\begin{aligned} \tilde{C}_1'\tilde{C}_1 &= C_1'\hat{Q}C_1 \\ \tilde{C}_1'\tilde{D}_{12} &= C_1'\hat{Q}D_{12} \\ \tilde{D}_{12}'\tilde{D}_{12} &= \hat{R} + D_{12}'\hat{Q}D_{12} \end{aligned} \tag{5.19}$$

EQ (5.19) yields:

$$\tilde{C}_1 = \begin{bmatrix} \sqrt{\hat{Q}}C_1 \\ 0 \end{bmatrix}, \quad \text{and} \quad \tilde{D}_{12} = \begin{bmatrix} \sqrt{\hat{Q}}D_{12} \\ \sqrt{\hat{R}} \end{bmatrix} \tag{5.20}$$

Since $\tilde{D}_{11} = [0]$, the state-space equation relating the performance variable vector z to the state vector x, and the control force vector u, can be expressed as:

$$z = \begin{bmatrix} \sqrt{\hat{Q}}C_1 \\ 0 \end{bmatrix} x + \begin{bmatrix} \sqrt{\hat{Q}}D_{12} \\ \sqrt{\hat{R}} \end{bmatrix} u \tag{5.21}$$

The performance vector z, when partitioned into two components, z_1 and z_2, can be expressed as:

$$z_1 = \sqrt{\hat{Q}}(C_1 x + D_{12} u) \tag{5.22}$$

and:

$$z_2 = \sqrt{\hat{R}}\, u \tag{5.23}$$

A comparison of EQ (5.22) and EQ (4.10) reveals that the z_1 component of the H_2 performance variable vector is simply the LQG performance variable vector given by weighted by the matrix $\sqrt{\hat{Q}}$. Similarly, EQ (5.23) implies that the control forces must be weighed by the matrix $\sqrt{\hat{R}}$. This similarity suggests that the performance variable vector z in the H_2 formulation must include the penalized variables (tractor and semitrailer bounce and pitch accelerations, and suspension and tire deflections) and the actuator forces. Moreover, the penalized variables as well as the actuator forces must be weighted by $\sqrt{\hat{Q}}$ and $\sqrt{\hat{R}}$, respectively. The penalized variables considered in the H_2 synthesis are thus identical to those described in section 4.3 of Chapter 4, which include ride quality, cargo safety, rattle space requirements and dynamic tire forces.

A relationship between $\tilde{B}_1$ and $\tilde{D}_{21}$, and the noise correlation W and V, also needs to be established to ensure that the H_2 and LQG formulations are identical. Noting that:

$$E\left\{\begin{bmatrix} B_1\xi(t) \\ D_{21}\zeta(t) \end{bmatrix}\begin{bmatrix} \xi'(\tau)B_1' & \zeta'(\tau)D_{21}' \end{bmatrix}\right\} = \begin{bmatrix} B_1WB_1' & 0 \\ 0 & D_{21}VD_{21}' \end{bmatrix}\delta(t-\tau) \tag{5.24}$$

The cross diagonal elements are zeros since there is no cross correlation between the road disturbance and sensors noise. From EQ (5.1) it is evident that the white plant noise ξ and white measurement noise ζ enter the H_2 formulation via $\begin{bmatrix} \tilde{B}_1 \\ \tilde{D}_{21} \end{bmatrix}$. The joint correlation function can thus be expressed as:

$$E\left\{\begin{bmatrix} \tilde{B}_1\tilde{w}(t) \\ \tilde{D}_{21}\tilde{w}(t) \end{bmatrix}\begin{bmatrix} \tilde{w}'(t)\tilde{B}_1' & \tilde{w}'(t)\tilde{D}_{21}' \end{bmatrix}\right\} = \begin{bmatrix} \tilde{B}_1\tilde{B}_1' & \tilde{B}_1\tilde{D}_{21}' \\ \tilde{D}_{21}\tilde{B}_1' & \tilde{D}_{21}\tilde{D}_{21}' \end{bmatrix}\delta(t-\tau) \tag{5.25}$$

EQ (5.24) and EQ (5.25) permit a comparison between the H_2 and LQG formulations. EQ (5.24) and EQ (5.25) yield:

$$\begin{aligned} \tilde{B}_1\tilde{B}_1' &= B_1WB_1' \\ \tilde{B}_1\tilde{D}_{21}' &= 0 \\ \tilde{D}_{21}\tilde{D}_{21}' &= D_{21}VD_{21}' \end{aligned} \tag{5.26}$$

The matrices $\tilde{B}_1$ and $\tilde{D}_{21}$ are ,therefore, defined as:

$$\begin{aligned} \tilde{B}_1 &= \begin{bmatrix} B_1\sqrt{W} & 0 \end{bmatrix} \\ \tilde{D}_{21} &= \begin{bmatrix} 0 & D_{21}\sqrt{V} \end{bmatrix} \end{aligned} \tag{5.27}$$

EQ (5.20) and (5.27) establish the requirements for the H_2 multivariable control problem to be equivalent to the LQG control problem. From the equivalency analysis, the matrices $\tilde{B}_1$, $\tilde{C}_1$, $\tilde{D}_{12}$, and $\tilde{D}_{21}$, are described by EQ (5.20) and (5.27), and $\tilde{D}_{11} = 0$. The matrices $\tilde{A}$ and $\tilde{B}_2$ are not effected by the H_2/LQG equivalency requirements, and thus are identical to the matrices A and B_2, defined by EQ (4.7) in Chapter 4. The matrices $\tilde{C}_2$ and $\tilde{D}_{22}$, relating the state vector x and control forces vector u to the observation vector y, will be defined in a following section.

5.2.1 Solution of the H_2 Control Problem

Designing an H_2 optimal controller for the tractor-semitrailer multivariable system involves essentially is determination of the optimal control force vector $\boldsymbol{u}$ and its relation to the observation vector $\boldsymbol{y}$. In the previous Chapter, all the state variables were assumed to be measurable, and thus the observation vector $\boldsymbol{y}$ was identical to the state vector $\boldsymbol{x}$. Minimization of the quadratic performance index was thus attained using full-state feedback in conjunction with appropriate feedback gains. Such a control scheme poses many complexities associated with measurement of the entire state of the vehicle, which is not feasible. Alternatively, the vehicle state may be estimated from the measurement of a limited number of states, preferably directly measurable, using a *Kalman* filter, referred to as the observer. The observer encompasses an exact model of the plant and plant parameters. The observer employs directly measurable states to yield an estimate of the entire state vector. The H_2 suspension design is, therefore, carried out in two stages: *(i)* design of an observer to estimate the entire state vector using the measurable limited-state of the vehicle; and *(ii)* implementation of the estimated state to derive the optimal full-state feedback controller to achieve a minimum performance index. Since the H_2 problem is formulated to be equivalent to an *LQG* problem, the H_2 controller $\boldsymbol{K}$ can be realized using the *LQG* methodology resulting in a full-state feedback gain $\boldsymbol{K}_c$ and a *Kalman* filter (observer) with residual gain $\boldsymbol{K}_o$.

Kalman et al [3] and *Abdel Hady* et al [4] proposed the following form of the observer [3,4]:

$$\dot{\boldsymbol{x}}_o = \tilde{\boldsymbol{A}}\boldsymbol{x}_o + \tilde{\boldsymbol{B}}_2\boldsymbol{u} + \boldsymbol{K}_o(\boldsymbol{y} - \tilde{\boldsymbol{C}}_2\boldsymbol{x}_o - \tilde{\boldsymbol{D}}_{22}\boldsymbol{u}) \tag{5.28}$$

Where x_o is the optimum estimate of the state variable x and K_o is the observer gain. The estimation error e_r is, hence, defined as the difference between the state vector x and its optimum estimate x_o. The observer gain K_o is selected to minimize the error covariance matrix $E[e_r\ e_r']$ [3],. This results in the filter gain matrix given by [5-7]:

$$K_o = \left(P_o \tilde{C}_2' + \tilde{B}_1 \tilde{D}_{21}'\right)\left(\tilde{D}_{21} \tilde{D}_{21}'\right)^{-1} \tag{5.29}$$

Where P_o is the filter error covariance matrix, derived from the solution of the following *Riccati* equation:

$$\tilde{A}P_o + P_o\tilde{A}' - \left(P_o\tilde{C}_2' + \tilde{B}_1\tilde{D}_{21}'\right)\left(\tilde{D}_{21}\tilde{D}_{21}'\right)^{-1}\left(P_o\tilde{C}_2' + \tilde{B}_1\tilde{D}_{21}'\right) + \tilde{B}_1\tilde{B}_1' = 0 \tag{5.30}$$

Since the observer and tractor-semitrailer models are driven by the identical input u, and since the observer gain K_o is formulated to minimize the error between the state vector x and its estimate x_o, EQ (5.28) yields a reasonably good approximation of the actual state [3,4]. The *Kalman* filter approach provides an estimate of the state vector x based upon the available measurements contained in the observation vector y. The estimated vector x_o is then used in conjunction with a full-state feedback gain matrix to derive the control forces vector u, given by:

$$u = -K_c x_o \tag{5.31}$$

Where K_c is the full-state feedback control gain matrix derived to minimize the performance index, and is given by:

$$K_c = \left(\tilde{D}_{12}'\,\tilde{D}_{12}\right)^{-1}\left(\tilde{B}_2' P + \tilde{D}_{12}'\,\tilde{C}_1\right) \tag{5.32}$$

where P is the solution of the following *Riccati* equation:

$$\tilde{A}'P + P\tilde{A} - \left(P\tilde{B}_2 + \tilde{C}_1'\tilde{D}_{12}\right)\left(\tilde{D}_{12}'\tilde{D}_{12}\right)^{-1}\left(P\tilde{B}_2 + \tilde{C}_1'\tilde{D}_{12}\right)' + \tilde{C}_1'\tilde{C}_1 = 0 \tag{5.33}$$

Upon substituting for u form EQ (5.31), the estimated state vector can be expressed as:

$$\dot{x}_o = \left(\tilde{A} - K_o\tilde{C}_2 - \tilde{B}_2K_c + K_o\tilde{D}_{22}K_c\right)x_o + K_o y \tag{5.34}$$

EQ (5.31) and (5.34) are combined to yield the controller matrix transfer function K mapping the output y to the control vector u. The controller gain matrix can be expressed by the following 2×2 block representation:

$$K = \left[\begin{array}{c|c} \tilde{A} - K_o\tilde{C}_2 - \tilde{B}_2K_c + K_o\tilde{D}_{22}K_c & K_o \\ \hline -K_c & 0 \end{array}\right] \tag{5.35}$$

alternatively:

$$\begin{aligned} \dot{x}_o &= A_c x_o + B_c y \\ u &= C_c x_o \end{aligned} \tag{5.36}$$

where:

$$\begin{aligned} &A_c = \tilde{A} - K_o\tilde{C}_2 - \tilde{B}_2K_c + K_o\tilde{D}_{22}K_c\ ; \\ &A_c = K_o \quad \text{and} \quad A_c = -K_c \end{aligned}$$

Upon substituting for the expression y from EQ (5.1), EQ (5.36) yields:

$$\dot{x}_o = A_c x_o + B_c \tilde{C}_2 x + B_c \tilde{D}_{21} \tilde{w} + B_c \tilde{D}_{22} u \tag{5.37}$$

Replacing u by $C_c x_c$, EQ (5.1) and (5.37) yield:

$$\begin{aligned} \dot{x} &= \tilde{A}x + \tilde{B}_2 C_c x_o + \tilde{B}_1 \tilde{w} \\ z &= \tilde{C}_1 x + \tilde{D}_{12} C_c x_o + \tilde{D}_{11} \tilde{w} \\ \dot{x}_o &= B_c \tilde{C}_2 x + \left(A_c + B_c \tilde{D}_{22} C_c\right) x_o + B_c \tilde{D}_{21} \tilde{w} \end{aligned} \tag{5.38}$$

The closed loop state-space description of the tractor-semitrailer can thus be expressed as:

$$\begin{aligned} \dot{\hat{x}} &= \hat{A}\hat{x} + \hat{B}\tilde{w} \\ z &= \hat{C}\hat{x} + \hat{D}\tilde{w} \end{aligned} \tag{5.39}$$

where:

$$\hat{x} = \begin{bmatrix} x \\ x_o \end{bmatrix}, \quad \tilde{w} = \tilde{w}, \quad \hat{A} = \begin{bmatrix} \tilde{A} & \tilde{B}_2 C_c \\ B_c \tilde{C}_2 & A_c + B_c \tilde{D}_{22} C_c \end{bmatrix},$$

$$\hat{B} = \begin{bmatrix} \tilde{B}_1 \\ B_c \tilde{D}_{21} \end{bmatrix}, \quad \hat{C} = \begin{bmatrix} \tilde{C}_1 & \tilde{D}_{12} C_c \end{bmatrix}, \quad \hat{D} = \tilde{D}_{11} = 0 \tag{5.40}$$

The H_2 performance index is thus given by:

$$J_{H2} = \|T_{wz}\|_2^2 = Tr(X\hat{C}'\hat{C}) \tag{5.41}$$

where X is the steady state closed-loop state covariance matrix, defined by:

$$X = \lim_{t \to \infty} E[\tilde{x}'(t)\ \tilde{x}(t)] \tag{5.42}$$

and is the solution of the algebraic *Lyapunov* equation:

$$\tilde{A}X + X\tilde{A}' + \tilde{B}\tilde{B}' = 0 \tag{5.43}$$

Since $\tilde{D} = \tilde{D}_{11} = [0]$, each component of the performance index can be evaluated using the following equation:

$$J_{H2i} = \sum_{m=1}^{46} \sum_{n=1}^{46} [\tilde{C}(i,m)][\tilde{C}(i,n)]X(m,n) \quad i = 1,2,\ldots,19 \tag{5.44}$$

5.3 LIMITED-STATE MEASUREMENT CASES

Measurement of many response variables, such as absolute velocities, absolute displacements and road elevations represent a major hurdle for applications of full-state feedback control systems in vehicles. Although absolute velocities and displacements can theoretically be obtained by integrating directly measurable acceleration signals, the signal integration poses various formidable tasks associated with filter designs and phase variations. Similarly, the measurement of road elevation necessitate body mounted road height sensors. In view of excessive hardware and signal processing requirements, high cost and poor reliability of active suspension systems employing full and perfect measurements, H_2 control schemes based upon measurement of limited and directly measurable states are analyzed. In this study, two distinct cases involving measurement of directly accessible states are proposed

5.3.1 *LSM1*-Relative Displacements and Velocities Across the Suspensions

Relative displacements and velocities across the suspensions can easily be obtained by mounting *LVT*s and *LVDT*s or string potentiometers between the tractor/semitrailer bodies and the tire axles. Since these instruments provide a direct measure of the relative velocities and displacements, the time delay associated with signal processing can be minimized. The elements of the error-free observation vector y are thus given by:

$$y_1 = x_1 + A_1 x_2 - x_5 \tag{5.45a}$$

$$y_2 = x_1 - B_1 x_2 - x_6 \tag{5.45b}$$

$$y_3 = x_1 - B_2 x_2 - x_7 \tag{5.45c}$$

$$y_4 = x_3 - B_3 x_4 - x_8 \tag{5.45d}$$

$$y_5 = x_3 - B_4 x_4 - x_9 \tag{5.45e}$$

$$y_6 = x_{10} + A_1 x_{11} - x_{14} \tag{5.45f}$$

$$y_7 = x_{10} - B_1 x_{11} - x_{15} \tag{5.45g}$$

$$y_8 = x_{10} - B_2 x_{11} - x_{16} \tag{5.45h}$$

$$y_9 = x_{12} - B_3 x_{13} - x_{17} \tag{5.45i}$$

$$y_{10} = x_{12} - B_4 x_{13} - x_{18} \tag{5.45j}$$

where y_1 to y_5 are the relative velocities, and y_6 to y_{10} are the relative displacements across the suspensions. Using string potentiometers with built-in signal conditioning provide a measure of both the displacements and velocities. A total of 5 sensors are therefore required to obtain the observation vector for the five-axle, tractor-semitrailer model suspension considered in this study.

5.3.2 *LSM2*-Tractor and Semitrailer Bounce and Pitch Accelerations

Accelerometers mounted on the tractor and semitrailer can provide the required signals for this active suspension scheme. The elements of the error-free observation vector $\boldsymbol{y}$ are, therefore, given by:

$$\begin{aligned} y_1 = -\big[&C_1(x_1 + A_1x_2 - x_5) + C_2(2x_1 - B_1x_2 - x_6 - B_2x_2 - x_7) + \\ &C_5(x_1 - B_5x_2 - x_3 - A_2x_4) + K_1(x_{10} + A_1x_{11} - x_{14}) + \\ &K_2(2x_{10} - B_1x_{11} - x_{15} - B_2x_{11} - x_{16}) + K_5(x_{10} - B_5x_{11} - x_{12} - A_2x_{13}) + \\ &u_1 + u_2 + u_3\big]/m_{s1} \end{aligned} \tag{5.46a}$$

$$\begin{aligned} y_2 = -\big[&C_1A_1(x_1 + A_1x_2 - x_5) + C_2[B_1(x_1 - B_1x_2 - x_6) + \\ &B_2(x_1 - B_2x_2 - x_7)] - C_5B_5(x_1 - B_5x_2 - x_3 - A_2x_4) + \\ &K_1A_1(x_{10} + A_1x_{11} - x_{14}) + K_2[B_1(x_{10} - B_1x_{11} - x_{15}) + \\ &B_2(x_{10} - B_2x_{11} - x_{16})] - K_5B_5(x_{10} - B_5x_{11} - x_{12} - A_2x_{13}) + \\ &A_1u_1 - B_1u_2 - B_2u_3)\big]/I_{y1} = 0 \end{aligned} \tag{5.46b}$$

$$\begin{aligned} y_3 = -\big[&C_3(x_3 - B_3x_4 - x_8 + x_3 - B_4x_4 - x_9) + C_5(x_3 + A_2x_4 - x_1 + B_5x_2) + \\ &K_3(x_{12} - B_3x_{13} - x_{17} + x_{12} - B_4x_{13} - x_{18}) + K_5(x_{12} + A_2x_{13} - x_1 + B_5x_{11}) + \\ &u_4 + u_5\big]/m_{s2} \end{aligned} \tag{5.46c}$$

$$\begin{aligned} y_4 = -\big[&-C_3[B_3(x_3 - B_3x_4 - x_8) + B_4(x_3 - B_4x_4 - x_9)] + \\ &C_5A_2(x_3 + A_2x_4 - x_1 + B_5x_2) - K_3[B_3(x_{12} - B_3x_{13} - x_{17}) + \\ &B_4(x_{12} - B_4x_{13} - x_{18})] + K_5A_2(x_{12} + A_2x_{13} - x_{10} + B_5x_{11}) - \\ &B_3u_4 - B_4u_5\big]/I_{y2} = 0 \end{aligned} \tag{5.46d}$$

where y_1 and y_2 are the bounce and pitch accelerations of the tractor sprung mass, and y_3 and y_4 are the bounce and pitch accelerations of the semitrailer sprung mass.

The elements of the matrices $\tilde{C}_2$ and $\tilde{D}_{2j}$ can be derived from the above equations

to yield an expression for the observation vector y. The coefficient matrices in EQ (5.1) are then formulated to describe the dynamics of the tractor-semitrailer. Using the controller described in EQ (5.35), the state-space equations of the closed loop vehicle system are evaluated from EQ (5.39). The different components of the performance index are then evaluated from EQ (5.44).

5.4 FREQUENCY DOMAIN ANALYSIS

The frequency performance characteristics of the actively suspended vehicle are evaluated for random road excitations. Since the road excitations are assumed to be stationary and Gaussian, the vector of system response variables, z, is also stationary and Gaussian [8-10]. The closed loop state-space description of the tractor-semitrailer, EQ (5.39), yields the frequency response function:

$$H = \left\{ \bar{C}\left(sI - \bar{A}\right)^{-1} \bar{B} + \bar{D} \right\} \tag{5.47}$$

where $H(j\omega), \in \mathbb{C}^{4\times n}$; is the complex frequency response function (n is 11 for *LSM1* and 5 for *LSM2*). The power spectral density of the response vector is, therefore, given by the following relation [11]:

$$S_z(\omega) = HH^* \tag{5.48}$$

where, *denotes the complex conjugate transpose. The diagonal elements of $S_z(\omega)$ provide the spectral densities of the output states z_i.

5.5 PERFORMANCE CHARACTERISTICS OF THE H_2 ACTIVE SUSPENSION

The performance characteristics of the *LSM1* and *LSM2* suspensions based on the H_2 control scheme are evaluated and compared to those of the "optimum" passive and full-state feedback active suspensions. The response characteristics are discussed in view of the different components of the performance index, specifically, the ride quality, cargo safety, suspension deflections and tire deflections. The results are further analyzed to determine the effectiveness of the *LSM1* and *LSM2* suspensions with considerably relaxed hardware requirements. The influence of sensor noise and actuator size on the suspension performance is further investigated. The response characteristics of the *LSM1* and *LSM2* suspensions are presented in terms of percent improvement (+) or percent deterioration (-) in performance, compared to that of the "optimum" passive suspension.

5.5.1 Influence of Sensors Noise and Actuators Size on Vehicle Ride Quality

The performance characteristics of an active suspension are strongly influenced by the sensor noise and the actuator effort. The significance of sensors noise and actuator effort is investigated through analysis of an active suspension based upon full-state measurement, by letting $\tilde{C}_2 = I$, and $\tilde{D}_{21} = \tilde{D}_{22} = 0$ in EQ (5.1). Since the H_2 problem is formulated to be equivalent to the *LQG* problem derived in Chapter 4, the weighting coefficient corresponding to the active suspension scheme *AS5*, identified in Chapter 4, are used.

Different components of the performance index of the active suspension are presented as function of the sensor noise intensity V_i (V_i=V_1=$\cdots$=V_n) and the actuator

weighting coefficients ρ_i ($\rho_i=\rho_1=\cdots=\rho_5$) in Figures 5.1 to 5.4. The performance characteristics are presented in terms of percent improvement (+) or percent deterioration (-) in relation with the performance of the "optimum" passive suspension.

The components of the performance index are evaluated from EQ (5.46) for varying magnitude of sensors noise V_i and actuator weighting coefficients ρ_i. For low sensor noise ($V_i < 10^{-8}$) and low penalty on power supply ($\rho_i < 10^{-6}$), the suspension performance is similar to that of the *AS5* presented in Chapter 4. This is attributed to the fact that the H_2 problem is formulated to be equivalent to the *LQG* problem. The suspension performance in terms of percent improvement remains nearly constant irrespective of variations in the sensor noise, $V_i < 10^{-8}$, and actuator effort $\rho_i < 10^{-6}$. The suspension performance, however, deteriorates rapidly with an increase in sensor noise, and approaches that of the passive suspension for $V_i > 10^{-2}$, irrespective of the actuator effort. The suspension performance also deteriorates with reduction in the actuator effort, as illustrated in the figures, and approaches that of the passive suspension irrespective of the sensor noise levels. The results presented in Figures 5.1 to 5.4 thus clearly illustrate that excessive measurement noise and/or inadequate actuator power results in very little or no improvement in the performance indices. The influence of sensors noise and actuator effort on the performance characteristics of the limited-state measurement active suspensions, *LSM1* and *LSM2* is investigated. The results (not presented) revealed trends similar to those obtained for the active suspension based on full-state measurement.

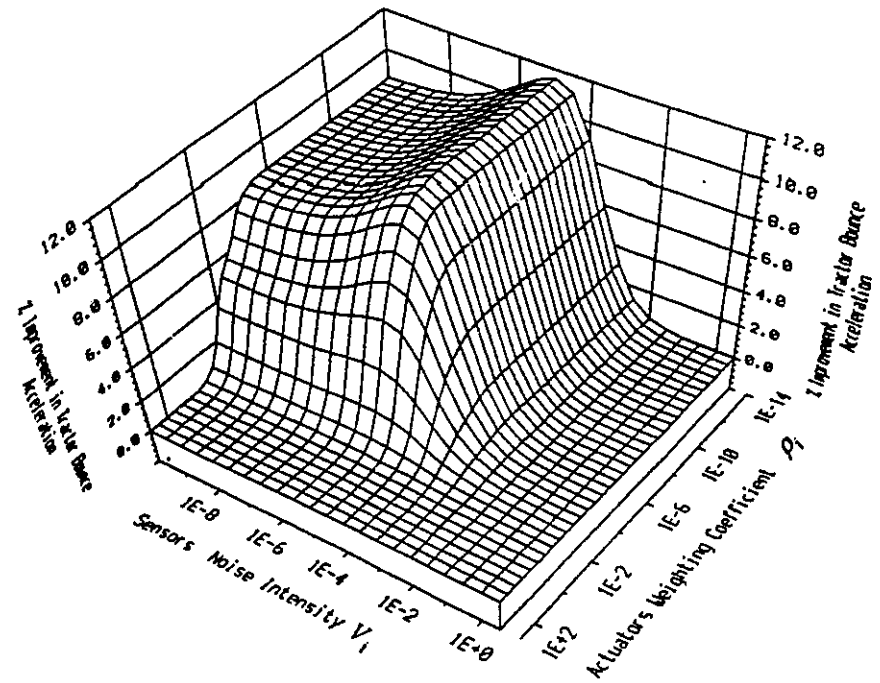

Figure 5.1a Percent improvement(+)/deterioration(-) in the mean square of the tractor bounce acceleration for varying noise intensity and actuators weighting coefficient (compared to passive).

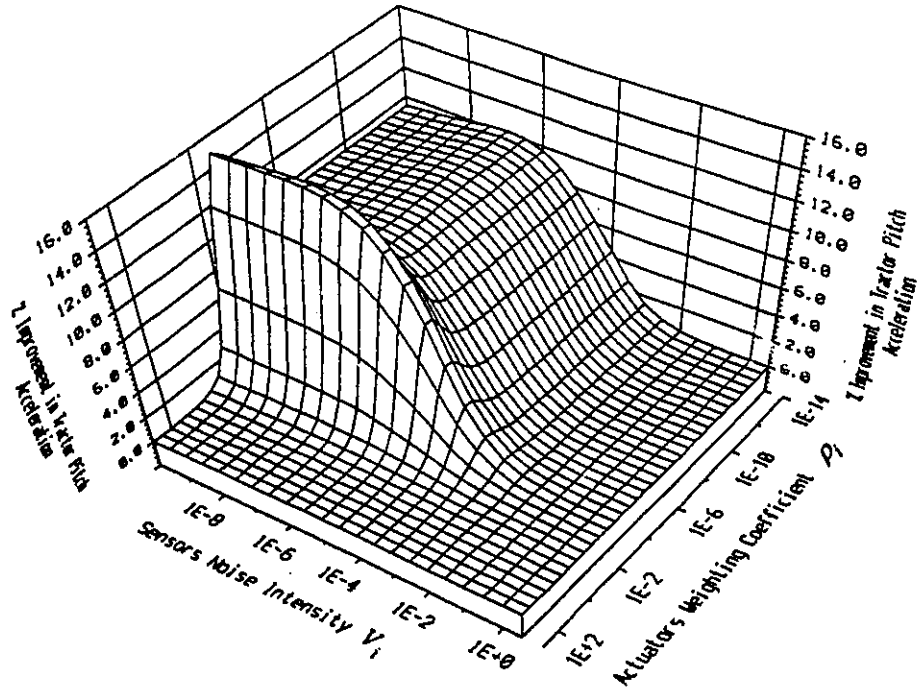

Figure 5.1b Percent improvement(+)/deterioration(-) in the mean square of the tractor pitch acceleration for varying noise intensity and actuators weighting coefficient (compared to passive).

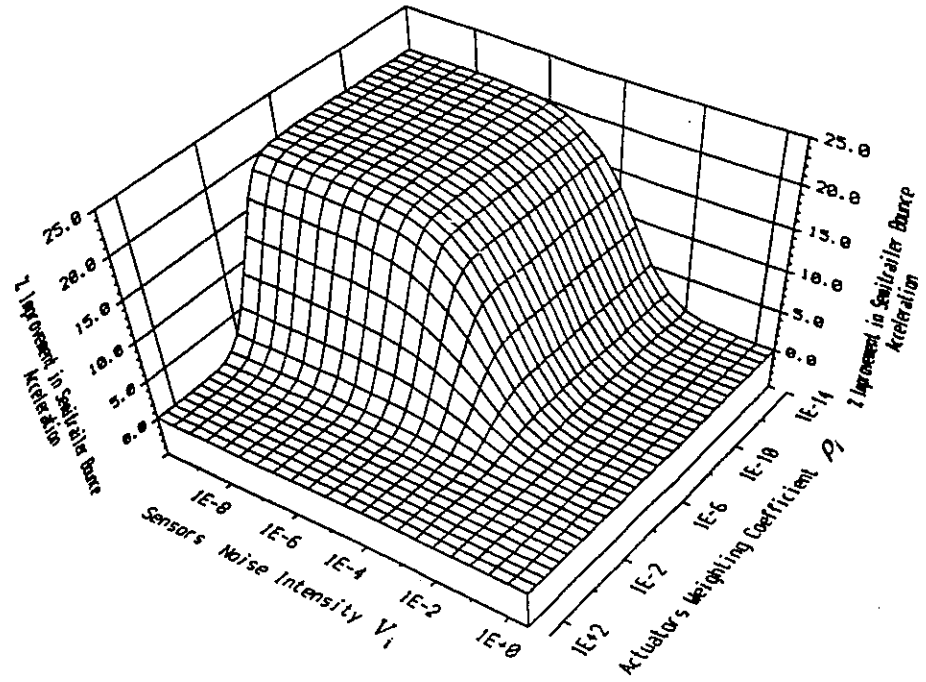

Figure 5.2a Percent improvement(+)/deterioration(-) in the mean square of the semitrailer bounce acceleration for varying noise intensity and actuators weighting coefficient (compared to passive).

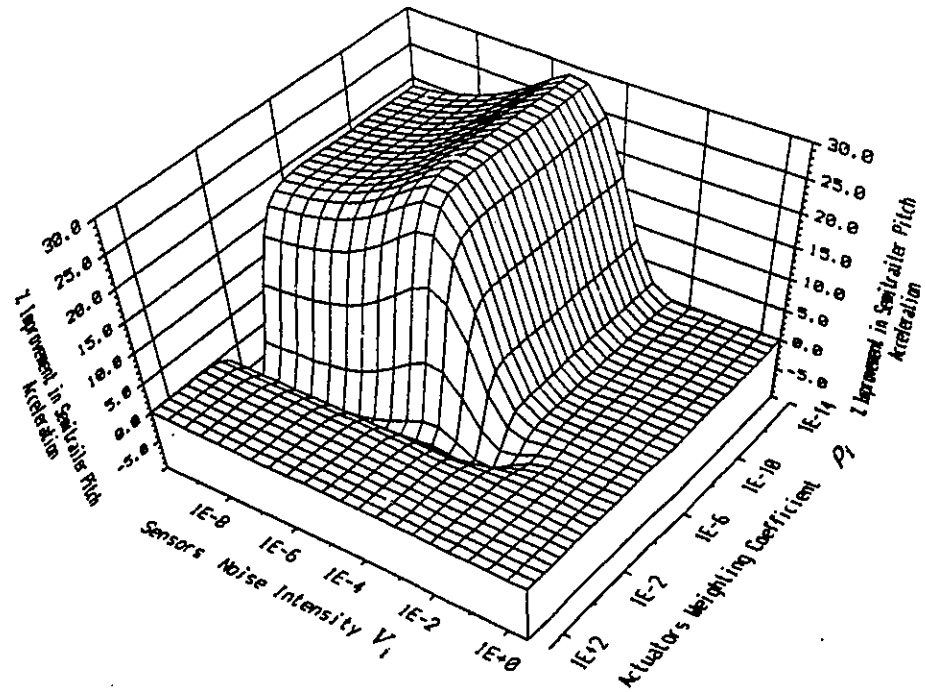

Figure 5.2b Percent improvement(+)/deterioration(-) in the mean square of the semitrailer pitch acceleration for varying noise intensity and actuators weighting coefficient (compared to passive).

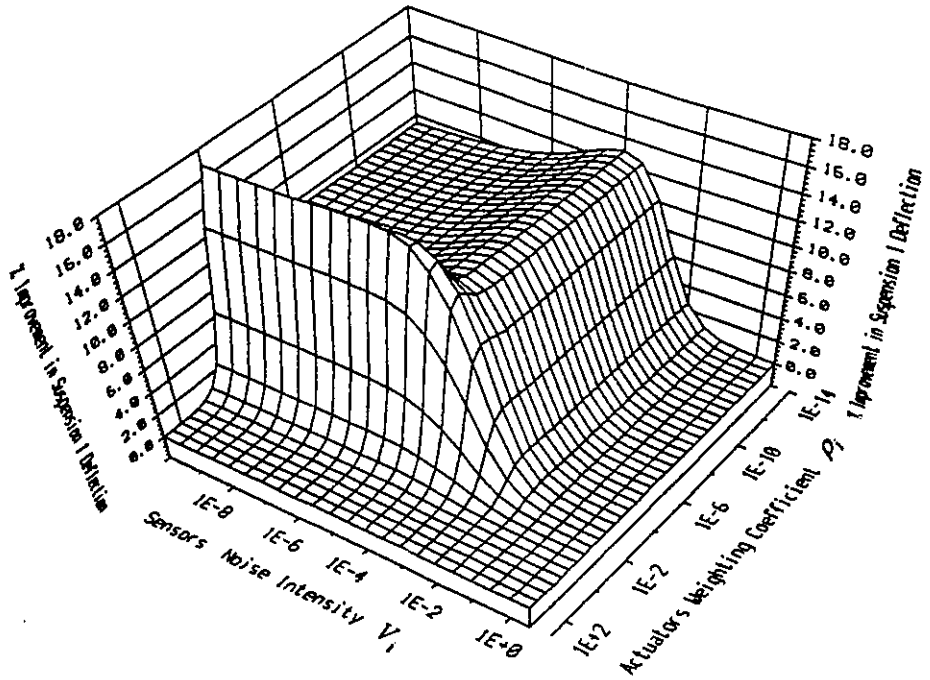

Figure 5.3a Percent improvement(+)/deterioration(-) in the mean square of suspension 1 deflection for varying noise intensity and actuators weighting coefficient (compared to passive).

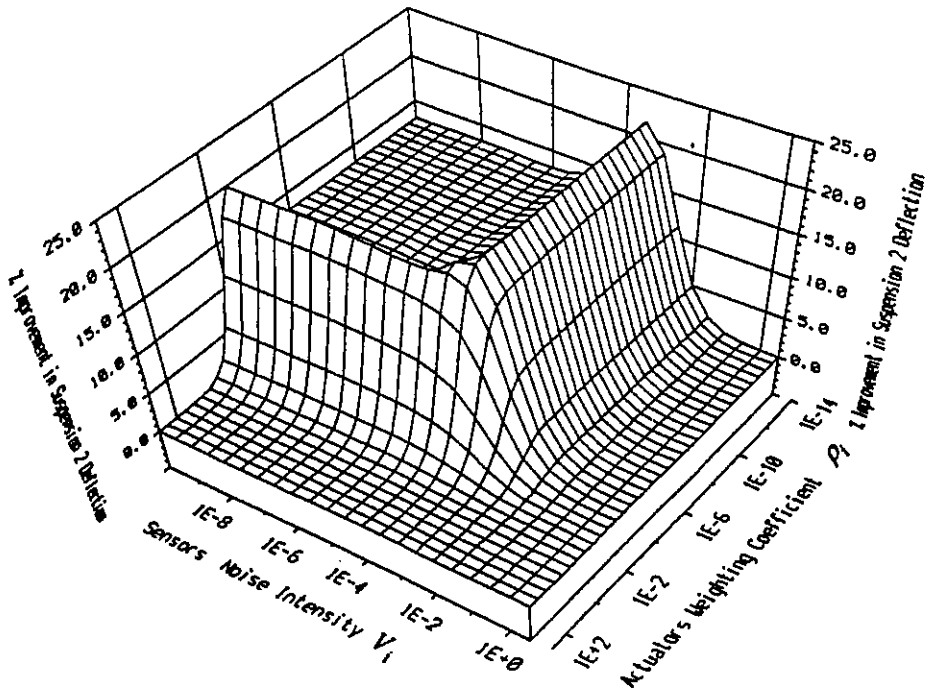

Figure 5.3b Percent improvement(+)/deterioration(-) in the mean square of suspension 2 deflection for varying noise intensity and actuators weighting coefficient (compared to passive).

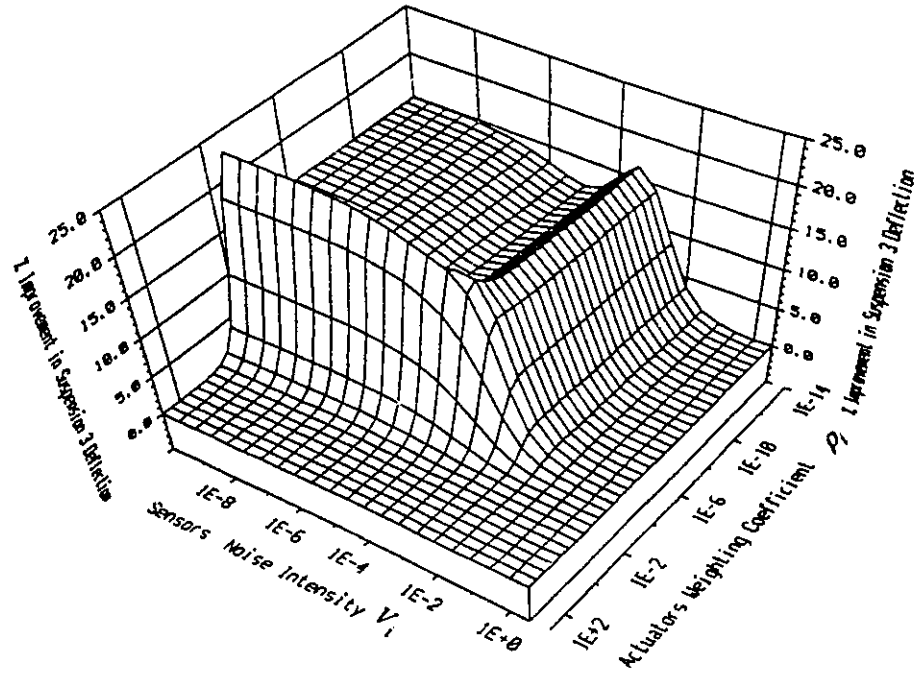

Figure 5.3c Percent improvement(+)/deterioration(-) in the mean square of suspension 3 deflection for varying noise intensity and actuators weighting coefficient (compared to passive).

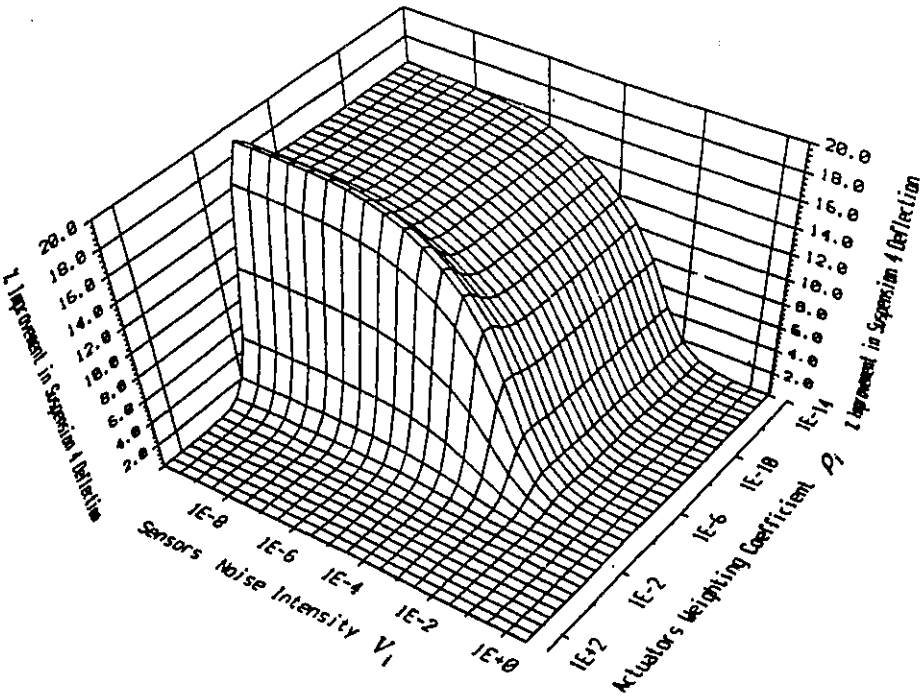

Figure 5.3d Percent improvement(+)/deterioration(-) in the mean square of suspension 4 deflection for varying noise intensity and actuators weighting coefficient (compared to passive).

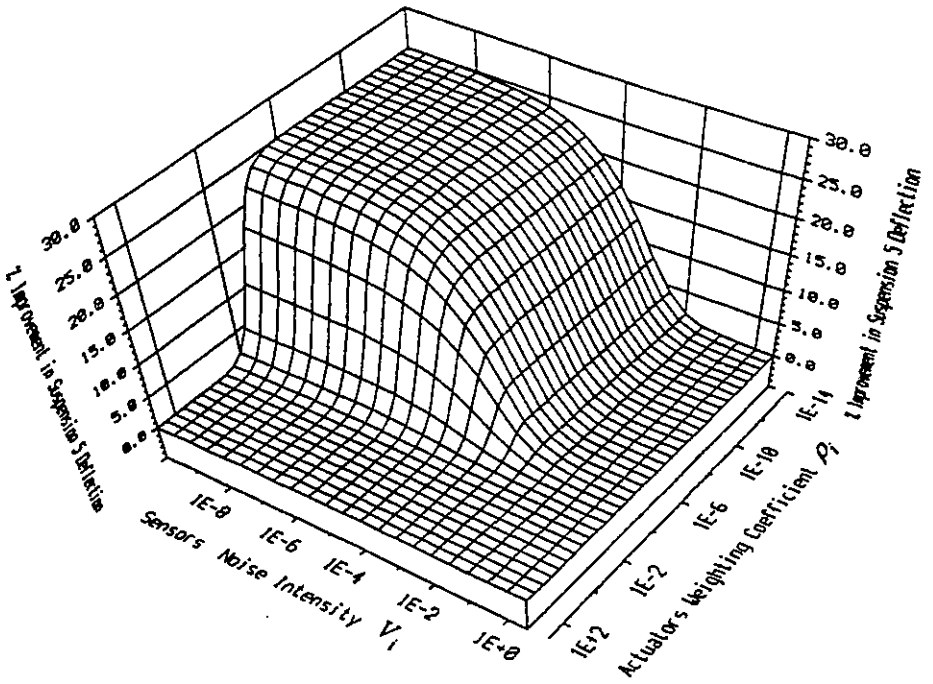

Figure 5.3e Percent improvement(+)/deterioration(-) in the mean square of suspension 5 deflection for varying noise intensity and actuators weighting coefficient (compared to passive).

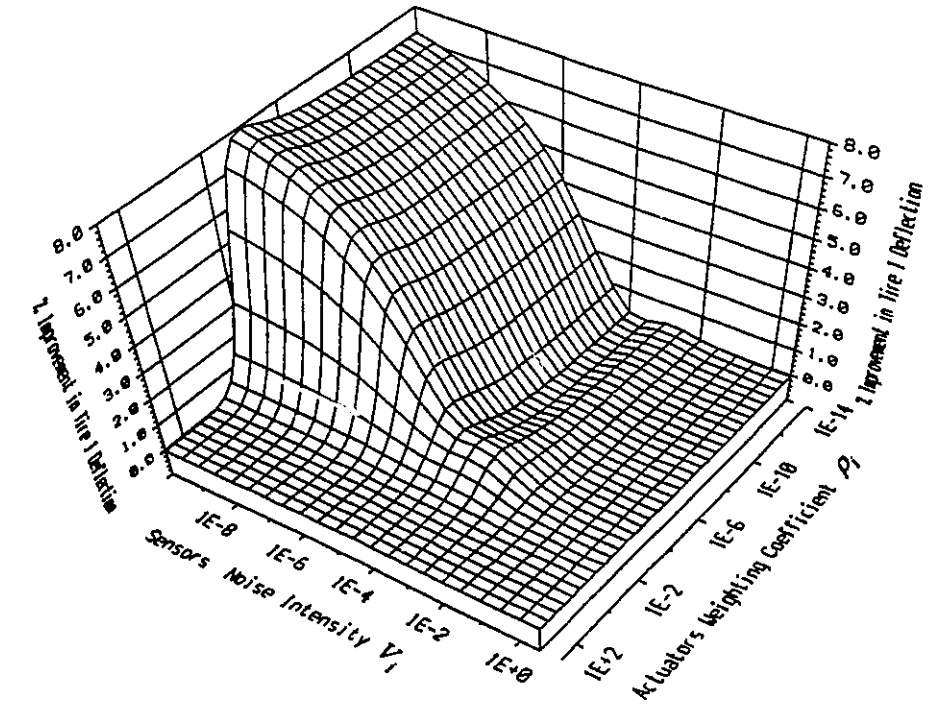

Figure 5.4a Percent improvement(+)/deterioration(-) in the mean square of tire 1 deflection for varying noise intensity and actuators weighting coefficient (compared to passive).

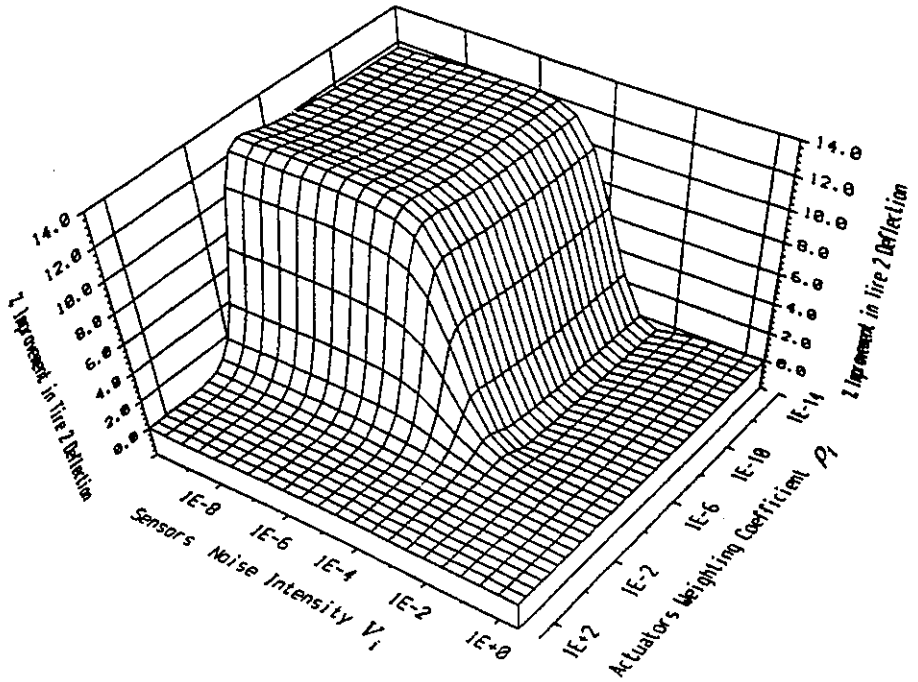

Figure 5.4b Percent improvement(+)/deterioration(-) in the mean square of tire 2 deflection for varying noise intensity and actuators weighting coefficient (compared to passive).

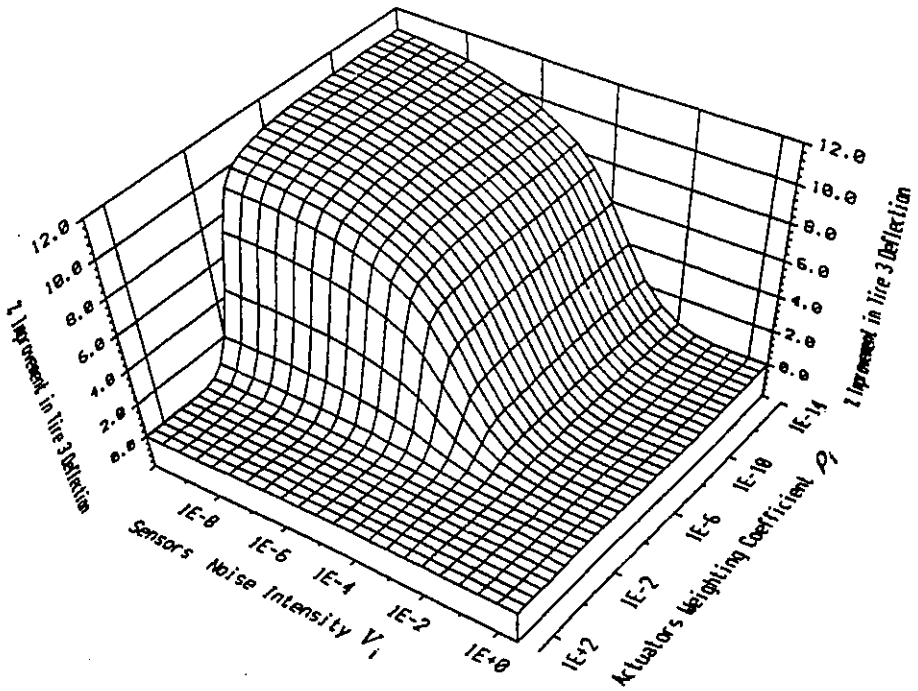

Figure 5.4c Percent improvement(+)/deterioration(-) in the mean square of tire 3 deflection for varying noise intensity and actuators weighting coefficient (compared to passive).

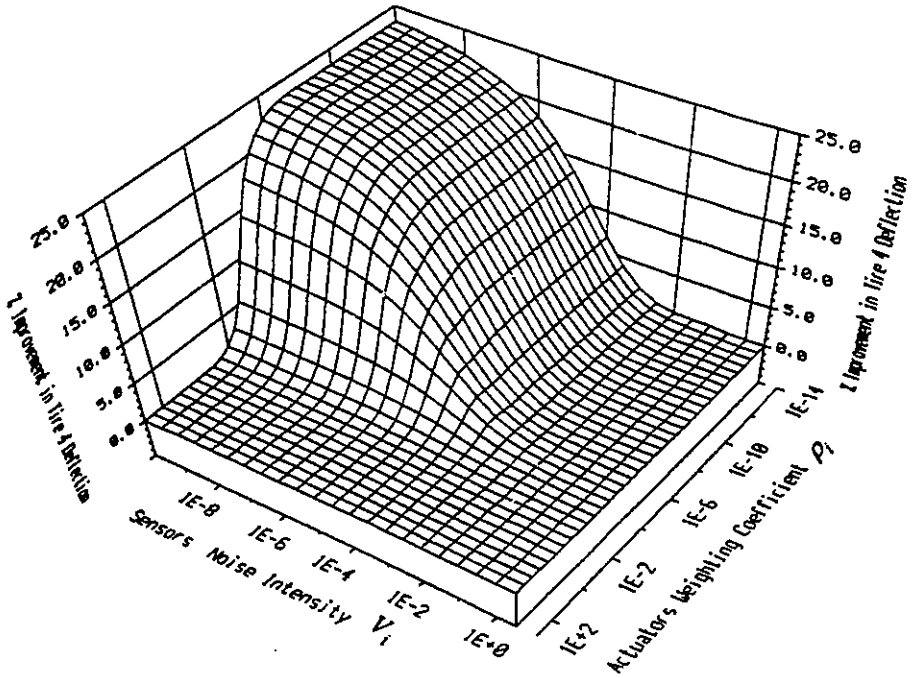

Figure 5.4d Percent improvement(+)/deterioration(-) in the mean square of tire 4 deflection for varying noise intensity and actuators weighting coefficient (compared to passive).

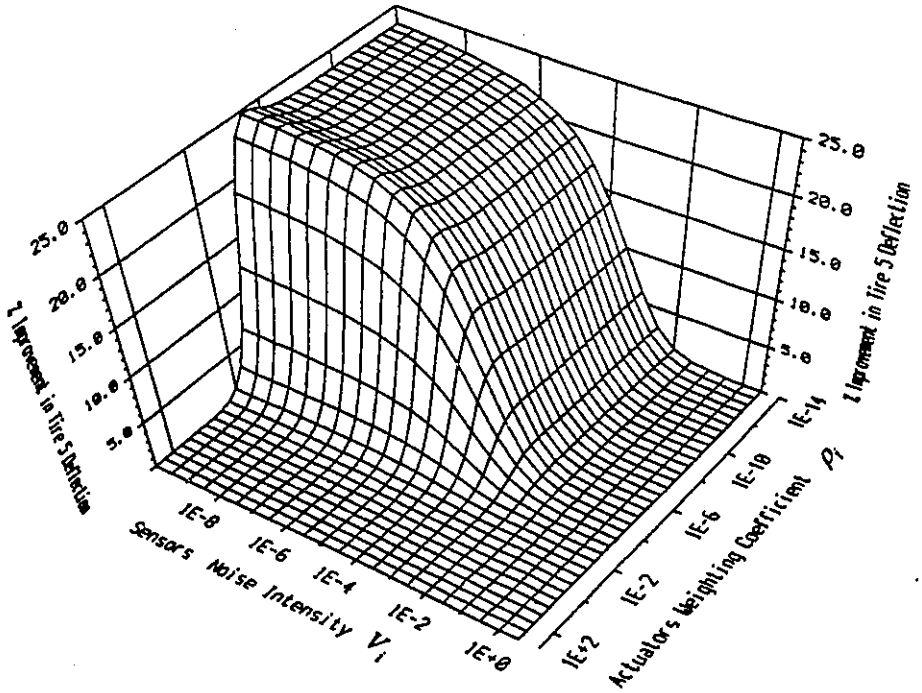

Figure 5.4e Percent improvement(+)/deterioration(-) in the mean square of tire 5 deflection for varying noise intensity and actuators weighting coefficient (compared to passive).

The performance characteristics of the active suspensions limited-state measurement (*LSM1* and *LSM2*) are compared to those of the full-state feedback active suspension for varying sensors noise. The actuator force weighting coefficient is selected as $\rho_i = 10^{-14}$, to ensure availability of adequate actuator effort. from the results presented in Figures 5.5 to 5.8, the following observations are made;

1. The three suspension systems offer similar % improvement in the performance for low level of sensors noise. This indicates that the state estimation can be accomplished with greater accuracy when signal noise levels are low. It is thus possible to achieve performance similar to that of the full-state feedback suspension, while using limited-state measurement. It should be noted that the *LSM1* is based upon feedback from measurement of relative velocities and relative displacements across the suspension systems, while *LSM2* is based upon measurements of the tractor and semitrailer bounce and pitch accelerations.

2. The discrepancy among the performance characteristics of the three suspension schemes increases with increase in noise intensity. For signal noise intensity $V_i > 10^{-2}$, none of the three suspension schemes offer a noticeable improvement in performance when compared to a passive suspension.

3. Using tractor and semitrailer bounce and pitch accelerations as the only available measurements (*LSM2*), it is possible to obtain a performance comparable to that based on full-state measurements.

4. The suspension scheme based on relative measurements (*LSM1*), while offering acceptable performance at low sensor noise, is very sensitive to increased corruption

in the measurable quantities. The performance of this scheme is, generally, not as favorable as that based on either full-state measurements or accelerations-only measurements (*LSM2*).

5. A moderate increase in the signal noise levels tends to improve the performance components related to tractor bounce and semitrailer pitch (*AS5* and *LSM2*), and relative deflection across the steering axle suspension (*AS5*). This improvement is, however, achieved at the cost of rapid degradation of all the other components of performance index.

6. The *LSM1* suspension scheme yields considerable reduction in the deflection across the tractor drive axles, while the deflections across the remaining axle suspensions increase. Although a white sensor noise of identical intensity is introduced within each channel of measurement (relative displacements and velocities), the influence of signal noise is dependent upon the signal-to-noise ratio of each channel. The signal noise thus tends to deteriorate the front axle suspension deflection more significantly due to its lower magnitude of dynamic deflection.

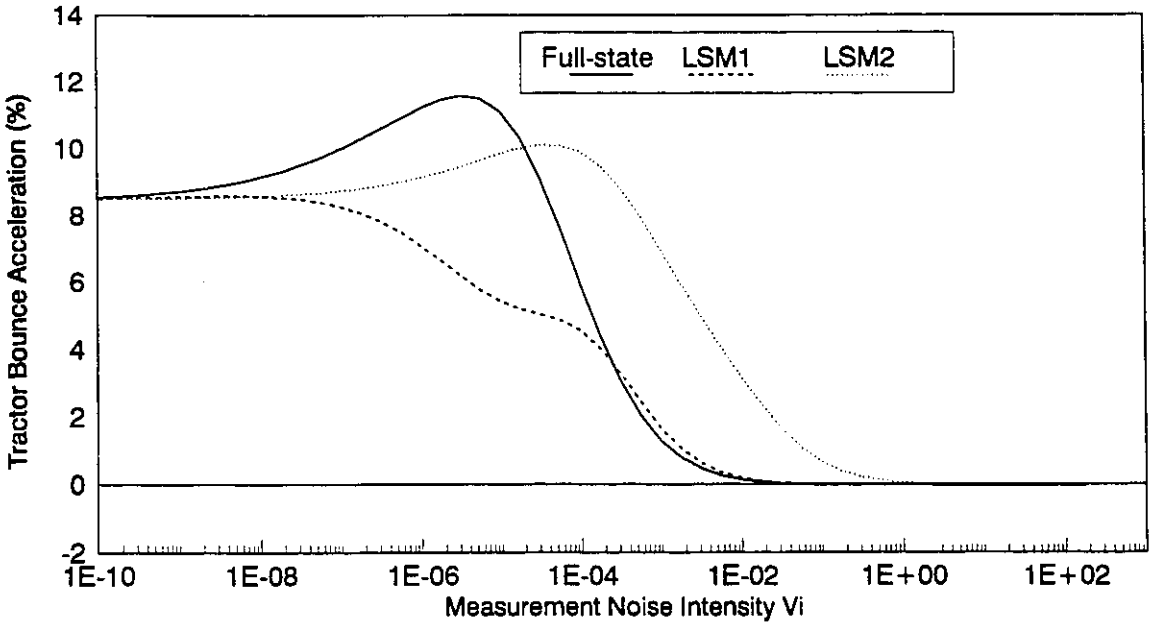

Figure 5.5a Percent improvement(+)/deterioration(-) in mean square of tractor bounce acceleration for varying sensors noise (compared to passive)

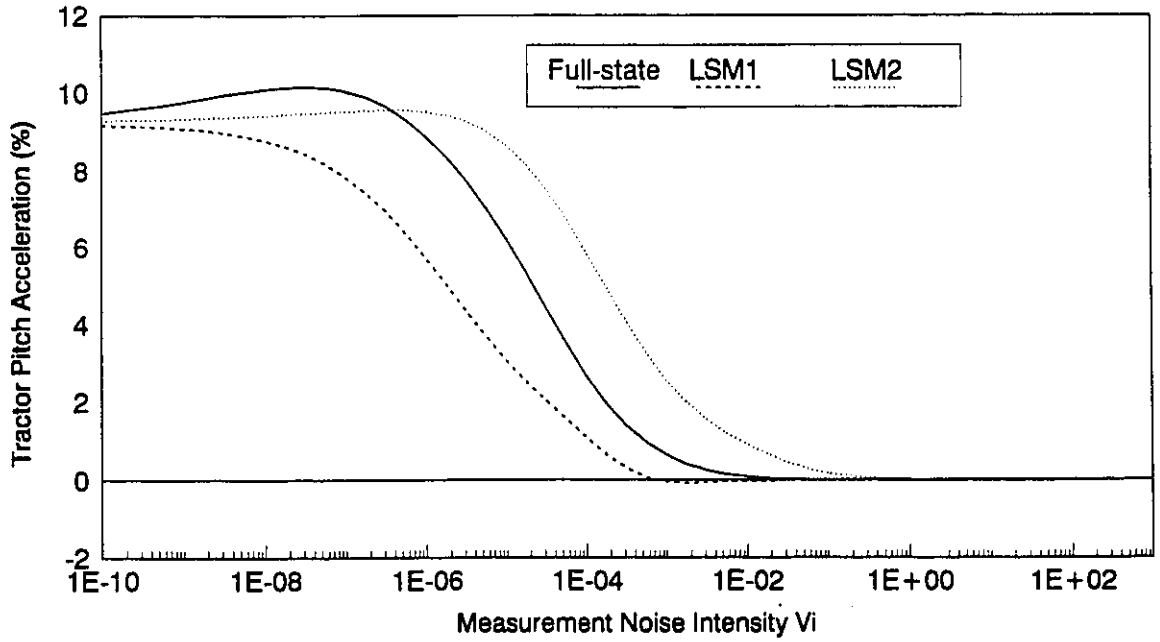

Figure 5.5b Percent improvement(+)/deterioration(-) in mean square of tractor pitch acceleration for varying sensors noise (compared to passive)

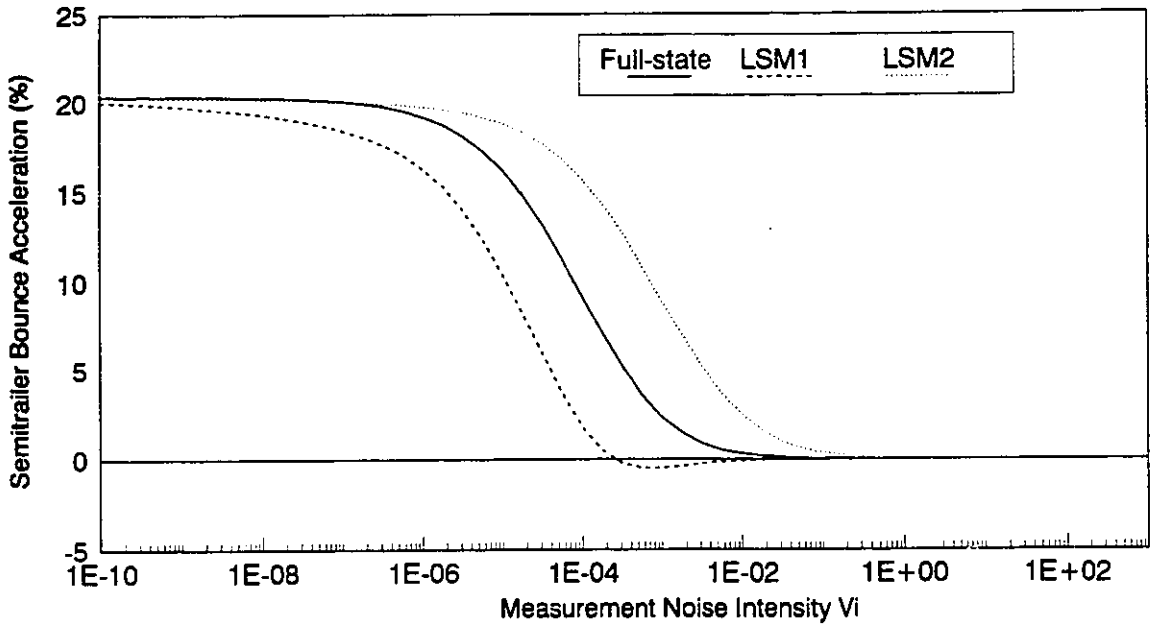

Figure 5.6a Percent improvement(+)/deterioration(-) in mean square of semitrailer bounce acceleration for varying sensors noise (compared to passive)

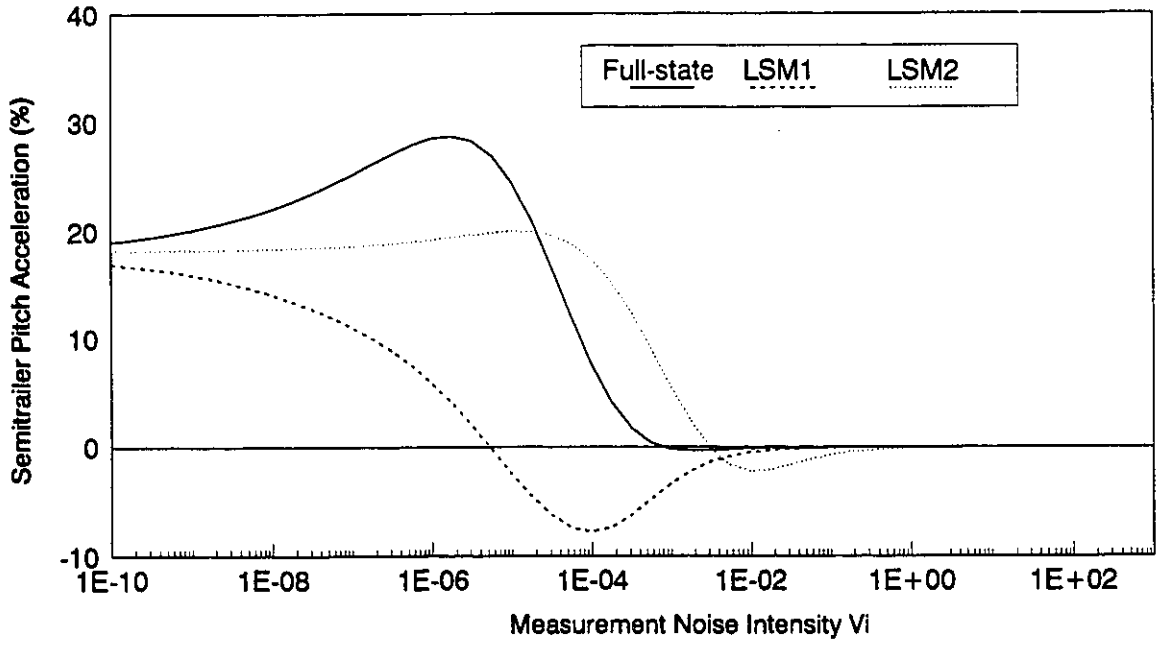

Figure 5.6b Percent improvement(+)/deterioration(-) in mean square of semitrailer pitch acceleration for varying sensors noise (compared to passive)

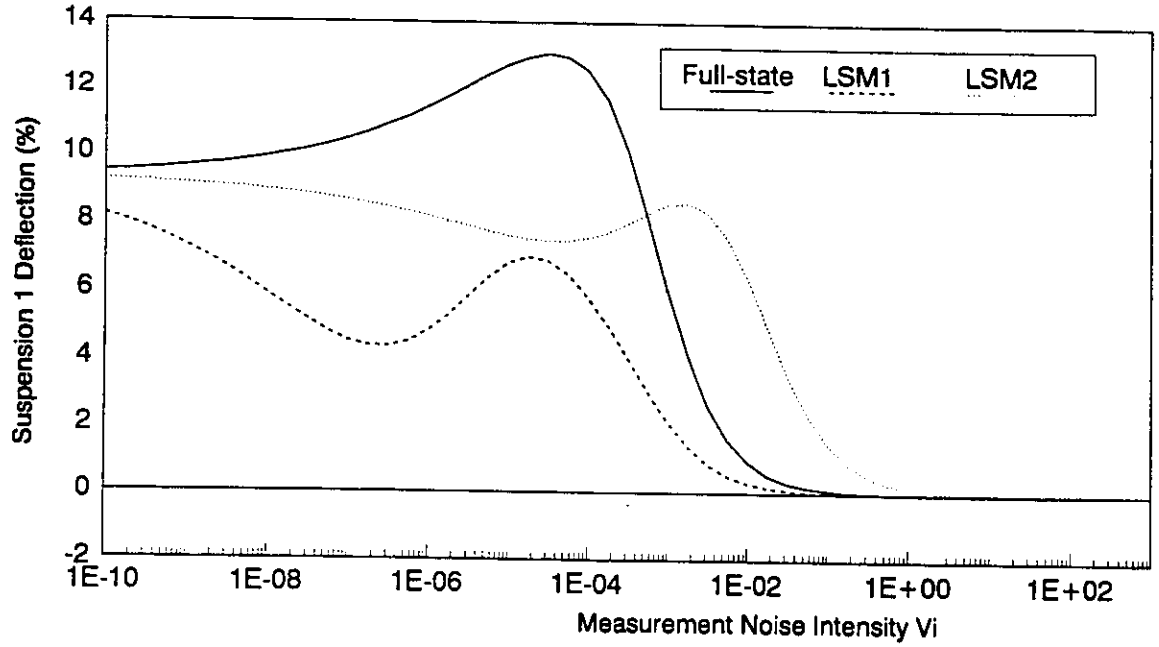

Figure 5.7a Percent improvement(+)/deterioration(-) in mean square of suspension 1 deflection for varying sensors noise (compared to passive)

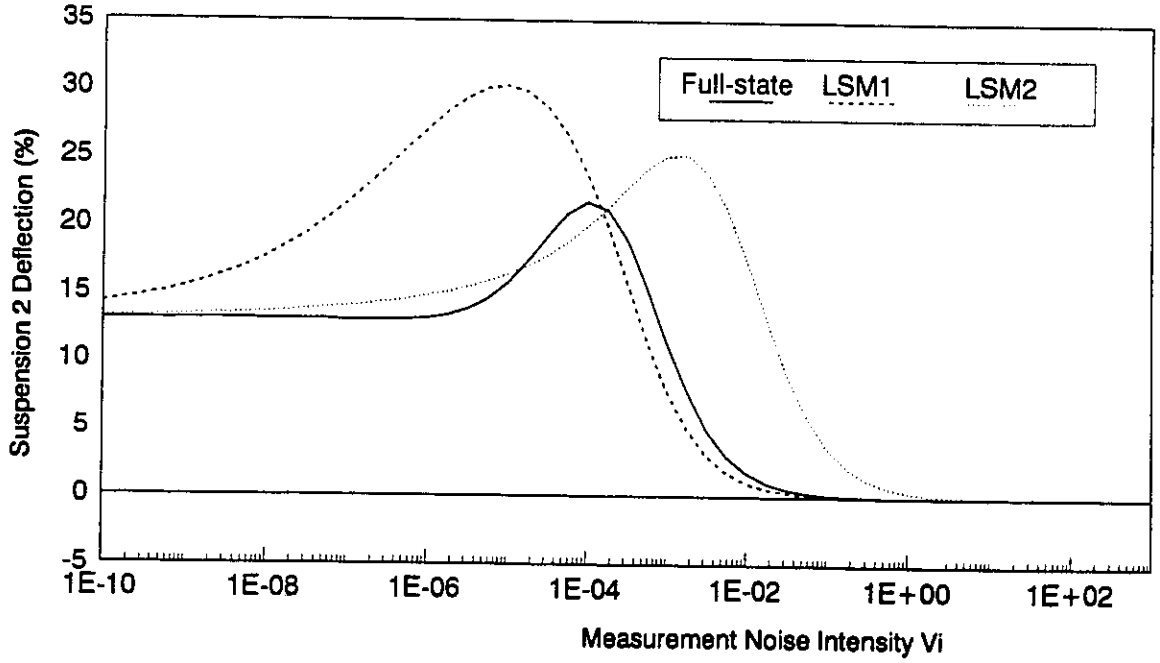

Figure 5.7b Percent improvement(+)/deterioration(-) in mean square of suspension 2 deflection for varying sensors noise (compared to passive)

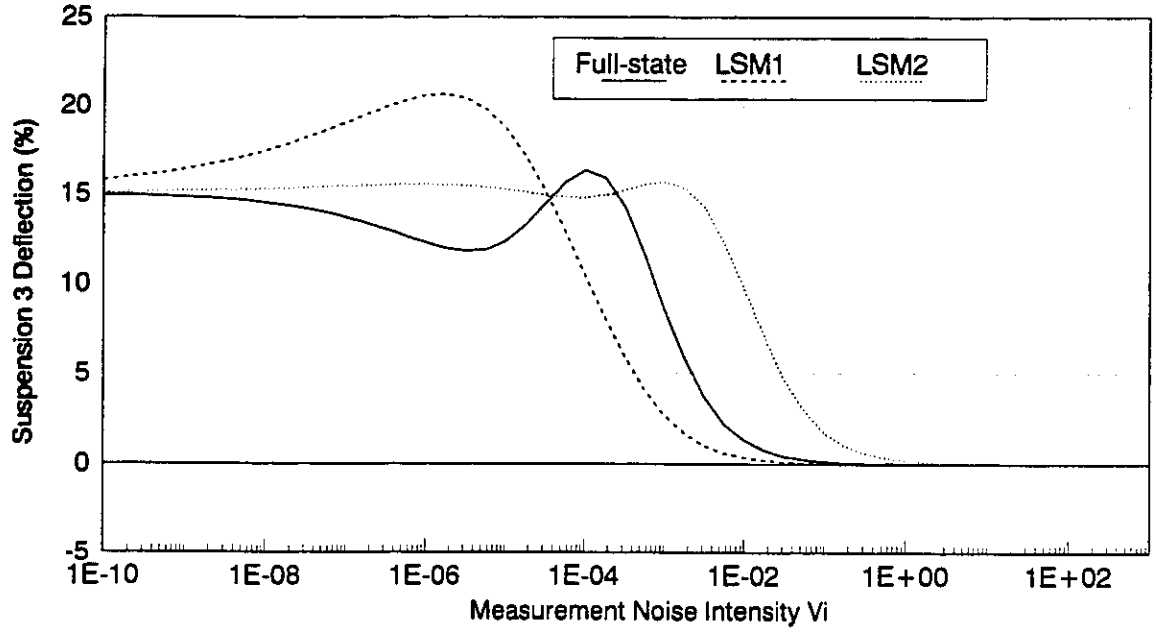

Figure 5.7c Percent improvement(+)/deterioration(-) in mean square of suspension 3 deflection for varying sensors noise (compared to passive)

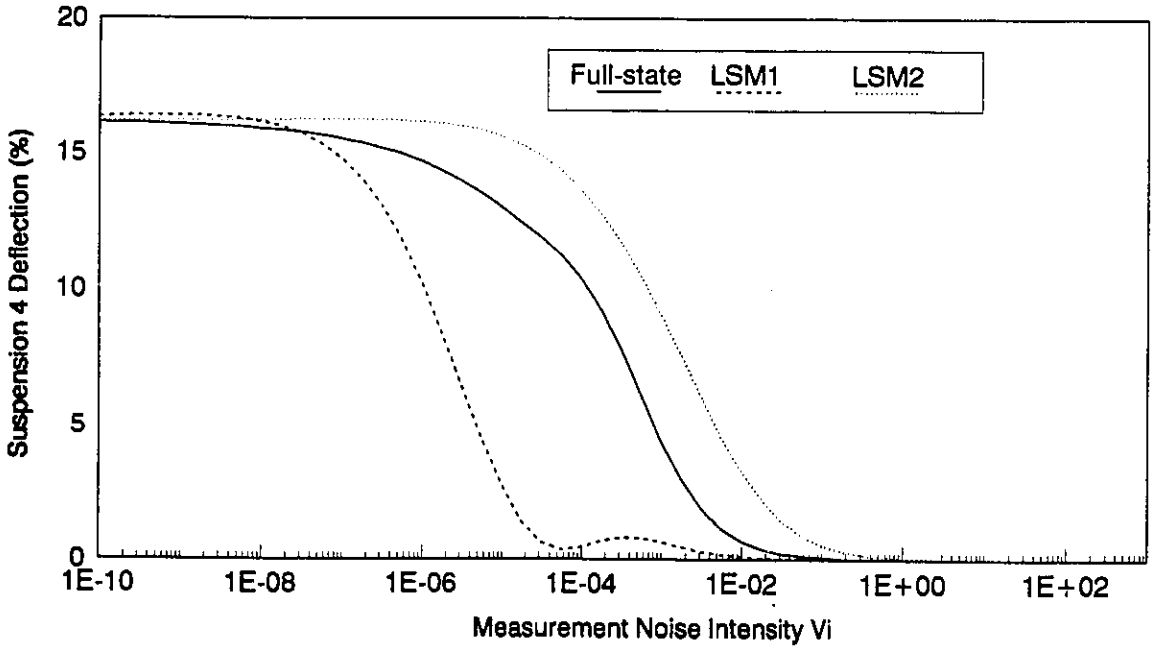

Figure 5.7d Percent improvement(+)/deterioration(-) in mean square of suspension 4 deflection for varying sensors noise (compared to passive)

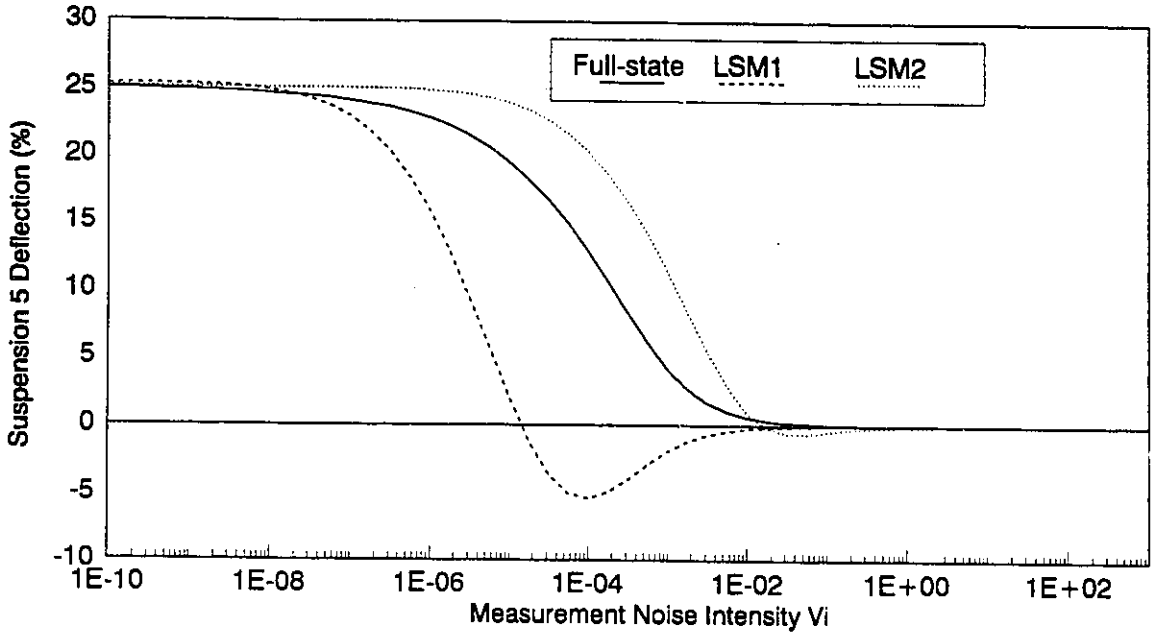

Figure 5.7e Percent improvement(+)/deterioration(-) in mean square of suspension 5 deflection for varying sensors noise (compared to passive)

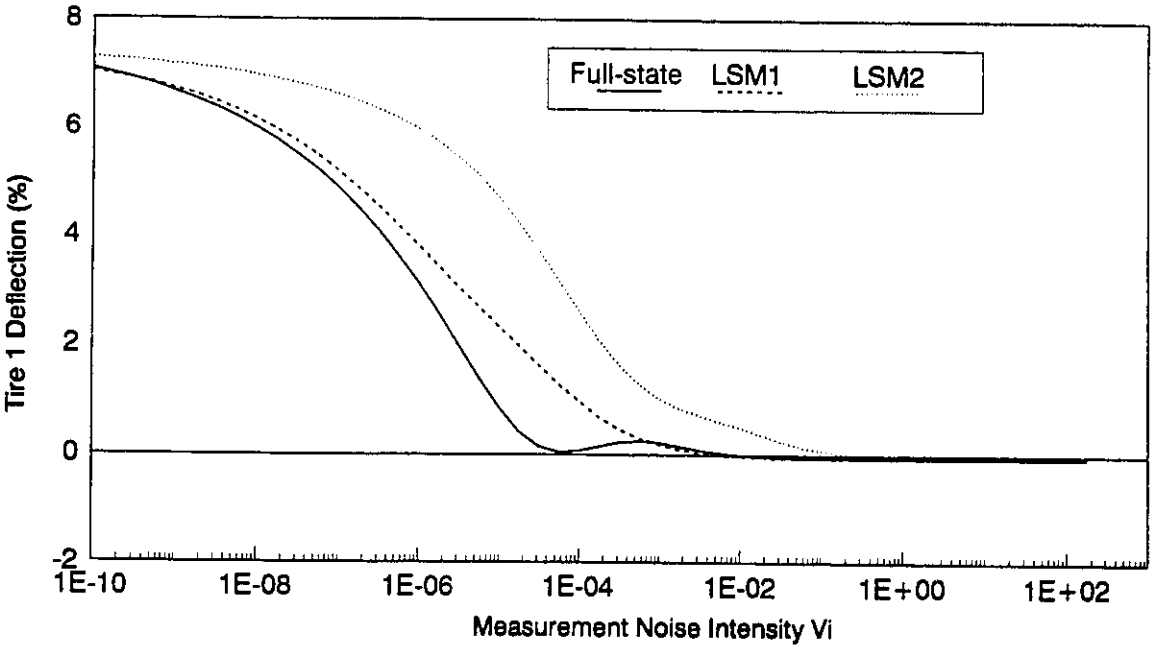

Figure 5.8a Percent improvement(+)/deterioration(-) in mean square of tire 1 deflection for varying sensors noise (compared to passive)

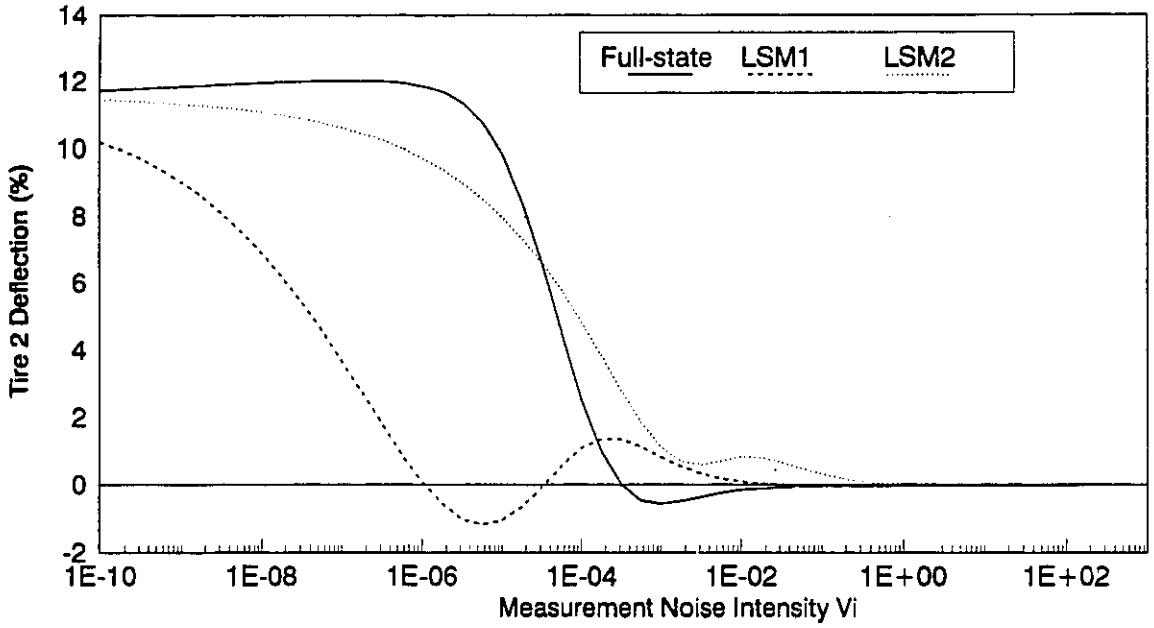

Figure 5.8b Percent improvement(+)/deterioration(-) in mean square of tire 2 deflection for varying sensors noise (compared to passive)

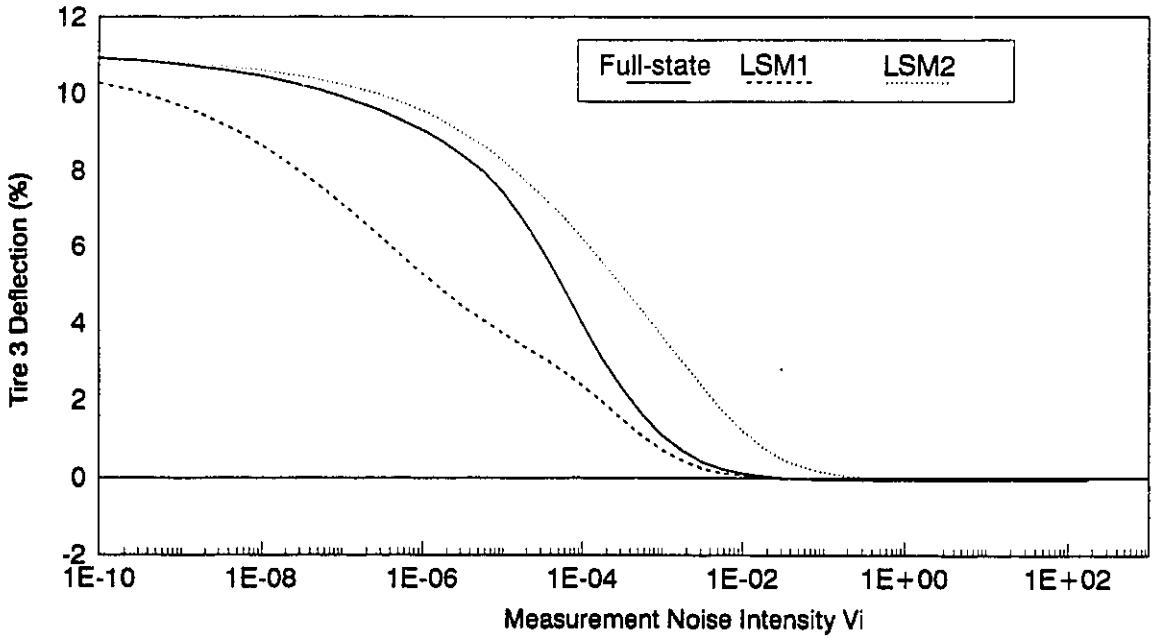

Figure 5.8c Percent improvement(+)/deterioration(-) in mean square of tire 3 deflection for varying sensors noise (compared to passive)

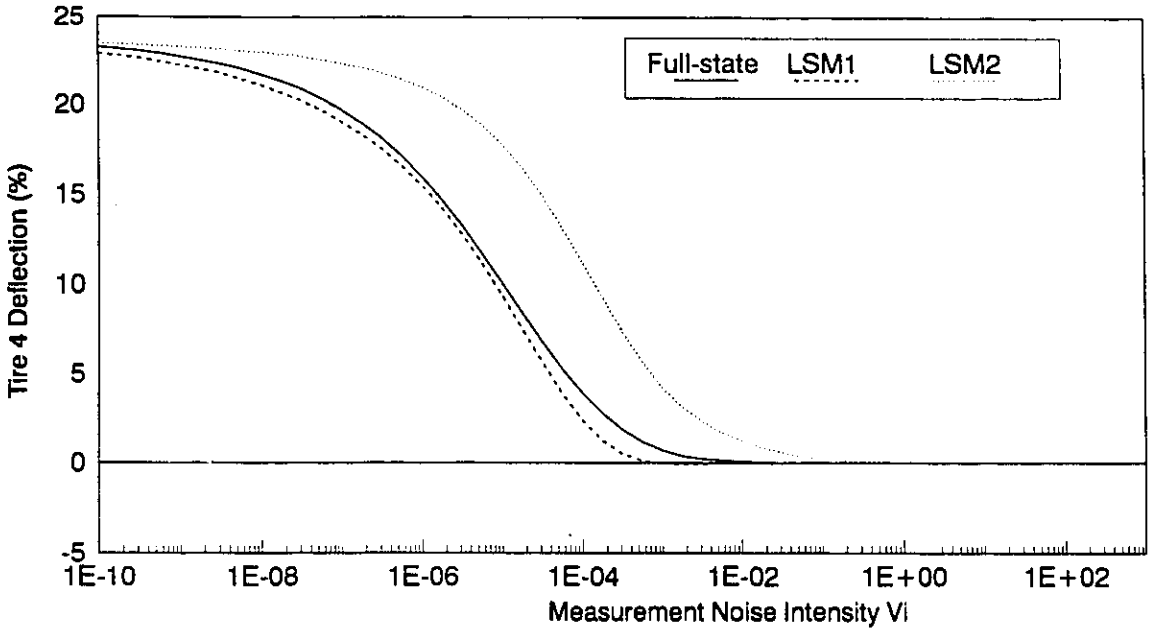

Figure 5.8d Percent improvement(+)/deterioration(-) in mean square of tire 4 deflection for varying sensors noise (compared to passive)

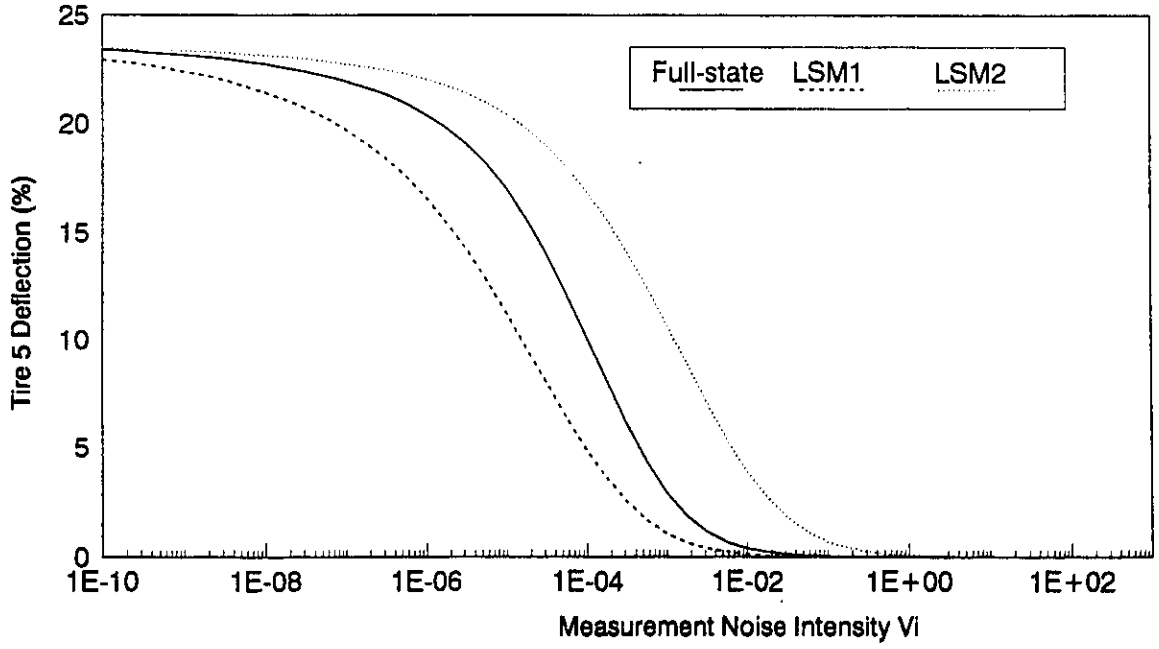

Figure 5.8e Percent improvement(+)/deterioration(-) in mean square of tire 5 deflection for varying sensors noise (compared to passive)

The influence of actuator effort on the performance characteristics of the three suspension systems is further investigated, while the sensors noise intensity are held at V_i=10^{-6}. Figures 5.9 to 5.12 illustrate the relative performance characteristics of the full-state, *LSM1* and *LSM2* active suspension systems as a function of the actuator weighting coefficients, ρ_i. The results clearly reveal that the performance characteristics approach those of the passive suspension when the actuator effort is reduced, irrespective of the suspension scheme. Since each active suspension system is configured as a fail-safe combination of the passive and active components, a reduction in the actuator effort will simply cause the suspension to operate in a passive mode. The performance characteristics, however, approaches those of the "optimum" passive suspension, since the passive components correspond to the optimum design described in Chapter 3. The fail-safe configuration of the active suspension, thus, enhances the reliability of the suspension systems. For adequate actuator effort ($\rho_i < 10^{-06}$), the following table summarizes the percent improvement/deterioration in performance of the three suspension schemes, compared to those of the "optimum" passive suspension.

Table 5.1 Percent reduction(+)/increase(-) in the mean square value of each of the performance variables for the 3 suspension schemes (V_i=10^{-6}) (compared to passive)

Performance variable	*Full-State* %	*LSM1* %	*LSM2* %
Tractor bounce acceleration	1.121e+01	7.094e+00	9.146e+00
Tractor pitch acceleration	8.898e+00	5.713e+00	9.531e+00
Semitrailer bounce acceleration	1.924e+01	1.631e+01	1.979e+01
Semitrailer pitch acceleration	2.859e+01	5.940e+00	1.923e+01
Suspension 1 Deflection	1.142e+01	4.793e+00	8.170e+00
Suspension 2 Deflection	1.314e+01	2.698e+01	1.480e+01
Suspension 3 Deflection	1.229e+01	2.063e+01	1.554e+01
Suspension 4 Deflection	1.465e+01	1.017e+01	1.613e+01
Suspension 5 Deflection	2.286e+01	1.589e+01	2.491e+01
Tire 1 force	3.118e+00	3.810e+00	5.974e+00
Tire 2 force	1.186e+01	8.321e-02	9.718e+00
Tire 3 force	9.051e+00	5.299e+00	9.546e+00
Tire 4 force	1.605e+01	1.554e+01	2.105e+01
Tire 5 force	2.044e+01	1.661e+01	2.205e+01

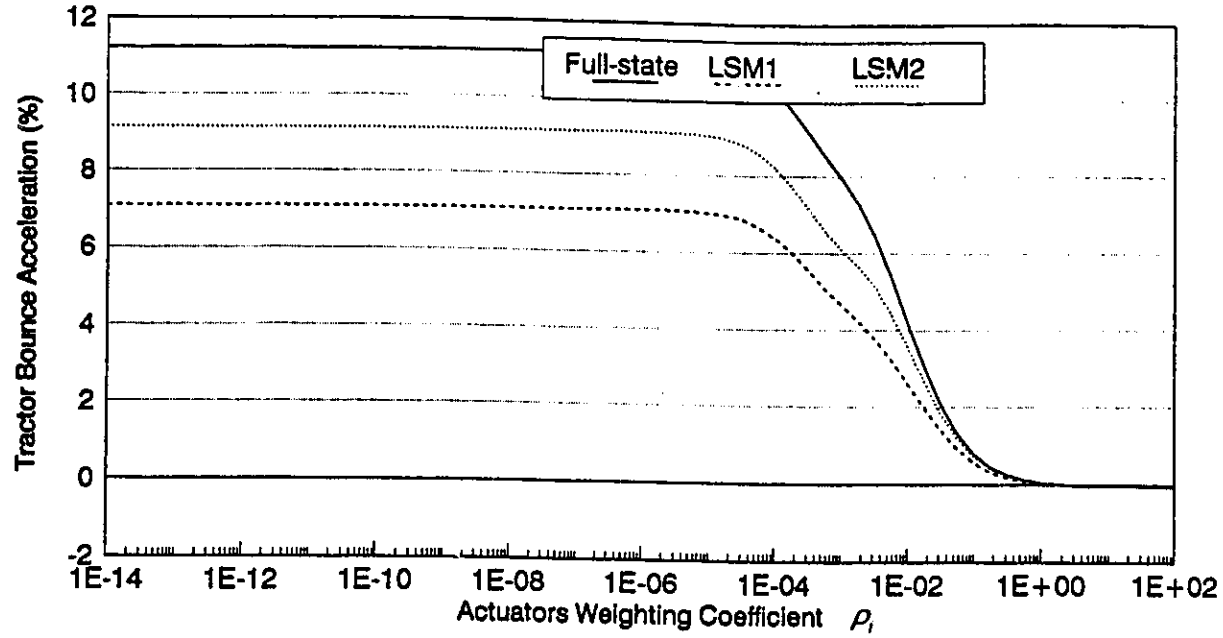

Figure 5.9a Percent improvement(+)/deterioration(-) in mean square of tractor bounce acceleration for varying actuators size (compared to passive)

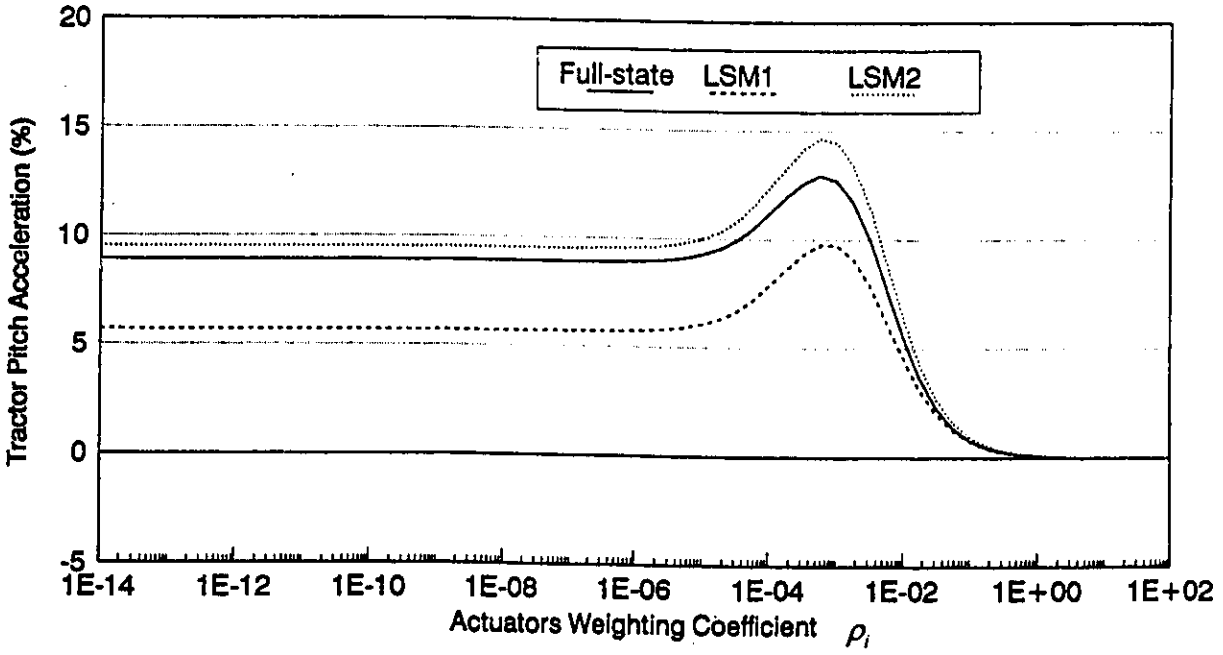

Figure 5.9b Percent improvement(+)/deterioration(-) in mean square of tractor pitch acceleration for varying actuators size (compared to passive)

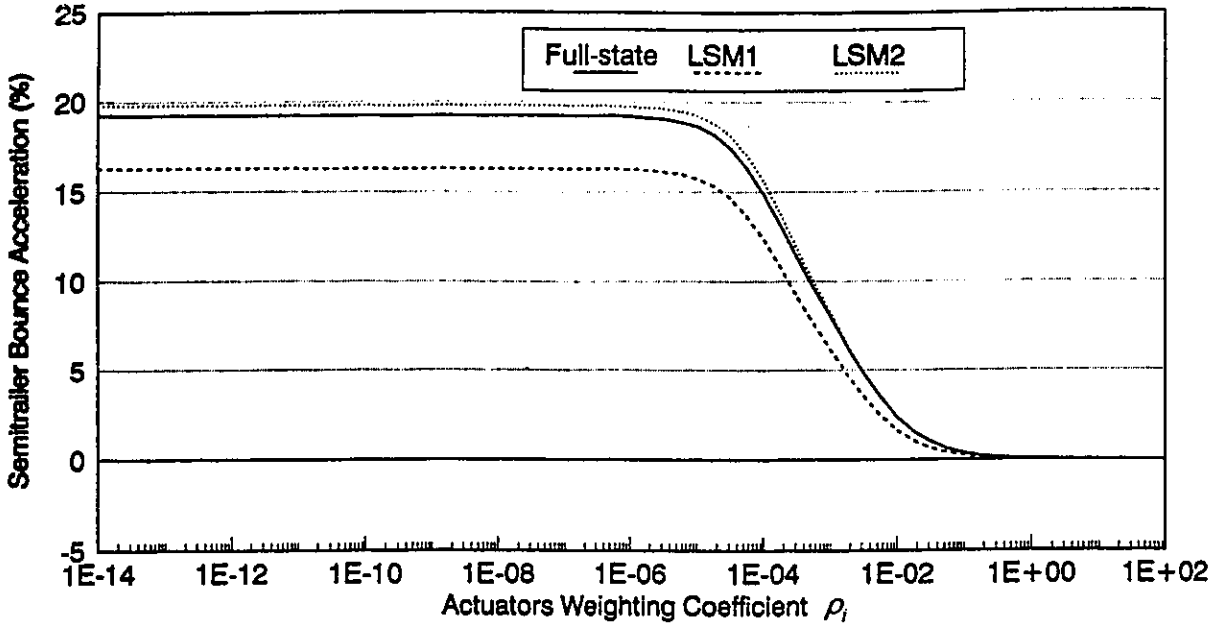

Figure 5.10a Percent improvement(+)/deterioration(-) in mean square of semitrailer bounce acceleration for varying actuators weighting coefficient (compared to passive)

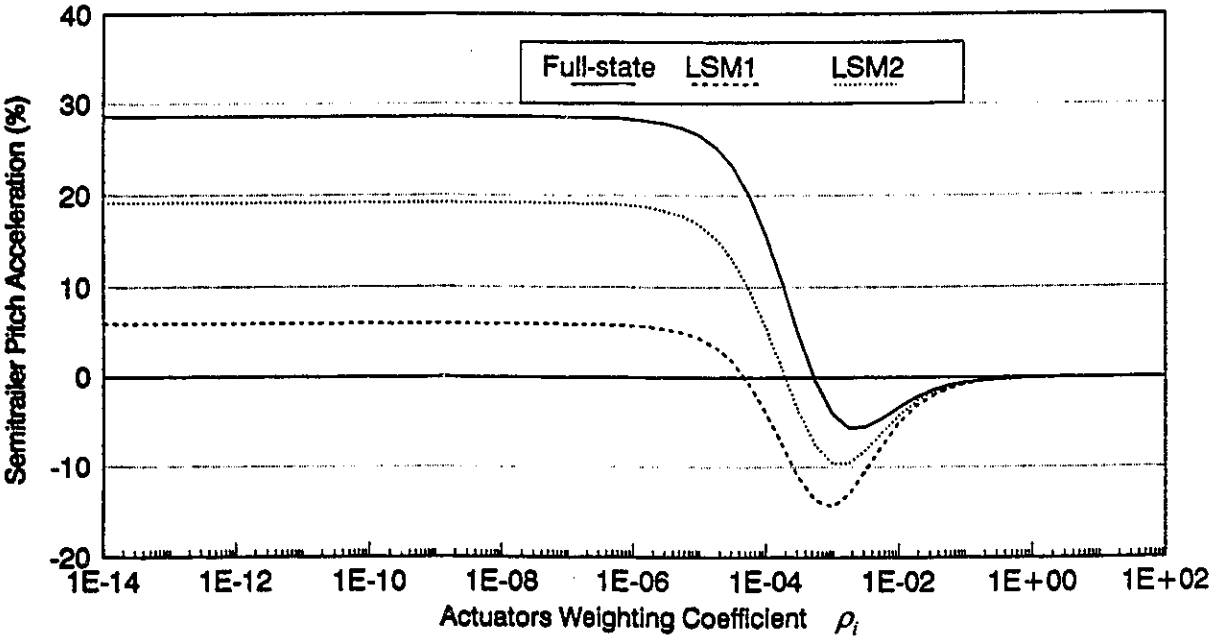

Figure 5.10b Percent improvement(+)/deterioration(-) in mean square of semitrailer pitch acceleration for varying actuators weighting coefficient (compared to passive)

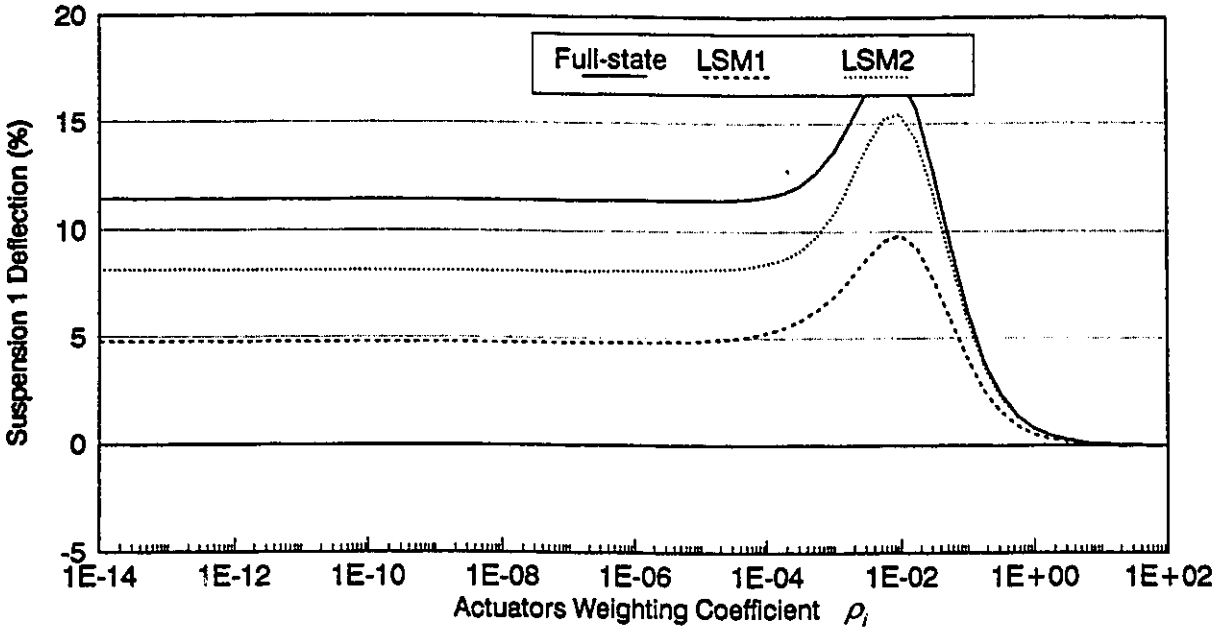

Figure 5.11a Percent improvement(+)/deterioration(-) in mean square of suspension 1 deflection for varying actuators weighting coefficient (compared to passive)

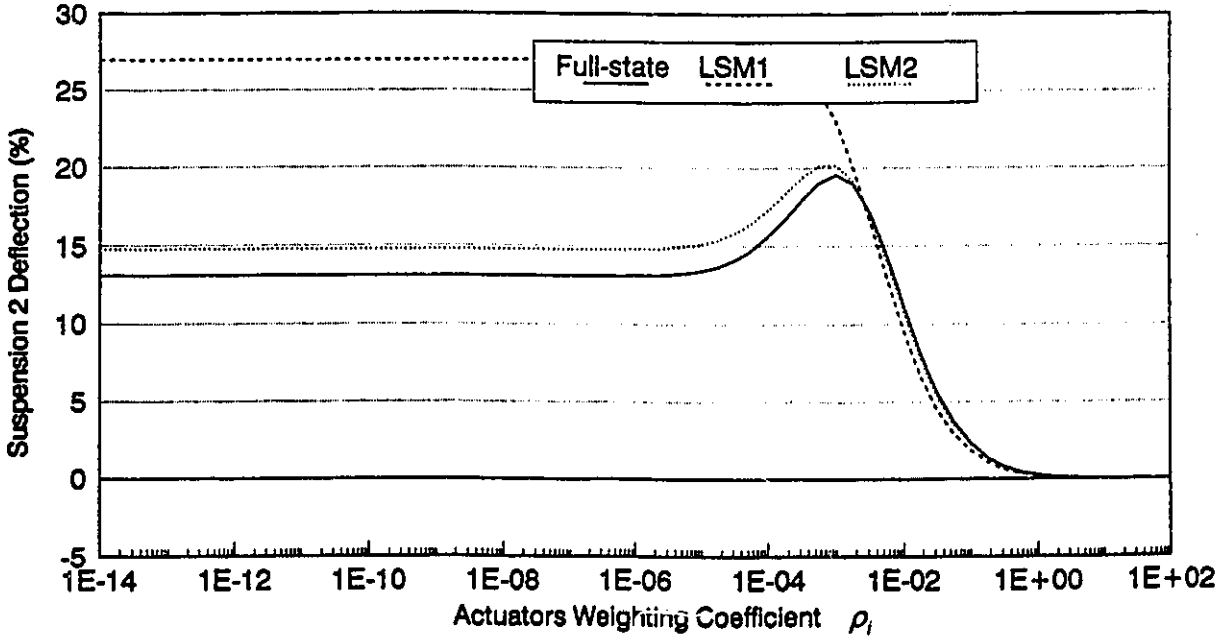

Figure 5.11b Percent improvement(+)/deterioration(-) in mean square of suspension 2 deflection for varying actuators weighting coefficient (compared to passive)

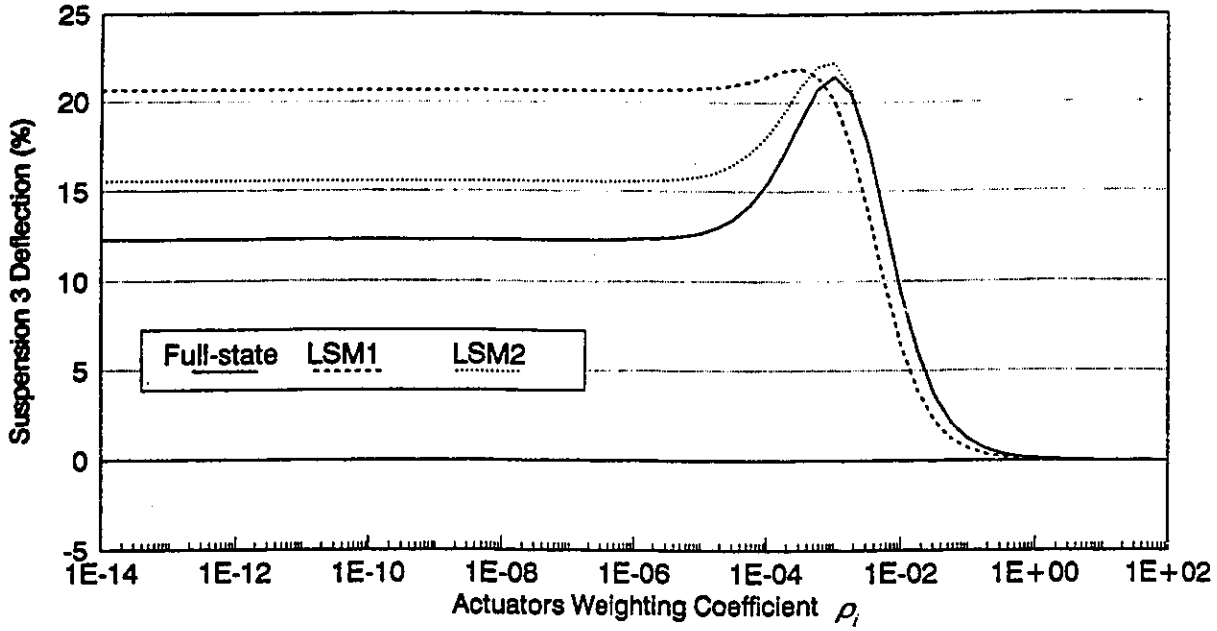

Figure 5.11c Percent improvement(+)/deterioration(-) in mean square of suspension 3 deflection for varying actuators weighting coefficient (compared to passive)

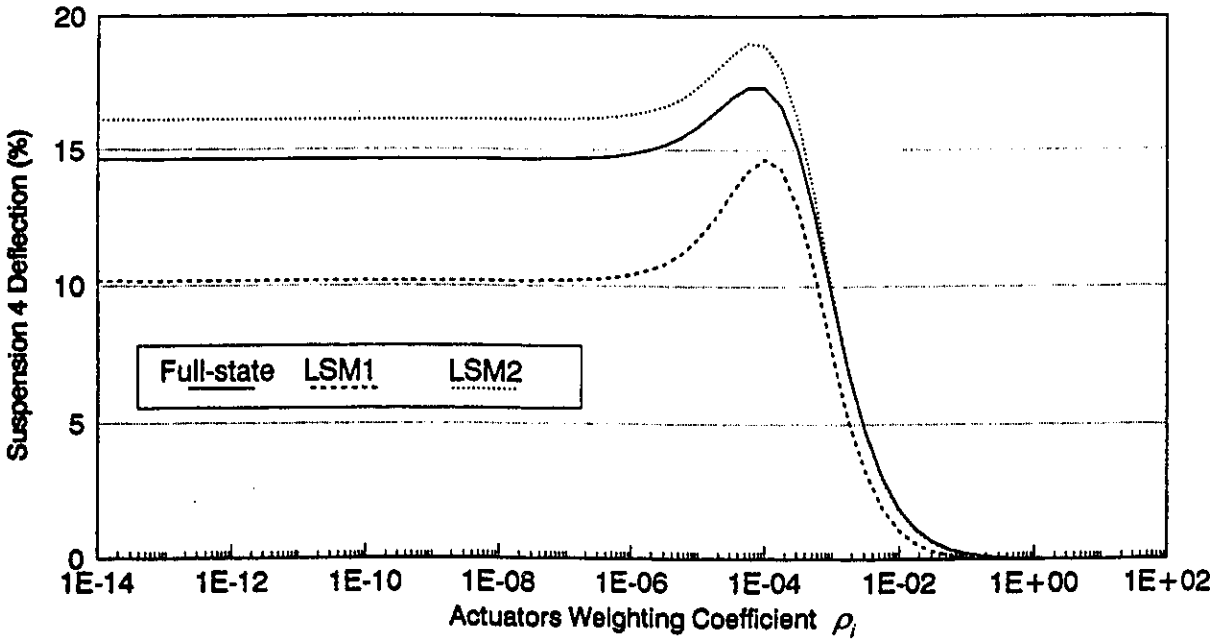

Figure 5.11d Percent improvement(+)/deterioration(-) in mean square of suspension 4 deflection for varying actuators weighting coefficient (compared to passive)

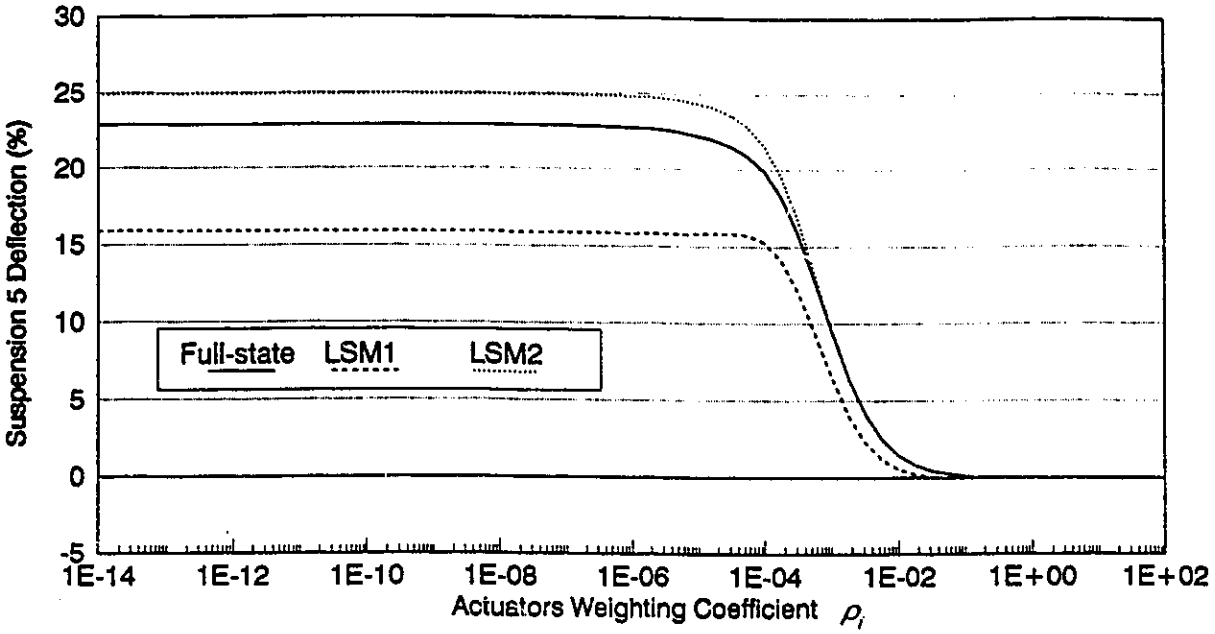

Figure 5.11e Percent improvement(+)/deterioration(-) in mean square of suspension 5 deflection for varying actuators weighting coefficient (compared to passive)

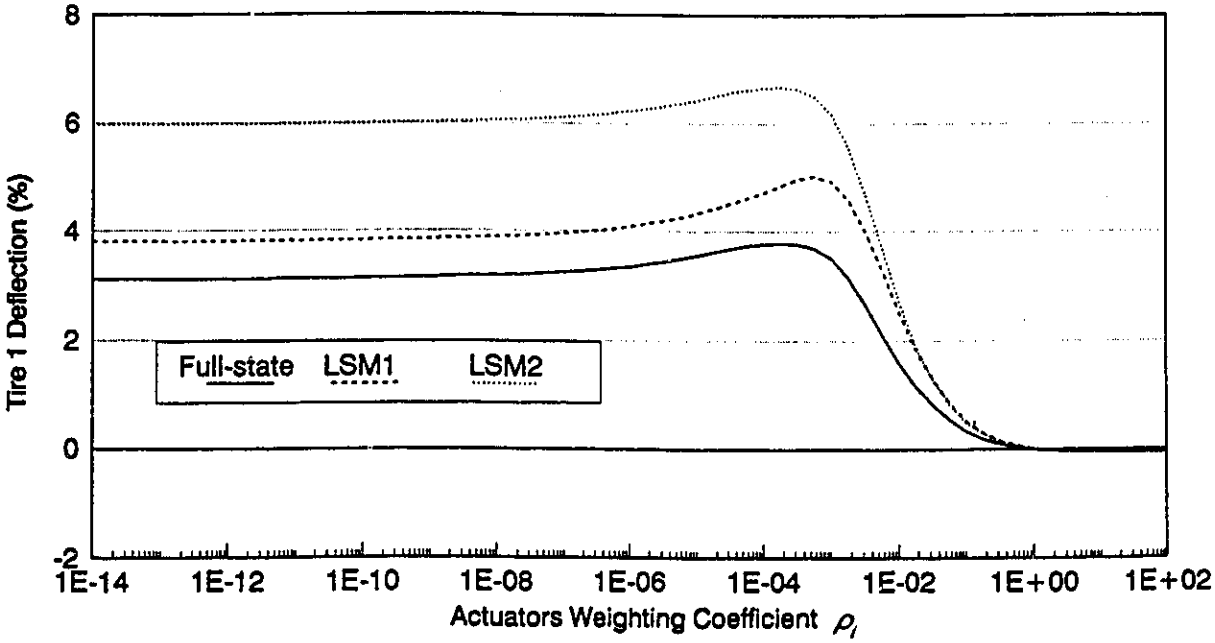

Figure 5.12a Percent improvement(+)/deterioration(-) in mean square of tire 1 deflection for varying actuators weighting coefficient (compared to passive)

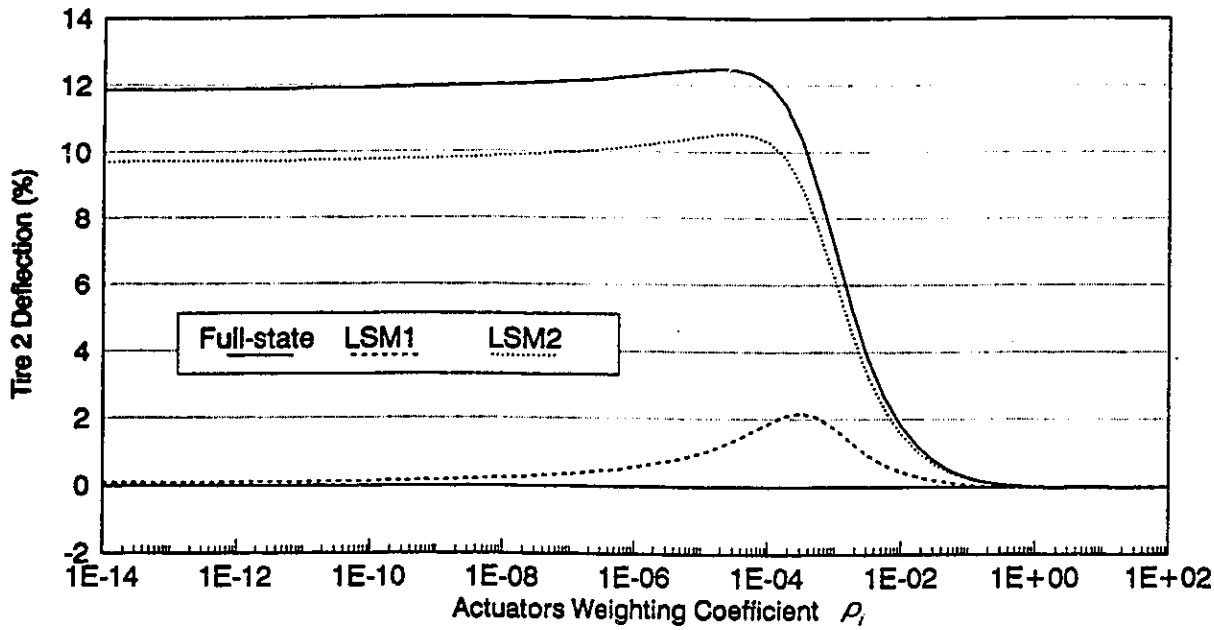

Figure 5.12b Percent improvement(+)/deterioration(-) in mean square of tire 2 deflection for varying actuators weighting coefficient (compared to passive)

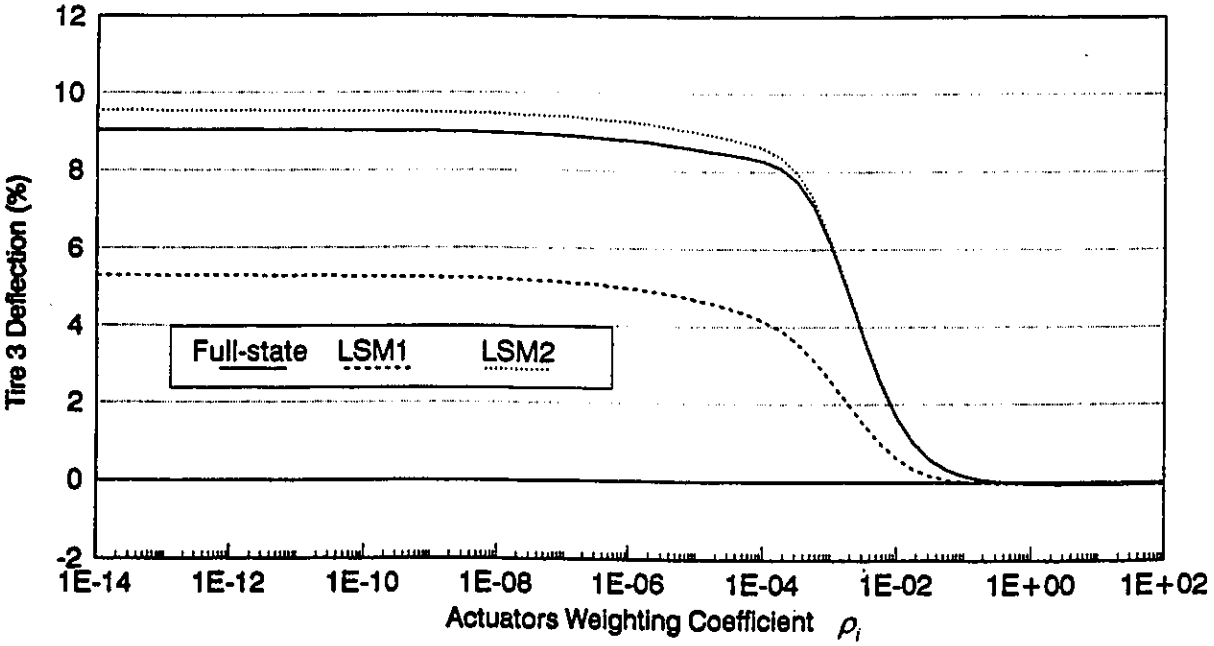

Figure 5.12c Percent improvement(+)/deterioration(-) in mean square of tire 3 deflection for varying actuators weighting coefficient (compared to passive)

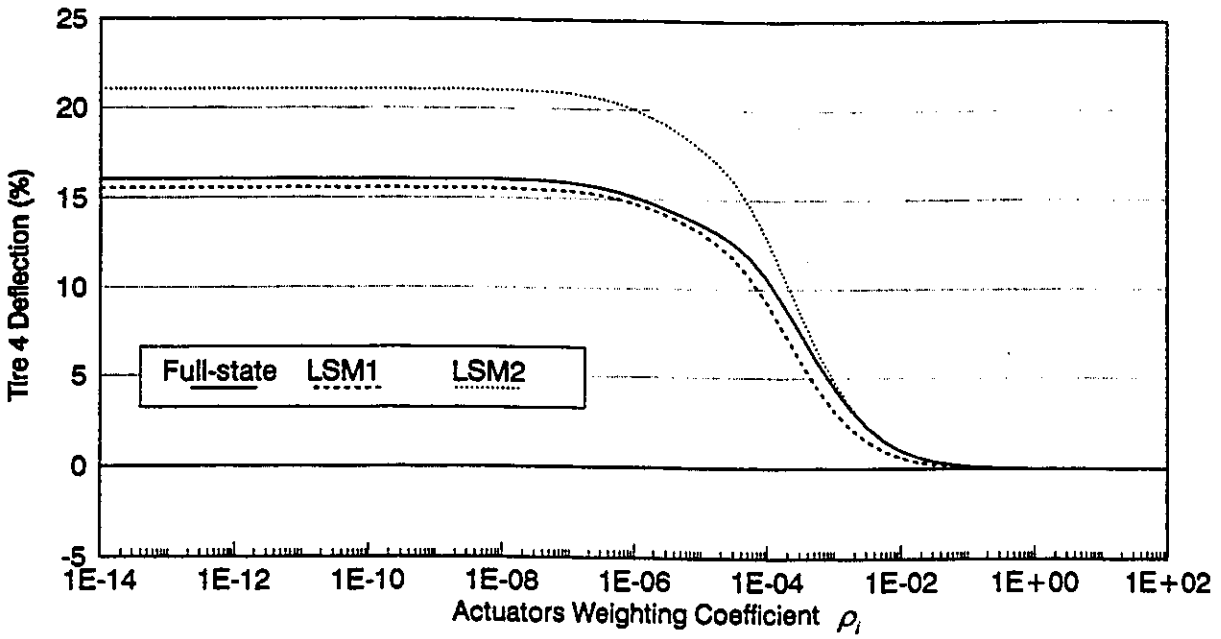

Figure 5.12d Percent improvement(+)/deterioration(-) in mean square of tire 4 deflection for varying actuators weighting coefficient (compared to passive)

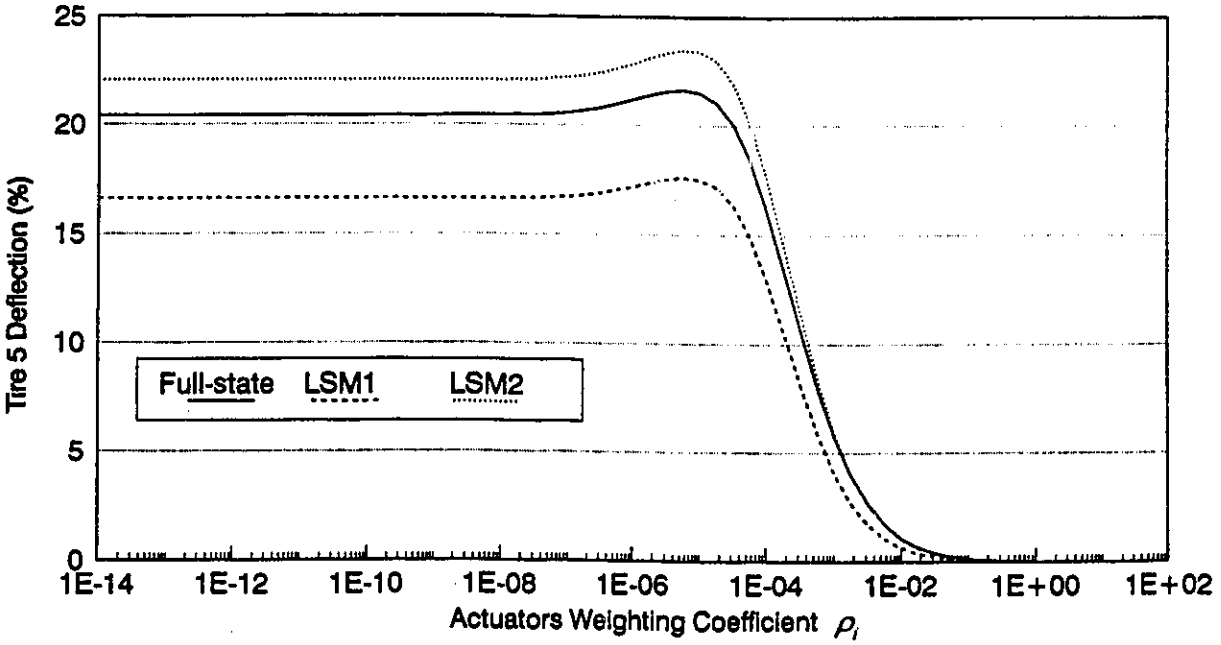

Figure 5.12e Percent improvement(+)/deterioration(-) in mean square of tire 5 deflection for varying actuators weighting coefficient (compared to passive)

The results summarized in Table 5.1 reveal that the *LSM2* suspension scheme, based upon measurement of vertical and pitch acceleration of the sprung masses, yields performance characteristics similar to those of the active suspension based upon full-state measurement. A comparison of the performance characteristics of the three suspension schemes further reveal that the *LSM2* suspension provides superior performance related to suspension and tire deflection, when compared to those of the full-state active suspension. The vertical acceleration response of the vehicle with *LSM2* suspension is quite comparable to that of the full-state active suspension. The *LSM2* suspension, however, yields slightly inferior performance related to semitrailer pitch acceleration, tractor bounce acceleration, deflection response of the front axle suspension, and deflection response of the second axle tire, when compared to that of the full-state active suspension. From the results, it is apparent that *LSM2* suspension based upon the measurement of limited states can provide performance similar to that of the full-state active suspension.

5.5.2 Frequency Response Characteristics of the Vehicle

The response characteristics of the vehicle with limited-state measurements active suspensions, *LSM1* and *LSM2*, are evaluated for random excitations arising from a rough road. EQ (5.48) is solved to derive the frequency spectra of the response characteristics in order to study the resonant behavior and frequency components of the different variants. The response characteristics are compared to those of the full-state feedback active suspensions to demonstrate the effectiveness of the *LSM1* and *LSM2* suspension schemes. The results are further compared to those of the "optimum" passive suspension to illustrate the performance potentials of the active systems. The analyses are performed with actuator weighting coefficients, $\rho_i = 10^{-14}$, and sensor noise intensity, $V_i = 10^{-06}$.

The frequency response spectra of different penalized variables of the active and passive suspensions are presented in terms of their respective *PSD*, as shown in Figures 5.13 to 5.16. The active suspensions effectively suppress the peak vertical acceleration response of the tractor and semitrailer *CG* near the bounce resonance of the vehicle, as shown in Figure 5.13a. The peak vertical acceleration response corresponding to the wheel hop is also somewhat lower than that due to "optimum" passive suspension. Active suspensions also suppress the pitch acceleration response considerably in the vicinity of the respective resonant frequencies, as illustrated in Figures 5.13b and 5.14b. The active suspension systems based upon full-state and only acceleration measurement (*LSM2*) yields considerably superior response characteristics, related to ride quality and cargo safety, when compared to the "optimum" passive and *LSM1* active suspension. The active suspension system based upon *LSM2* scheme yields performance characteristics either similar or superior to the full-state feedback active suspension. The performance characteristics, related to ride quality and cargo safety, of the *LSM1* suspension, however, are considerably inferior to the *LSM2* and full-state active suspensions.

All the active suspension schemes considered in this study yield considerable reduction in the dynamic deflection response of the suspensions in the vicinity of the respective sprung mass resonant frequencies, as shown in Figure 5.15. The suspension deflection response of the active suspensions to excitation frequencies above 3 Hz approaches that of the optimum passive suspension. Active suspensions based upon the *LSM1* scheme yields lowest peak deflection response of the of drive axle suspensions, while the *LSM2* scheme yields lowest peak deflection response of semitrailer axle suspensions. The performance characteristics related to suspension rattle space requirements of the *LSM2* suspension are quite similar to those of the full-state active suspension, and considerably superior to those of the "optimum" passive suspension.

Figure 5.16 illustrate a comparison of the response spectra of the tire forces of the vehicle with "optimum" passive and different active suspension systems. Vehicle with "optimum" passive suspension results in peak tire forces near the resonant frequencies of the sprung and unsprung masses. Vehicle with active suspension exhibits peak tire frequencies slightly higher than those observed for the passive suspension. Active suspensions, however, result in significant reduction in the magnitude of peak tire forces corresponding to sprung masses resonant frequencies. The *LSM2* active suspension based upon measurement of sprung mass accelerations yield lowest tire forces, as shown in the figures.

The results presented in Figures 5.13 to 5.16 reveal that the early conclusions based on the expected values hold, and an active suspension that satisfies all the performance criteria is possible. A suspension based on full-state or acceleration-only measurements (*LSM2*) improves the tractor and semitrailer response, and reduces the tire forces throughout most of the frequency range. The major drawback of these schemes is the high rattle space requirements at low frequencies as shown in Figure 5.15. A suspension based on relative velocity and displacement measurements (*LSM1*) offers a better rattle space control, when compared to the other schemes. Although remaining superior to a passive suspension, *LSM1* results in certain deterioration in the tractor and semitrailer acceleration, and tire force response, as shown in Figures 5.13, 5.14 and 5.16.

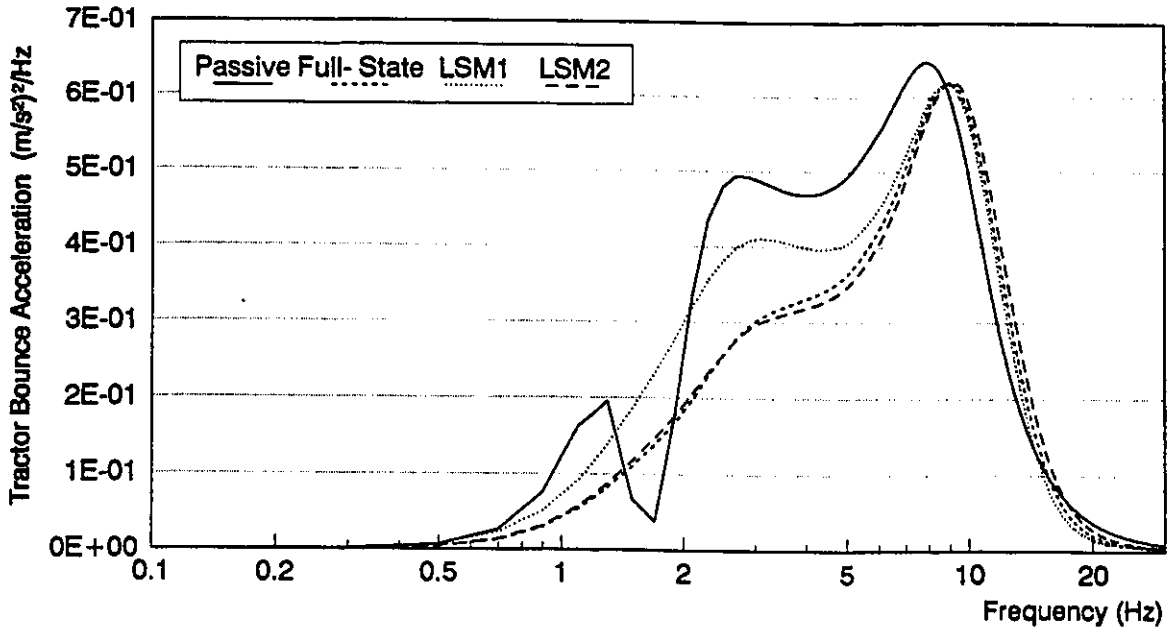

Figure 5.13a PSD of tractor bounce acceleration for passive and active systems

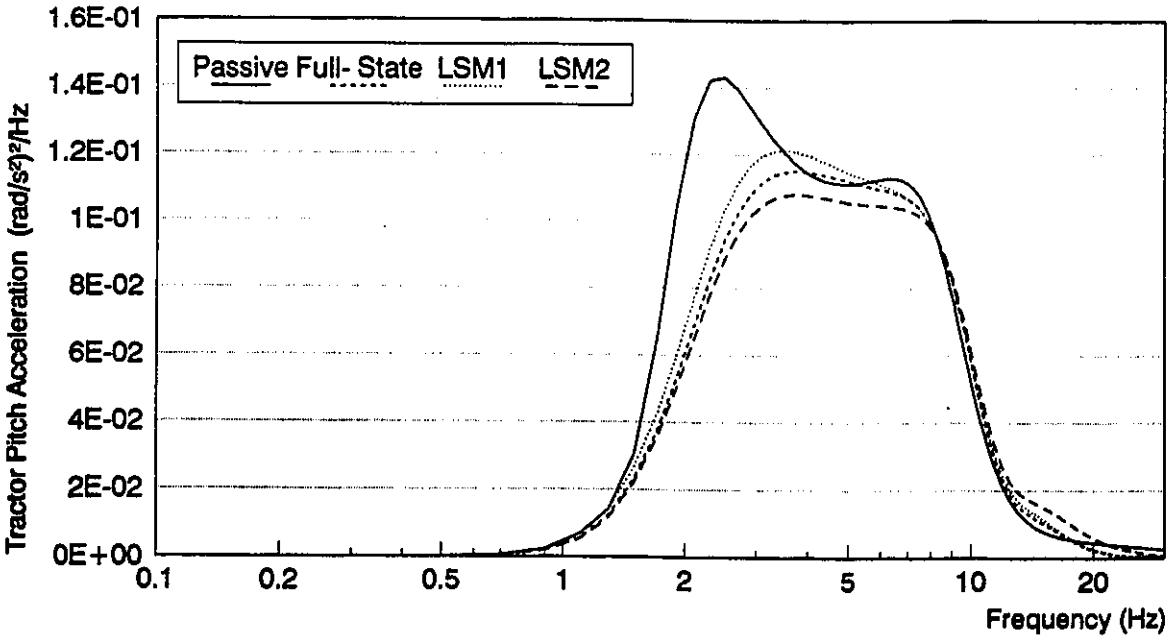

Figure 5.13b PSD of tractor pitch acceleration for passive and active systems

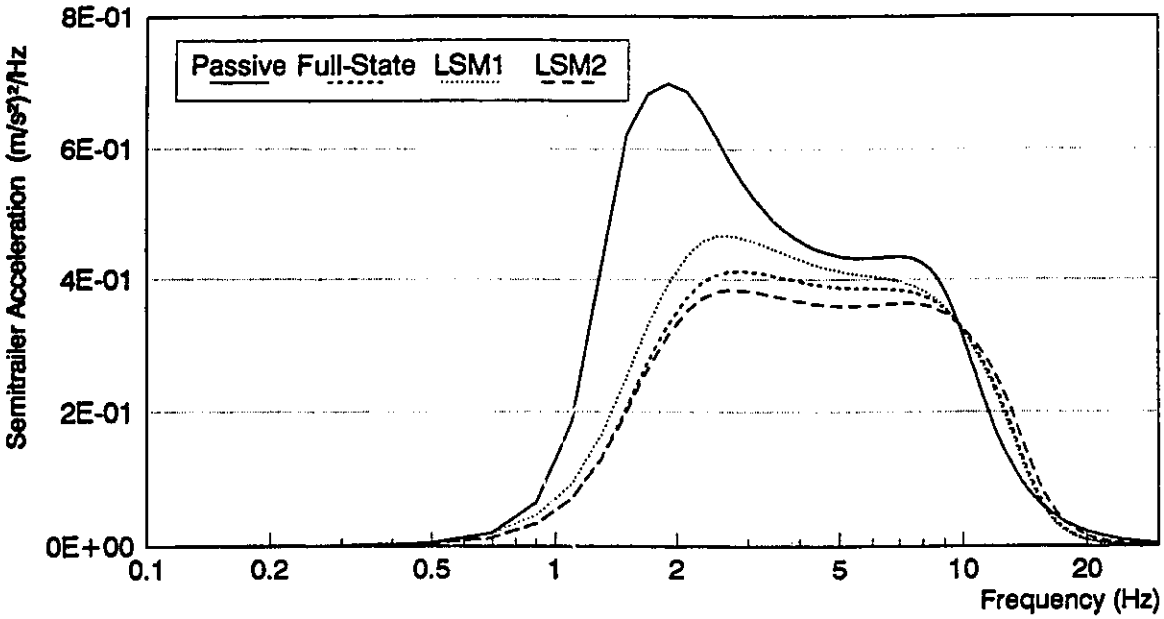

Figure 5.14a PSD of semitrailer bounce acceleration for passive and active systems

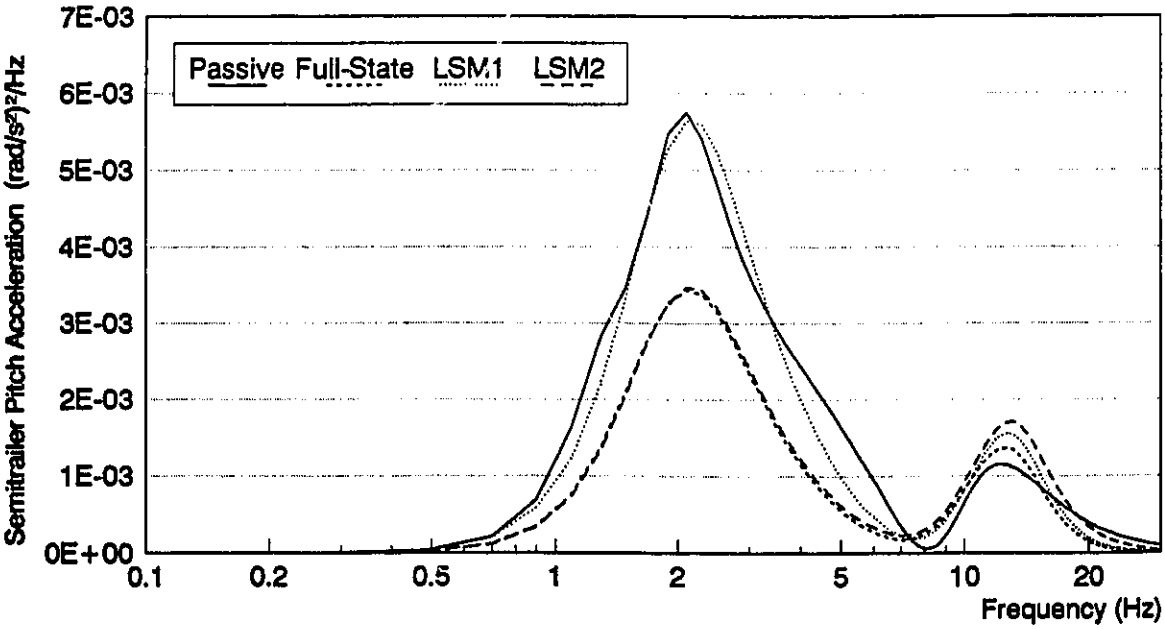

Figure 5.14b PSD of semitrailer pitch acceleration for passive and active systems

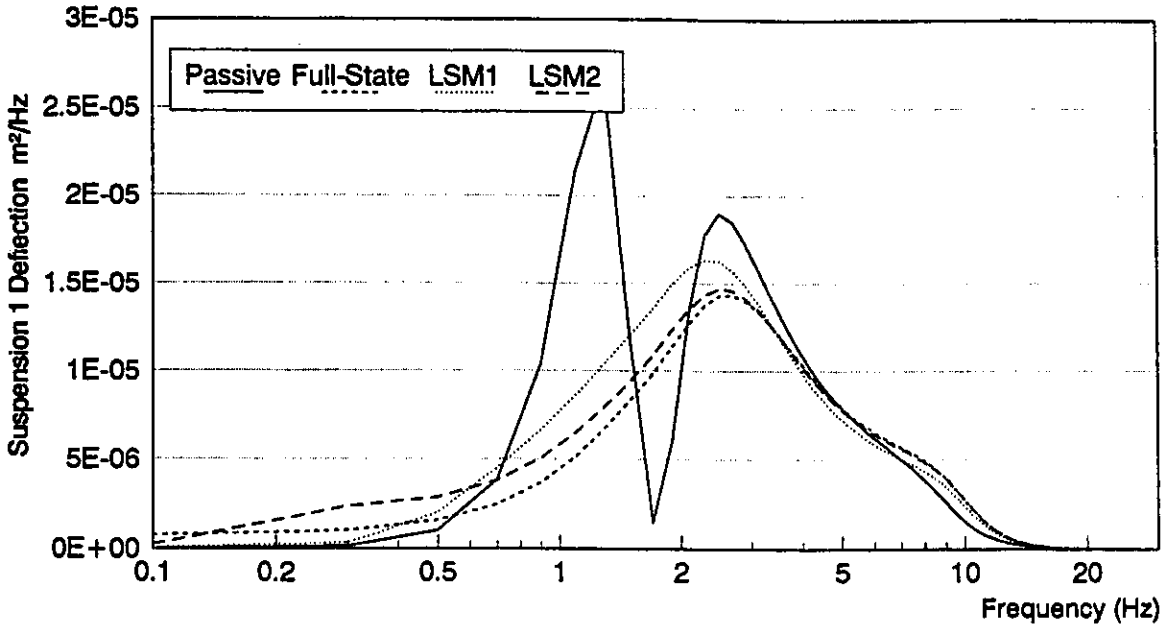

Figure 5.15a PSD of suspension 1 deflection for passive and active systems

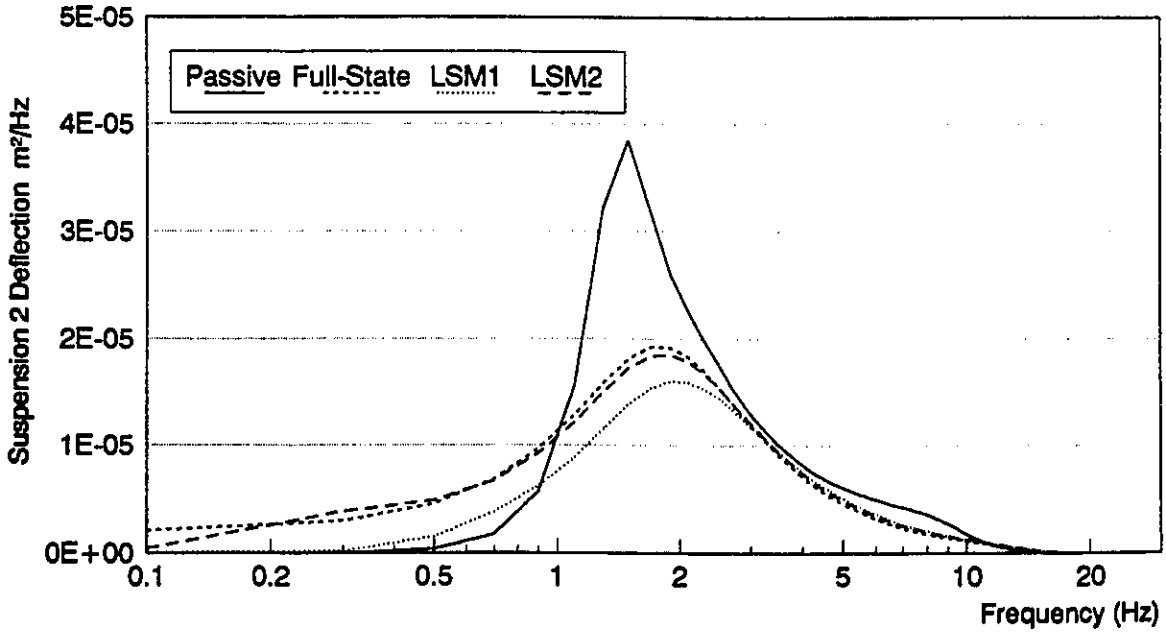

Figure 5.15b PSD of suspension 2 deflection for passive and active systems

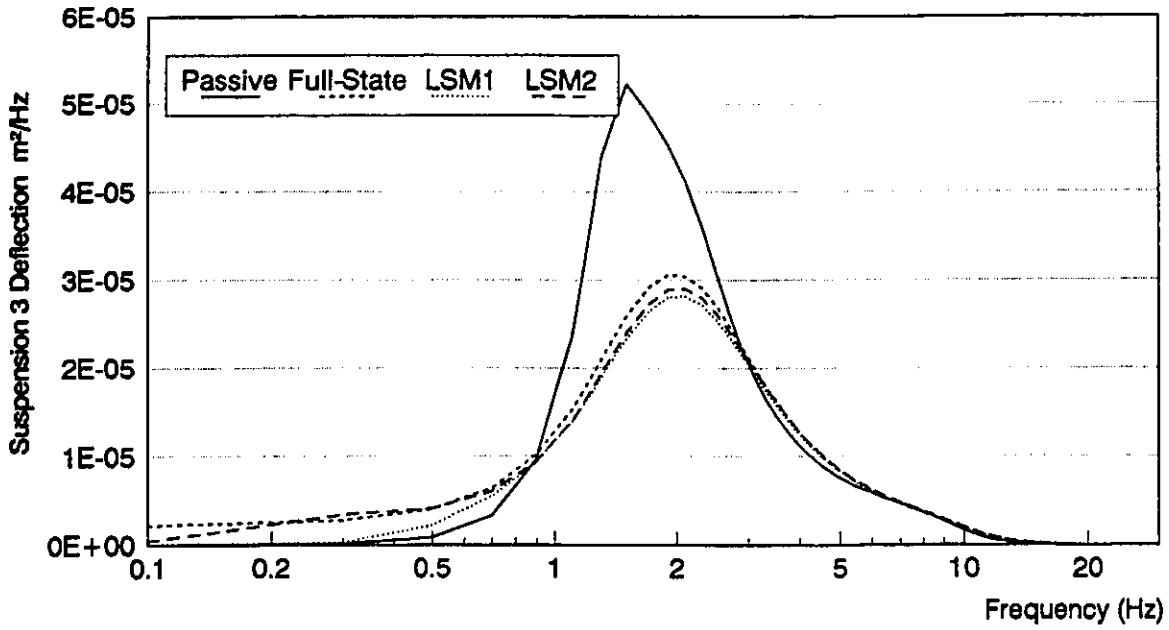

Figure 5.15c PSD of suspension 3 deflection for passive and active systems

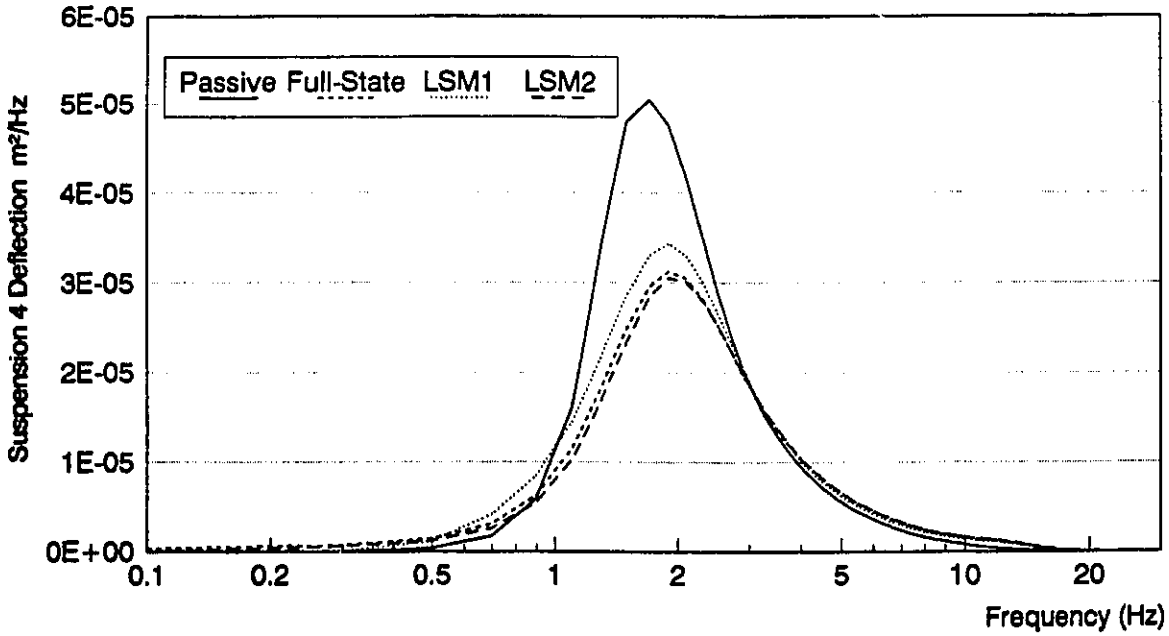

Figure 5.15d PSD of suspension 4 deflection for passive and active systems

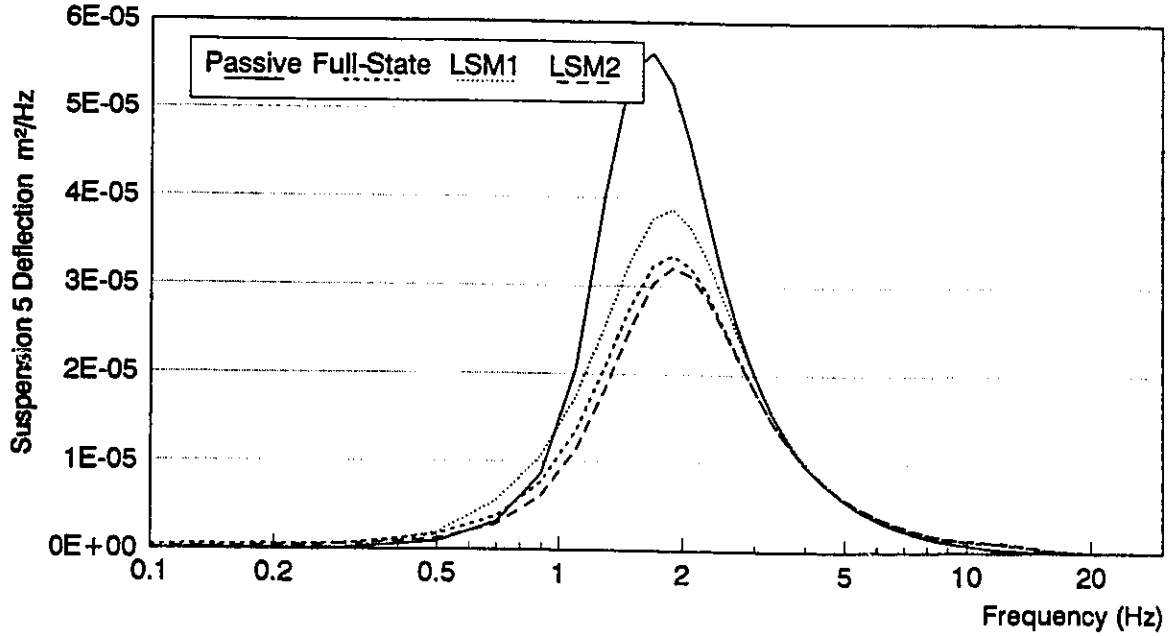

Figure 5.15e PSD of suspension 5 deflection for passive and active systems

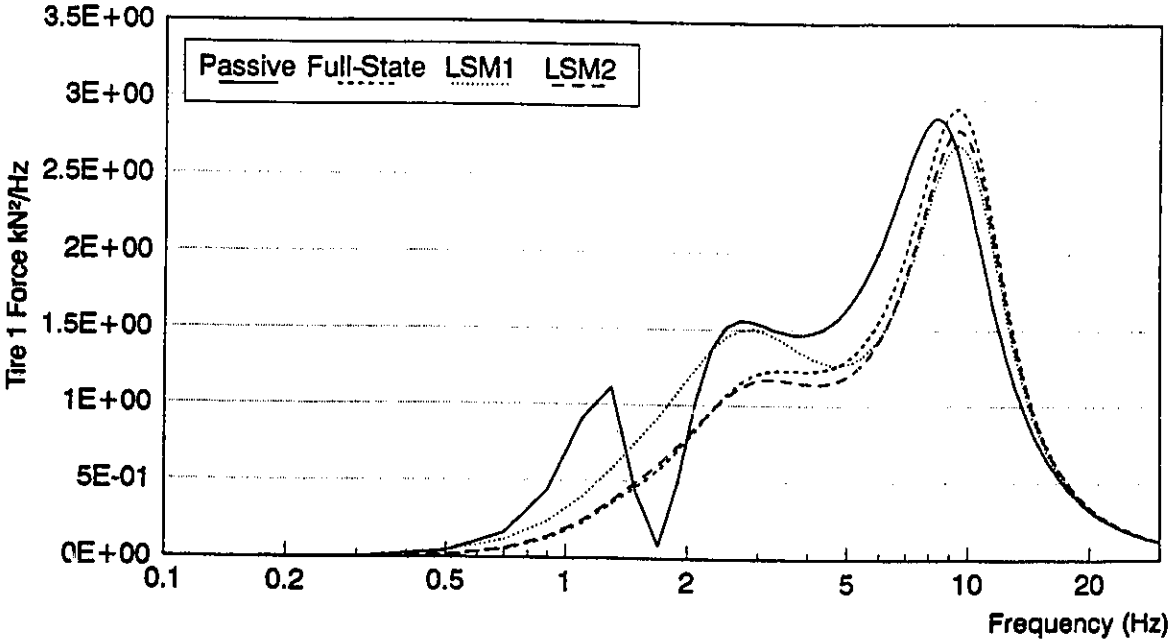

Figure 5.16a PSD of tire 1 force for passive and active systems

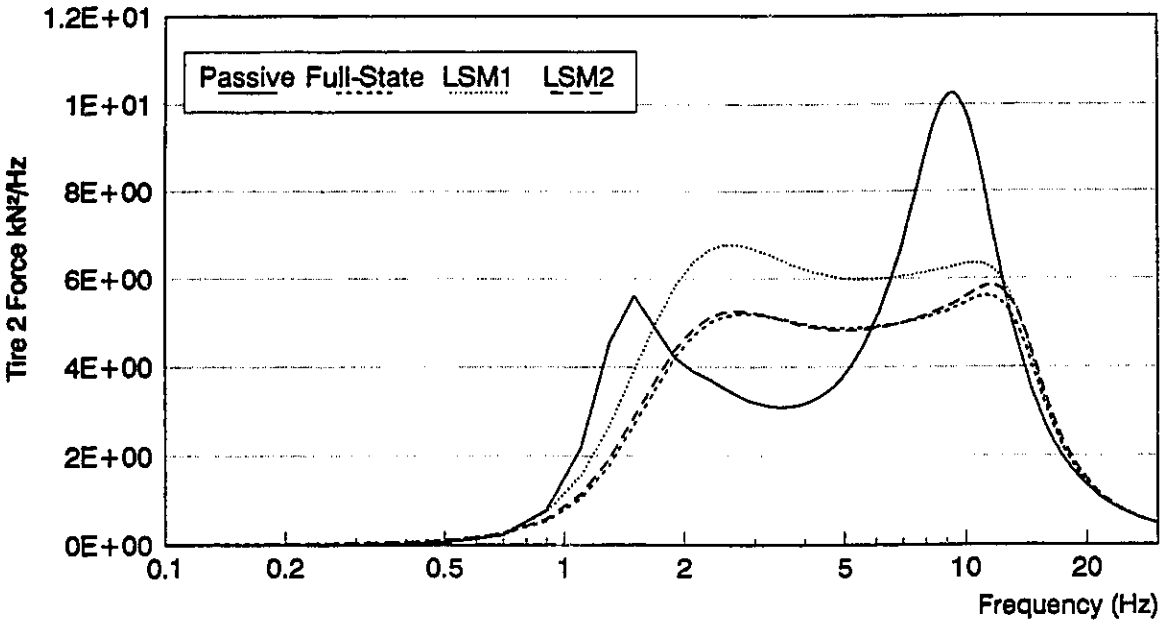

Figure 5.16b PSD of tire 2 force for passive and active systems

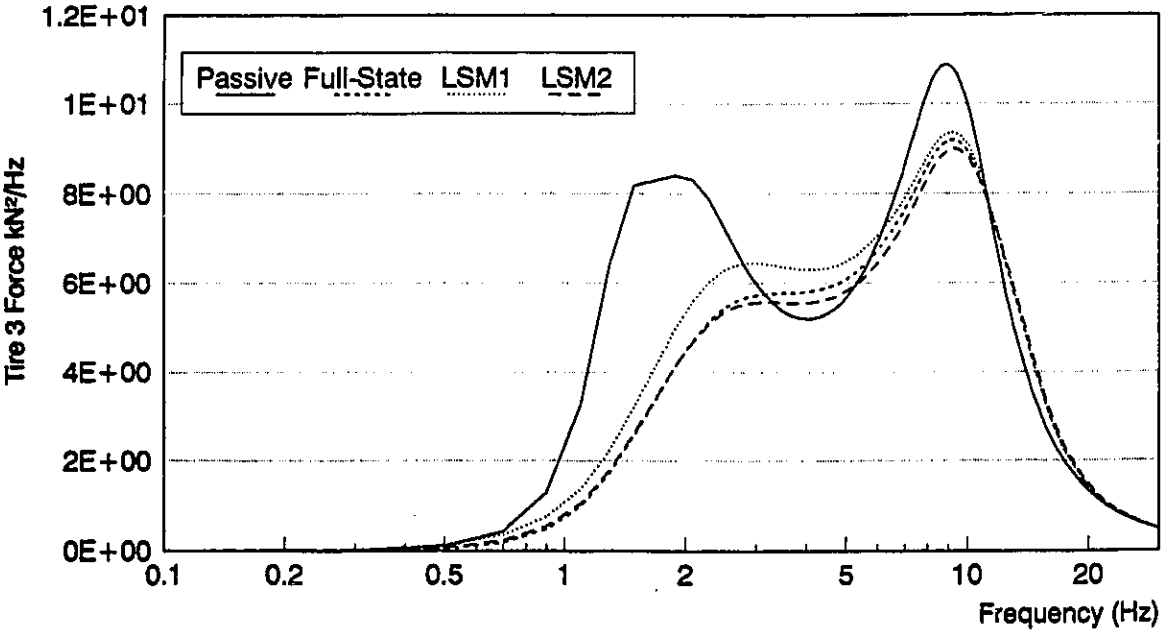

Figure 5.16c PSD of tire 3 force for passive and active systems

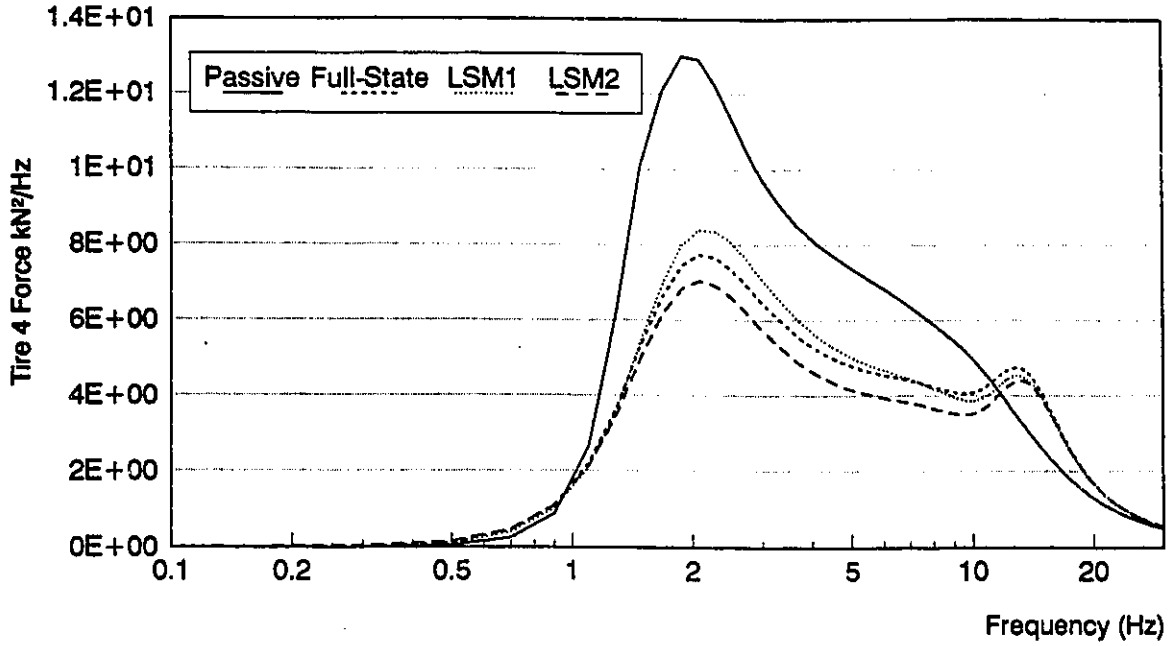

Figure 5.16d PSD of tire 4 force for passive and active systems

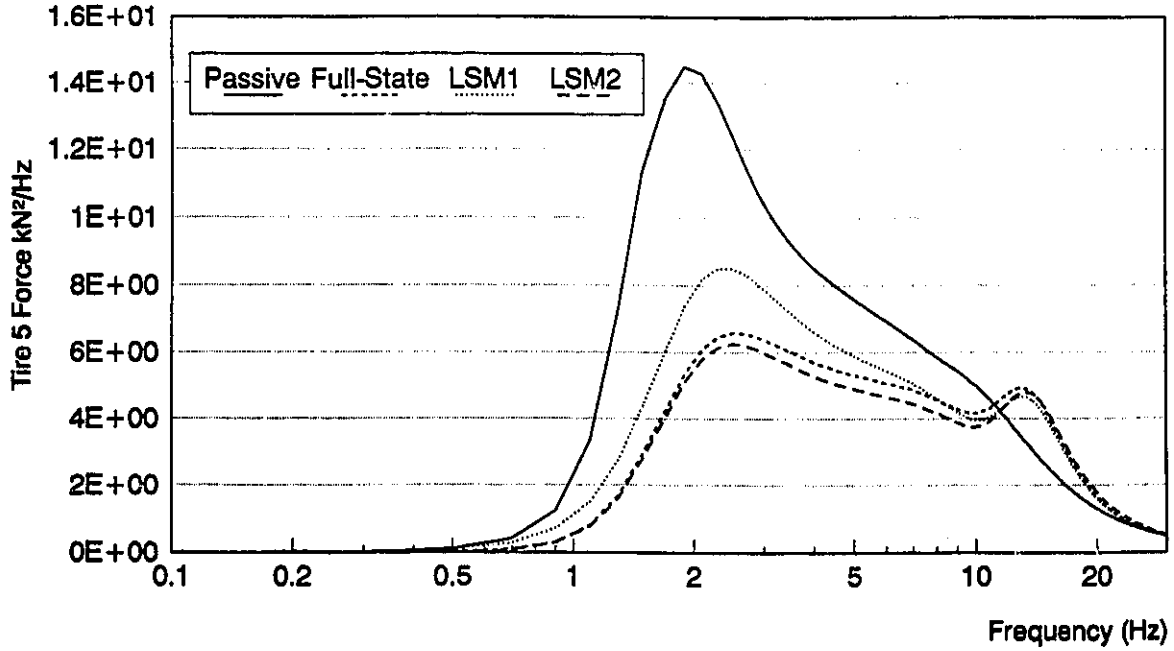

Figure 5.16e PSD of tire 5 force for passive and active systems

5.5.3 Influence of Vehicle Speed on Active Suspension Performance

The control gains for the active suspensions are optimized for a vehicle traveling at a speed of 90 *km/h*. The influence of variations in vehicle speed on the performance components is investigated to determine the effectiveness of the control gains in the entire speed range. The active suspensions based on full-state measurements, relative velocity and displacement measurements (*LSM1*) or acceleration measurements (*LSM2*) are designed at a vehicle speed of 90 *km/h* and the resulting control gain matrices are used to compute the performance variants corresponding to different operating speeds in the 10-120 *km/h* range.

Figures 5.17 to 5.20 illustrate the mean square vertical and pitch acceleration response of the tractor and semitrailer sprung masses as a function of the vehicle speed. The mean square responses increases with increase in vehicle speed irrespective of the suspension system. The full-state, *LSM1* and *LSM2* suspensions yield improved vertical acceleration response of both sprung masses. The tractor pitch response of the active suspensions is lower than that of the passive suspension in almost the entire speed range. The passive suspension, however, yields superior semitrailer pitch response at speeds below 60 *km/h*. The active suspensions based upon full-state and *LSM2* schemes yield important vertical and pitch acceleration performance at higher speeds when compared to the response behavior of passive and *LSM1* active suspensions.

Based on the mean square values, the three active suspension schemes are guaranteed to offer improved tractor bounce and pitch and semitrailer bounce throughout the vehicle speed range. The semitrailer pitch performance, however, is compromised at low speeds for *LSM1* (below 80 *km/h*) and for *LSM2* (below 60 *km/h*) as shown in Figure 5.18b. Similarly, the rattle space requirements are higher for these two schemes at low

speeds as shown in Figure 5.19. The active suspension systems based upon full-state, *LSM1* and *LSM2* schemes yield reduced tire forces throughout the speed range, as shown in Figure 5.20. Generally, the performance of the active suspensions compared to the optimum passive suspension is enhanced as the vehicle speed increases and thus these active systems would be more beneficial at highway speeds.

5.5.4 Influence of Road Roughness on Suspensions Performance

Active suspension designed for specific road profiles are known to provide best performance for excitations arising from roads with similar profiles. The performance characteristics are known to vary with the road roughness. In this study, the control gains for the active suspensions were selected for excitations arising from a rough road. The performance characteristics of the selected suspension systems are further evaluated for varying road profiles to study the effectiveness of the active suspension systems. The components of the performance index are evaluated for three types of roads (asphalt, concrete and rough roads). The results are presented in terms of percent improvement(+) or percent deterioration (-) in the mean square values of the penalized variables with reference to those of the "optimum" passive suspension.

Figures 5.21 to 5.30 illustrate the relative performance characteristics of three active suspension schemes for excitations arising from three different roads. The results clearly reveal that active suspensions offer definite improvement in all the components of the performance index irrespective of pavement roughness. For the three types of roads, *LSM1* seems most suited for reducing the rattle space requirements at the expanse of higher tire forces. Using acceleration measurements (*LSM2*) it is possible to achieve a performance close to that of a suspension based on full-state measurements, irrespective of the road roughness.

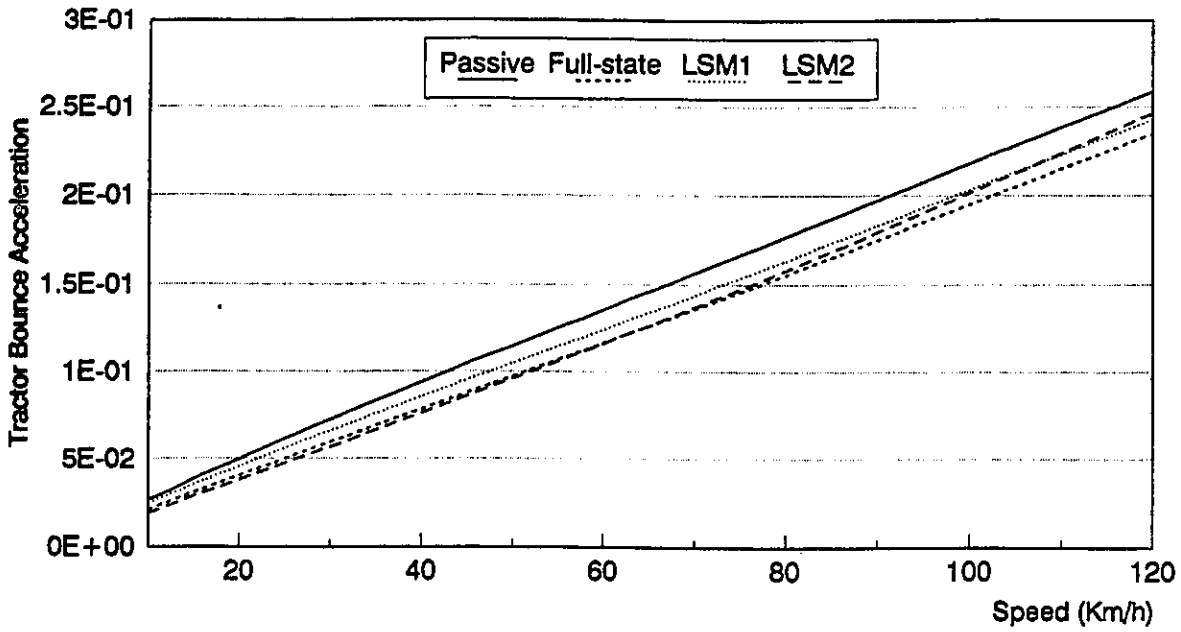

Figure 5.17a Effect of vehicle speed on mean square of tractor bounce acceleration for passive and active systems

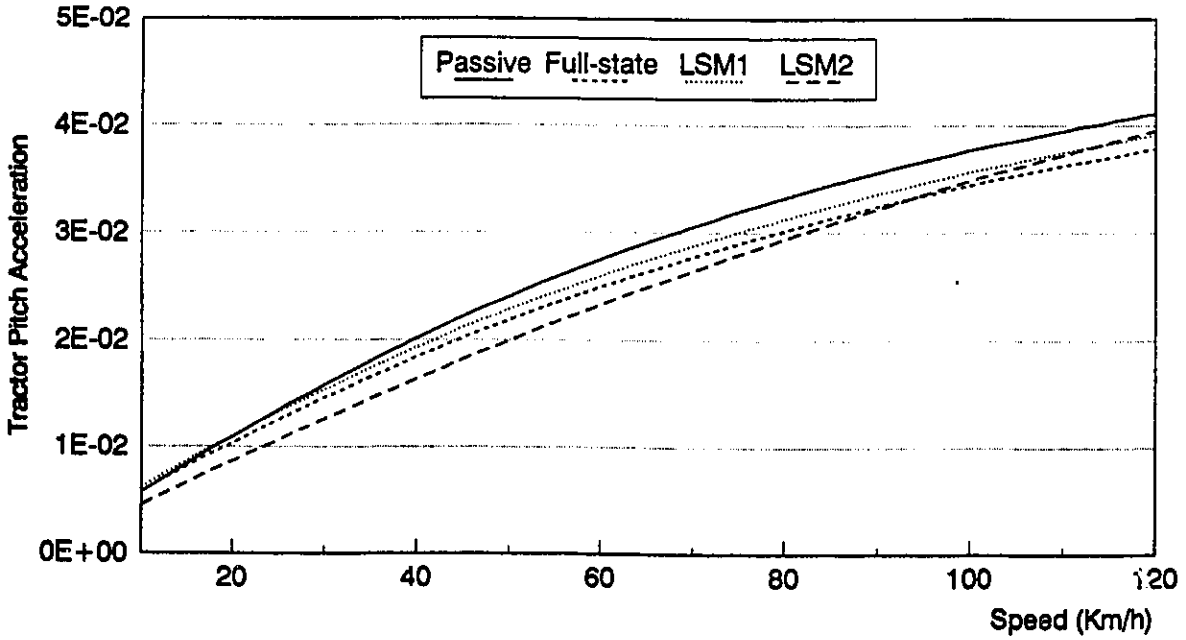

Figure 5.17b Effect of vehicle speed on mean square of tractor pitch acceleration for passive and active systems

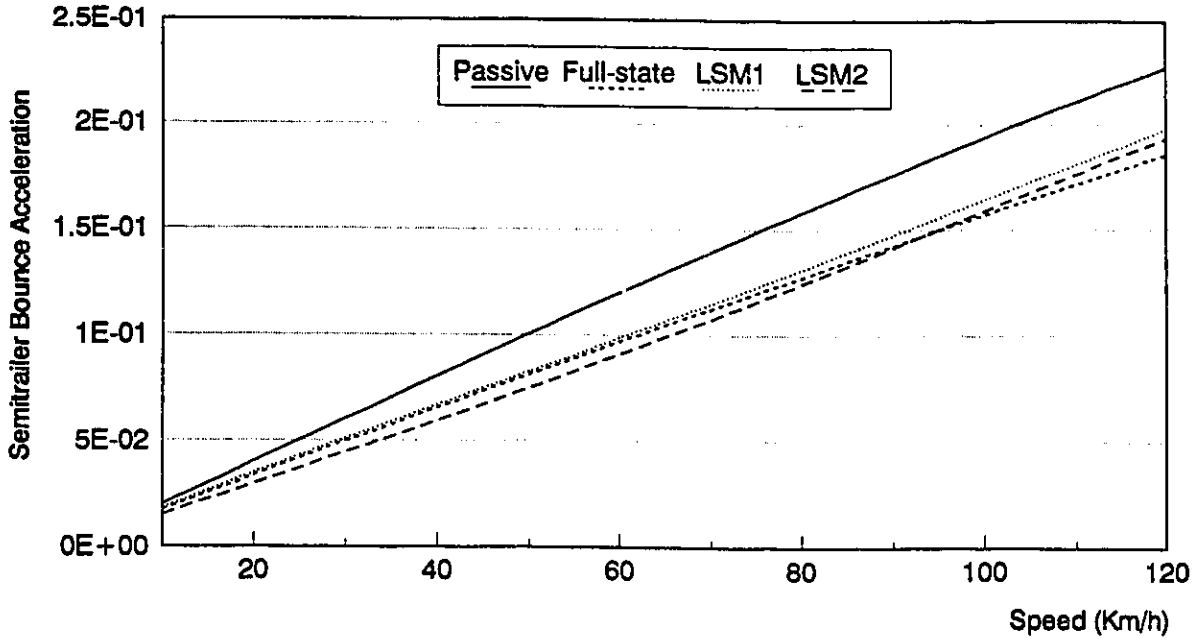

Figure 5.18a Effect of vehicle speed on mean square of semitrailer bounce acceleration for passive and active systems

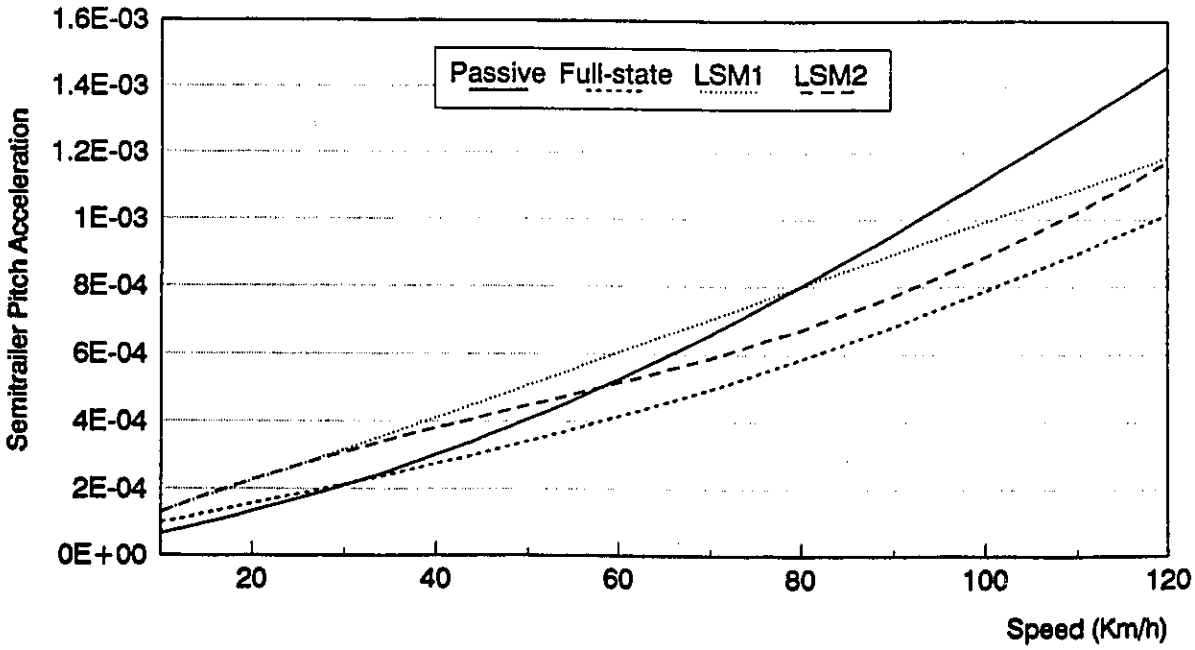

Figure 5.18b Effect of vehicle speed on mean square of semitrailer pitch acceleration for passive and active systems

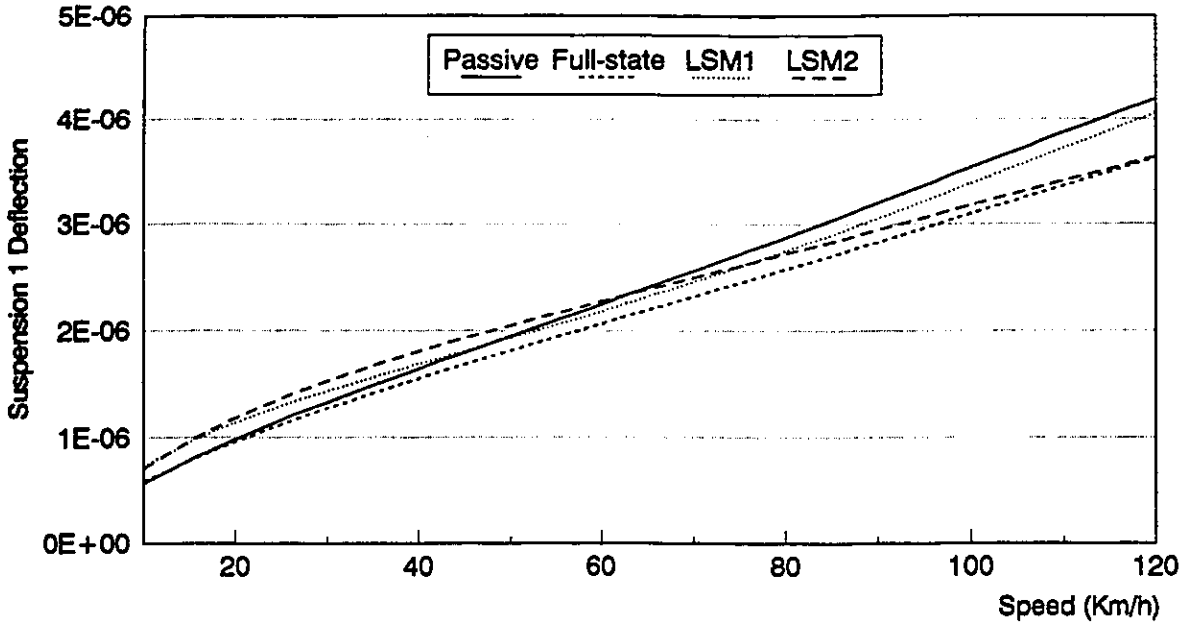

Figure 5.19a Effect of vehicle speed on mean square of suspension 1 deflection for passive and active systems

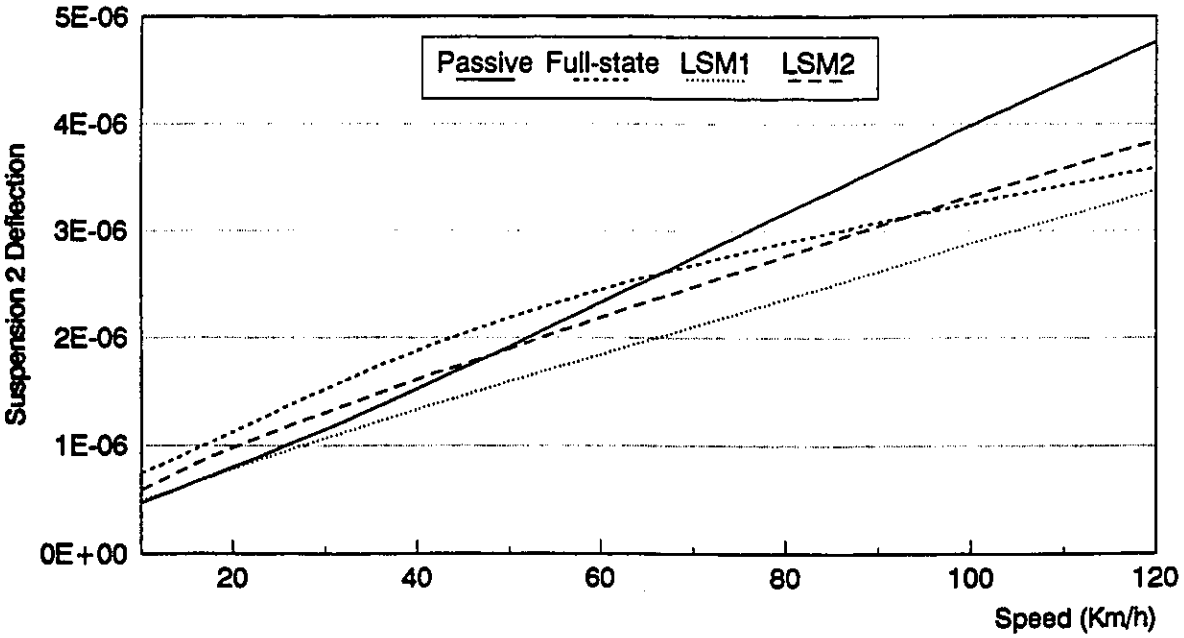

Figure 5.19b Effect of vehicle speed on mean square of suspension 2 deflection for passive and active systems

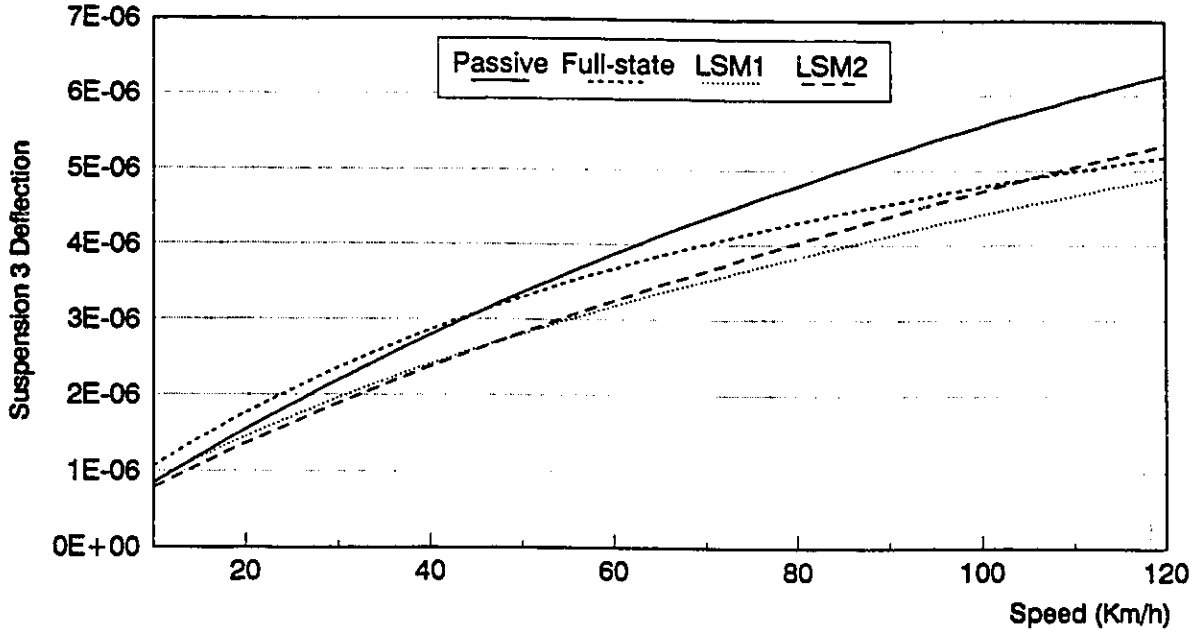

Figure 5.19c Effect of vehicle speed on mean square of suspension 3 deflection for passive and active systems

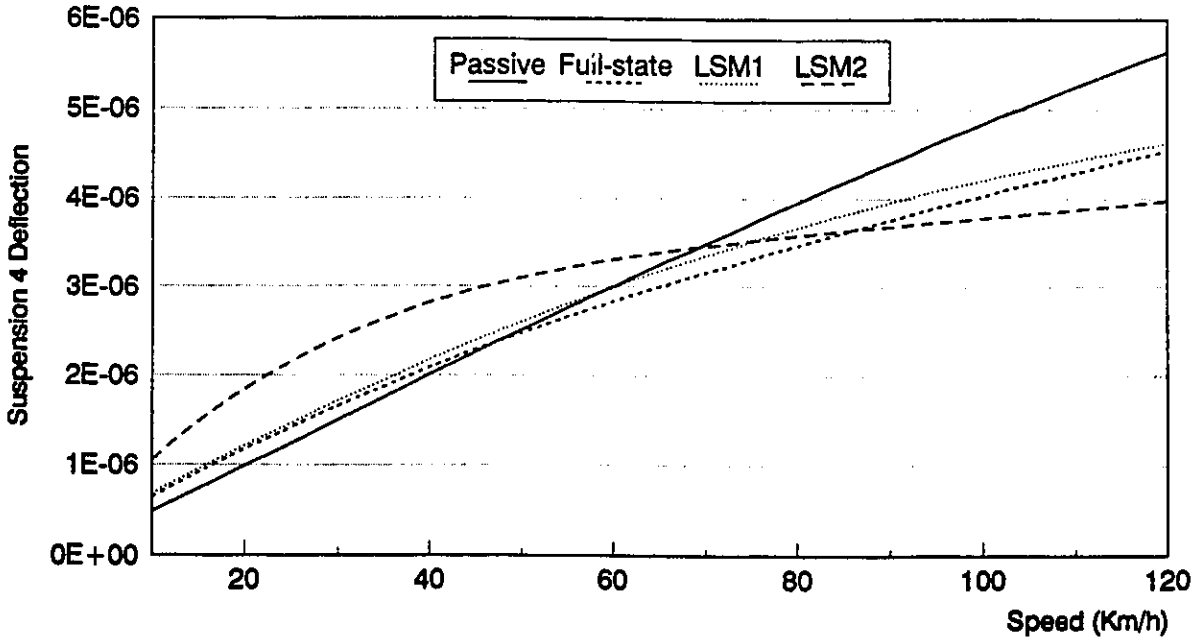

Figure 5.19d Effect of vehicle speed on mean square of suspension 4 deflection for passive and active systems

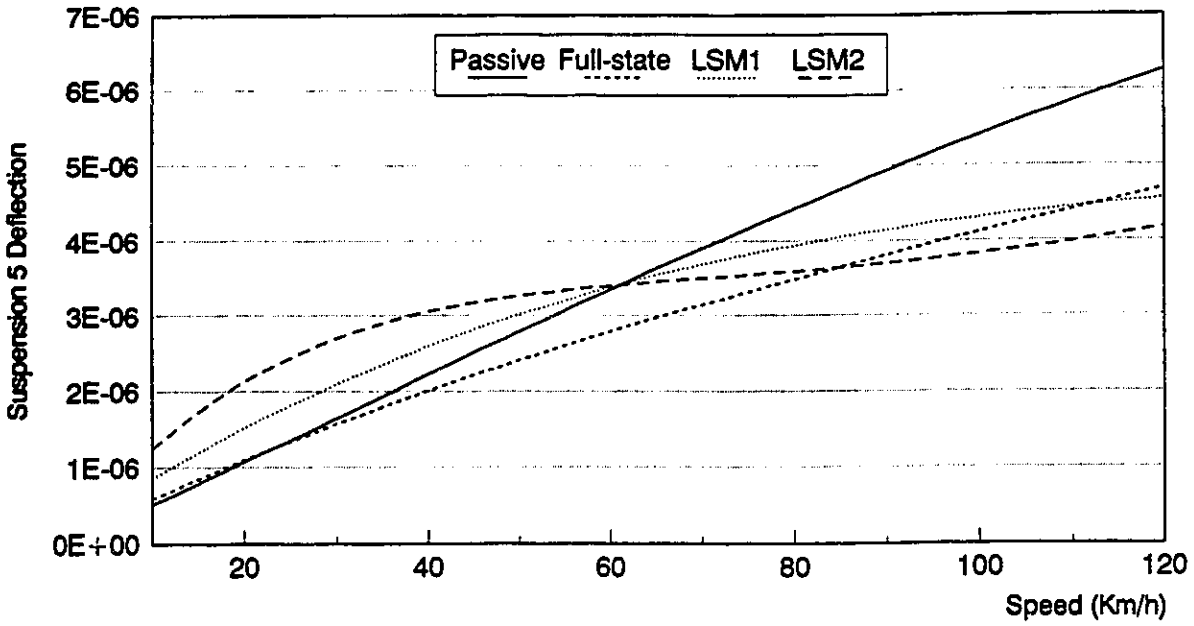

Figure 5.19e Effect of vehicle speed on mean square of suspension 5 deflection for passive and active systems

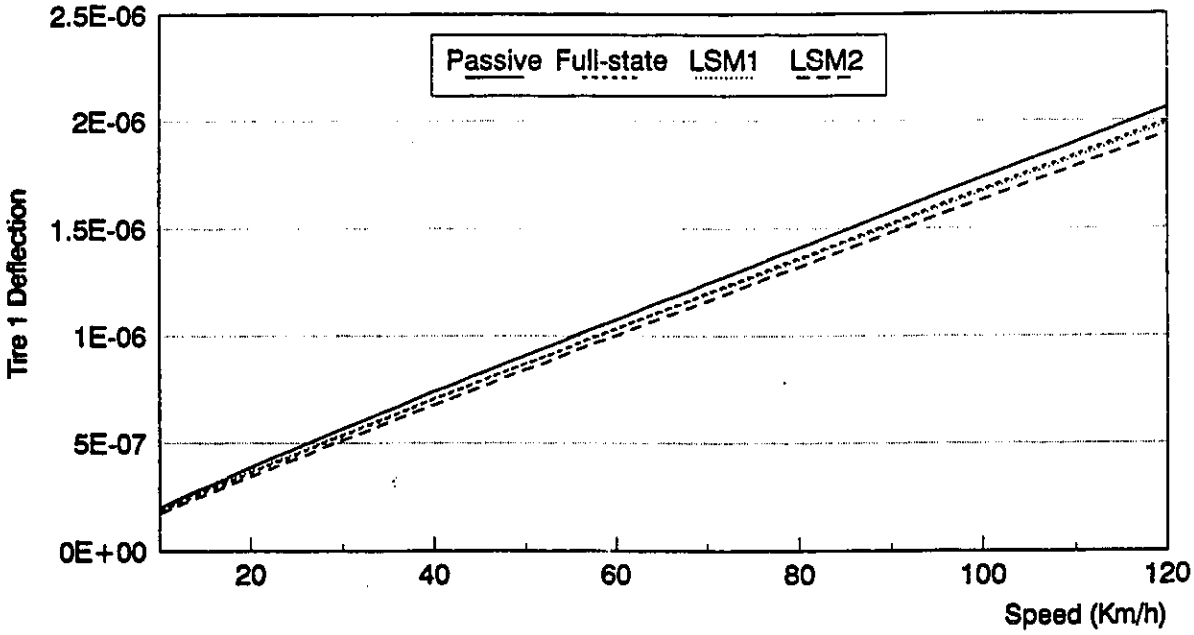

Figure 5.20a Effect of vehicle speed on mean square of tire 1 deflection for passive and active systems

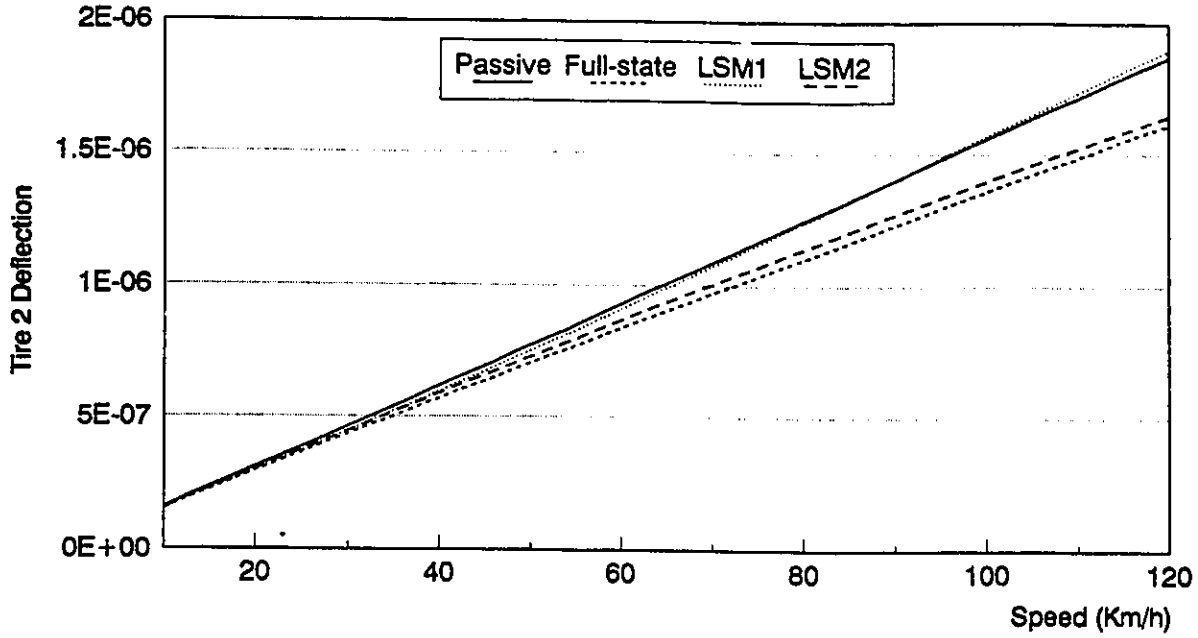

Figure 5.20b Effect of vehicle speed on mean square of tire 2 deflection for passive and active systems

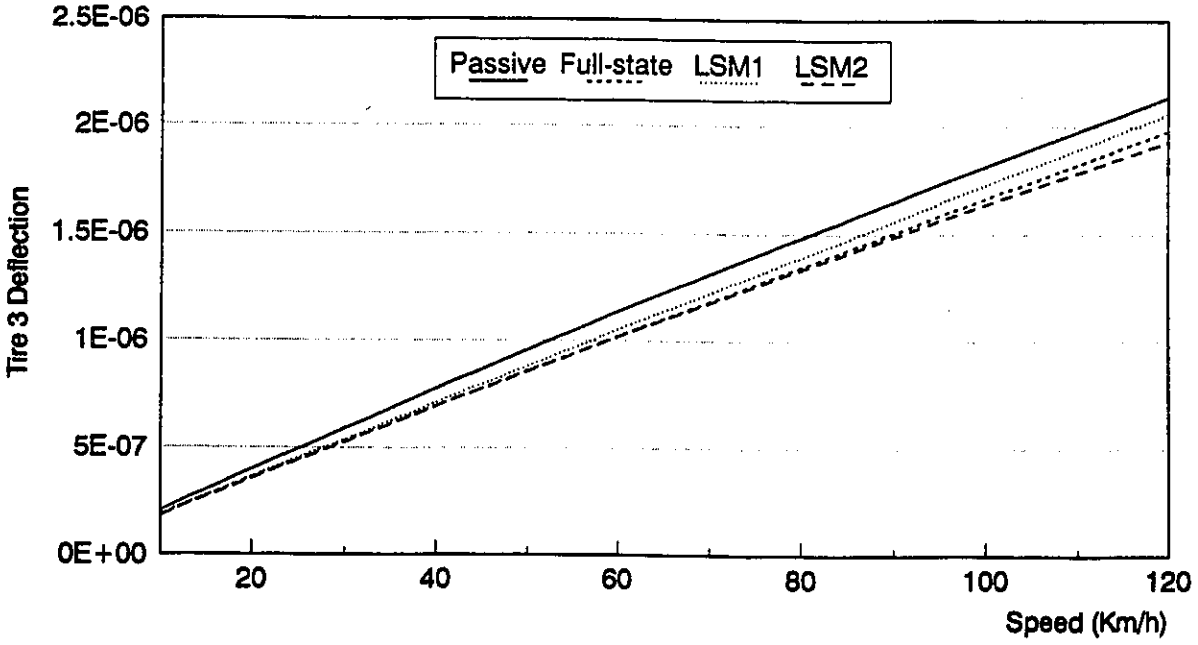

Figure 5.20c Effect of vehicle speed on mean square of tire 3 deflection for passive and active systems

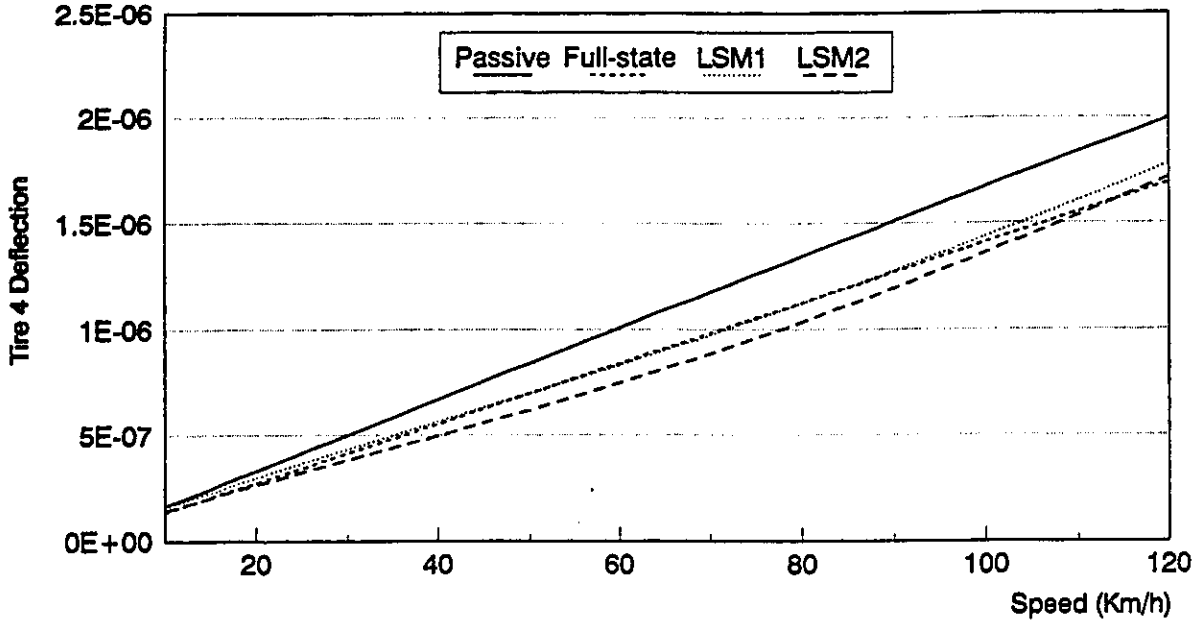

Figure 5.20d Effect of vehicle speed on mean square of tire 4 deflection for passive and active systems

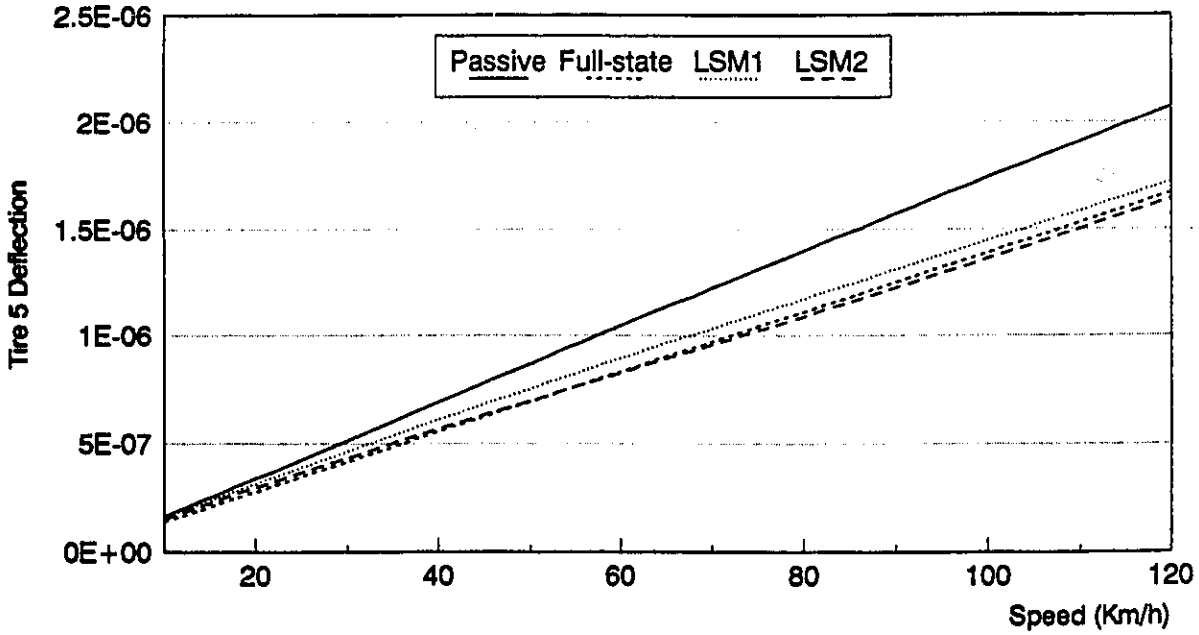

Figure 5.20e Effect of vehicle speed on mean square of tire 5 deflection for passive and active systems

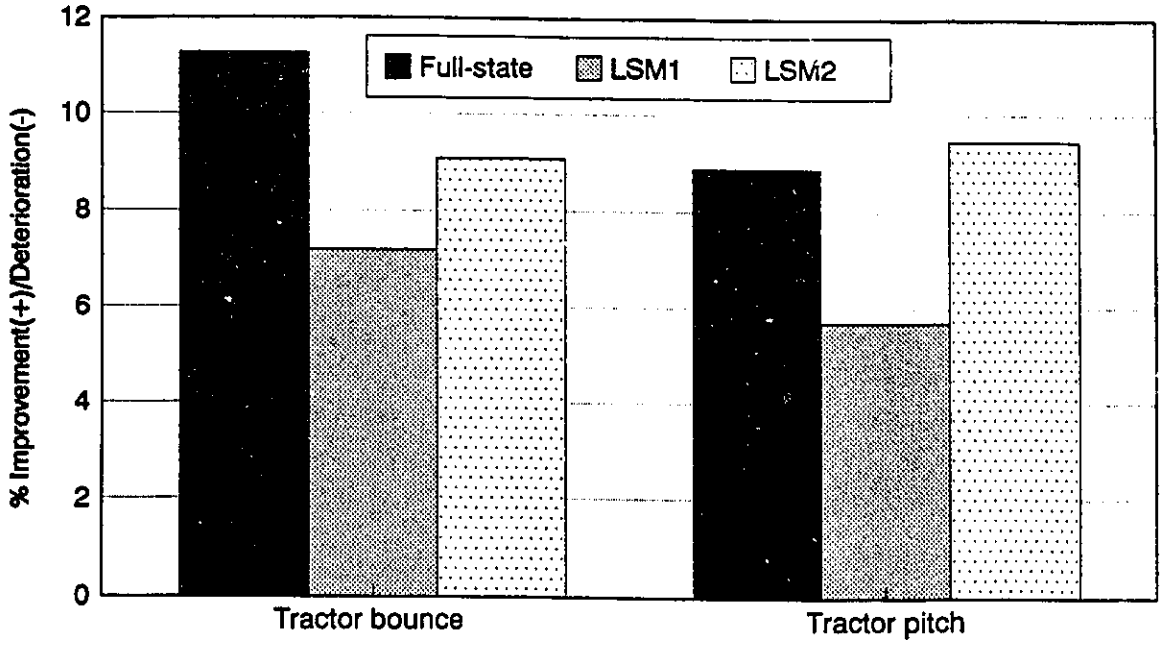

Figure 5.21 Percent improvement(+)/deteriration(-) in the mean square of tractor bounce and pitch accelerations (compared to passive; smooth road)

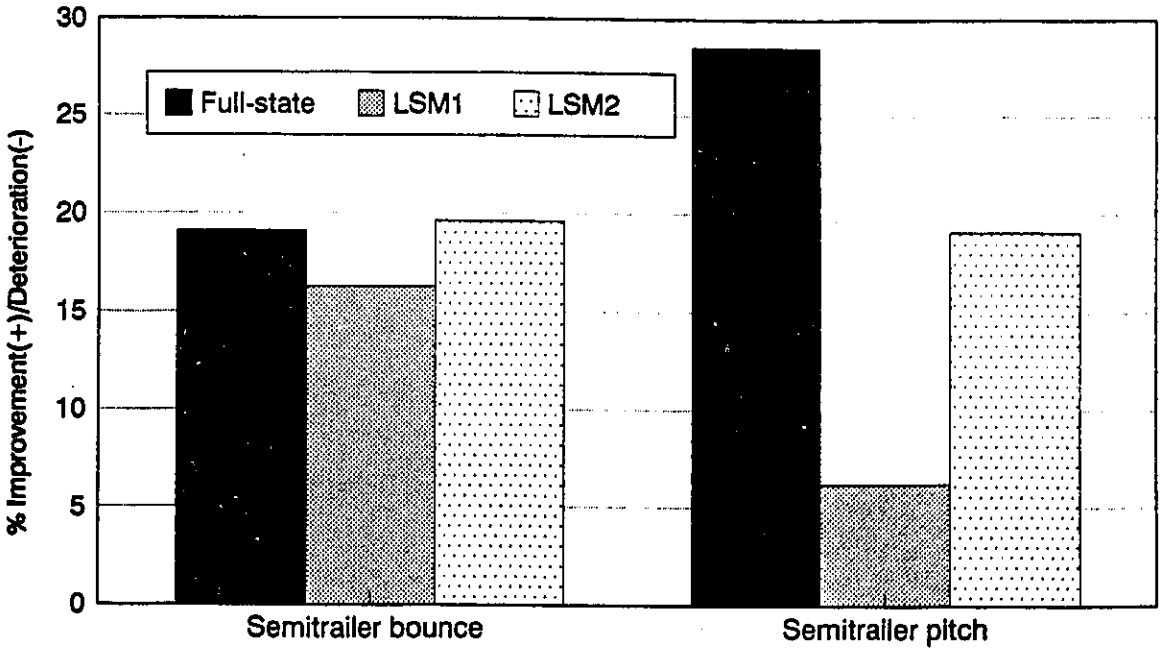

Figure 5.22 Percent improvement(+)/deteriration(-) in the mean square of semitrailer bounce and pitch accelerations (compared to passive; smooth road)

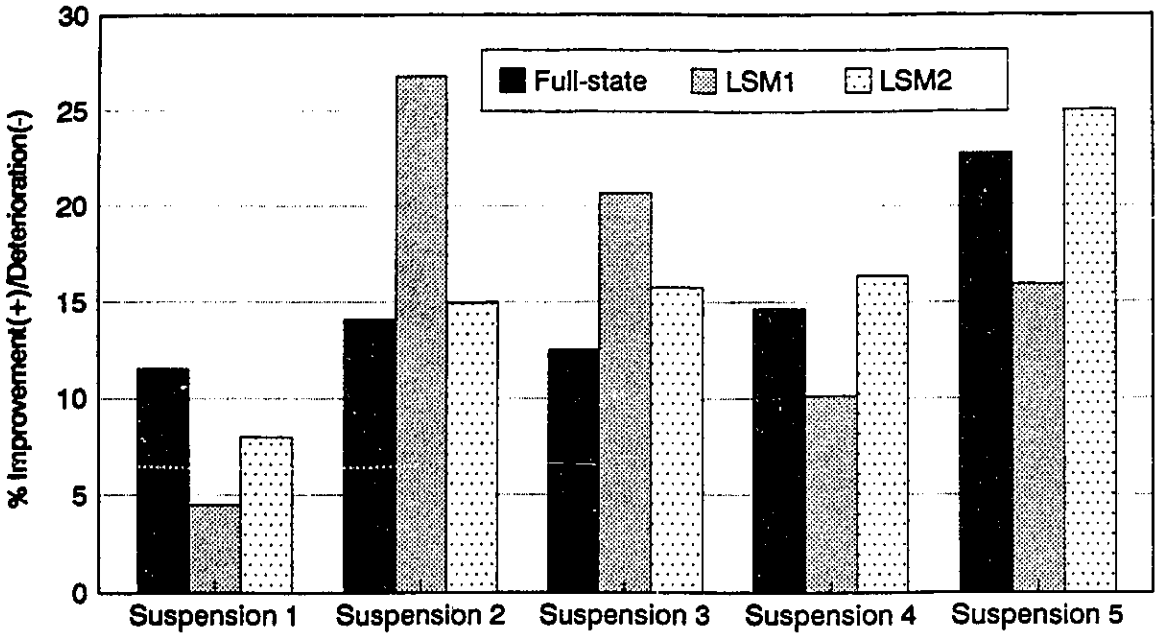

Figure 5.23 Percent improvement(+)/deteriration(-) in the mean square of tire deflections (compared to passive; smooth road)

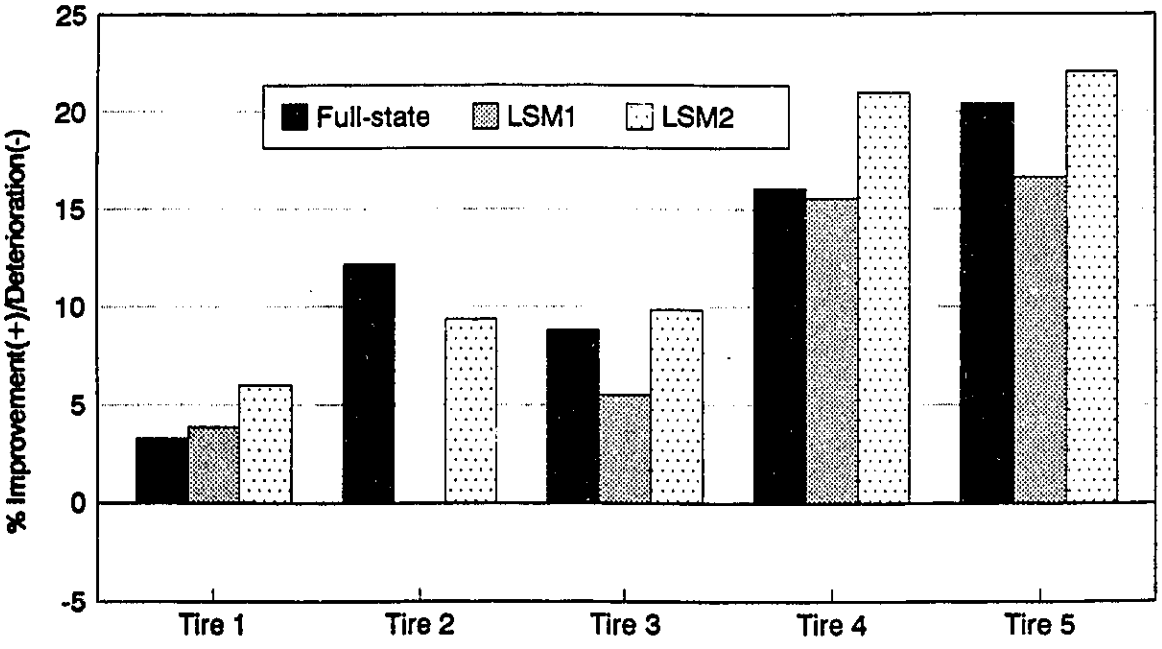

Figure 5.24 Percent improvement(+)/deteriration(-) in the mean square of tire deflections (compared to passive; smooth road)

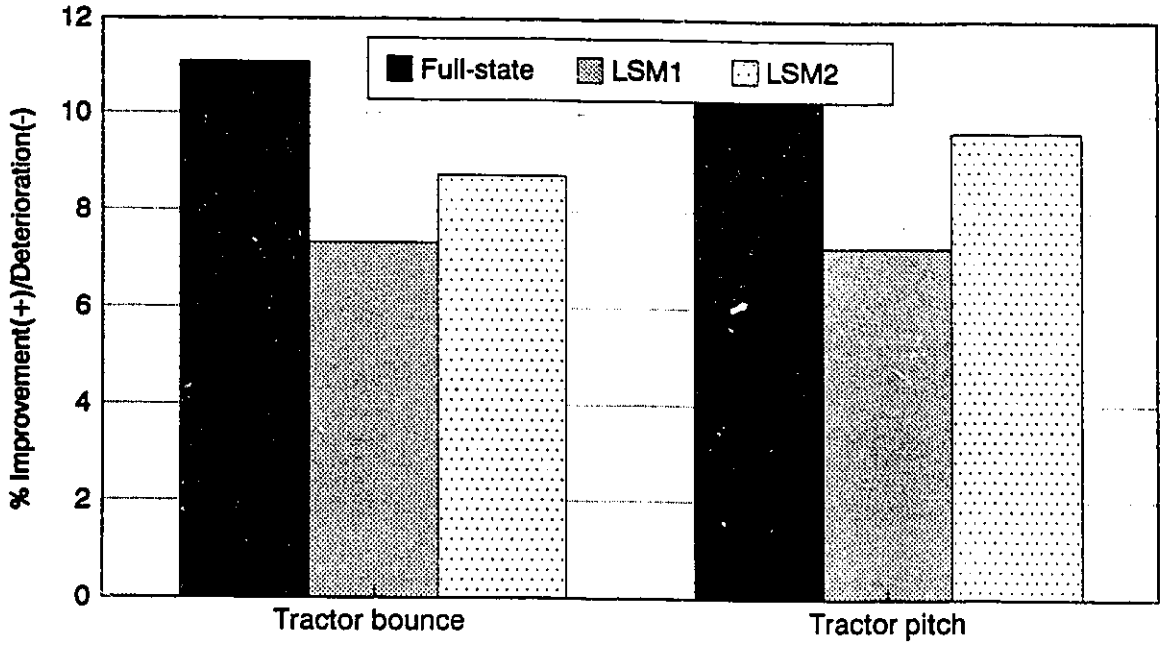

Figure 5.25 Percent improvement(+)/deteriration(-) in the mean square of tractor bounce and pitch accelerations (compared to passive; medium rough road)

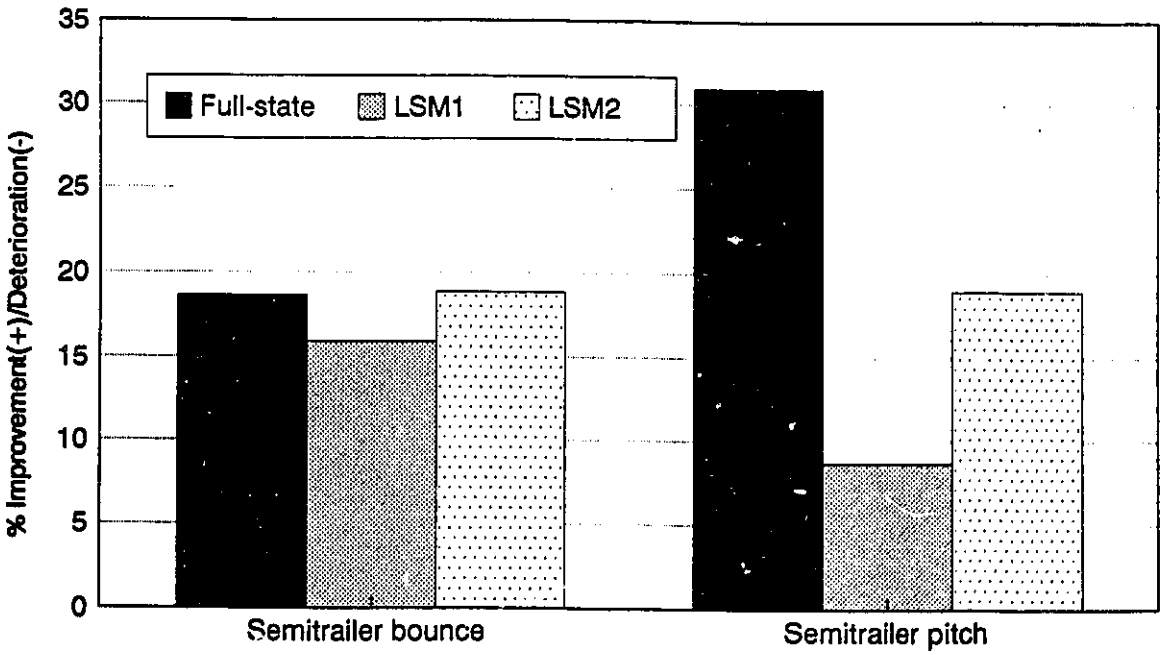

Figure 5.26 Percent improvement(+)/deteriration(-) in the mean square of semitrailer bounce and pitch accelerations (compared to passive; medium rough road)

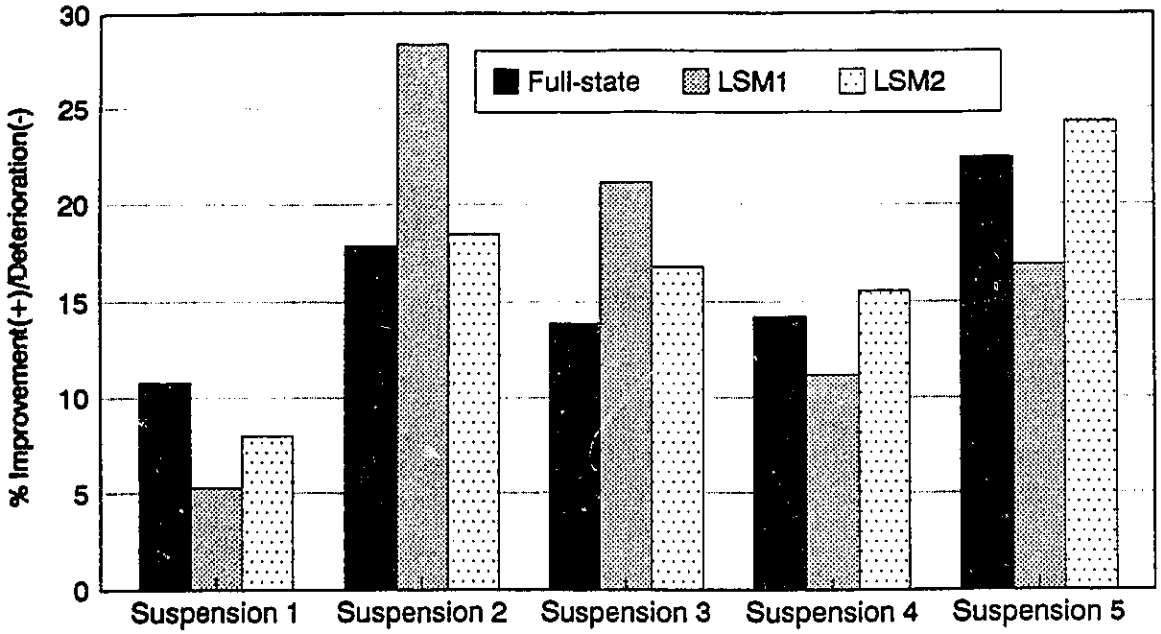

Figure 5.27 Percent improvement(+)/deteriration(-) in the mean square of tire deflections (compared to passive; medium rough road)

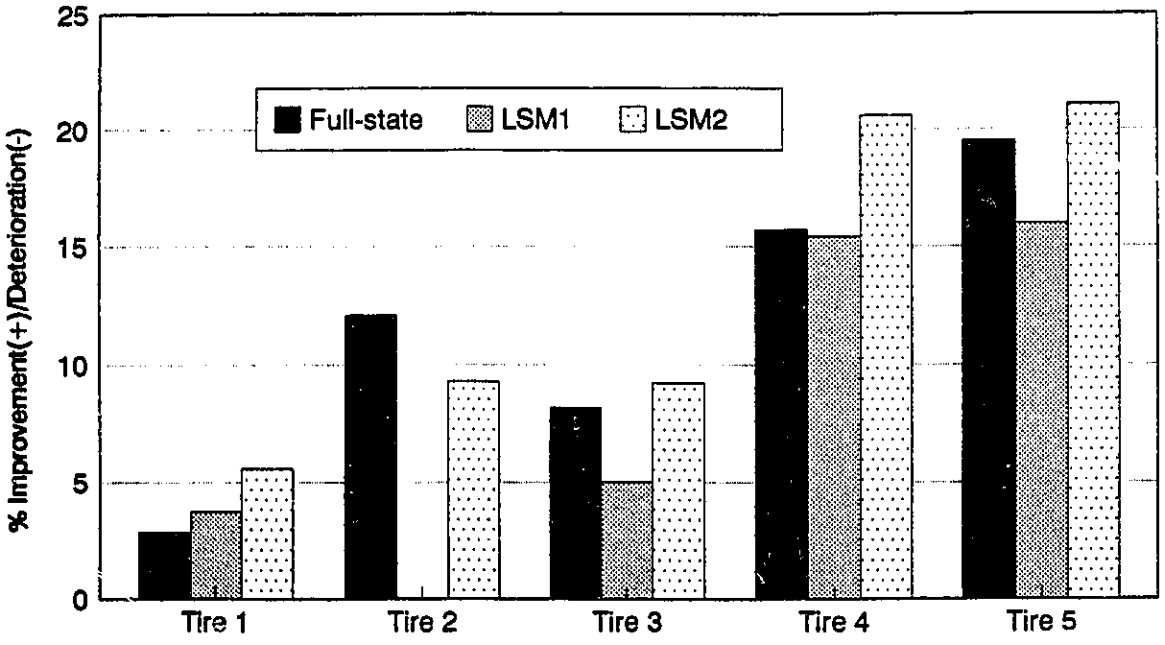

Figure 5.28 Percent improvement(+)/deteriration(-) in the mean square of tire deflections (compared to passive; medium rough road)

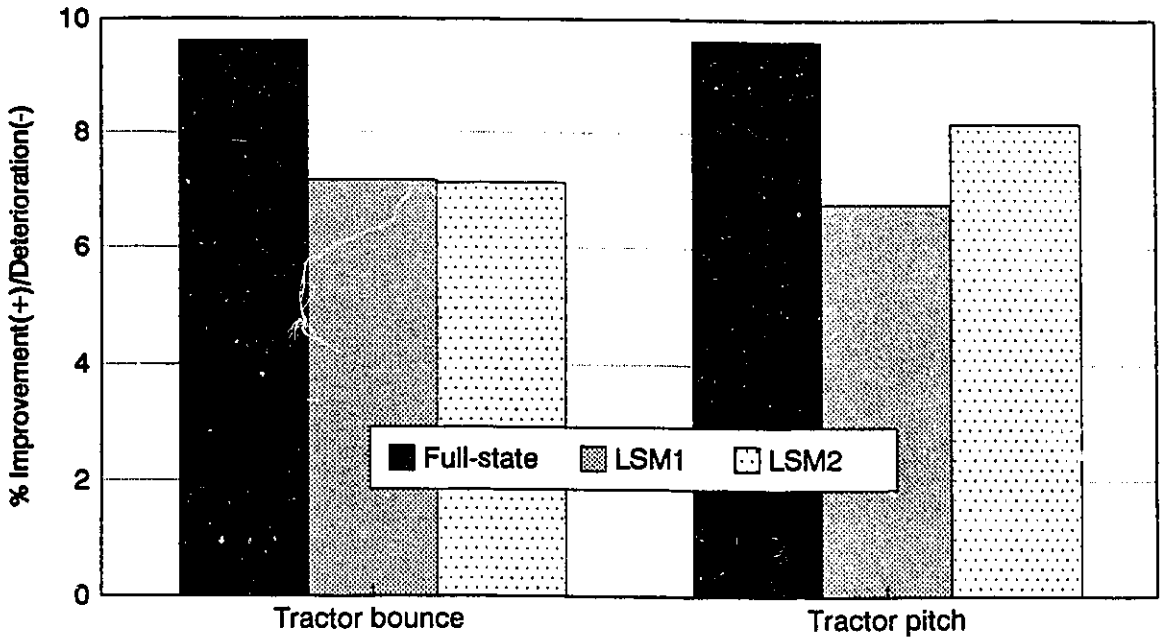

Figure 5.29 Percent improvement(+)/deteriration(-) in the mean square of tractor bounce and pitch accelerations (compared to passive; rough road)

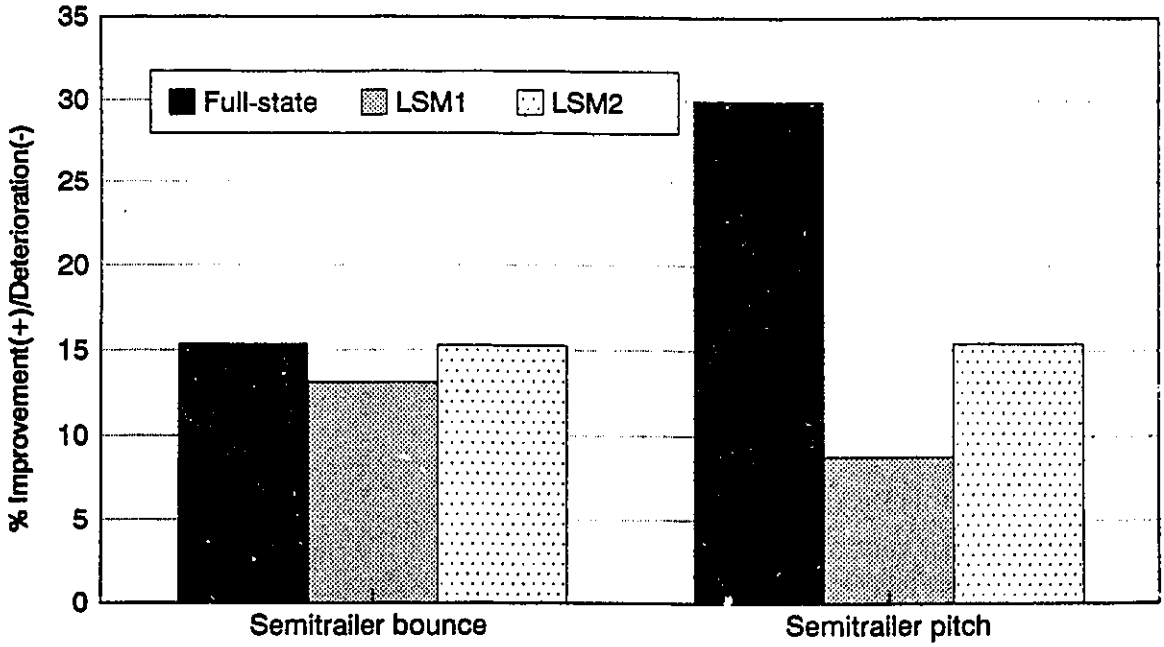

Figure 5.30 Percent improvement(+)/deteriration(-) in the mean square of semitrailer bounce and pitch accelerations (compared to passive; rough road)

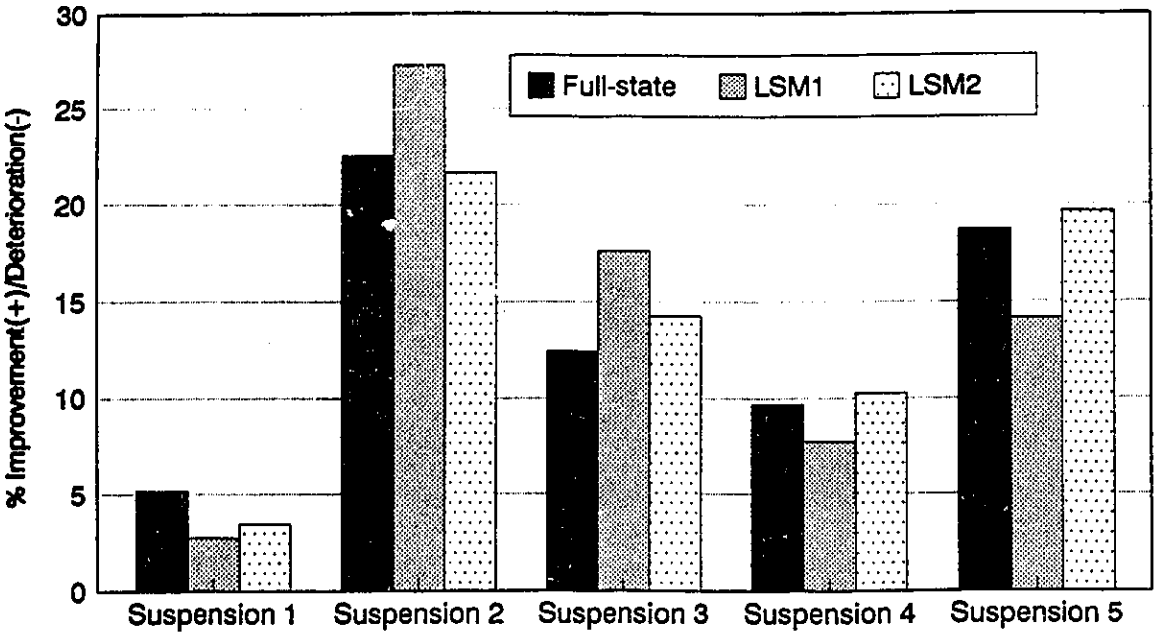

Figure 5.31 Percent improvement(+)/deteriration(-) in the mean square of tire deflections (compared to passive; rough road)

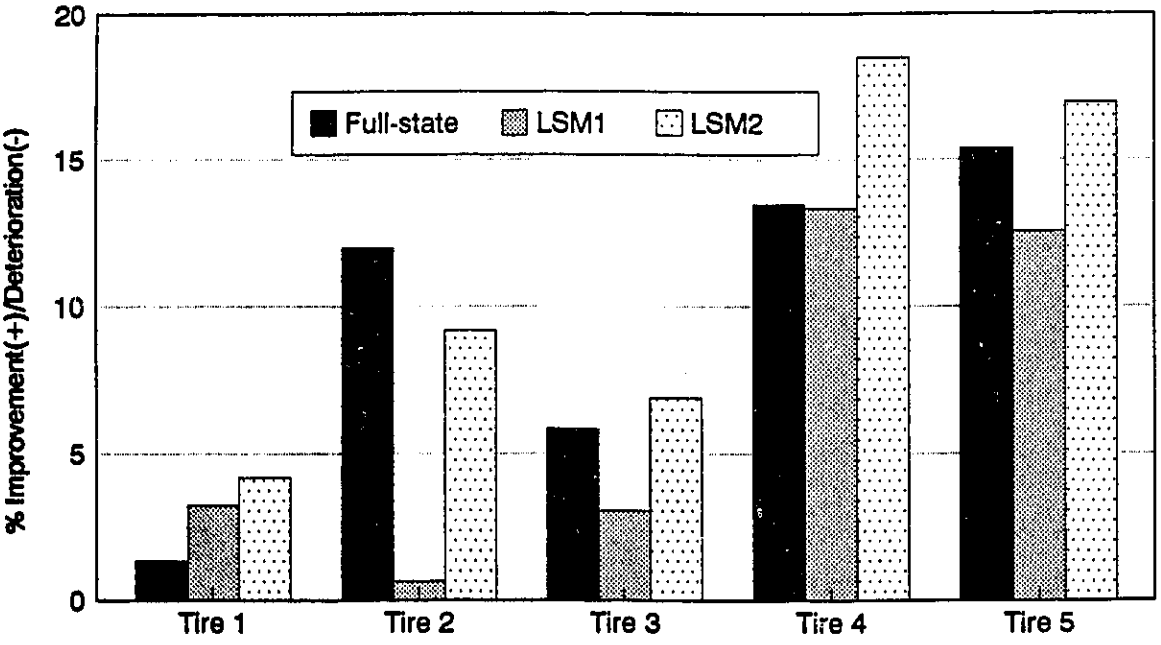

Figure 5.32 Percent improvement(+)/deteriration(-) in the mean square of tire deflections (compared to passive; rough road)

5.6 SUMMARY

The performance potentials of an active suspension based upon limited-state feedback are investigated in an attempt to reduce the cost, complexities and hardware requirements of a full-state feedback active suspensions. H_2 control technique is used to develop an active suspension incorporating uncertain measurement variables and limited-state feedback. For consistency and ease of comparison, the problem is formulated to be equivalent to an *LQG* problem. Two suspension schemes based upon limited-state measurements are formulated: *LSM1* based upon measurement of the relative displacements and velocities across the suspensions; and *LSM2* based upon vertical and pitch accelerations of the sprung masses. The effects of variations in the sensor noise intensity along with actuators effort, on the suspension performance are examined. It is shown that excessive sensor noise and/or limited actuator effort result in degradation of the suspension performance. The active suspension, however, approaches that of a passive suspension. This feature makes the active suspension operate in a fail-safe manner in the event of excessive sensor noise or lack actuator power. A comparison of the frequency response characteristics of passive and the three active suspensions revealed that all the active suspensions offer a performance superior to that of a passive suspensions throughout most of the frequency range. The major drawback of these schemes is that they generally require larger rattle space at low frequency. This can be partially solved by using a suspension that uses relative displacement and velocity measurement (*LSM1*). This scheme, however, is not well suited for semitrailer pitch control and tire forces reduction. An active suspension that is optimized to operate at 90 *km/h* on a rough road continues to provide superior performance for different speeds and road profiles.

5.7 REFERENCES

1. J. C. Doyle, K. Glover, P. P. Khargonakar and B. A. Francis, *"State-Space Solution to Standard H_2 and H_∞ Control Problems,"* IEEE transactions on Automatic Control, Vol. 34 No. 8, August 1989, pp. 831-846.

2. S. B. Kiriczi and R. Kashani, *"Control of Active Suspension with Parameter Uncertainty and Non-White Road Unevenness Disturbance Input,"* SAE Publication No. 902283,

3. R. E. Kalman and R. S. Bucy, *"New Results in Linear Filtering and Prediction Theory,"* Trans. ASME ser. D, Journal of Basic Engineering, Vol. 83, 1961, pp. 95-108.

4. M. B. A. Abdel Hady and D. A. Crolla E., *"Active Suspension Control Algorithms for a Four Wheel Vehicle Model,"* International Journal of Vehicle Design, Vol. 13, No. 2, 1992, pp. 144-158.

5. J. Doyle and G. Stein, *'Multivariable Feedback Design: Concepts for Classical/Modern Synthesis.'* IEEE Transactions on Automatic Control, AC-26, 1981, pp. 4-16.

6. M. J. Safanov, A. J. Laub and G. Hartman, *'Feedback Properties of Multivariabe Systems: The Role and Use of Return Difference Matrix.'* IEEE Transactions on Automatic Control, AC-26, 1981, pp. 47-65.

7. G. Stein, and M. Athans, *'The LQR/LTR Procedure for Multivariable Feedback Control Design.'* IEEE Transactions on Automatic Control, AC-32, 1987, pp. 105-114.

8. C. J. Dodds, *"The Laboratory Simulation of Vehicle Service Stress,"* Journal of Engineering for Industry, ASME Transactions, Vol. 96, No. 2, May 1974, pp. 391-398

9. C. J. Dodds and J. D. Robson, *"The Description of Road Surface Roughness,"* Journal of Sound and Vibration, Vol. 31, No. 2, 1973, pp. 175-184.

10. J. D. Robson, *"Road Surface Description and Vehicle Response,"* International Journal of Vehicle Design, Vol. 1, No. 1, 1979, pp. 25-35.

11. J. S. Bendat and A. G. Piersol, *"Random Data: Analysis and Measurement Procedures,"* Whiley-Interscience, 1971, Toronto, Ontario, Canada.

CHAPTER 6

PAVEMENT DAMAGE EVALUATION

6.1 INTRODUCTION

It has been long recognized that heavy vehicles are largely responsible for tire forces generated pavement deterioration. A number of analytical and experimental studies on heavy vehicles have concluded that the dynamic component of the total tire force can account for anywhere from 2 to 50 % of the wheel generated road damage [1]. The road damage has been related to the magnitude of dynamic tire loads transmitted to the roads. In addition to truck size and weight, various other design and operating factors affect the magnitude of wheel loads transmitted to the pavement. The axle configuration, axle loads, gross vehicle weight, suspension type, tire inflation pressure, vehicle speed and road roughness, are known to affect the dynamic tire loads in a significant manner [2]. Despite significant relaxation in the freight vehicle weights and dimension regulations in the recent years, the trucking industry has indicated continued interest in further relaxation in vehicle weights and dimension. The axle loads and the dynamic tire loads may thus be expected to increase further. Among the various design factors that influence the dynamic tire loads, the suspension designs merit special consideration to control the magnitude of dynamic tire loads transmitted to the pavement. Heavy vehicle suspensions, however, are designed

to achieve a compromise among the improved ride quality, cargo safety and rattle space requirements. Recognizing the effects of suspension design on truck-pavement interactions, dynamic pavement loading need to be prioritized along with the other existing suspension design requirements.

The population of heavy vehicles on our highways, along with growing demand to increase their weights and dimensions, have prompted serious concerns related to the dynamic wheel loads transmitted to the pavements. The dynamic wheel loads of heavy vehicles are known to be among the major causes of pavement deterioration. Passive suspensions, while being very reliable and easily implementable, fall short of satisfying the various conflicting design requirements, as demonstrated in Chapter 3. With recent advances in optimization techniques, automatic control, and availability of sophisticated and reliable hardware, active suspensions offer considerable performance potentials to achieved improved compromise among the various conflicting design requirements. The overwhelming improvement of ride quality resulting from the use of active suspensions seems to have overshadowed their effect on tire generated pavement damage. It has been established that vehicle ride quality and dynamic tire loads are strongly related to various vibration modes of the vehicle. An analogy between the ride qualify and tire loads has been further established [3,4]. The aim of this chapter is to evaluate the effect of advanced suspensions on tire generated pavement damage. The effects of variations in vehicle speed, road roughness, suspension stiffness and damping, tire stiffness, semitrailer axles spacing, and semitrailer *CG* location on the dynamic load coefficients are investigated for the "optimum" passive as well as the active suspensions.

Damages to the pavement structures can be primarily attributed to the traffic loads and the environment. Pavement damage caused by wheel loads is of primary concern for heavy vehicle design. While there is considerable civil engineering literature concerned

with theoretical and experimental studies of road damage caused by heavy vehicle, it is, however, mostly based on the assumption that vehicles apply a constant (static) tire force to the road. These studies have achieved limited success due to the complexities associated with the road damage mechanisms. Although considerable research efforts have been expended to predict the pavement failure, a satisfactory agreement between theory and experiment has not yet been achieved [5]. It is not uncommon for such analyses to underestimate pavement fatigue lives by a factor of 100 [6-8].

Since the mechanisms of road surface failures are not well understood, it has been suggested that vehicle configurations be assessed in terms of their relative pavement damage potentials. Pavement damage potentials of a heavy vehicle are frequently assessed in terms of the *Dynamic Load Coefficient* (*DLC*), defined as the ratio of the root mean square of the dynamic tire forces to the mean tire load. The *DLC* is thus strongly dependent upon road surface roughness, vehicle speed, suspension and tire properties, vehicle and axles configuration, geometry and mass distribution of the vehicle etc.

6.2 ASSESSMENT OF ROAD DAMAGE

Vehicle generated road damage is directly related to the magnitude of tire forces transmitted to the pavement. The tire forces transmitted to the road consist of two components: a static load and the fluctuating or dynamic load. The static load depends on the geometry and mass distribution of the vehicle, and the load sharing characteristics of the suspension systems. Dynamic tire forces, on the other hand, are the result of vehicle vibration caused by road roughness. The intensity of these vibrations and hence the severity of the dynamic tire forces primarily depend upon the suspension design and vehicle and axle configuration.

Dynamic tire forces and their interaction with the pavement is a complex process. The extent of damage caused by these loads to pavements depend on the road structure and material characteristics, as well as the nature of the applied loads. Although a number of methods have been proposed to estimate the serviceability index or service lives of pavements, serious concerns have been raised on the validity of the methods [8]. In view of the complexity associated with the pavement mechanisms and lack of generally acceptably assessment methods, the performance potentials of suspension systems are assessed in terms of the relative magnitudes of the dynamic tire loads.

6.2.1 The Fourth Power Law: Applied to Static Load

A common unit for defining the road damage potential of various classes of vehicles has been sought to normalize and objectively compare the extent of damage caused by different classes and vehicle configurations. The first attempts to normalize road damage were based on identification of broad vehicle groups [9]. Each group contains a number of broadly "similar" vehicles, which are assigned a common pavement-damage-potential index. This, however, was a rugged attempt to quantify tire generated road damage and hence did not capture the effect of essential vehicle elements such as actual static axle forces.

The most important result to quantify and compare road damage due to static toad was attained through extensive road tests conducted by the *AASHO* (*The American Association of State Highway Officials)* [10-12]. Analysis of measured date revealed that the decrease in pavement "serviceability" caused by heavy vehicles can be related to the fourth power of the static axle load. Consequently the number of *Equivalent Standard Axle Loads* (*ESAL*) *N*, attributed to static loads was defined as [10-12]:

$$N = (P_{stat} / P_0)^4 \tag{6.1}$$

where, P_{stat} is axle static load and P_0 is a reference axle load taken as 80 *kN*. While the *Fourth Power Law* remains widely used as an effective tool, its validity has been questioned and exponents as high as 12 have been cited [13,14]. To demonstrate the significance of the *Fourth Power Law*, consider an axle carrying a static load resulting in *N ESAL*, if the load is doubled *N* is multiplied by 2^4. This indicates that while the static load is only doubled, the damage potential is multiplied by 16.

6.2.2 Dynamic Tire Forces

While there is considerable civil engineering literature concerned with theoretical and experimental studies of road damage caused by heavy vehicle loads, it is, however, mostly based on the assumption that vehicles apply a constant (static) tire force to the road. Dynamic forces that are caused by the interaction of a heavy vehicle with road surface roughness constitute a significant portion of the total tire forces. Peak tire forces can be as much as twice their static values, and *RMS* levels are typically 20-30% of the static forces [15,16],. The road damage assessment thus necessitates appropriate considerations of the dynamic tire forces.

The magnitude of the dynamic tire forces depends on the road surface roughness, vehicle speed, suspension and tire properties, vehicle and axle configuration, geometry and mass distribution of the vehicle, etc. A parameter frequently used to characterize the magnitude of dynamic tire forces is the *Dynamic Load Coefficient* (*DLC*), defined as:

$$DLC = \frac{RMS\ dynamic\ tire\ force}{Static\ tire\ force}. \tag{6.2}$$

where:

$$RMS\ dynamic\ tire\ force\ = \left[\int_0^{\infty} S_f(\omega)\ d(\omega)\right]^{0.5} \tag{6.3}$$

and $S_f(\omega)$ is the power spectral density of the tire force. Heavy vehicles typically exhibit *DLC* in the range of 0.1 to 0.3 [15-18]. *DLC* values as high as 0.4 have also been reported [2].

The approach to the problem of estimating the extent of the of road damage due to dynamic tire forces was based on an extension of the *Fourth Power Law* (normally used for static loads) to dynamic loads. Using the assumption that road damage depends on the fourth power of the dynamic wheel force at a point on the road, it has been shown that the expected value of the fourth power of the instantaneous wheel force is given by [19]:

$$\Phi = E[P^2(t)] = (1 + 6\bar{s}^2 + 3\bar{s}^4)P_{stat}^4 = RSF \times P_{stat}^4 \tag{6.4}$$

where,

$P(t)$ = The instantaneous tire force at time t,

P_{stat} = Static tire force,

$\bar{s}$ = Coefficient of variation of dynamic tire force (the *DLC*),

$RSF = (1 + 6\bar{s}^2 + 3\bar{s}^4)$ = Dynamic Road Stress Factor.

The *RSF* approach was used in a limited number of studies to estimate the pavement damage caused by dynamic tire forces and to introduce new legislation relevant to axle configuration and loads [16, 20-22].

While EQ (6.4) presents an attempt to mathematically characterize the road damage due to dynamic tire forces, its accuracy is subjected to considerable criticism [5,23-24], since *RSF* is based on the inherently uncertain fourth power law. Moreover, *RSF* method neglects the sensitivity of the road response to variations in the speed and frequency of the applied loads, and assumes that each suspension system on a vehicle does not influence the tire forces generated by other axles [3]. However, since the *RSF* is directly related to the *DLC*, it is expected that suspensions should rank in the same order whether the wheel loads are compared in terms of road stress factor (*RSF*) or the dynamic load coefficient (*DLC*). In view of the considerable criticism of the *Fourth Power Law* and its use to characterize the pavement damage, the *DLC* is used in this study to assess the relative performance characteristics of various suspension systems.

6.3 DETERMINATION OF THE *DLC*

The road friendliness of the various suspension schemes is assessed in terms of their respective dynamic load coefficients, using EQ (6.2). The dynamic load coefficient necessitates the evaluation of the *RMS* value of the dynamic tire forces which is related to the power spectral density, as described in EQ (6.3). The *PSD* of the tire forces obtained from the frequency domain analyses performed in the previous chapters, is used to evaluate the *DLC* due to tire forces transmitted to the pavement.

In this section, the effects of suspension type on the *DLC* and thus the road friendliness of the vehicle is assessed for the following suspension systems:

- The "optimum" passive suspension system determined based on the covariance analysis presented in Chapter 3. The "optimum" suspension parameters are listed in Table 3.3.

- The active suspension schemes developed in Chapters 4 and 5, assuming white noise corrupted measurements ($V_i = 10^{-6}$) for the limited-state measurements and availability of sufficient control effort ($\rho_i = 10^{-14}$). The active suspension based upon full-state feedback control is considered with the weighting coefficients corresponding to *AS5* presented in Table 4.2. These active suspensions are based on the following accessible measurements:

    1. Ideal full-state measurement with no sensors noise
    2. Relative velocity and displacement measurements (*LSM1*)
    3. Acceleration measurements (*LSM2*)

The dynamic wheel loads are strongly related to road roughness, vehicle suspension, speed and axle configurations. The vehicle models are analyzed to determine the influence of different design and operating factors on the *DLC*. The *DLC* of the various suspension systems are also evaluated for three types of roads characterized by EQ (2.2). The coefficients of road roughness are summarized in Table 6.1. In addition to the suspension type and road roughness, the *DLC* and the road friendliness of the vehicle is assessed for variations in vehicle speed ranging from 10 to 125 *km/h*. The effects of the suspension and tire parameters, as well as the semitrailer axles spacing and cargo placement on the *DLC* are also investigated.

Table 6.1 Roughness parameters for asphalt and concrete roads

Type of road	α *(1/m)*	σ *(m)*
Asphalt *(smooth)*	0.15	0.0033
Concrete *(medium rough)*	0.20	0.0056
Concrete *(rough)*	0.40	0.0120

6.3 RESULTS AND DISCUSSIONS

The influence of relevant vehicle design parameters and operating conditions on the dynamic load coefficient due to tire forces is investigated and the results are analyzed to recommend suspension designs to enhance the road-friendliness of the vehicles. Unless specified, the results are derived for the nominal vehicle model parameters described in Chapter 2 subject to excitations arising from a rough road at a speed of 90 *km/h*. The effects of road surface roughness, vehicle speed, suspension and tire properties, configuration, geometry and mass distribution of the vehicle on the *DLC* are evaluated and discussed in the following subsections.

6.3.1 Effect of Road Roughness on the *DLC*

The *DLC* is strongly dependent upon the road roughness, irrespective of the suspension type and properties. An increase in road roughness results in increased dynamic load coefficient due to tire forces. The *DLC* is investigated for vehicle interaction with smooth, medium rough and rough roads with roughness parameters listed in Table 6.1.

The *DLC* due to tire forces of the vehicle equipped with the "optimum" passive suspension are illustrated in Figure 6.1, as a function of the road roughness. The results clearly show the dependency of the *DLC* on the road roughness. The *DLC* of all the tire forces on rough roads is observed to be nearly 6 times that obtained under smooth roads. This emphasizes the importance of initial road construction and proper road maintenance. The contribution of the dynamic load tires to pavement deterioration would be much smaller for a smooth road and hence the degradation would be much slower.

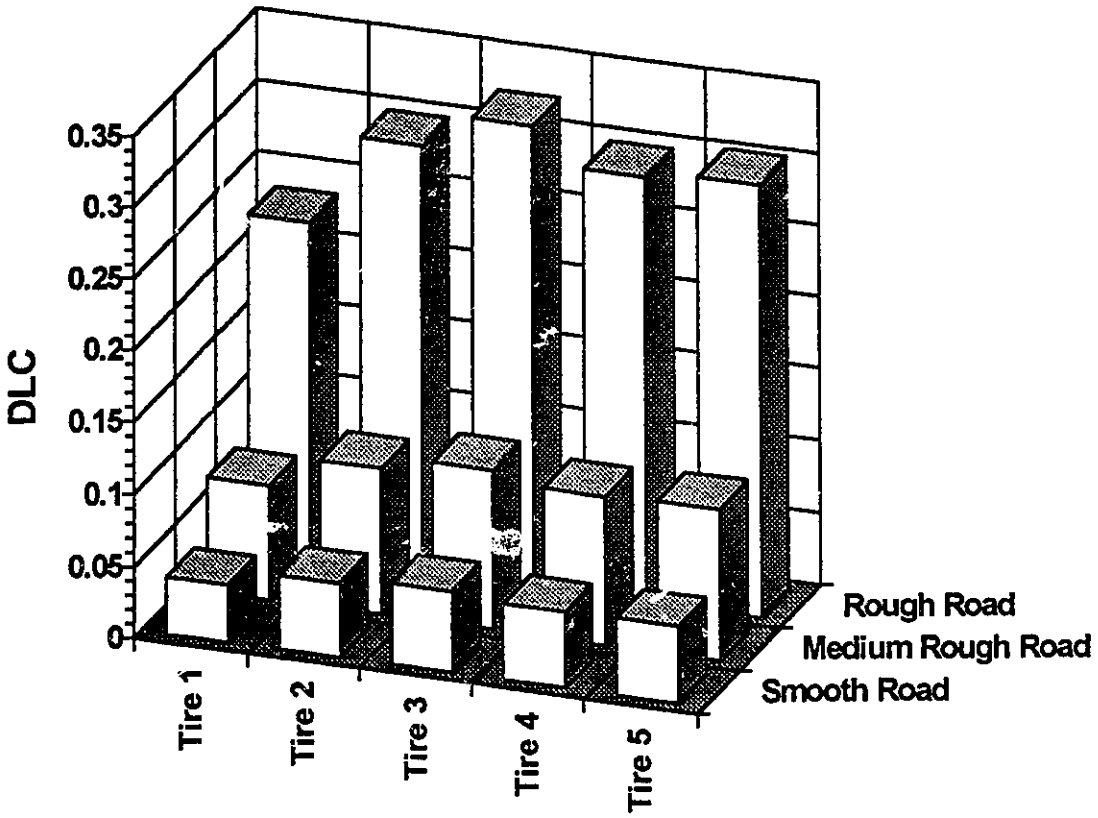

Figure 6.1 DLC of the tractor-semitrailer tires for different types of roads (passive suspension)

Figure 6.2 presents the tire force response characteristics of three active suspension systems (full-state or ideal active, *LSM1* and *LSM2*) as a function of the road roughness. The *DLC* is strongly related to the restoring and dissipative properties of the vehicle suspension. Active systems with suspension properties that change with changing excitations and response characteristics thus offer considerable potential to reduce the *DLC*. The response characteristics are presented in terms of percent decrease (+) or percent increase (-) in *DLC* when compared to those due to the "optimum" passive suspension. An ideal active suspension, with full-state measurement and no sensor noise, offers the highest reduction in the *DLC* irrespective of the road roughness, as shown in Figure 6.2. An ideal active suspension, however, poses considerable complexities with its implementation due to requirements associated with measurement of the augmented state vector. Alternatively, *LSM2* active suspension, based upon measurement of vertical and pitch accelerations, offers considerable reduction in the *DLC*. The *LSM1* suspension, based upon measurement of the relative velocities and displacements offers least improvement in *DLC*, as shown in the figure. Both of these suspensions are, however, much easier to implement due to ease of measurement of the limited state using accelerometers, *LVDT*, *LVT* and string potentiometers. The *LSM2* suspension yields reduction in *DLC* comparable to that of an ideal active suspension for all the tractor-semitrailer tires, irrespective of the road roughness. The reduction in the *DLC* varies from 3 to 13.5 % for different tires and roads. The most significant reduction can be achieved for the semitrailer tires. *LSM1* results in a reduction of all the vehicle tire *DLC* except the second tire where an increase of less than 0.2% is noticed. This increase, however, does not represent a major drawback of this particular scheme since the reduction in the *DLC* of all the other tires is significant.

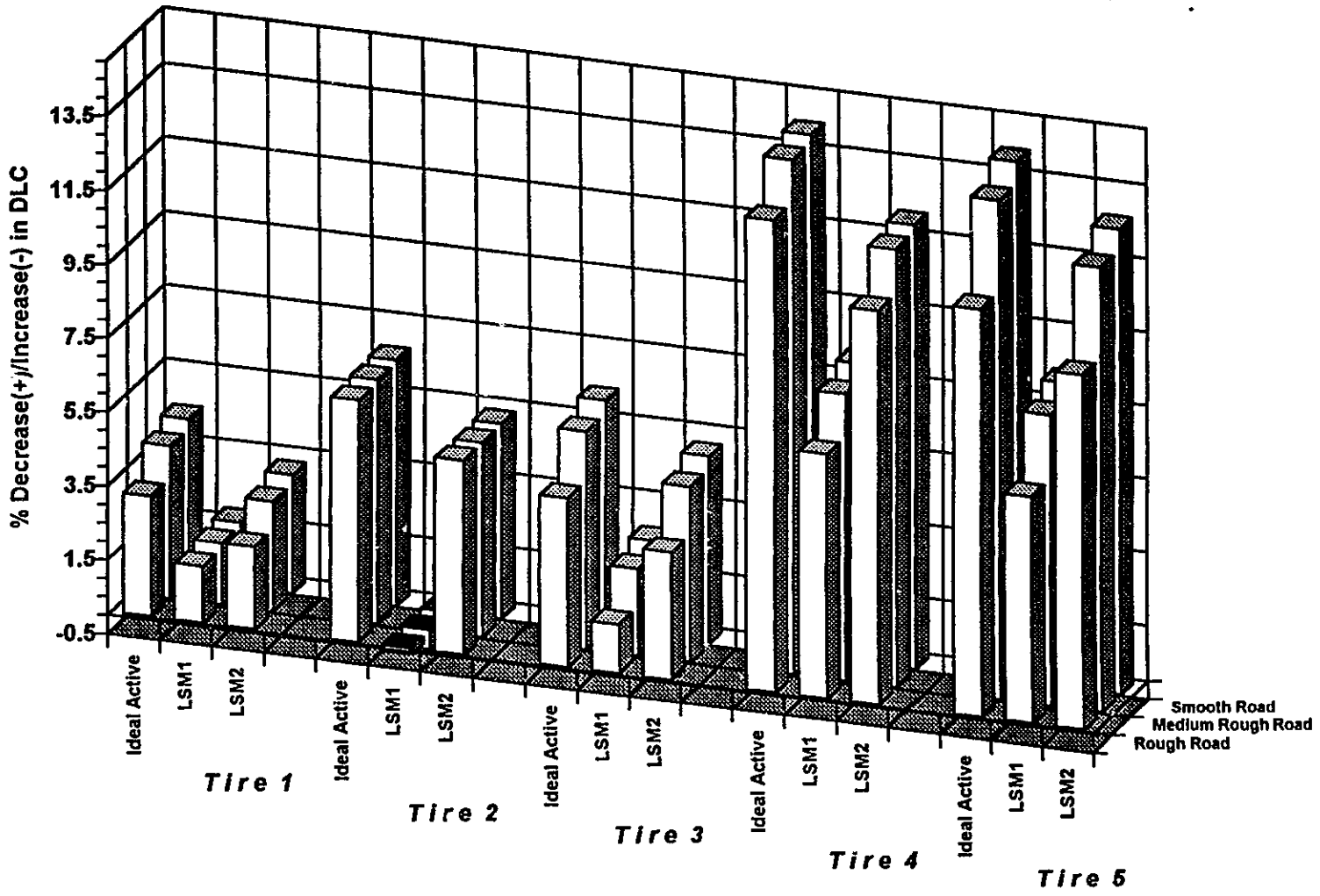

Figure 6.2 Percent improvement(+)/deterioration(-) in the the DLC of the tractor-semitrailer tires using different suspension schemes (relative to passive)

6.3.2 Effect of Vehicle Speed on the *DLC*

The influence of variations in vehicle speed on the *DLC* due to tire forces is investigated for the 10 to 125 *km/h* speed range. Figure 6.3 illustrate the *DLC* of tire forces for "optimum" passive, and ideal, *LSM1* and *LSM2* active suspensions as a function of vehicle speed. The results are presented for excitation arising from a rough road. The *DLC* increases rapidly with increase in the vehicle speed, irrespective of the suspension type, as shown in the figures. The active suspension schemes, in general, result in lower *DLC* throughout the speed range. A suspension scheme based on acceleration measurements (*LSM2*) results in a *DLC* similar to that of an ideal active suspension throughout the speed range. *LSM1*, however, results in only marginal reduction in the *DLC*. This is especially true for the second tire. As the speed is increased from 10 to 125 *km/h*, the *DLC* almost triples regardless of the suspension scheme. The effectiveness of the active suspensions, specifically the ideal and *LSM2*, in reducing the *DLC* becomes apparent as the vehicle speed increases. Since freight vehicles operate mostly at high speeds, and the *DLC* approach high values at these speeds, the performance potentials of the active systems becomes more apparent.

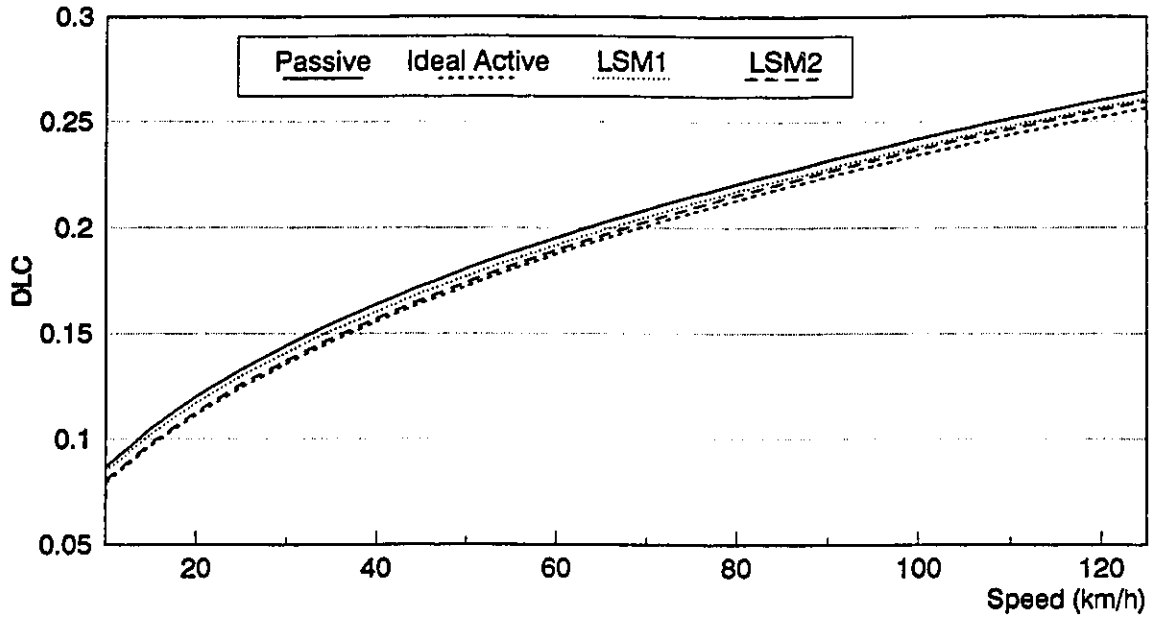

Figure 6.3a Effect of vehicle speed on the DLC of tire 1 for different types of suspensions

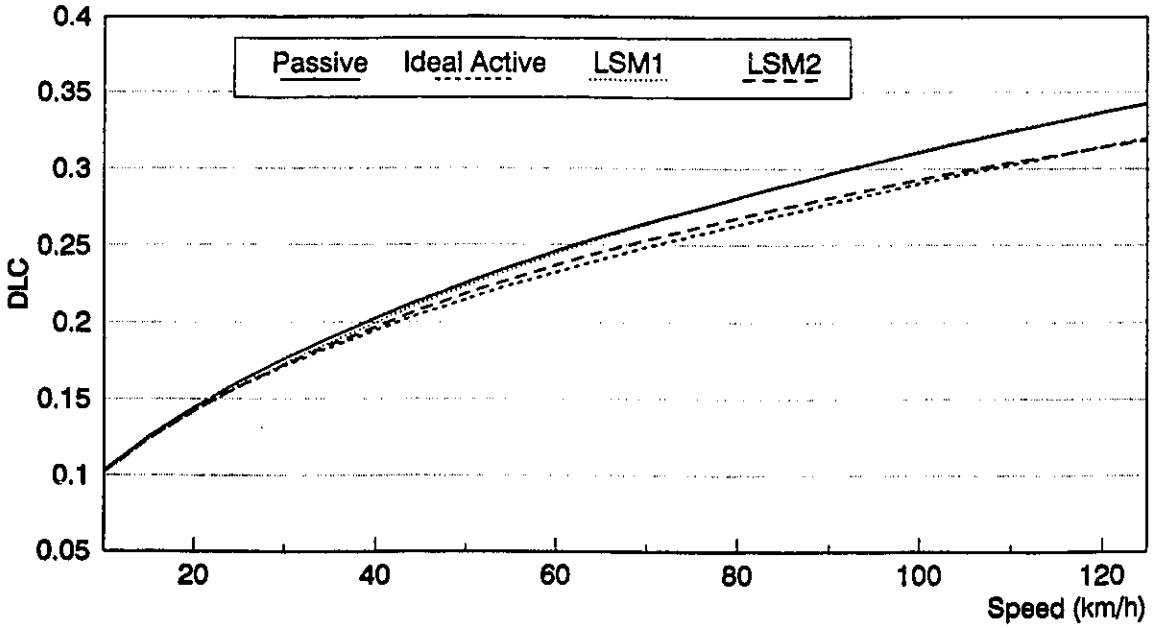

Figure 6.3b Effect of vehicle speed on the DLC of tire 2 for different types of suspensions

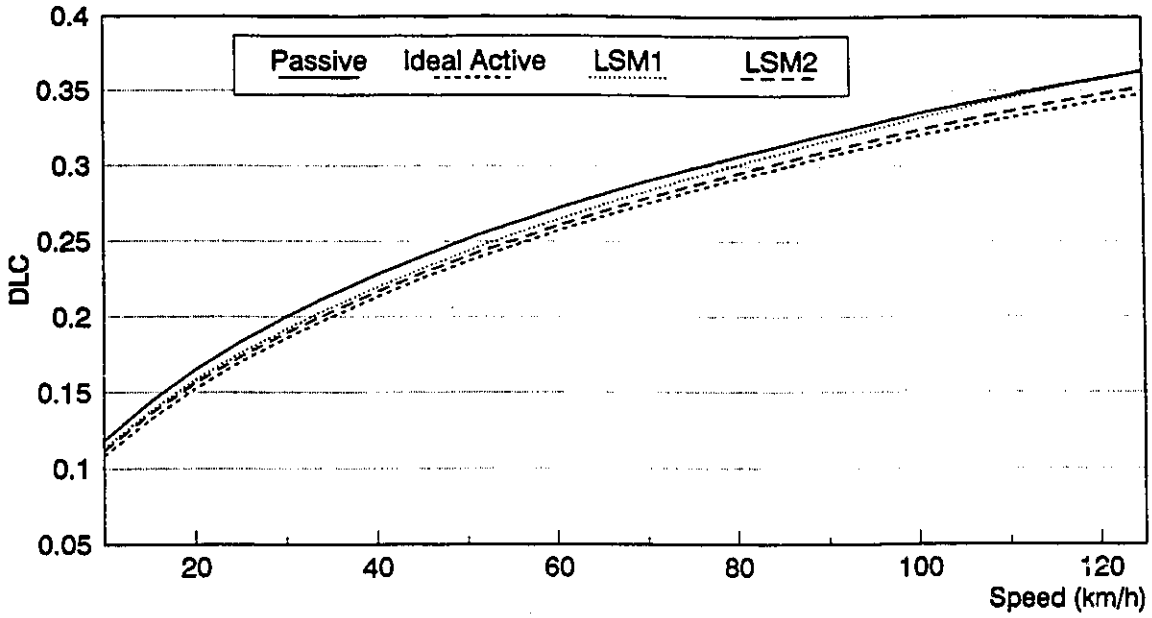

Figure 6.3c Effect of vehicle speed on the DLC of tire 3 for different types of suspensions

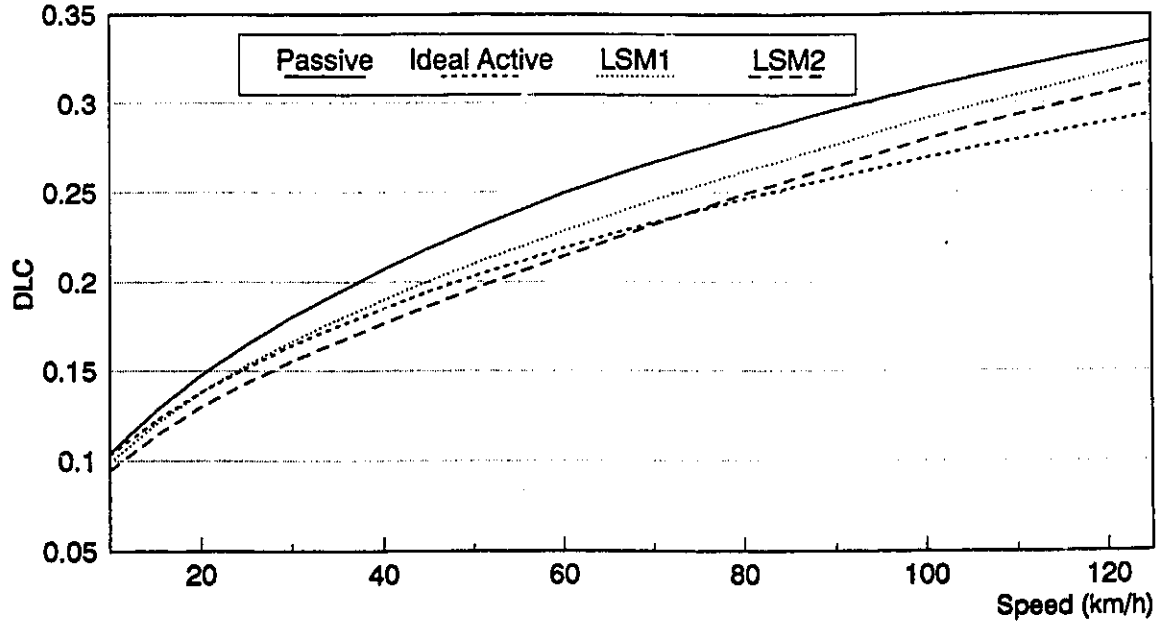

Figure 6.3d Effect of vehicle speed on DLC of tire 4 for different types of suspensions

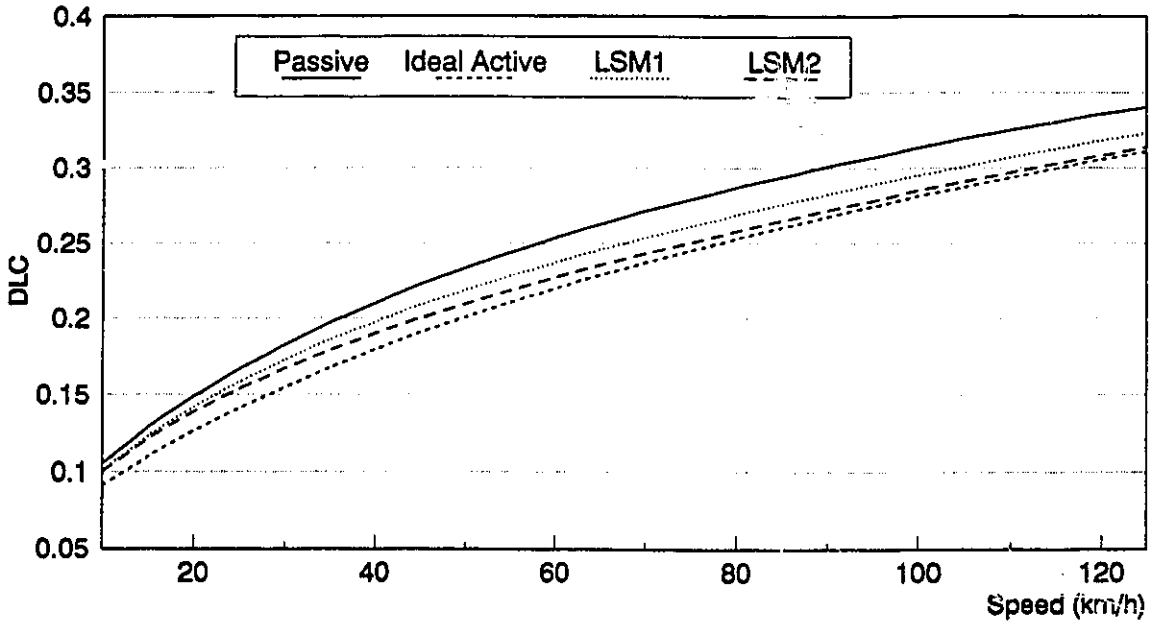

Figure 6.3e Effect of vehicle speed on the DLC of tire 5 for different types of suspensions

6.3.3 Effect of Suspension Stiffness and Damping Properties on the *DLC*

The restoring and dissipative properties of vehicle suspensions strongly influence the *DLC* of tire loads transmitted to the pavements.

The effect of suspension parameters variation on the *DLC* is investigated only for a passive suspension. As discussed in Chapter 4, active suspensions can always be tuned for variations in passive suspension parameters resulting in almost insignificant changes in the vehicle behavior. Since the passive suspension parameters were derived to achieve a compromise among the ride quality, cargo safety, tire dynamic forces and suspension deflections, the resulting suspension design may not yield the best performance related to dynamic tire forces. The nominal suspension parameters, presented in Chapter 3, are varied and their influence on the *DLC* is investigated to propose suspension designs to enhance road friendliness of the vehicle.

Figures 6.4 and 6.5 illustrate the effect of variations in the suspension stiffness and damping properties on the *DLC* of the tractor-semitrailer tires. The variations in the suspension parameters are presented in terms of % of nominal values. The results illustrate a strong influence of variation in the suspension damping on the *DLC*, while the influence of variation in the stiffness is relatively small. Heavily or lightly damped suspensions cause high dynamic tire forces. Increasing the damping by 50%, for instance, can result in a 14% increase in the *DLC* of tires 4 and 5. On the other hand, reducing the suspensions damping by 50% can result in approximately 13% increase in the *DLC* of tires 2 and 3.

The nominal suspension damping parameters determined in Chapter 3, correspond to 0% variation in damping in Figure 6.4, seem to offer a compromise between the *DLC* of all the tractor-semitrailer tires. At the nominal suspension damping value the *DLC* of tire 1

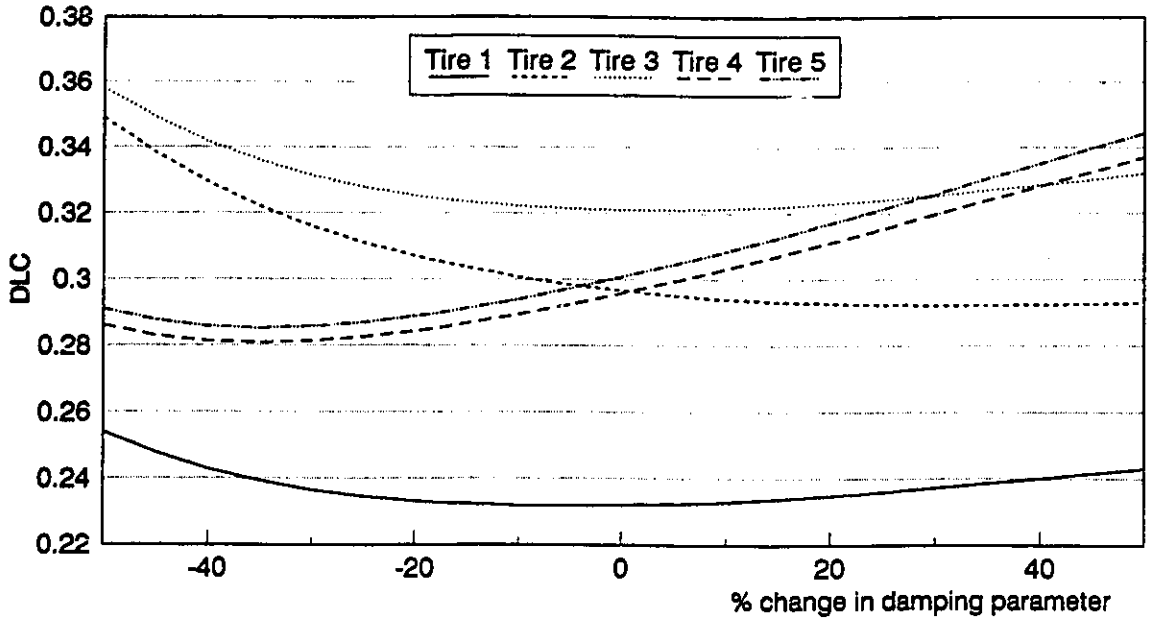

Figure 6.4 Effect of variation in nominal suspension dampings on the DLC (passive suspension)

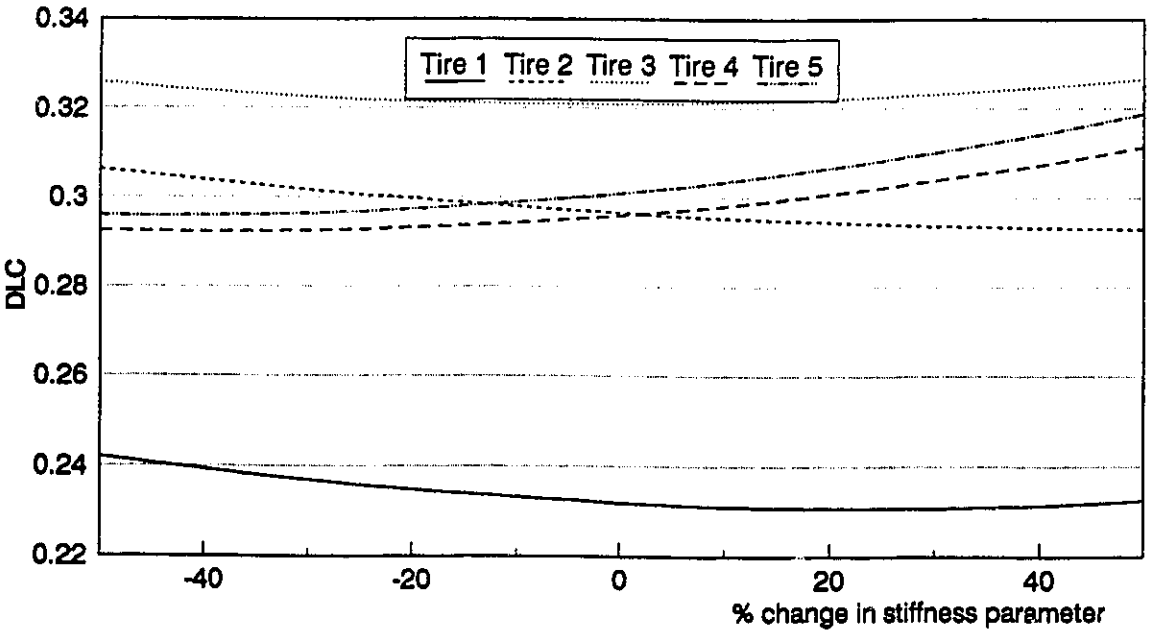

Figure 6.5. Effect of variation in nominal suspension stiffnesses on the DLC (passive suspension)

is minimum while the *DLC* of all the other tires is between 0.29 and 0.32. Similarly, the nominal stiffness suspension parameters determined in Chapter 3 are found to eliminate large discrepancies between the *DLC* of different tractor-semitrailer tires, as shown in Figure 6.4.

Since the nominal suspension damping and stiffness parameters are optimized for a vehicle operated at a 90 *km/h* speed, these parameters may not be best suited for operation at a different speed. Since the magnitude of vehicle vibrations and thus the tire loads are strongly related to vehicle speed, suspension tuning may be necessary to minimize the *DLC* corresponding to different speeds. The *DLC* of tire loads are thus investigated for varying speed, and suspension parameters to arrive at the desired suspension design at different speeds. The restoring and dissipative properties of the suspensions that yield minimum *DLC* are thus identified at each operating speed.

Figures 6.6 and 6.7 present the required change in the stiffness and damping properties of the passive suspension to achieve minimum *DLC* in the 10-125 *km/h* speed range. While tires on axles 1 and 3 yield minimum *DLC* with the nominal suspension damping, a slight reduction in semitrailer axle suspensions damping is desired to achieve minimum *DLC* in the entire speed range. The second axle suspension requires small increase is suspension damping for minimum *DLC*. The desired variation in suspension damping of all the axles, however, is relatively insensitive to variations in the speed. More significant variation in the suspension stiffness, however, may be desirable to achieve minimum *DLC* at different speeds, as shown in Figure 6.7. Higher vehicle speed necessitates higher suspension stiffness value to reduce the *DLC*. However, variations in the damping and stiffness properties of the passive suspension might not always be possible since they can significantly jeopardize the other design objectives, such as ride quality, cargo safety and suspension rattle space requirements.

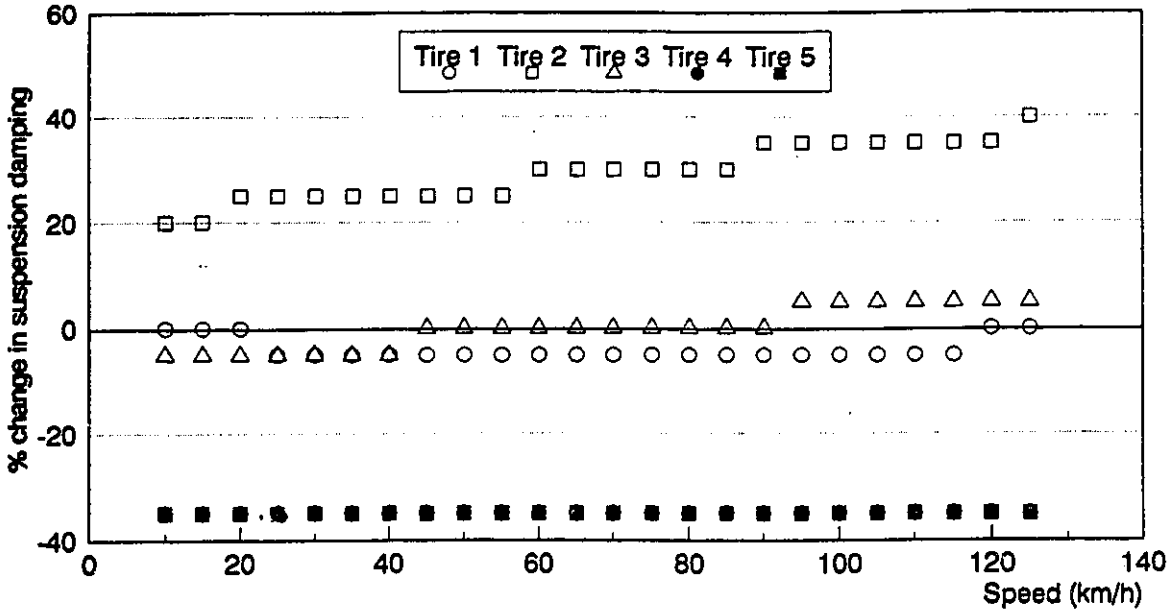

Figure 6.6 Required percent variation in damping for least DLC at a given speed (passive suspension)

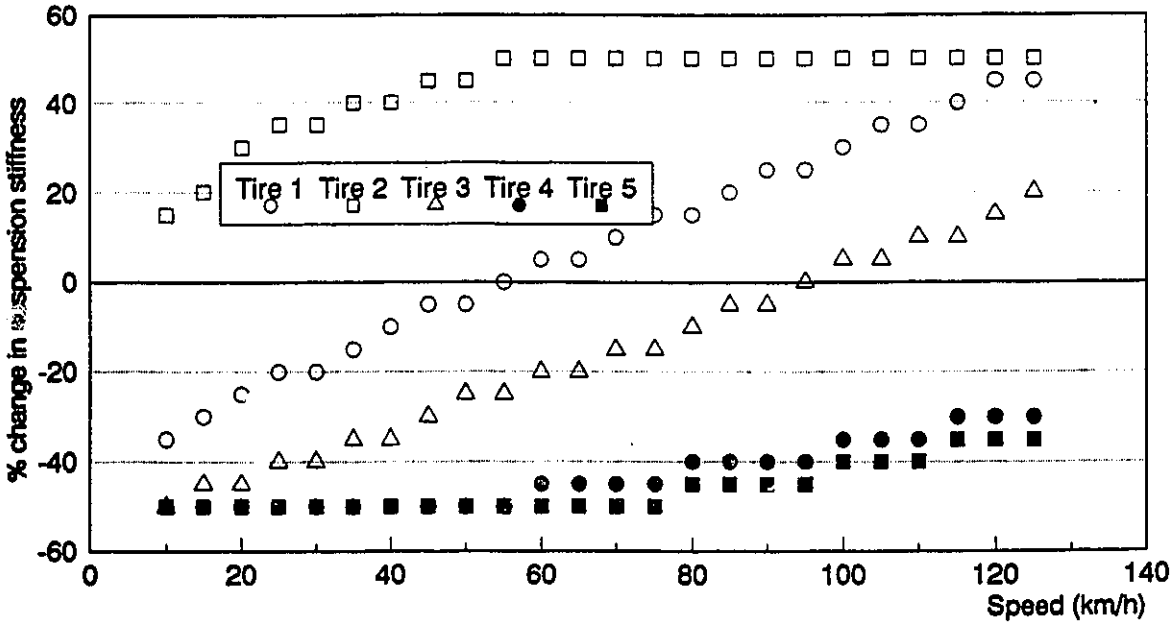

Figure 6.7 Required percent variation in stiffness for least DLC at a given speed (passive suspension)

6.3.4 Influence of Stiffness Properties of the Tires on the *DLC*

The dynamic wheel loads transmitted to the pavement are directly influenced by the restoring properties of the tires. The tire properties, however, affect the load carrying capacity, ride quality, traction and braking, handling, and stability performance of the vehicle in a highly complex manner. An excessive variations in the tire stiffness may be detrimental to the directional stability and traction/braking performance of the vehicle. The influence of tire stiffness on the *DLC* is thus investigated for ±25% variations about the nominal stiffness values. An increase in the tire stiffness yields considerable increase in the *DLC* for all the axle tires, irrespective of the suspension design, as shown in Figure 6.8. An increase in tire stiffness, realized by increase in the inflation pressure, tends to reduce the contact patch area. The dynamic tire forces thus distributed over reduced contact area can cause excessive road damage. The results show that the performance characteristics of the active suspensions deteriorate considerably with increase in the tire stiffness, and approaches that of a the passive suspension. A reduction in tire stiffness is thus desirable to achieve low *DLC* due to tire forces. Table 6.2 summarizes the % reduction in *DLC* caused by 25 % reduction in the tire stiffness for a passive suspension. A reduction of up to 21% in the *DLC* of the second tire can be achieved by reducing the tire stiffness by 25%. Table 6.3 illustrate the percent reduction in *DLC* of the *LSM2* active suspension when compared to those of the passive suspension for nominal and softer (25% reduction in stiffness) tires. The results show that further reduction in the *DLC* is possible when active suspension is employed. The *DLC* due to the last axle tire decreases by 12.6% when *LSM2* suspension is used in conjunction with the nominal tires. The *DLC* further reduces to 21.2% when tire stiffness is reduced by 25%. Combined tire stiffness reduction and active suspension can, therefore, significantly reduce the *DLC* of the tractor-semitrailer tires. Based on passive suspensions, most research has indicated that lower tire pressures usually results in reduced wheel loads which confirms the results obtained here.

Table 6.2 Percent reduction(+)/increase(-) in the *DLC* of the tractor-semitrailer tires resulting from a 25% reduction in the tire stiffness (passive suspension)

Tire i ↓	*%*
1	1.98e+01
2	2.12e+01
3	1.94e+01
4	1.41e+01
5	1.38e+01

Table 6.3 Effect of tire stiffness reduction on the percent reduction(+) of the *DLC* (*LSM2* compared to passive)

% reduction in tire stiffness → *Tire i* ↓	*% reduction in DLC for 0% reduction in tire stiffness*	*% reduction in DLC for 25% reduction in tire stiffness*
1	2.22e+00	5.79e+00
2	1.26e+01	1.49e+01
3	7.77e+00	1.35e+01
4	1.25e+01	1.82e+01
5	1.26e+01	2.12e+01

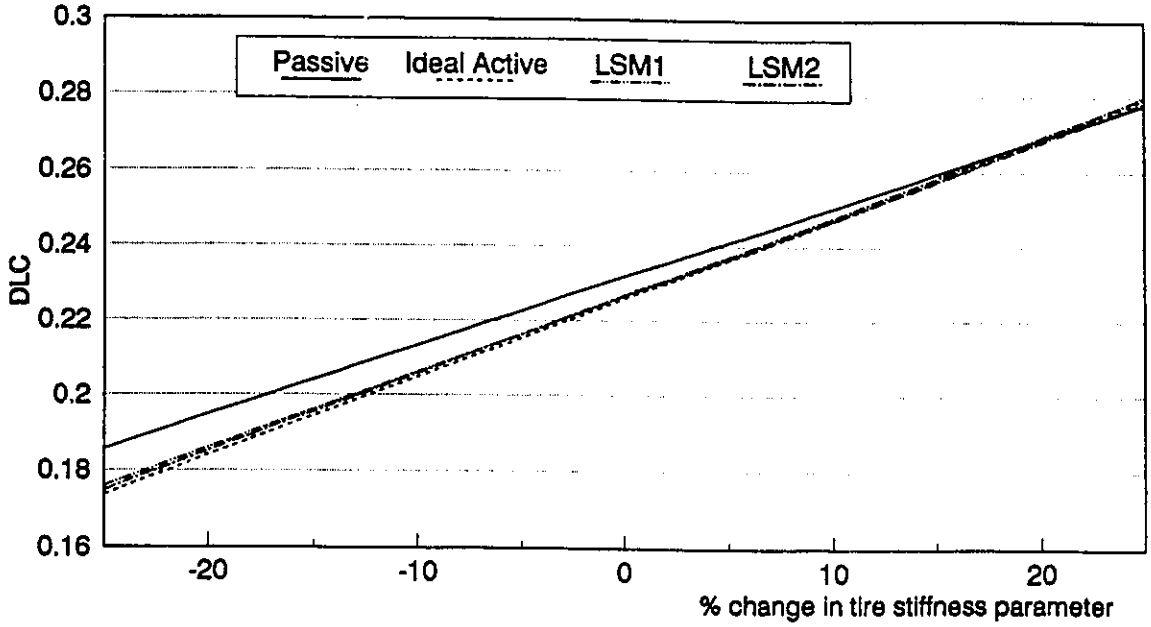

Figure 6.8a Effect of tire stiffness variation on the DLC of tire 1 for different types of suspensions

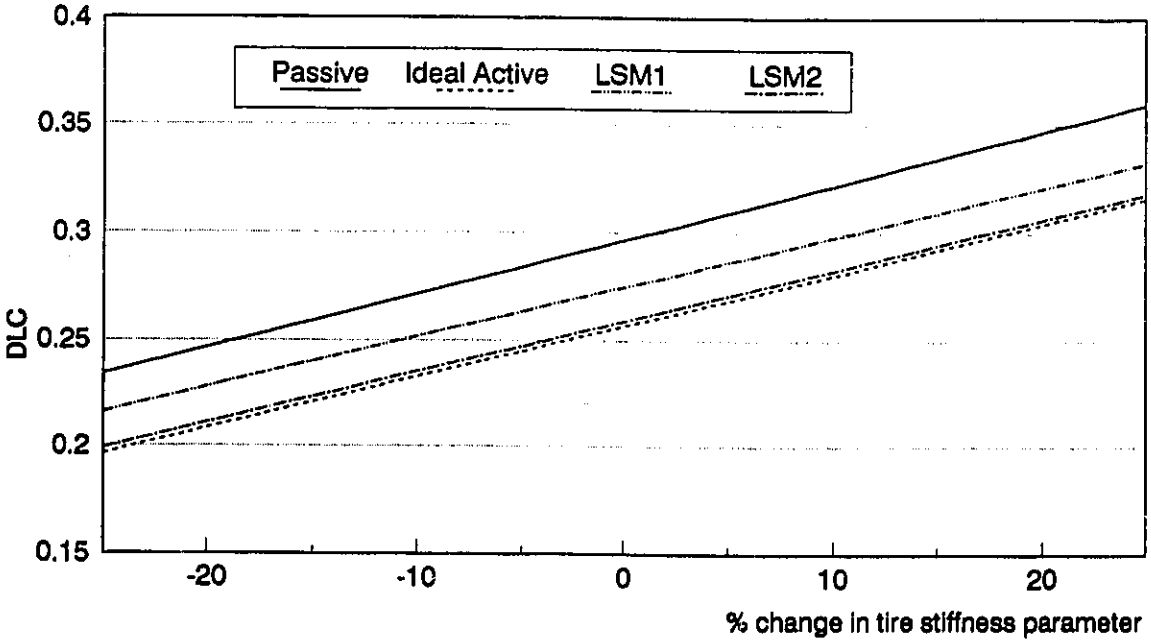

Figure 6.8b Effect of tire stiffness variation on the DLC of tire 2 for different types of suspensions

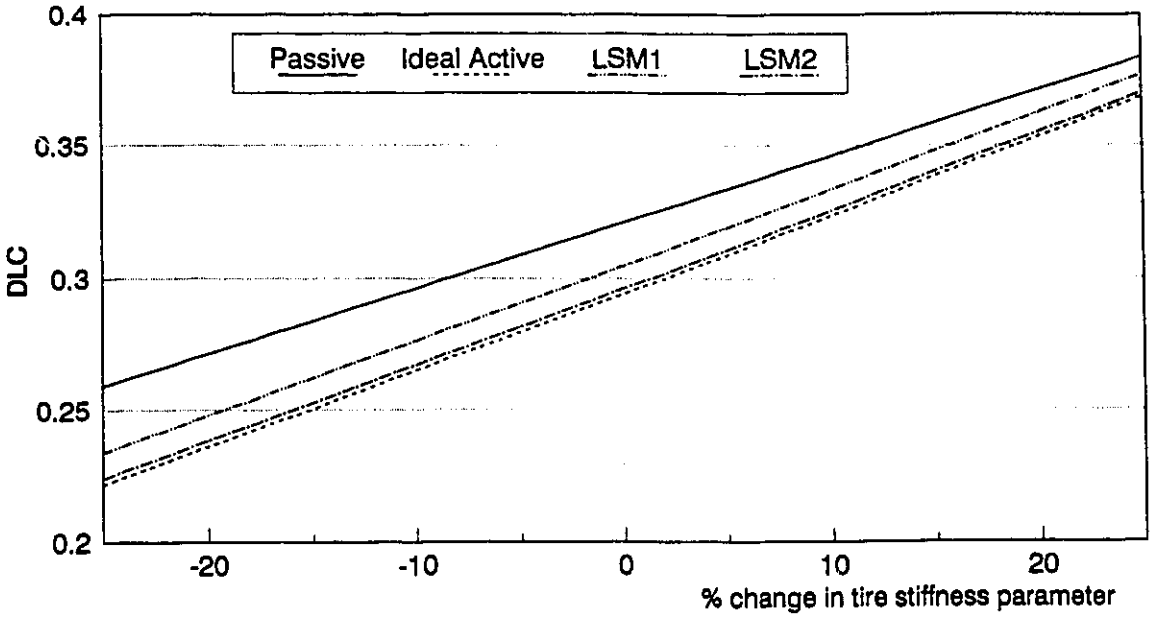

Figure 6.8c Effect of tire stiffness variation on the DLC of tire 3 for different types of suspensions

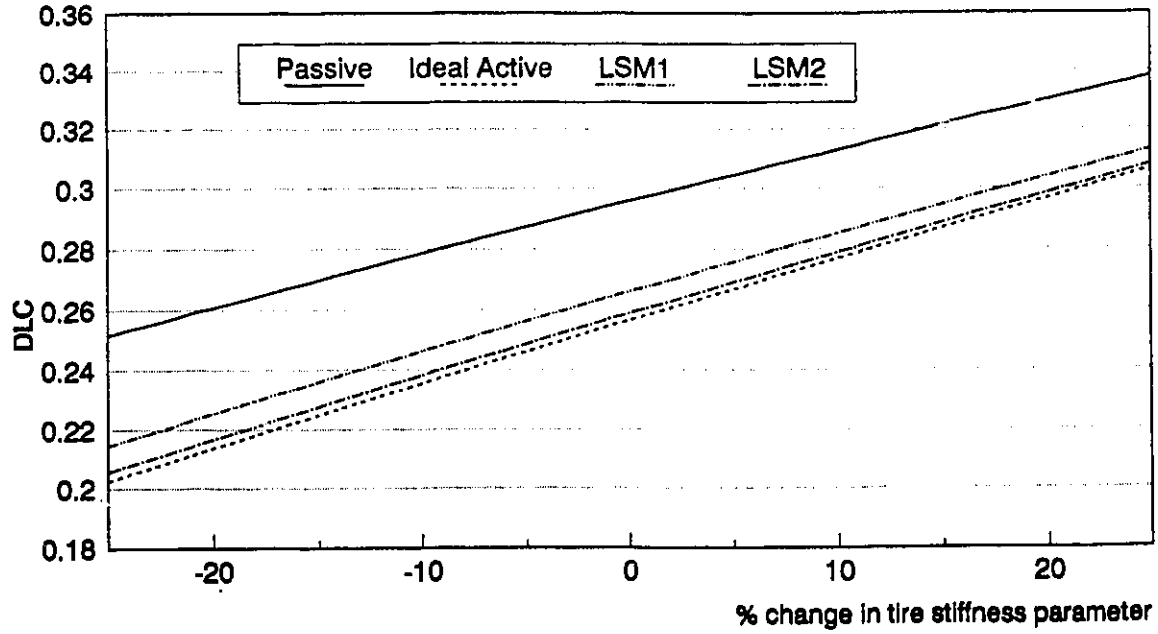

Figure 6.8d Effect of tire stiffness variation on the DLC of tire 4 for different types of suspensions

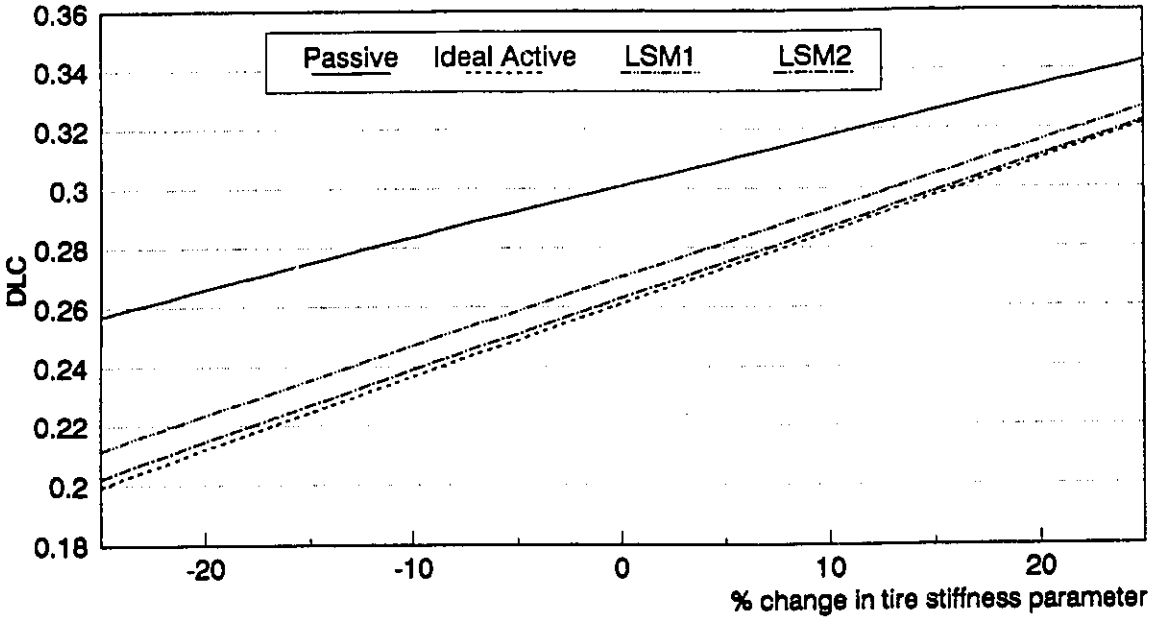

Figure 6.8e Effect of tire stiffness variation on the DLC of tire 5 for different types of suspensions

6.3.5 Effect of Semitrailer Axle Spacing on the *DLC*

Figures 6.9 illustrate the influence of variations in the semitrailer axle spacing on the *DLC* due to the tire forces. The axle spacing is varied from $1.2m$ to $2m$. While the variation in trailer axle spacing do not influence the *DLC* of tire forces on the tractor axles, the *DLC* due to trailer axle tire forces vary with the axle spacing. A widely spaced axle yields reduced *DLC* due to lead axle tire force, with an increase in the trailing axle tire *DLC*, as shown in the figures. The change in the *DLC* is, however, small (about 3%) and does not warrant an increase in the axle spacing.

6.3.6 Effect of Loading Patterns on the *DLC*

Cargo placement affects the load distribution among the different axles. The variations in the longitudinal location of the semitrailer *CG* thus affects the *DLC* in a significant manner. The longitudinal location of *CG* distance from the fifth wheel is varied from 4 to 8m, and its effect on the *DLC* of the forces is presented in Figures 6.10 and 6.11.

An increase in the longitudinal distance between the articulation and the trailer *CG* location tends to reduce the static loads on tractor axles, and increase the load on the trailer axle. The *DLC* due to forces on the tractor axle tires, however, increase, as shown in Figure 6.10. The *DLC* due to tractor tire forces approaches more than twice the value, when *CG* location is varied from 4 to $8m$. The corresponding *DLC* due to trailer axle tires approaches near 50% of the value. Moving the load to the back of the semitrailer increases the fraction of static load carried by the semitrailer tires. Since the *DLC* is defined as the ratio of the *RMS* dynamic tire force and the static tire force, an increase in the static force would obviously result in a decrease in the *DLC* as shown in Figures 6.10d and 6.10e.

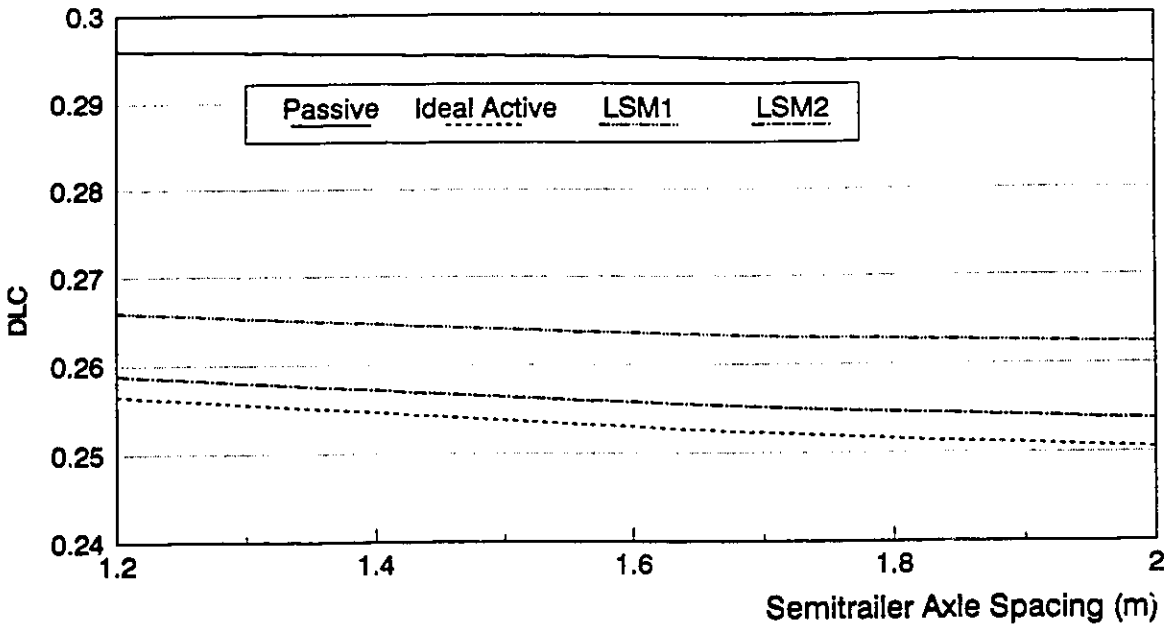

Figure 6.9a Effect of semitrailer axle spacing on the DLC of tire 4 for differrent types of suspensions

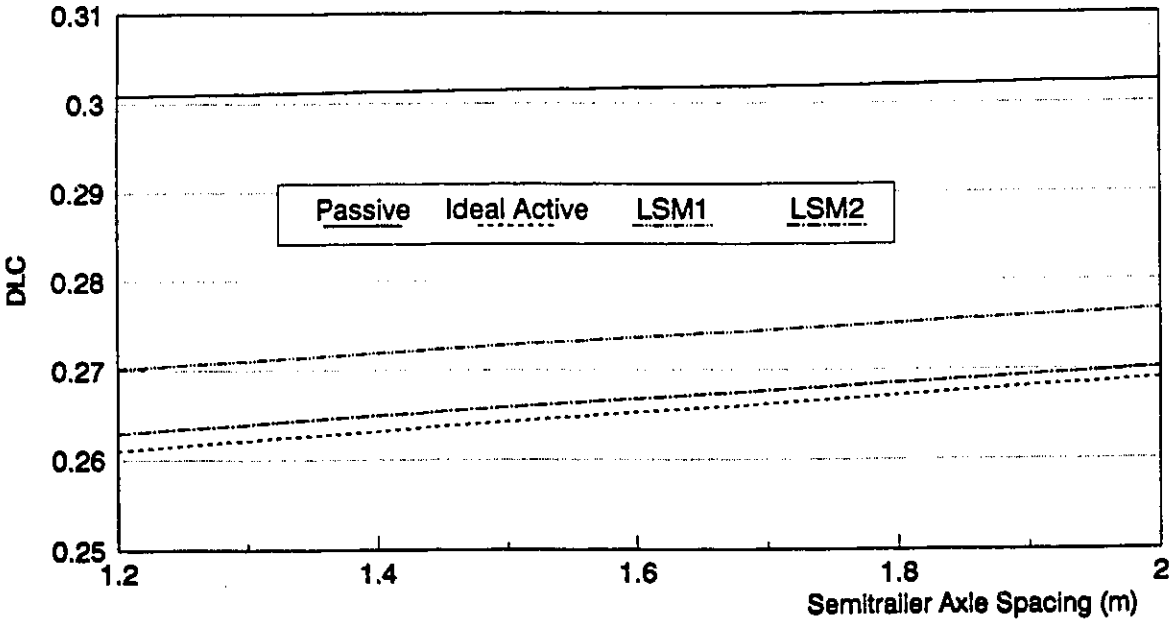

Figure 6.9b Effect of semitrailer axles spacing on the DLC of tire 5 for different types of suspensions

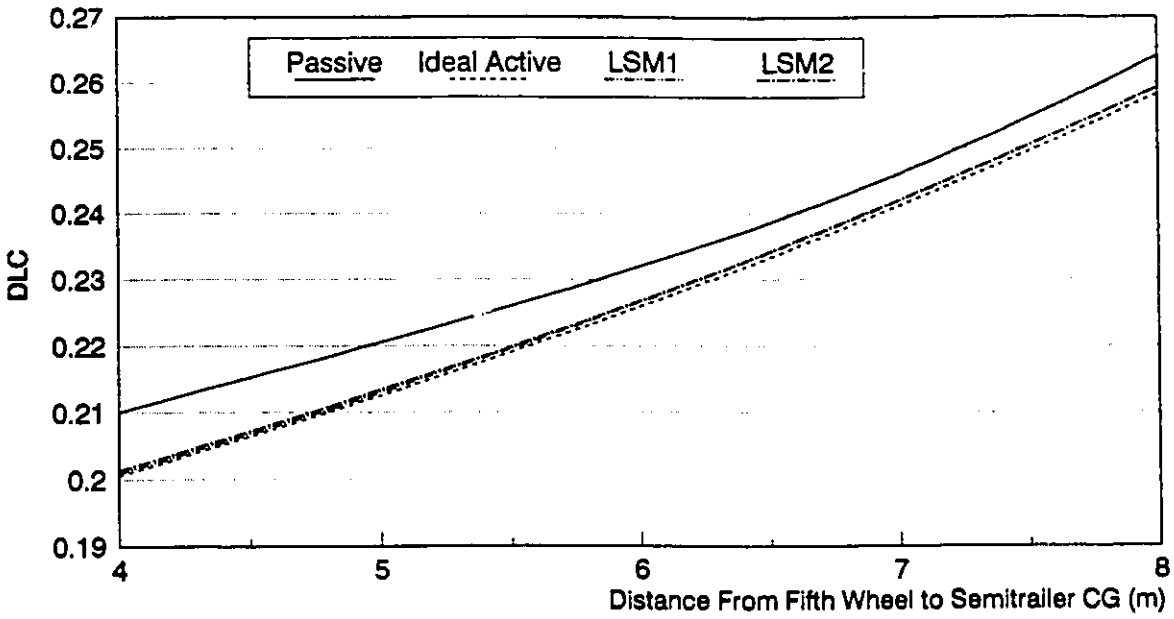

Figure 6.10a Effect of semitrailer CG location on the DLC of tire 1 for different types of suspensions

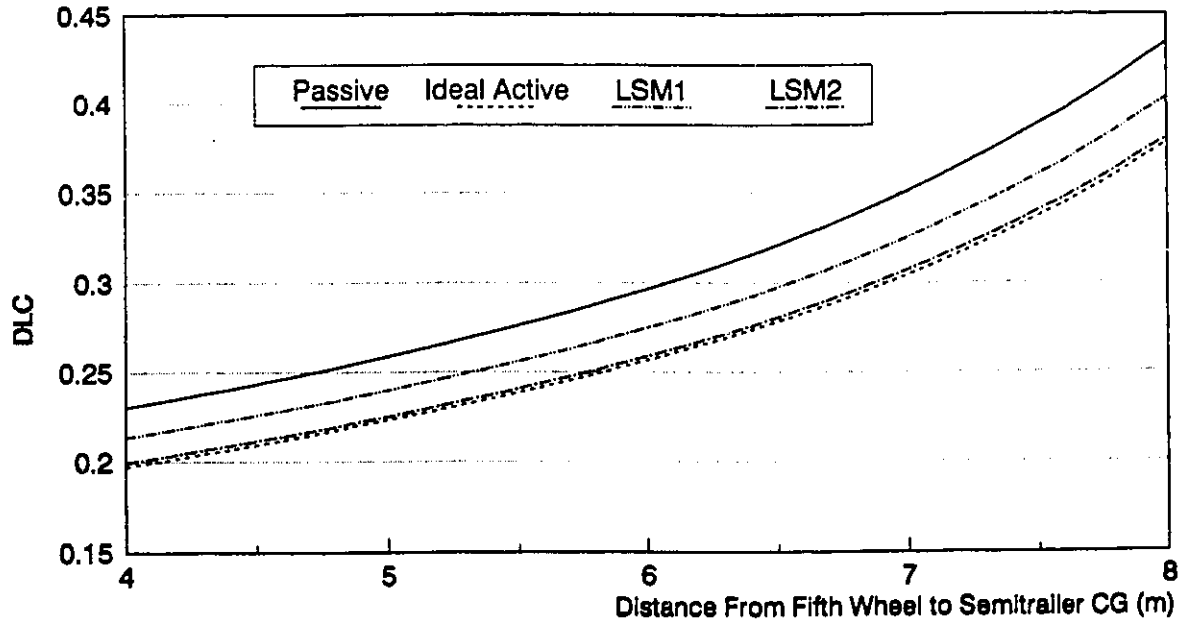

Figure 6.10b Effect of semitrailer CG location on the DLC of tire 2 for different types of suspensions

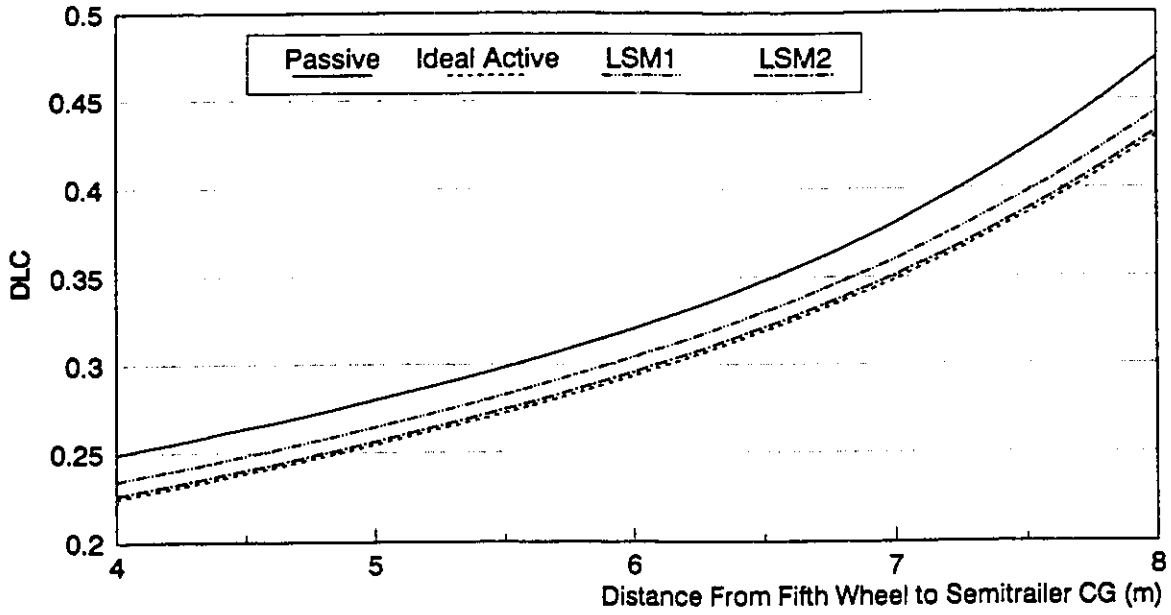

Figure 6.10c Effect of semitrailer CG location on the DLC of tire 3 for different types of suspensions

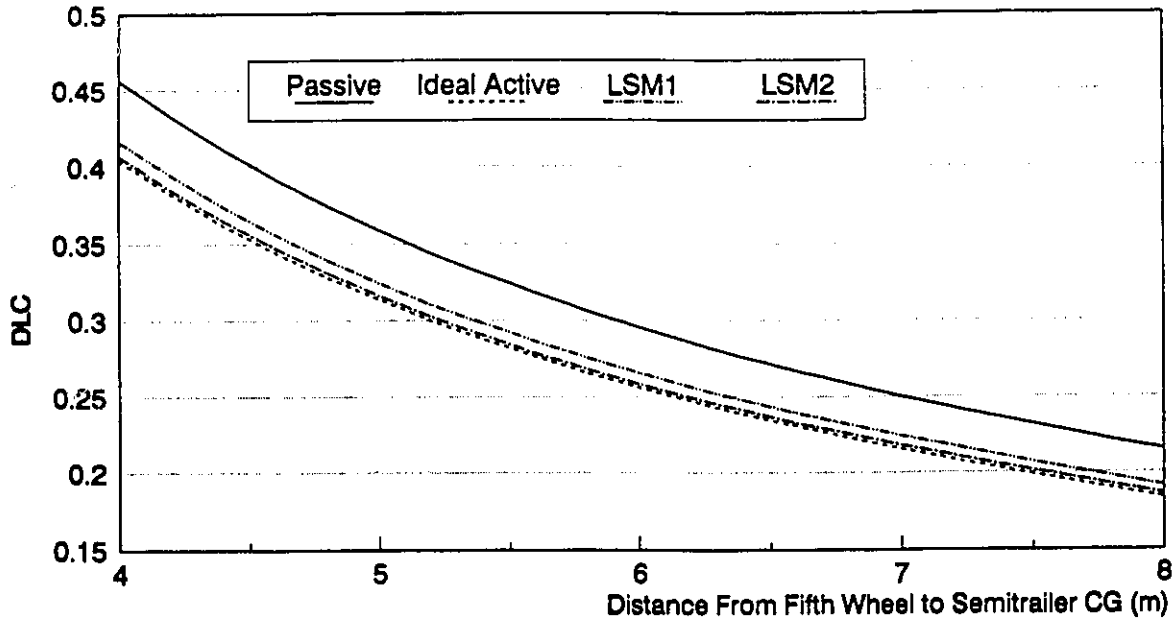

Figure 6.10d Effect of semitrailer CG location on the DLC of tire 4 for different types of suspensions

Choosing the proper location of the semitrailer *CG* can be accomplished, however, by investigating the *DLC* of all the vehicle tires simultaneously, as shown in Figure 6.11. In order to avoid excessive *DLC* at a particular tire, the semitrailer *CG* should be located between 5.5 and 6 *m* from the fifth wheel. This particular choice would result in a *DLC* of about 0.3 for tires 2, 3, 4 and 5. If the semitrailer *CG* is, however, moved to the front (4 *m* from the fifth wheel), the *DLC* of tires 2 and 3 can be reduced to less than 0.25 (about 23% decrease). Unfortunately this reduction is accompanied by an increase in the *DLC* of tires 4 and 5 to about 0.45, which is an increase of about 50%, and thus is unacceptable.

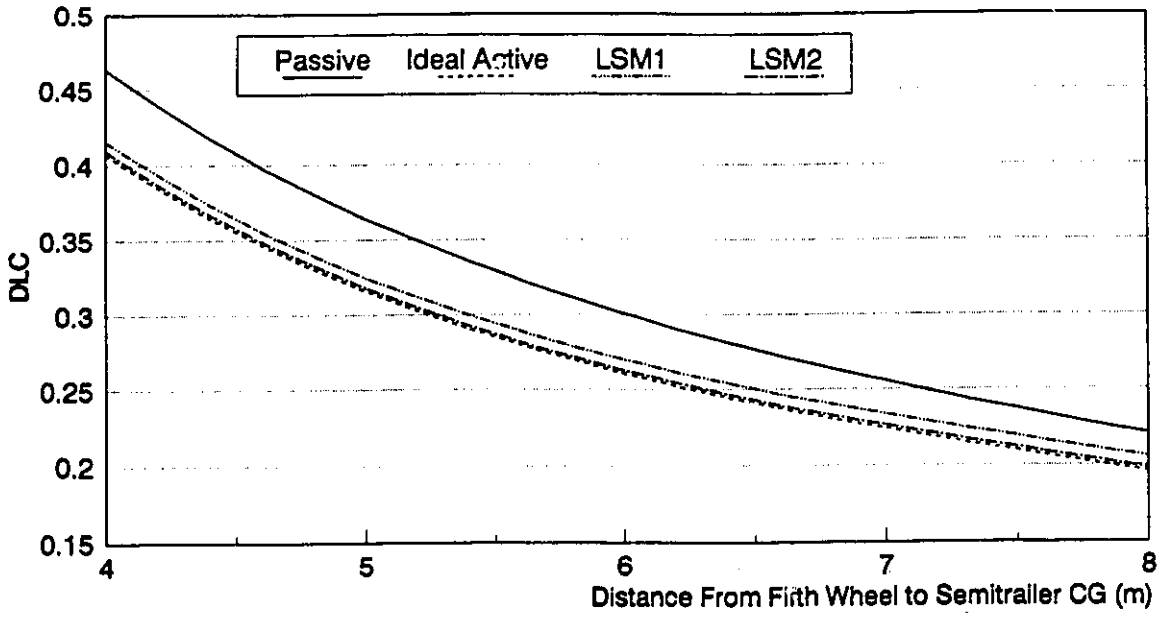

Figure 6.10e Effect of semitrailer CG location on the DLC of tire 5 for different types of suspensions

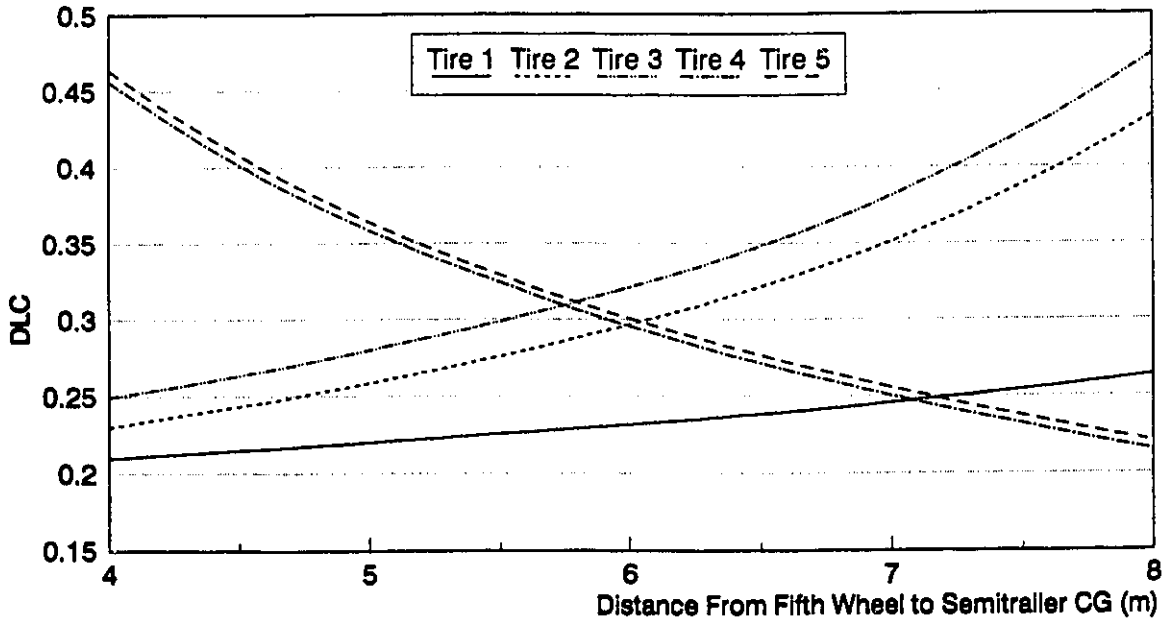

Figure 6.11 Effect of semitrailer CG location on the DLC of tractor-semitrailer tires (passive suspension)

6.4 SUMMARY

The effect of different vehicle design and operating parameters on the dynamic tire forces is investigated using the dynamic load coefficient (*DLC*) of tire forces. The results show that a realistic active suspension scheme that uses limited state measurements and accounts for sensor noise, can reduce the *DLC* by more than 13% (for tire 4 and 5). This scheme was also shown to be superior to a passive suspension regardless of the vehicle speed and road roughness. The two major factors that have considerable influence on the *DLC* are the vehicle speed and the road roughness. An increase in road roughness and the vehicle speed results in increased *DLC* due to all the tractor semitrailer tire forces. For the case of a passive suspension, proper choice of the damping and stiffness is necessary to achieve low *DLC*. The *DLC*, however, is more sensitive to variations in suspension damping. Increasing the tire stiffness increases the *DLC* of all the tractor-semitrailer tires regardless of the type of suspension scheme used. However, the percent reduction in the *DLC* using active suspension schemes is more significant for tires with low stiffness..

6.5 REFERENCES

1. OECD Road Research Group, *"Road Research: Impact of Heavy Freight Vehicles,"* Paris, France : OECD, 1983, pp. 58-77,154.

2. P. F. Sweatman, *"A Study of Dynamic Wheel Forces in Axle Group Suspensions of Heavy Vehicles,"* Australian Road Research Board, Special Report, SR No. 27, 1983.

3. D. Cebon, *"Vehicle Generated Road Damage: a Review,"* Vehicle System Dynamics, 18 (1989), pp. 107-150

4. S. Rakheja et al., *"Ride Vibrations of Articulated Vehicles and Significance of Secondary Suspension,"* SAE 1989 Noise and Vib. Conf., SAE Publ. No. P-222, May 16-18, pp. 139-147.

5. E. N. Thrower, *"A Parametric Study of a Fatigue Prediction Model for Bituminous Road Pavement,"* TRRL Report LR892, 1979.

6. K. R. Peattie, *"Flexible Pavement Design,"* Applied Science Publishers Ltd. London, 1978, ed. Pell PS.

7. P. Ullidtz and B. K. Larsen, *"Mathematical Model for Predicting Pavement Performance,"* Transp. Res. Rec. 949, TRB, 1983, pp. 32-44.

8. D. Cebon, *"Theoretical Road Damage Due to Dynamic Tire Forces of Heavy Vehicles. Part 1: Dynamic Analysis of Vehicles and Road Surfaces. Part 2: Simulated Damage Caused by a Tandem-Axle Vehicle"*, Proc. Instn. Mech. Engrs., Vol 202, No. C2, pp. 103-117, 1988.

9. F. W. Cron, *'HIghway Design for Motor Vehicles- A Historical Review. Part 1: The Beginning of Traffic Measurement,'* Public Roads, 38 (3) pp. 85-95, 1974.

10. The AASHO Road Test, Report 5 *"Pavement Research,"* Highway Research Board, Special Report 61E, Washington DC 1962

11. The AASHO Road Test, Report 6 *"Special Studies,"* Highway Research Board, Special Report 61F, Washington DC 1962

12. F. H. Scrivner and H. C. Duzan, *'Application of AASHO Road Test Equations to Mixed Traffic,'* Proceedings of a conference on the AASHO Road Test, St. Louis, Mo., National Academy of Sciences, National Research Council, Special Report 73, 1962.

13. Anon, '*Impacts of Heavy Freight Vehicles*.' OECD, Paris, 1982.

14. J. T. Christison, K. O. Andersonand B. P. Shields, '*In Site Measurements of Strains and Deflections in a Full-Depth Asphaltic Concrete Pavement*,' Proc. Assoc. Asphalt Paving Technology, 47 pp. 398-430, 1978.

15. J. H. F. Woodrooffe, P. A. LeBlanc and K. R. LePierre, *"Effects of Suspension Variations on the Dynamic Wheel Loads of a Heavy Articulated Highway Vehicle,"* Vehicle Weights and Dimensions Study, Vol. 11, Canroad Transportation Research Corporation, Canada, 1986.

16. C. G. B. Mitchell and L. Gyenes, *" Dynamic Pavement Loads Measured for a Variety of Truck Suspensions,"* 2nd International Conference on Heavy Vehicle Weights and Dimensions, Kelowna, British Columbia, 1989.

17. G. Hu, *"Use of a Road Simulator for Measuring Dynamic Wheel Loads"*, SAE 881194, SP765, Vehicle/Pavement interaction, Indianapolis, November 7-10, 1988, pp. 61-68.

18. R. D. Ervin, R. L. Nisonger, M. Sayers, T. D. Gillespie and P. S. Fancher, *"Influence of Truck Size and Weight Variables on Stability and Control Properties of Heavy Trucks,"* University of Michigan Report No. UMTRI-83-10/2, April 1983.

19. J. Eisenmann, *"Dynamic Wheel Load Fluctuation- Road Stress,"* Strasse und Autobahn, 3 1978.

20. W. D. Hahn, "*Effects of Commercial Vehicle Design on Road Stress - Quantifying the Dynamic Wheel Loads for Stage 3: Single Axles, Stage 5: Triple Axles, as a Function of the Springing and Shock Absorption System of the Vehicle,"* Institut fur Kraftfahrwesen, Universität Hannover, Report No. 453, 1987.

21. W. D. Hahn, *"Effects of Commercial Vehicle Design on Road Stress - Vehicle Research Results,"* Institut fur Kraftfahrwesen, Universität Hannover, 1985.

22. P. Von Becker *"Commercial Vehicle Design-Road Stress: Effect on Transport Policy Decision,"* Strasse und Autobahn, 12, 1985 pp. 493-498.

23. R. R. Addis and R. A. Whitmarsh, *"Relative Damaging Power of Wheel Loads in Mixed Traffic,"* Transport and Road Research Laboratory, Laboratory Report LR979, 1981.

24. D. F. Kinder and M. G. Lay, *"Review of the Fourth Power Law,"* ARRB, Internal Report AIR000-248, 1988.

CHAPTER 7

CONCLUSIONS AND RECOMMENDATIONS FOR FUTURE WORK

7.1 HIGHLIGHTS OF THE STUDY

In this thesis, an analytical investigation of passive and active suspension systems for articulated freight vehicles is undertaken to study their performance potentials to enhance ride quality, cargo safety, and reduce tire induced road damage. The study is carried out in five sequential phases, and highlights of each phase of the study are described below.

1 • ***Development of a representative vehicle model:*** Based upon the reported surveys on heavy vehicle population in Canada, a candidate vehicle comprising a three-axle tractor and a two-axle semitrailer is identified for the study. The candidate vehicle is represented by an in-plane nine degrees-of-freedom dynamical system model incorporating sprung masses due to tractor and semitrailer, and unsprung masses due to the five axles. Each axle suspension is represented by a parallel combination of a linear spring and a viscous damper in parallel. Although passive vehicle suspensions, invariably, exhibit progressively hardening force-deflection and variable force-velocity properties, the linear suspension parameters yield significant insight

into vehicle response behavior with relatively simple analysis. The tire terrain interactions are represented by the linear force-deflection properties of tires assuming point contact with undeformable road. The random road undulations are analytically characterized and the time delays between the consecutive tire-road contact points are analytically modeled using *Padé* approximation. The road roughness model is incorporated within the nine-DOF vehicle model to derive an augmented heavy vehicle model.

2 • ***Passive suspension design and optimization***: The validity of the mathematical vehicle model is asserted by comparing the analytical and experimental frequency response characteristics of the selected response variables. The desired performance characteristics, such as ride quality, cargo safety, dynamic tire forces and suspension rattle space, are related to the generalized response coordinates to formulate the performance index. A performance criteria that includes tractor and semitrailer bounce and pitch accelerations, suspension deflections, and dynamic tire loads, is then formulated to assess the performance characteristics of the passively suspended vehicle. *"Optimum"* restoring and dissipative properties of the passive suspension system are tuned to achieve the performance criteria based on covariance analysis technique. The effects of varying the damping and stiffness properties of the suspension on the frequency response characteristics are further investigated to verify the conclusions drawn from the covariance analysis.

3 • ***Ideal active suspension design:*** An ideal fail-safe active suspension scheme based on full state feedback is formulated using *Linear Quadratic Gaussian* (*LQG*) control techniques. Passive damping and stiffness elements are incorporated in the active suspension system to yield a fail-safe configuration and to reduce the power requirement of the active actuators. A performance index comprising the weighted

control forces and weighted response variables is formulated. A methodology is also presented to determine the weighting factors. The performance characteristics of the ideal active suspension are compared to those of the "optimum" passive suspension to determine their potential performance benefits.

4 • ***Limited-state active suspension design:*** A more realistic active suspension scheme, based on H_2 synthesis, is developed to reduce the hardware requirements of an ideal active suspension. The suspension scheme is employed to solve the inherent hardware and signal processing requirements, high cost and poor reliability of a full state feedback active suspension design. Two suspension schemes, *LSM1* and *LSM2*, based upon limited state measurement of readily available quantities are investigated. The *LSM1* scheme is based on the measurement of relative displacements and velocities across the suspension, while the *LSM2* is based on the measurement of bounce and pitch accelerations of tractor and semitrailer sprung masses. The performance characteristics of the proposed suspension designs are compared to those of the full state measurement active suspension and the "optimum" passive suspension systems in view of the sensors noise and actuator power requirements.

5 • ***Effects of different suspension systems and vehicle configuration on tire dynamic forces:*** The effects of the passive and the various active suspension schemes on the dynamic tire forces are thoroughly investigated. Road friendliness of the heavy vehicle is assessed in terms of the dynamic load coefficient (*DLC*). Effects of the restoring and dissipative properties of the suspensions, road roughness, vehicle velocity, tire stiffness, semitrailer axle spacing and loading patterns of the *DLC* are also investigated.

7.2 CONCLUSIONS OF THE INVESTIGATION

The conclusions drawn from the investigation are summarized in the following sections.

7.2.1 Development of a Vehicle Ride Model and Road Roughness Characterization

- Based on reported surveys of heavy vehicle population in Canada, tractor-semitrailers are the most commonly used heavy vehicle configuration.
- An inplane 9 *DOF* tractor-semitrailer ride model can yield a significant insight into all the relevant performance characteristics.
- Road irregularities can be characterized mathematically by a single sided power spectral density. This formulation is shown to yield a reasonably good approximation of the actual road spectra.
- Appropriate consideration of the time delays between the first and subsequent tire-road contact points can be incorporated in the road roughness model through *Padé* approximation.

7.2.2 Optimization and Ride assessment of a Passive Suspension

- A performance index formulated to include ride quality, cargo safety, rattle space requirements and dynamic tire forces, encompass all the relevant design objectives and is thus well suited for suspension system design.
- The validity of the mathematical vehicle model is asserted by comparing the analytical and experimental frequency response characteristics of selected variables. The results of a road measurement study undertaken by *CONCAVE Research*

Centre on a similar vehicle are examined and it is observed that the model and the measured response characteristics show similar trends in the unsprung mass frequency and the corresponding magnitude. The magnitudes of model and measured acceleration response characteristics corresponding to the resonant frequencies of the drive axle are comparable. The similar trends observed for the simulation and the measured response characteristics reveal the adequacy of the vehicle model and the road characterization.

Different components of the objective function often pose conflicting design requirements. To select the "optimum" passive suspension parameters and thus realize an acceptable compromise among the different performance objectives, a study of effects of parameters on the components of the performance index is undertaken using covariance analysis. The results show that:

- Soft suspension is required to improve the vehicle ride quality and the cargo safety.
- There exists an ideal damping value for a given suspension stiffness to improve the ride quality and cargo safety.
- A soft suspension, while desirable to achieve good ride quality and cargo safety, contradicts the handling and roll stability as well as the static suspension deflection requirements.
- There is an optimal suspension stiffness value for a given value of damping to achieve low suspension deflection for the tractor axle suspensions. The existence of the optimal value is specifically apparent for lightly damped suspensions.
- A heavily damped suspension is desirable to reduce the suspension deflections. The deflection response of a heavily damped suspension, however, is relatively insensitive to variations in suspension stiffness.

- The study of the influence of suspension parameters on the dynamic deflection response of the tires revealed the existence of optimal suspension damping and stiffness parameters to achieve low dynamic deflection of each of the axle tires.
- The tire deflection tends to increase for extremely low and high damping values, irrespective of the suspension stiffness.

The results of the covariance analysis clearly illustrate the difficulties associated with designing a suspension to simultaneously satisfy all the design objectives. A set of nominal suspension parameters is, therefore, derived to achieve a compromise among the different components of the performance index. Since the results obtained from the covariance analysis, are based on the mean square values of the penalized variables and thus yield an overall measure of the performance. A study of the resonant behavior and frequency components of the response characteristics necessitates the frequency response analysis. The suspension parameters are varied to further tune the suspension design and to achieve better compromise among the different performance objectives. An examination of the response characteristics reveals that the only adjustment deemed necessary was the increase in the damping coefficients of the fourth and fifth suspensions. The effects of varying the damping and stiffness properties of the suspension on the frequency response characteristics are further investigated and reveal that:

- The selection of adequate suspension damping, for a given suspension stiffness, was found to involve a compromise between performance at low and high frequencies.
- For a given stiffness, an increase in the suspension damping results in improved ride quality, cargo safety and tire forces only at low frequencies.
- The rattle space requirements, however, decrease throughout the frequency range with increase in suspension damping.
- The nominal damping parameters were found to provide an overall good

performance without compromising the static suspension deflection requirements. The investigation thus demonstrated the effectiveness and convenience of the covariance technique in selecting the nominal suspension.

7.2.3 Design of an Ideal Fail-Safe Active Suspension for the Tractor-Semitrailer

Linear Quadratic Gaussian (*LQG*) control techniques are employed to design an ideal active suspension scheme based on full state feedback. The ideal active suspension scheme is formulated to minimize a quadratic performance measure that includes ride quality, cargo safety, suspension and tire dynamic deflections, and power requirement. The active suspension suggested is a parallel combination of passive elements and a feedback controlled force generator. The investigation of the active suspension scheme revealed that:

- Although the presence of the passive elements in the active suspension was found to have no effect on the performance characteristics of the vehicle for properly selected feedback gains, passive elements were found to affect the power requirements of the active suspension in a significant manner.
- The results clearly show the existence of an ideal range of passive suspension stiffness and damping values to realize the active suspension with minimum actuator forces magnitude.
- The damping and stiffness values of passive elements, derived from the analysis of the passive suspension, are used to realize the fail-safe active suspension. Although the selected passive suspension components do not yield minimal power requirements, the power demand is quite close to the optimal.
- The performance characteristics of an active suspension is shown to be strongly dependent on the choice of the weighting coefficients in the performance index.

- An initial set of weighting coefficients selected using the covariance study of the passive suspension is found to yield a balanced weighting of all the performance variables.

To realize a compromise among the different components of the performance index, a total of 5 sets of weighting coefficients are selected through an iterative procedure. The suspension schemes based on these weighting coefficients are designated as *AS1* to *AS5*. All the five active suspension schemes, in general, were found to yield improved performance when compared to the passive suspension. Each of these schemes, however, accentuates certain particular aspects of the performance index.

Based on frequency domain analysis, the performance characteristics of the penalized variables for the five active and the "optimum" passive suspensions are investigate to verify the conclusions drawn from the covariance analysis. The following conclusions were drawn from the study:

- All the five active suspension schemes are found to offer improved ride quality and better cargo safety almost in the entire frequency range.
- Substantial benefits can be observed with all of the 5 active suspension schemes especially at low frequencies, which is a critical frequency region in ride quality evaluations.
- The active suspensions, irrespective of the weighting coefficients, do not provide a significant improvement in the vertical and pitch responses characteristics of the tractor and semitrailer sprung masses near the wheel hop frequencies.
- The magnitudes of relative deflection response across all the five axle suspensions also reduces considerably when proposed active suspensions are employed. The active suspensions, however, yield high suspension deflection at low frequencies,

especially below 0.9 *Hz*.

- Active suspension systems yield significant reduction in dynamic tire forces at low frequencies. The reduction of the dynamic tire forces, however, is not evident near wheel hop frequencies.
- The suspension scheme *AS5* yields the most significant reduction in the dynamic tire forces in the entire frequency range. This active suspension scheme is thus desirable when the design objectives involve a specific emphasis on the pavement fatigue caused by dynamic tire loads transmitted to the road.

The performance characteristics are evaluated for variations in the vehicle speed to study the effectiveness of the active suspensions. The control gain for the active suspensions *AS1* to *AS5*, selected for a vehicle speed of 90 *km/h*, are used to evaluate the response characteristics in the 10-120 *km/h* speed range. The results of the study show that:

- The ideal active suspensions provide significant improvement in the ride quality and cargo safety, irrespective of the vehicle speed and the active suspension scheme.
- The relative magnitude of deflection response of the active suspensions are comparable to those of the passive suspension and thus no extra rattle space requirements is necessary for the active systems.
- Except for *AS3*, all the active systems show lower tire deflections throughout the speed range.
- The performance of the active suspensions, in general, is enhanced as the vehicle speed increases. Since freight vehicles operate mostly at high speeds, the performance potentials of the active systems become more significant.
- The active suspensions yield improved performance related to all the design objectives. The suspension performance related to ride quality, cargo safety and tire

forces can be further improved by relaxing the rattle space requirements.

7.2.4 Design and Ride Assessment of a Realistic Active Suspension with Sensors Noise and Limited State Measurements

In view of hardware and signal processing requirements, high cost and poor reliability of a full state feedback active suspension design, a thorough analysis of a more realistic active suspension scheme, based on H_2 synthesis, is undertaken. The assumption of full and perfect measurement of the states is relaxed in the design of the H_2 active suspension. The proposed active suspension system is also formulated incorporating the sensor signal noise. Two suspension schemes, *LSM1* and *LSM2*, based upon limited state measurement of readily available quantities are investigated. The *LSM1* scheme is based on the measurement of relative displacements and velocities across the suspension, while the *LSM2* is based on the measurement of bounce and pitch accelerations of tractor and semitrailer sprung masses. The response characteristics of *LSM1* and *LSM2* are discussed in view of the different components of the performance index, specifically, the ride quality, cargo safety, suspension deflections and tire deflections, and compared to those of the "optimum" passive and full-state feedback active suspensions. The influence of sensor noise and actuator size on the suspension performance is further investigated. The results reveal that:

- For low sensor noise and low penalty on power supply, the suspension performance is similar to that of a full-state feedback active suspension systems. The suspension performance, however, deteriorates rapidly with an increase in sensor noise, and approaches that of the passive suspension, irrespective of the actuator effort.
- The suspension performance also deteriorates with reduction in the actuator effort and the active suspension performance approaches that of the passive suspension

irrespective of the sensor noise levels.

- Excessive measurement noise and/or inadequate actuator power results in very little or no improvement in the performance indices.
- The three suspension systems offer similar % improvement in the performance for low level of sensors noise and sufficient actuator effort. This indicates that the state estimation can be accomplished with greater accuracy when signal noise levels are low. It is thus possible to achieve performance similar to that of the full state feedback suspension, while using limited state measurement.
- The discrepancy among the performance characteristics of the three suspension schemes, increases with increase in noise intensity.
- Using tractor and semitrailer bounce and pitch accelerations as the only available measurements (*LSM2*), it is possible to obtain performance comparable to that of the suspension based on full state measurements.
- Since each active suspension system is configured as a fail-safe combination of the passive and active components, a reduction in the actuators effort will simply cause the suspension to operate in a passive mode. The performance characteristics, however, approach those of the "optimum" passive suspension, since the passive components correspond to the optimum design.
- Using any of the active suspension schemes, the tire forces are reduced throughout the whole speed range.
- Generally, the performance of the active suspensions compared to the optimum passive suspension is enhanced as the vehicle speed increases and thus these active systems would be more beneficial at high speeds.
- Superior performance of the active suspensions schemes is maintained regardless of the road roughness.

7.2.5 Evaluation of the Road Friendliness of the Various Suspension Schemes

The road friendliness of vehicles with various suspension schemes is assessed in terms of their respective dynamic load coefficient. The influence of relevant vehicle design parameters and operating conditions on the dynamic load coefficients of the vehicle tires is investigated to attempt to reduce the tire dynamic forces and thus the pavement damage. It is shown that:

- The *DLC* of all the tractor-semitrailer tires are significantly affected by the road roughness regardless of the type of suspension.
- The *DLC* more than triples for a tractor-semitrailer traveling on a rough road compared to one traveling on a medium rough road for the passively suspended vehicle. This emphasizes the importance of initial road construction and proper road maintenance. The contribution of the dynamic load tires to pavement deterioration would be much smaller for a smooth road and hence the degradation would be much slower. As the road ages, its roughness increases and hence its rate of deterioration due to dynamic tire loads also increases.
- The level of *DLC* reduction of *LSM2* is comparable to that of an ideal active suspension for all the tractor semitrailer tires, irrespective of the levels of road roughness. This reduction in *DLC* varies from 3 to 13.5 % and the most significant reduction can be achieved for the semitrailer tires.
- Increased speed results in increased *DLC* and hence increased pavement deterioration rate, irrespective of the suspension scheme used. As the speed is increased from 10 to 125 *km/h*, the *DLC* almost triples irrespective of the suspension scheme.
- Active suspension schemes generally result in lower *DLC* throughout the speed range of interest.

- A suspension scheme based on acceleration measurements (*LSM2*) results in a *DLC* which approaches that of an ideal active suspension throughout the speed range.
- For the case of a passive suspension, it is shown that variations in the suspension damping have greater effect on the *DLC* than variations in the stiffness. Too much or too little damping can cause high dynamic tire forces.
- Increasing the damping by 50%, for instance, can result in a 14% increase in the *DLC* of the semitrailer tires. On the other hand, reducing the suspensions damping by 50% can result in approximately 13% increase in the *DLC* of the tractor drive axle tires.
- The chosen "optimum" stiffness and damping parameters for the passive suspension offer a compromise between the *DLC* of all the tractor-semitrailer tires. At the nominal suspension damping value the *DLC* of steering axle tire is minimum while the *DLC* of all the other tires is between 0.29 and 0.32.
- Increased tire stiffness increases the *DLC* for the tractor-semitrailer tires irrespective of the suspension type.
- In the case of a passive suspension, a reduction of up to 21% in the *DLC* of the second tire can be achieved by reducing the tire stiffness by 25%.
- The percent reduction in the *DLC* using active suspension schemes is shown to be more significant at low tire stiffness.
- Semitrailer axles spacing has no noticeable effect on the *DLC* of the tractor tires, but reduces the *DLC* of tire 4 and increases that of tire 5. This increase/decrease in the *DLC* is, however, small (about 3%) and does not warrant the axle spacing increase.
- Moving the cargo and hence the *CG* location towards the back of the semitrailer increase the *DLC* of the tractor tires and reduces that due to semitrailer tires.

7.3 RECOMMENDATIONS FOR FURTHER WORK

The present research work yields significant insight into the effects of passive and active suspension systems on the performance characteristics of articulated heavy vehicles. Following tasks are recommended to further enhance the investigation.

- The *LQG* design is known to have an infinite gain margin, at least 50% gain reduction tolerance and at least ±60 *degrees* phase margin in each control input channel. The H_2 (and H_∞) technique, however, can be extended to investigate the robustness of the optimal feedback control system in the presence of plant parameter uncertainties and high order dynamics. Since the uncertainties in the vehicle model are mostly structured, structured singular values can be employed to assess the robustness limits of the system.

- Future dynamic studies of the suspension should include the nonlinear characteristics of the suspensions and tires. Linear analysis methods can still be used for the design of the passive and active systems by employing linearization techniques.

- The dynamics of the controllers, associated time delays, and nonlinearities should be incorporated in the active suspension modeling to enhance the confidence in the analysis.

- Attempts should be made to develop a comprehensive analytical model of the active system hardware. A simple 2 *DOF* physical system model can be initially used to further investigate the possible practical implications of the various active suspension schemes.

- Road tests using an instrumented vehicle fitted with an active suspension prototype should be undertaken to validate the potentials of different control schemes. The test track may also need to be instrumented with sub-surface strain gauges to accurately record the dynamic wheel loads. The ride quality can best be assessed by recording the acceleration response at the driver seat interface and compared with the reduced comfort *RMS* acceleration limits proposed by *ISO* 2631.